THE UNIVERSITY OF QUEENSLAND

AUSTRALIA

Trophic ecology of shallow and deep reef-building corals

Veronica Zoya Radice

B.A. Biology

A thesis submitted for the degree of Doctor of Philosophy at

The University of Queensland in 2019

Faculty of Science

School of Biological Sciences

Coral Reef Ecosystems Laboratory

Abstract

Oceanic hydrodynamic mechanisms have a fundamental role in shaping coral reef ecosystems. Consequently, regional processes such as deep-water upwelling affect nutrient fluxes and the function of coral reefs at a local scale. Despite the importance of upwelling to marine ecosystems worldwide, there is limited knowledge about how this dynamic oceanographic process affects reef-building coral communities. Although depth is used to group different reef zones, the extent of nutrient fluxes across reef slopes is dependent on complex biophysical drivers. As mixotrophic organisms, reef-building corals rely on resources provided by their endosymbiotic dinoflagellates (herein 'symbionts'; autotrophy) as well as energy from feeding on particulate organic matter in the water column (heterotrophy). Although reduced light availability in deeper reefs may lead to a reduced dependence on autotrophy and a potential increase in heterotrophy, potential shifts in trophic strategies can be decoupled with depth due to the complex nature of the coral holobiont (Chapter 1).

Chapter 2 investigated the influence of upwelling on the trophic ecology of a community of reef-building corals common to shallow and deep reefs in the remote atoll system of the Maldives, Indian Ocean. Due to the structure of the central Maldives atolls, we considered different fore reef exposures including oceanic reefs and reefs facing the shallower Inner Sea. Trophic strategies of three species of coral (*Galaxea fascicularis*, *Pachyseris speciosa*, and *Pocillopora verrucosa*) were analyzed using carbon and nitrogen stable isotope ratios ($\delta^{13}C$ and $\delta^{15}N$) of coral hosts, their symbionts, and potential food sources of corals including particulate organic matter and plankton. Further, *in situ* seawater temperature was recorded to characterize water column mixing and potential differences in resource availability associated with depth. The results indicated that the water column was well mixed between 10 and 30 m reef depth and coral host isotopic ratios indicated an atoll-wide reliance on deep-water nitrogen across depth. However, coral host isotopic ratios indicated species-specific trophic strategies that revealed distinct patterns among the three species of coral. Only one coral species (*G. fascicularis*) had different $\delta^{13}C$ values between shallow and deep reefs, indicating an autotrophy strategy in shallow reefs but reduced autotrophy and a potential increase in heterotrophy in deep reefs. In contrast, *P. verrucosa* and *P. speciosa* showed consistent isotopic ratios regardless of reef depth. Among the three species, *P. verrucosa* was relatively more heterotrophic while *P. speciosa* depended more on autotrophy across the reef slope.

The ability to shift trophic strategies to increase heterotrophic feeding is important to the survival and recovery of corals subject to thermal stress conditions. In 2016 a global thermal stress event impacted coral reefs worldwide, including the Maldives, and caused mass coral bleaching and mortality. Eight

months after the thermal stress event in the Maldives, the same coral reefs were surveyed to investigate potential shifts in isotopic niches due to changes in trophic strategy (Chapter 3). Changes in the coral isotopic niches were observed following the thermal stress event. Shallow *G. fascicularis* had a decreased isotopic niche that was consistent with reduced autotrophy while the isotopic niche size of deep populations of *G. fascicularis* increased. The latter supports the ability of *G. fascicularis* to increase heterotrophic feeding in response to thermal stress. Increased isotopic niche size of both shallow and deep *P. speciosa* supports an increase in heterotrophy that in turn helped maintain autotrophy, its main trophic strategy. Minimal changes in the isotopic niche sizes of *P. verrucosa* were consistent with its dependence on heterotrophy.

Chapter 4 used a different set of biochemical tracers – fatty acids – to investigate the role of heterotrophy in the same three species of reef-building coral. The composition and various indices of fatty acids were compared among the three coral host species and their symbionts, including established indices applied in a novel context of coral trophic ecology. Further, a linear discriminant analysis was used to estimate the contribution of polyunsaturated fatty acids derived from various potential sources (symbionts and a diverse taxonomic range of plankton) to the three coral host species. This chapter provides insight into the importance of heterotrophy in coral nutrition, especially in productive reef systems, and provides extensive evidence of the utility of fatty acids in understanding coral trophic ecology.

In summary, this thesis examined a range of biochemical evidence associated with the trophic strategies of reef-building corals. Comparing these coral species with diverse trophic strategies, the relative contribution of autotrophy and heterotrophy was estimated for each species (Chapter 5). Despite the general dependence on symbiont autotrophy, the three species of coral hosts showed different abilities to utilize heterotrophy for nutrition. Although local oceanography plays a key role in nutrient cycling in reef systems, the inherent physiology of the coral holobiont strongly influences the ecological niche. Despite differences between shallow and deep reefs, diverse nutritional strategies enable corals to occupy the same habits while maintaining different trophic niches.

Declaration by author

This thesis is composed of my original work, and contains no material previously published or written by another person except where due reference has been made in the text. I have clearly stated the contribution by others to jointly-authored works that I have included in my thesis.

I have clearly stated the contribution of others to my thesis as a whole, including statistical assistance, survey design, data analysis, significant technical procedures, professional editorial advice, financial support and any other original research work used or reported in my thesis. The content of my thesis is the result of work I have carried out since the commencement of my higher degree by research candidature and does not include a substantial part of work that has been submitted to qualify for the award of any other degree or diploma in any university or other tertiary institution. I have clearly stated which parts of my thesis, if any, have been submitted to qualify for another award.

I acknowledge that an electronic copy of my thesis must be lodged with the University Library and, subject to the policy and procedures of The University of Queensland, the thesis be made available for research and study in accordance with the Copyright Act 1968 unless a period of embargo has been approved by the Dean of the Graduate School.

I acknowledge that copyright of all material contained in my thesis resides with the copyright holder(s) of that material. Where appropriate I have obtained copyright permission from the copyright holder to reproduce material in this thesis and have sought permission from co-authors for any jointly authored works included in the thesis.

Publications included in this thesis

Peer-reviewed manuscript:

Incorporated as Chapter 2

Radice VZ, Hoegh-Guldberg O, Fry B, Fox MD, and Dove S (2019). Upwelling as the major source of nitrogen for shallow and deep reef-building corals across an oceanic atoll system. *Functional Ecology* 1-15. DOI: 10.1111/1365-2435.13314

Contributor	Statement of Contribution
Veronica Z. Radice (Candidate)	Conception and design (70%) Analysis and Interpretation (75%) Drafting and production (70%)
Sophie G. Dove	Conception and design (10%) Analysis and Interpretation (10%) Drafting and production (15%)
Michael D. Fox	Analysis and Interpretation (5%)
Brian Fry	Conception and design (10%) Analysis and Interpretation (10%) Drafting and production (15%)
Ove Hoegh-Guldberg	Conception and design (10%) Drafting and production (5%)

Refereed conference abstracts:

Radice VZ, Fry B, Hoegh-Guldberg O, Fox MD, and Dove S (2018). Shifts in trophic strategies of reef-building corals following seawater temperature anomaly. **Oral Presentation**. 11th International Conference on the Applications of Stable Isotope Techniques to Ecological Studies.

Radice VZ, Hoegh-Guldberg O, Fry B, Fox MD, and Dove S (2018). Stable isotopes indicate role of upwelling and coral heterotrophic feeding following mass bleaching in remote coral reefs of the Maldives. **Oral Presentation**. Australian Marine Sciences Association Conference.

Radice VZ, Hoegh-Guldberg O, Fry B, and Dove S (2016). Investigating the influence of upwelling on stable isotope compositions of coral from the shallow and deep slope. **Oral Presentation**. 13th International Coral Reef Symposium.

Other publications during candidature

Peer-reviewed manuscript:

Fox MD, Williams GJ, Johnson MD, **Radice VZ**, Zgliczynski BJ, Kelly ELA, Rohwer FL, Sandin SA, and JE Smith (2018). Gradients in Primary Production Predict Trophic Strategies of Mixotrophic Corals across Spatial Scales. *Current Biology* 28, 3355–3363. DOI: 10.1016/j.cub.2018.08.057

Refereed conference abstract:

Wepfer PH, Nakajima Y, Sutthacheep M, **Radice VZ**, Richards Z, Ang P, Fujimura A, Sudek M, Reimer J, Chen A, Teraneo TI, Toonen R, Mikehyev A, Economo EP, and S Mitarai (2018). The phylogeography of the reef-building coral genus *Galaxea* across its global distribution. Oral Presentation. 4th Asia-Pacific Coral Reef Symposium.

Contributions by others to the thesis

Sophie Dove, Brian Fry, and Ove Hoegh-Guldberg contributed to the conception and design of the project. Michael Brett, Sophie Dove, Michael Fox, Brian Fry, and Ove Hoegh-Guldberg contributed to the analysis and interpretation of research data. Sophie Dove, Brian Fry, and Ove Hoegh-Guldberg contributed to drafting significant parts of the work or critically revising it. Kristen Brown, Dominic Bryant, Sophie Dove, Craig Heatherington, Kelly Latijnhouwers, and Ove Hoegh-Guldberg contributed to field data collection.

Statement of parts of the thesis submitted to qualify for the award of another degree

No works submitted towards another degree have been included in this thesis.

Research Involving Human or Animal Subjects

No animal or human subjects were involved in this research.

Acknowledgements

An enormous thank you to my advisors – Brian, Sophie, and Ove – and to my committee members Selina Ward and Salit Kark. Thank you to the two thesis examiners who provided valuable feedback for improving this thesis. Thank you Ove and Sophie for the opportunity to join your lab. It was with great excitement that I boarded a plane with a one-way ticket to Australia, the land down under where I knew no one. I have made such a beautiful life here. Thank you for supporting me and giving me the freedom to develop my own research ideas and projects. It was such a unique opportunity to focus my research in the understudied central Indian Ocean. Thank you for your support both within the offices of UQ and also out in the field (although I wish you had seen the reefs of the Maldives before the mass coral bleaching). I have learned a great deal from you both, thank you.

Brian – thank you for opening up my mind to the amazing but often mysterious world of isotopes. I am so thankful that this first introduction to isotopes blossomed into essentially the basis of my entire thesis. From attending the Stable Isotopes in Biosphere Systems workshop, to our cherished Isotope Hour group at Griffith University (I wish we could continue), to having you as an advisor and good friend these past 5 years, it's been (and will continue to be!) an incredible journey learning about isotopes. Thank you for your patience, kindness, and silly jokes. I always enjoy visiting you at Griffith, and despite the complexity of the science you always keep things light and fun, with much encouragement. I really appreciate your enthusiasm for my research although I hope that my coral isotope mysteries didn't cause you to lose too much sleep. Although you're apparently retiring, I hope we can continue to discuss isotopes and research ideas in the years to come.

Mike Brett – I am thankful for our chance meeting during your sabbatical at Griffith. Just as I was learning about new trophic markers, it was great to learn first hand about fatty acids from you. Thank you for the great discussions about coral fatty acids – I'm happy that you share my excitement in investigating the complexities of coral trophic strategies, and I hope this research is a starting point for future collaborative work. Thank you for the opportunity to learn about fatty acids and to visit your lab at the University of Washington.

Thank you to the XL Catlin Seaview Survey team and the team at the Global Change Institute, especially Pete Dalton, Susie Green, Dave Harris, Rachael Hazell, Sara Naylor, Shari Stepanoff, and Abbie Taylor. Thank you to Mike Phillips and Craig Heatherington for supporting my diving and boating activities at UQ, and for the extensive dive training during the ADAS course. Thank you to MBRS for organizing the boat handling course.

Thank you to everyone involved in the Maldives field expeditions, from the logistics to permits to diving to working with smelly corals to mental support. Thank you for not only making this research possible (this entire thesis!), but also in a safe manner. Thank you to the Maldives Ministry of Fisheries and Agriculture, especially Adam Ziyad and Ahmed Shifaz. Thank you to the Maldives Marine Research Centre, especially Shiham Adam and Nizam Ibrahim. Thank you to the Maldives Environmental Protection Agency, especially Hussain Ibrahim. Thank you to the IUCN Maldives, especially Gabriel Grimsditch and Ahmed Basheer. Thank you to Dominic Bryant, Alexander Bryant, and Mary Bryant for your invaluable help with organizing our research activities in the Maldives. It's always such a relief when things run so smoothly! Thank you to the crews of the M/V Emperor Voyage, especially Niyam and Mario, and the M/V Emperor Atoll, especially Issie and Tuna, you had a critical role in the success and safety of the research expeditions. A huge thank you to my dive buddies Craig Heatherington and Kelly Latijnhouwers (2015 expedition) and Kristen, Sophie, Susie, Dom, Ove, and Chris (2017 expedition), and for your surface support in processing all of the coral and seawater samples. Thank you to Pete for being an absolute legend across all of the Seaview Survey trips – thanks for always having my back, and for your guidance, patience, and support. Also, thanks Pete for leading by example and for the important lessons at sea. Thank you to Adam Andrews for his generous help in videotaping and photographing coral reefs in the Maldives to help identify potential focal species for this thesis. I also thank Stina Boman and Sébastien Pauner from Casa Mia Mathiveri for their assistance in retrieving temperature loggers on the reef. Thank you to the Maldives Meteorological Society for providing wind data from Hulhule.

Thank you to my awesome collaborators and friends. Mike Fox, I'm thankful that we met at ICRS back in 2016! As we have so many common ideas and unanswered questions, I hope our current work is a jumping off point for future research projects. Patricia Wepfer, although we have yet to meet in person, I feel like we already know each other. It has been great chatting over Skype and discussing various ideas about *Galaxea*. I hope we will have the opportunity to meet and expand on this project in the future. Thank you to Sean J. Yeung and Alex Lowe for your lab support during my visit to the University of Washington.

Thank you to all of the members of the Coral Reef Ecosystems Lab for their support throughout my Ph.D. A special thank you to Hayley, Aaron, Annamieke, and Gio for your support both in Brisbane and at Heron Island. Thank you to Nathan Caromel for all of his support during my field work at HIRS, I could not have done it without you.

To my Ph.D. crew – Kristen, Michelle, Anj, Ale, Dom, Francisco, Rene, Matt, Robert, Tania, and Catherine. Thank you for being the best lab mates and friends. We share so many special memories from Brisbane and far flung field work locations, from work and from our down time enjoying life (and many beers). A shout out to Dom – it's been awesome working alongside each other across the central Indian Ocean, thanks for your continued support and encouragement. Thank you Michelle for being not only a best friend but the dream office mate – thanks for brightening each day in the office, for our chats over tea and chocolate, and for your constant support throughout each step of the way. Thank you Kristen for being the best of friends and sharing this Ph.D. journey with me, in all corners of the world. We have such awesome memories from all of the trips, but also from Brisbane – thanks to you and Tysen for all the weekend fun.

Thank you to the post-docs – Pim, Carolina, Doro, Andreas, Ben, Beto, Emma, Julie, Manuel, Maria, Steven Robbins, and Uli. A special thank you to Pim for his friendship and guidance – I hope we will soon be able to work on a project together.

Thank you to all of those who have inspired, encouraged, and mentored me as I began my scientific research journey – Erik Cordes, Danielle DeLeo, James Dutko, Blake Hill, Yvette Langdon, Jifen Li, Mary Mullins, Andrea Quattrini. Thank you for inspiring a young, eager scientist.

Thank you to Rich McGarvey, Beth and Tom McKenna, Sal, and Bill Lamoreaux for introducing me to the underwater world of Dutch Springs. However murky and cold it may have been, those early diving experiences were pivotal in my dive training. Thank you for your expertise, your high standards, your love for teaching others to dive, and of course, your friendship.

To my dearest Kirsten, Brock, and Penny – thank you for welcoming me into your home with open arms. I am so grateful for your constant support, especially everything you did for me during my visit to UW. It was basically my dream life living with you guys, we just needed Terry to join us. Kirsten, thank you for your unwavering support, love, and constant cheer from across the Pacific.

To my dear friends scattered across the world, near and far – Jamie, Pauline, Charlotte, Elise, Rhian, Tino, Kene, Maddie, Margaux, Meghan, Natasha. Thank you for your friendship and support throughout this journey. To Ed and Jerri Weiss, thank you for your love and support over the years. To my French class and Benoît at the Alliance Française Brisbane – thank you for your great

company, laughs, and the welcome distraction from my thesis. I'm happy to be finally reviving my French.

To my wonderful family – thank you to all of you for your support and encouragement over the years. Although it has been tough being so far from home, I know we are always thinking of each other. I love and miss you all so very much. Thank you to my extended Poole family – I am thankful to share the experience of enjoying the reefs of PNG!

Thank you to my family for the inspiration to pursue scientific research. To Babushka Valya and Dedushka Oleg – I wish I could tell you about my research, and have chats about isotopes (who could've guessed I'd be working with isotopic data after my grandfather worked with isotopes in the 1970s!). Thank you to all of the scientists who came before me, including my great-grandmother Zoya, with whom I share a love for the ocean (and physiology!).

Thank you Anton for your love and support. It's been tough being so far apart, especially with both of us having been enrolled in graduate programs. Here's to more reunions in cool places – wherever we may next find ourselves!

Thank you Mama and Papa for your unwavering support. Thank you for showing me the wonders of the natural world, and for giving me such a broad exposure not only to science but to everything including languages, art, history, and sports. Ultimately it was the early excitement in all of the above, and especially nature and science, that inspired me to pursue research. Despite being on opposite sides of the world, quite literally, you are my biggest supporters. I appreciate all of your encouragement, advice, and letters, and I'm thankful for our reunions in various parts of the world.

Terry – I would not be where I am today or the person who I am today without you. Thank you for your constant support day in and day out. Thank you for your creativity and for showing me how there is always a way. Thank you for your genuine enthusiasm for my research, and for helping me work out ideas at every step of the way. Thank you for using all of your amazing skills to help me build such a wide range of equipment for my field work. Thank you for listening about isotopes and mixing models, corals and symbionts, monsoon seasons and seawater (and making fun silly songs!). Thank you for teaching me so many new things and for working through some data with me. Most importantly, thank you for sharing your love for the ocean with me. I love being out on or in the water together, and I hope for many, many more days out on the blue with you.

Financial support

This research was funded by the XL Catlin Seaview Survey, Australian Research Council (ARC) Centre of Excellence for Coral Reef Studies CE140100020 (SD and OHG), the ARC Linkage LP110200874 (SD and OHG), and the ARC Laureate FL120100066 (OHG). It was also supported by the University of Queensland Research Training Tuition Fee Offset, the XL Catlin Ocean Scholar Scholarship, and the University of Washington Dale A. Carlson Endowed Faculty Support Fund. Multiple awards supported conference attendance, including a University of Queensland School of Biological Sciences Graduate Student Conference Travel Award, an ARC Centre of Excellence for Coral Reef Studies Conference Support Award, and an Australian Coral Reef Society Conference Student Travel Award.

Keywords

Climate change, deep coral reef, fatty acid trophic marker, heterotrophy trophic strategy, Indian Ocean, Island Mass Effect, isotope ecology, Maldives, particulate organic matter, upwelling

Australian and New Zealand Standard Research Classifications (ANZSRC)

ANZSRC code: 060203, Ecological Physiology, 50%

ANZSRC code: 040203, Isotope Geochemistry, 30%

ANZSRC code: 050101, Ecological Impacts of Climate Change, 20%

Fields of Research (FoR) Classification

FoR code: 0602, Ecology, 50%

FoR code: 0402, Geochemistry, 30%

FoR code: 0501, Ecological applications, 20%

Dedications

This thesis is dedicated to all scientists of the past, present, and future. I am grateful to be a part of a community of people that continually wonder about and investigate the mysteries of the natural world. Thank you for sharing your knowledge, and continuing to build our understanding of this beautiful blue planet.

This thesis is dedicated to all of my family. A special dedication to all of the scientists in my family, from whom I have derived great inspiration.

I dedicate this thesis to Mama and Papa, for helping me find the sea.

The sea, once it casts its spell, holds one in its net of wonder forever.

~ Jacques-Yves Cousteau

Table of Contents

List of Figures & Tables

from the second part of the survey (8-16 April 2015). Data are shown from both shallow and deep reefs because reef depth did not affect POM isotopic ratios.

Figure 2.4. Coral host carbon ($\delta^{13}C$) and nitrogen ($\delta^{15}N$) isotope ratios by coral species, reef depth (shallow versus deep), and reef exposure (oceanic versus Inner Sea). The three species of reef-building corals (*Galaxea fascicularis*- black, *Pachyseris speciosa*- red, *Pocillopora verrucosa*- blue) were collected from shallow (10 m) and deep (30 m) reefs in the central Maldives. Coral host $\delta^{13}C$ and $\delta^{15}N$ values (mean ± SE) are grouped by oceanic reef exposure (a and b, respectively) and by Inner Sea reef exposure (c and d, respectively).

Figure 2.5. The effect of coral host species, reef depth, and reef exposure on symbiont carbon ($\delta^{13}C$) and nitrogen ($\delta^{15}N$) isotope ratios. Symbionts were isolated from three species of reef-building corals (*Galaxea fascicularis*- black, *Pachyseris speciosa*- red, *Pocillopora verrucosa*- blue) collected from shallow (10 m) and deep (30 m) reefs in the central Maldives. Symbiont $\delta^{13}C$ and $\delta^{15}N$ values (mean ± SE) are grouped by oceanic reef exposure (a and b, respectively) and by Inner Sea reef exposure (c and d, respectively).

Figure 2.6. Isotopic niches of shallow (solid line, △) and deep (dash line, ○) reef-building corals from the central Maldives. Carbon ($\delta^{13}C$) and nitrogen ($\delta^{15}N$) isotope ratios of a) coral hosts *Galaxea fascicularis*, *Pachyseris speciosa*, and *Pocillopora verrucosa* and b) their symbionts are shown with maximum likelihood standard ellipses representing isotopic niches.

Table 2.1. A linear mixed effects model was used to test the variables coral species (*Galaxea fascicularis*, *Pachyseris speciosa*, *Pocillopora verrucosa*), reef depth (shallow or deep), and reef exposure (oceanic or Inner Sea) on coral host and symbiont carbon ($\delta^{13}C$) and nitrogen ($\delta^{15}N$) isotope ratios (DF- degrees of freedom; SE- standard error).

Table S2.1. Life history strategies of the three scleractinian symbiotic coral species in this study (Darling et al. 2012; Madin et al. 2016a, 2016b).

Table S2.2. Summary of reef sites surveyed during a 19-day cruise (inter-monsoon period; 29 March to 16 April 2015) in the central Maldives, as marked in the map (Fig. 2a) created in ArcMap 10.3.1 using the layer *Global Distribution of Coral Reefs* (2010) from the UNEP-WCMC Millennium Coral

Reef Mapping Project (UNEP-WCMC et al. 2010). Yes/No (Y/N) designation indicates whether particulate organic matter (POM) or coral were sampled at a site.

Table S2.3. A linear mixed effects model was used to test the variables reef depth (shallow or deep), reef exposure (oceanic or Inner Sea), and sampling period (Period 1 or Period 2) on the carbon ($\delta^{13}C$) and nitrogen ($\delta^{15}N$) isotope ratios of particulate organic matter sampled from the reef water column.

Table S2.4. Summary of carbon and nitrogen isotope ratios ($\delta^{13}C$ and $\delta^{15}N$; mean ± SD), molar C:N ratio (± SD), isotopic niche size (Bayesian standard ellipse area), and colony abundance (mean number of colonies ± SD, sampled with equal sampling effort from each depth and reef exposure) for three species of corals and their symbionts.

Figure S2.1. Monthly average chlorophyll-*a* concentrations in the central Indian Ocean (mg m^{-3}; 4-km MODIS-Aqua satellite) during the months preceding and following the survey (March-April 2015). The black box outlines the central Maldives atolls that were surveyed.

Figure S2.2. Monthly sums of daily wind direction counts (numbered) for the months preceding and following the survey period (March-April 2015). Wind direction changes according to the monsoon seasons, from the NE (Jan-Mar; NE monsoon) to the SW (Apr-Jun; SW monsoon). Wind data are from site 1/27 (Hulhumale, North Malé; see map in Fig. 2a) obtained from the Maldives Meteorological Service (www.meteorology.gov.mv/).

Figure S2.3. Variability in seawater temperature (5 min interval; March-April 2015) from shallow (10 m) and deep (30 m) reefs at three locations (a, b, and c) on the western oceanic rim of the Maldives archipelago (sites 4, 5, and 6 shown on map in Fig. 4a). d) Average daily seawater temperatures from shallow and deep reefs (average of three sites shown in a, b, and c) with standard error (grey scale shading) and maximum monthly mean (MMM) sea surface temperature (NOAA Coral Reef Watch; Malé, Maldives).

Figure S2.4. Particulate organic matter (POM) and daily wind direction from coral reefs across the central Maldives (numbers along x-axis indicate coral reef site, see map in Fig. 2.2a). a) POM nitrogen isotope ratios ($\delta^{15}N$) from shallow (10 m) and deep (30 m) reefs and b) carbon isotope ratios ($\delta^{13}C$) from shallow and deep reefs shown in chronological order of the survey. The same site, represented by the asterisk (*), was visited at the start and the end of the survey.

Figure S2.5. Isotopic niche sizes of coral hosts represented by Bayesian standard ellipse areas (black circle) of three species of coral (*Galaxea fascicularis*, *Pachyseris speciosa*, *Pocillopora verrucosa*) from shallow (10 m) and deep (30 m) reefs in the Maldives. Posterior distribution credibility intervals (50%, 75%, and 95%) shown in grey scale.

Figure S2.6. Isotopic niche sizes of symbionts represented by Bayesian standard ellipse areas (black circle) of symbionts isolated from three species of coral (*Galaxea fascicularis*, *Pachyseris speciosa*, *Pocillopora verrucosa*) from shallow (10 m) and deep (30 m) reefs in the Maldives. Posterior distribution credibility intervals (50%, 75%, and 95%) shown in grey scale.

Figure 3.1. Seawater temperature from shallow (10 m) and deep (30 m) reefs in the central Maldives. a) Monthly seawater temperature (April 2015 to October 2016) from shallow and deep reefs of three sites. b) Daily sea surface temperature (SST; NOAA Coral Reef Watch Virtual Station) and shallow reef and deep reef seawater temperature (average of three sites shown in 2a) between January and September 2016. Monthly maximum mean (MMM) of SST and $MMM_{adjusted}$ (adjusted relative to SST) of shallow and deep reefs are shown. Shading indicates the mass coral bleaching event in the Maldives (April through July 2016; Ibrahim et al. 2017).

Table 3.1. Carbon and nitrogen ($\delta^{13}C$ and $\delta^{15}N$) stable isotope ratios and C:N ratios (mean ± SD) of three coral host species and their symbionts collected from shallow (10 m) and deep (30 m) reefs in the year before (2015) and after (2017) the thermal stress event in the Maldives.

Table 3.2. Multi-factorial analysis of variance (ANOVA) tested the effect of sampling year (2015 versus 2017) relative to the 2016 thermal stress event and reef depth (10 m versus 30 m) on the carbon ($\delta^{13}C$) and nitrogen ($\delta^{15}N$) isotope values of three species of coral hosts and their symbionts.

Figure 3.2. Isotopic niches of shallow (10 m: △, solid line ellipse) and deep (30 m: ○, dashed line ellipse) coral hosts a) *Galaxea fascicularis*, b) *Pachyseris speciosa*, and c) *Pocillopora verrucosa* one year before (2015) and eight months after (2017) the thermal stress event in the Maldives. Maximum likelihood standard ellipses were fitted to multivariate isotopic data ($\delta^{15}N$ and $\delta^{13}C$) with variation of individual samples shown.

Figure 3.3. Isotopic niches of shallow (10 m: △, solid line ellipse) and deep (30 m: ○, dashed line ellipse) symbionts of a) *Galaxea fascicularis*, b) *Pachyseris speciosa*, and c) *Pocillopora verrucosa* one year before (2015) and eight months after (2017) the thermal stress event in the Maldives. Maximum likelihood standard ellipses were fitted to multivariate isotopic data ($\delta^{15}N$ and $\delta^{13}C$) with variation of individual samples shown.

Figure 3.4. Isotopic niche sizes of coral hosts and their symbionts from shallow (10 m) and deep (30 m) reefs before ('Pre') and after ('Post') thermal stress event in the Maldives in 2016. Standard ellipse area and Bayesian standard ellipse area (SEA and SEA-B, respectively) of a) *Galaxea fascicularis* coral hosts and b) symbionts, c) *Pachyseris speciosa* coral hosts and d) symbionts, e) *Pocillopora verrucosa* coral hosts and f) symbionts. The SEA (red square) and mode of SEA-B (black circle) are plotted on top of grey scale shading indicating posterior distribution credibility intervals (50%, 75%, and 95%). For a given species/tissue type/depth, a change in isotopic niche size after the thermal stress event is signified with an asterisk (*) in the plots (probability of >90%). Note different scale of y-axis between hosts (left panel) and symbionts (right panel).

Figure 3.5. Comparisons of carbon and nitrogen cycling between coral hosts and their symbionts a) *Galaxea fascicularis*, b) *Pachyseris speciosa*, and c) *Pocillopora verrucosa* before (green) and after (red) the thermal stress event. For example, $\Delta^{13}C$ is the difference between $\delta^{13}C_{Host}$ and $\delta^{13}C_{Symbionts}$ for a given species from shallow (triangle) or deep (circle) reefs.

Table S3.1. Coral reefs surveyed across the central Maldives in 2017. POM was sampled at each site. All sites except those marked with an asterisk (*) were previously surveyed in 2015. Seawater temperature was measured at three sites (‡) between April 2015 and October 2016. Plankton tows (†) were conducted in 2017.

Table S3.2. The visible abundance of sampled coral colonies (mean ± SD) was used to estimate the distribution of coral species across depths (shallow 10 m versus deep 30 m) and reef exposures between sampling years (5 reefs in the Inner Sea and 5 Oceanic reefs surveyed in 2015 and 2017).

Table S3.3. Isotopic niche metrics for three species of coral hosts and their symbionts from shallow (10 m) and deep (30 m) reefs sampled before (2015) and after (2017) the thermal stress event in the Maldives in 2016. Standard ellipse area (SEA) and small sample size corrected standard ellipse area (SEAc) are shown along with carbon isotope ($\delta^{13}C$) and nitrogen isotope ($\delta^{15}N$) ranges.

Figure S3.1. Inorganic nutrients of seawater collected in the central Maldives. Nitrate (NO_3^-), ammonium (NH_4^+), and phosphate (PO_4^{-3}) concentrations were measured in seawater collected from 10 m, 20-29 m, 30-39 m, and 40-50 m reef depth (boxplot shows the median). Nitrite was undetectable for a majority of the samples. Letters denote statistical difference with mean concentration shown in parentheses.

Figure S3.2. The nitrogen isotope ratios ($\delta^{15}N$) and oxygen isotopic ratios ($\delta^{18}O$) of dissolved nitrate (NO_3^-) in seawater collected from 10 m, 30-39 m, and 40-50 m reef depth in the central Maldives. The $\delta^{15}N$-NO_3^- values and $\delta^{18}O$-NO_3^- values are shown in relation to NO_3^- concentration (a, b), the inverse of the NO_3^- concentration (c, d), and the log of the NO_3^- concentration (e, f).

Figure S3.3. Nitrogen and oxygen isotopic ratios ($\delta^{15}N$ and $\delta^{18}O$, respectively) of dissolved nitrate from the reef water column in the Maldives. Group 1 (dashed line) represents sources of atmospheric nitrate characterized by enriched $\delta^{18}O$ values, while Group 2 (solid line) represents nitrate derived from marine sources. The star symbol indicates the isotopic signature of deep-water nitrate with $\delta^{15}N$ around +5‰ and $\delta^{18}O$ around +3‰.

Figure S3.4. Different regimes of the reef water column are characterized by the isotopic variability of particulate organic matter (POM) collected before and after the 2016 thermal stress event in the Maldives. The concentration of particulate organic nitrogen (PON) is shown in relation to a) POM nitrogen isotope ratios ($\delta^{15}N$) and b) POM carbon isotopes ratios ($\delta^{13}C$); the concentration of particulate organic carbon (POC) is shown in relation to c) POM $\delta^{15}N$ values and d) POM $\delta^{13}C$ values; POM molar C:N ratios are shown in relation to e) POM $\delta^{15}N$ values and f) POM $\delta^{13}C$ values.

Figure S3.5. Total number of colonies sampled in 2015 and 2017 as a proxy for the visible abundance of coral species a) *Galaxea fascicularis*, b) *Pachyseris speciosa*, and c) *Pocillopora verrucosa* across shallow (10 m) to deep (30 m) reef slopes. Sum of colony fragments shown only for reefs that were surveyed both years, with a sampling target of a maximum of nine colonies per species per depth per year from five Inner Sea sites (Bodu Hura, Dhiggaru Falhu, Hulhuvehi, Kandimma Falhu, and Reethi Rah) and five Oceanic reef sites (Dinoluga, Maafushi, Mathiveri, Medhu Faru, and Veyvah; see Table S3.1).

Figure 4.1. Principal component analysis based on the composition of total (30) fatty acids in a) coral hosts *Galaxea fascicularis*, *Pachyseris speciosa*, and *Pocillopora verrucosa* and b) their associated symbionts with 80% concentration ellipses shown.

Figure 4.2. Established fatty acid indices are applied in a novel context as potential indicators of coral trophic strategies (autotrophy versus heterotrophy). The ratio of fatty acids 18:1n-7 to 18:1n-9 shows the relative proportion of photosynthesis-derived versus zooplankton-derived nutrition for *Galaxea fascicularis*, *Pachyseris speciosa*, and *Pocillopora verrucosa* a) coral hosts and b) their associated symbionts. An additional index of photosynthesis- versus animal-derived nutrition considers the input of typically photosynthesis-derived fatty acids (16:1n-7 and 18:1n-7) relative to typically animal-derived fatty acids (18:1n-9, 20:1n-9, and 22:1n-11) for c) coral hosts and d) their associated symbionts. Statistical differences are designated within each boxplot with letters (i.e., A and B).

Figure 4.3. The fatty acid index of the sum of long-chain MUFA (LC-MUFA; ∑20:1 and ∑22:1) was used to evaluate the relative proportion of nutrition derived from copepods for *Galaxea fascicularis*, *Pachyseris speciosa*, and *Pocillopora verrucosa* a) coral hosts and b) their associated symbionts. Statistical differences are designated within each boxplot with letters (i.e., A and B).

Figure 4.4. Linear discriminant analysis (LDA) based on PUFA composition (18:2n-6, 18:3n-3, 18:3n-6, 18:4n-3, 20:4n-6, 20:5n-3, 22:6n-3) was used to estimate the proportional contribution of different sources of PUFA to the coral host PUFA composition of the species a) *Galaxea fascicularis*, b) *Pachyseris speciosa*, and c) *Pocillopora verrucosa* with 95% confidence ellipses.

Table 4.1. Proportional contributions of polyunsaturated fatty acids derived from copepods, diatoms, and host-specific symbionts expressed as the 95% confidence intervals (CI) and means estimated from a bootstrapped linear discriminant analysis. The particulate-derived source includes the external particulate sources of copepods and diatoms.

Table S4.1. Fatty acid composition (mean ± SD of % total fatty acids) of three species of coral hosts and their symbionts from the Maldives (n=10 samples for each species of host or symbiont).

Table S4.2. Classification of different potential sources of polyunsaturated fatty acids (18:2n-6, 18:3n-6, 18:3n-3, 18:4n-3, 18:5n-3, 20:4n-6, 20:5n-3, 22:6n-3) evaluated in the original model of the linear discriminant analysis.

Figure S4.1. Comparison of the proportional difference of thirty fatty acids between coral hosts (red) and symbionts (green) for three species of corals a) *Galaxea fascicularis*, b) *Pachyseris speciosa*, and c) *Pocillopora verrucosa*. Number inside colored circle is the difference between coral host and symbiont fatty acid percentage, with color and x-axis position relative to zero signifying which partner has a greater proportion of a given fatty acid. A blank space is shown if there was zero percent of a given fatty acid. A negative number of host fatty acid percent difference is due to the position (left) in relation to zero on the x-axis.

Figure S4.2. The relationship between symbiont and host fatty acid proportions of fatty acids (a-n), isolated from individual coral colonies of *Galaxea fascicularis* (red), *Pachyseris speciosa* (green), and *Pocillopora verrucosa* (blue).

Figure S4.3. Principal component analysis based on composition of 12 polyunsaturated fatty acids (all PUFA, see Table S4.1) in *Galaxea fascicularis*, *Pachyseris speciosa*, and *Pocillopora verrucosa* a) coral hosts and b) their associated symbionts, with 80% concentration ellipses shown.

Figure S4.4. Proportion of the sum of long-chain MUFA (LC-MUFA) between symbionts and coral host of individual colonies *Galaxea fascicularis* (red), *Pachyseris speciosa* (green), and *Pocillopora verrucosa* (blue).

Figure S4.5. Linear discriminant analysis (LDA) based on the PUFA composition (18:2n-6, 18:3n-3, 18:3n-6, 18:4n-3, 18:5n-3, 20:4n-6, 20:5n-3, 22:6n-3) of coral hosts and potential food sources (original model). Potential sources include copepods, cryptophytes, diatoms, and symbionts specific to each coral host species a) *Galaxea fascicularis*, b) *Pachyseris speciosa*, and c) *Pocillopora verrucosa* (95% confidence level ellipse).

Figure S4.6. Linear discriminant analysis (LDA) based on the polyunsaturated fatty acid composition (18:2n-6, 18:3n-3, 18:3n-6, 18:4n-3, 20:4n-6, 20:5n-3, 22:6n-3) of coral hosts, most likely potential food sources (as per final LDA model), host-associated symbionts, and cultured symbionts. Despite the low sample size of cultured symbiont fatty acid data available in the literature, the cultured symbiont samples group closely together and do not clearly cluster with host-associated symbionts.

Table 5.1. Model A- Carbon isotope mixing model estimates of the relative importance of autotrophy and heterotrophy for three species of reef-building coral. The end member for Autotrophy was derived by adding 1.0‰ to the most autotrophic coral (average $\delta^{13}C$ of deep host *P. speciosa* from 2015, prior to the 2016 thermal stress event), and the Heterotrophy end member is the average $\delta^{13}C$ value of plankton. The $\delta^{13}C$ values and proportions of contributions from Autotrophy and Heterotrophy are shown as average ± standard error, calculated using IsoError. Shallow (2015) and deep (2015 and 2017) populations of *G. fascicularis* were considered separately because of different average $\delta^{13}C$ values between depths.

Table 5.2. Model B- Carbon isotope mixing model estimates of the relative importance of autotrophy and heterotrophy for three species of reef-building coral. The end member for Autotrophy is the average of 20% of the most positive $\delta^{13}C$ values of symbionts, and the Heterotrophy end member is the average $\delta^{13}C$ value of plankton. The $\delta^{13}C$ values and proportions of contributions from Autotrophy and Heterotrophy are shown as average ± standard error, calculated using IsoError. Shallow (2015) and deep (2015 and 2017) populations of *G. fascicularis* were considered separately because of different average $\delta^{13}C$ values between depths.

Table 5.3. Model C- Carbon isotope mixing model estimates of the relative importance of autotrophy and heterotrophy for three species of reef-building coral. The end member for Autotrophy is the average of species-specific symbiont $\delta^{13}C$ values, and the Heterotrophy end member is the average $\delta^{13}C$ value of plankton. The $\delta^{13}C$ values and proportions of contributions from Autotrophy and Heterotrophy are shown as average ± standard error, calculated using IsoError. Shallow (2015) and deep (2015 and 2017) populations of *G. fascicularis* were considered separately because of different average $\delta^{13}C$ values between depths.

Table 5.4. Summary of estimates of Autotrophy and Heterotrophy contribution (average ± SE) calculated by averaging the results from carbon isotope mixing models A, B, and C (see Tables 5.1, 5.2, and 5.3).

List of Abbreviations used in the thesis

ANOVA: analysis of variance

Chl *a*: chlorophyll *a*

CO_2: carbon dioxide

DIC: dissolved inorganic carbon

DIN: dissolved inorganic nitrogen

DHW: degree heating weeks

LC-MUFA: long chain monounsaturated fatty acid

MMM: maximum monthly mean

NOAA: National Oceanic and Atmospheric Administration

PAR: photosynthetic active radiation

PCA: principal component analysis

PERMANOVA: permutational multivariate analysis of variance

POC: particulate organic carbon

POM: particulate organic matter

PON: particulate organic nitrogen

PUFA: polyunsaturated fatty acid

SAFA: saturated fatty acid

SD: standard deviation

SE: standard error

SST: sea surface temperature

$\delta^{13}C$: carbon stable isotope ratio

$\delta^{15}N$: nitrogen stable isotope ratio

$\delta^{18}O$: oxygen stable isotope ratio

Chapter 1:

General Introduction

1.1 Coral reefs under climate change

The study of the complex interaction between organisms, ecosystems, and the environment is central to understanding changes that are occurring at both local and global scales (Hoegh-Guldberg and Bruno 2010). Interest in studying trophic interactions has increased as evidence of rapid global climate change has continued to build in both terrestrial and aquatic environments (Harrington et al. 1999). However, it is a challenge to understand how climate change impacts marine trophic ecology while at the same time building the necessary insights for charting a course of change in which the most damaging aspects of issues such as ocean warming and ocean acidification are minimized (Winder and Schindler 2004; Hoegh-Guldberg et al. 2007).

A multitude of human-derived pressures challenge the structure and function of marine ecosystems at a global scale (Halpern et al. 2008; Hoegh-Guldberg and Bruno 2010). Despite projections that go back decades (Hoegh-Guldberg 1999), coral reefs continue to face the effects of climate change and many reef ecosystems as a whole have already shifted into different states (Hoegh-Guldberg et al. 2007; Hughes et al. 2017). Besides local pressures such as eutrophication and overfishing, encompassing climate change affects reefs worldwide at an ever-alarming rate (Carpenter et al. 2008). Due to human emissions of carbon dioxide building in the Earth's atmosphere, the frequency and duration of elevated seawater temperatures are increasing (Veron et al. 2009). Thermal stress destabilizes the symbiosis between corals and their dinoflagellate endosymbionts (herein 'symbionts'). During 'coral bleaching' there is a breakdown in the symbiosis between the coral host and its symbionts, which causes the (generally white) coral skeleton to become visible through the translucent host tissue (Hoegh-Guldberg 1999; Weis 2008).

The central focus of this thesis is understanding the trophic ecology of tropical coral reef ecosystems. Tropical coral reef ecosystems typically occupy low-nutrient 'oligotrophic' ocean waters and are renowned for their ability to build large limestone reef systems that support a vast array of other organisms (Darwin 1842). It is critical to understand how the consequences of a changing climate are affecting the ecology of coral reefs, which are in rapid decline (Walther et al. 2002). This thesis focuses on how the trophic strategies of corals respond to the environmental conditions in an oceanic atoll system in the central Indian Ocean.

1.2 Coral trophic strategies across environmental gradients

Both tropical and cold-water coral reefs are remarkable for their persistence in time and space (Hoegh-Guldberg et al. 2017), with their dependence on a number of key environmental variables ultimately determining their distribution and abundance (Kleypas et al. 1999). Across the slope between shallow and deep reefs, gradients of abiotic factors (e.g., light and temperature) and dissolved nutrient and particulate resource availability create different ecological niches (Leichter et al. 1998; Lesser et al. 2009). Coral trophic strategies respond to these environmental factors, and ultimately serve a key role in defining the niche of corals (Porter 1976; Knowlton and Jackson 1994). Life history and trophic strategies are key factors in determining population structure over depth (Muscatine et al. 1989a; Vermeij and Bak 2003). Reef-building symbiotic corals can depend on both 1) autotrophy- obtain nutrients from their photosynthetic symbionts and 2) heterotrophy- coral host feeding on particulate organic matter from the reef water column (Goreau et al. 1971). Goreau et al. (1971) considered corals "voracious carnivores." Indeed, corals can feed on a variety of particulate resources including zooplankton, phytoplankton, bacteria, flagellates, and detritus with heterotrophic feeding accounting for a major source of carbon and nitrogen for coral metabolism and calcification (Sorokin 1973; Houlbrèque and Ferrier-Pagès 2009; Leal et al. 2014). Under anomalously warm ocean conditions that cause coral bleaching, some coral species utilize heterotrophy to meet the demands of daily energy requirements (Grottoli et al. 2006). Carbon derived from symbiont autotrophy is generally used for short-term metabolic needs (e.g., respiration) in contrast to carbon derived from host heterotrophy (e.g., proteins, membranes; Bachar et al. 2007; Hughes et al. 2010). Autotrophically-derived carbon consists of both a fast turnover pool as well as carbon that is used more slowly, with dissolved inorganic carbon (DIC) for photosynthesis obtained primarily from seawater rather than host-respired DIC (Furla et al. 2000; Tanaka et al. 2018).

Carbon sources derived from autotrophy versus heterotrophy have important implications for coral recovery from thermal stress events, with carbon derived from heterotrophy being essential (Baumann et al. 2014). Coral species respond differently to thermal stress events, in part due to their ability to increase heterotrophic feeding (Grottoli et al. 2006). The availability of particulate organic matter, often affected by local oceanographic processes, can support some corals to increase heterotrophy (Fox et al. 2018). Increased food availability in deep reefs (e.g., 30 m) can support higher growth rates of coral relative to shallower reefs (Leichter et al. 1998). However, species-specific dependence on heterotrophy and particulate-rich reef waters can uncouple trophic zonation over depth (Leichter and Genovese 2006; Alamaru et al. 2009; Williams et al. 2018). Because heterotrophic feeding is typically considered facultative, species-specific patterns are evident over

small changes in depth (Palardy et al. 2005). For example, spatial variation in the deep water delivery of nutrients and particulate resources can structure coral trophic strategies across regions and over depth within a single reef system (Fox et al. 2018; Williams et al. 2018).

In tropical coral reefs, depth-related environmental variables including downwelling irradiance, temperature, and nutrients drive the distribution and abundance of coral community structure over depth (Leichter and Genovese 2006; Frade et al. 2008b; Bongaerts et al. 2013). Surface irradiance, measured by photosynthetically active radiation (PAR), is reduced greatly by approximately 10-fold at 30 m depth, with PAR nearing ~1% around 100 m depth depending on the site's water clarity (Fricke and Meischner 1985; Fricke et al. 1987; Kahng et al. 2012). Irradiance is also affected by water column turbidity, which can have implications for niche boundaries of coral species (Anthony and Connolly 2004). In some species, the crystal structure of the skeletons of reef-building corals can help increase light absorption by symbionts (Enríquez et al. 2005; Kahng et al. 2012). As light decreases, symbiont photobiology can adjust to increase light capture (Falkowski and Dubinsky 1981; Dubinsky et al. 1984; Muscatine et al. 1984) and/or symbiont clades (family Symbiodiniaceae) can change over depth (Rowan and Knowlton 1995; Bongaerts et al. 2013, 2015). Although symbiont zonation is prevalent in some species across high-light shallow reefs down to lower-light mesophotic depths (Bongaerts et al. 2015), species-specific traits of the coral host are equally important in determining the photobiological response of the holobiont (Frade et al. 2008a) and symbiont zonation is not always apparent even over large depth gradients of 0-60 m depth (Cooper et al. 2011). Increased chlorophyll concentrations (per area) in corals from deep (>20 m) reefs indicate either enhanced photosynthetic efficiency and/or increased heterotrophic feeding (Frade et al. 2008a; Lesser et al. 2010; Ziegler et al. 2014).

1.3 Oceanography of the Maldives archipelago

Oceanographic processes serve an important role in shaping tropical coral reefs. Various aspects of chemical, biological, and physical oceanography affect coral reefs at local and regional scales, including wave energy affecting reef structure and processes such as upwelling bringing deep-water nutrients to surface waters (Lowe and Falter 2015). Elevated concentrations of inorganic nutrients stimulate phytoplankton blooms, which serve as a critical food source for benthic and pelagic organisms in typically low-nutrient coral reef ecosystems in the tropics. The interaction between island/atoll topography and water circulation that causes enhanced phytoplankton productivity is referred to as the Island Mass Effect (Doty and Oguri 1956). Although the Island Mass Effect is

Table 1.1. Summary of wind direction measured in in the central Maldives (Hulhule, North Malé) for the northeast (NE) and southwest (SW) monsoon seasons (January 2005 to December 2017). Data are shown as counts of daily wind direction using N, S, E, W cardinal direction convention. To visualize seasonal wind patterns, a heat map is applied to show frequency of daily wind directions (red color shows 0 counts of a wind direction while green represents the highest frequency). Daily wind data were obtained from the Maldives Meteorological Service (2018).

Season	Year	N	NNE	NE	ENE	E	ESE	SE	SSE	S	SSW	SW	WSW	W	WNW	NW	NNW
NE	2005	8	12	4	28	39	1	0	0	0	0	0	14	18	11	14	2
NE	2006	10	9	10	39	39	6	3	1	1	3	1	5	7	6	6	3
NE	2007	13	2	12	47	37	2	0	0	1	2	0	1	13	9	2	8
NE	2008	14	4	16	24	24	4	1	0	2	2	0	7	18	14	6	12
NE	2009	10	7	5	43	38	1	2	0	0	2	1	13	10	7	6	6
NE	2010	10	3	8	36	26	2	0	0	0	1	4	9	22	15	8	6
NE	2011	28	4	12	27	24	2	2	0	0	3	5	5	6	18	6	8
NE	2012	11	16	18	33	29	3	1	0	1	2	1	5	9	9	5	4
NE	2013	9	9	6	47	25	4	3	1	1	3	3	4	13	7	3	9
NE	2014	6	4	10	49	42	1	0	0	3	0	2	4	10	5	2	3
NE	2015	8	5	21	45	26	4	2	1	2	0	0	4	16	2	8	4
NE	2016	12	11	20	38	18	3	0	0	2	1	2	6	16	6	2	5
NE	2017	15	7	10	37	16	1	1	1	0	0	1	10	16	8	7	9
SW	2005	0	0	0	0	0	0	0	1	1	2	9	26	62	28	11	3
SW	2006	2	1	0	0	0	1	1	3	14	15	6	25	53	17	11	4
SW	2007	1	0	2	0	0	0	1	3	6	13	12	34	55	16	7	0
SW	2008	7	0	1	0	0	0	0	3	5	17	9	29	43	30	2	6

SW	2009	0	0	0	0	0	0	1	0	5	7	11	56	56	16	0	1
SW	2010	2	0	0	0	1	0	1	0	2	7	13	37	58	19	7	5
SW	2011	0	0	0	0	2	0	0	1	10	14	9	31	50	26	5	3
SW	2012	1	0	0	1	1	1	3	4	4	4	9	26	56	31	10	0
SW	2013	0	0	0	0	0	0	1	3	8	5	9	50	51	12	10	3
SW	2014	0	0	0	0	0	0	0	1	0	5	5	60	49	27	3	1
SW	2015	2	0	0	0	1	0	0	0	10	5	17	40	62	11	1	0
SW	2016	0	0	1	0	0	0	1	0	0	0	0	23	91	32	5	0
SW	2017	0	0	0	0	0	0	0	1	1	4	13	47	49	21	11	4

prominent across the Pacific Ocean (Gove et al. 2016), its influence on coral reef atolls/islands in the central Indian Ocean remains to be characterized (Sasamal 2006).

The archipelago of the Republic of Maldives is situated along the north-south Laccadive-Chagos ridge in the central Indian Ocean (7°N-0°S, 72-74°E). The oceanic ridges of the atoll system drop off to >2,000 m depth while the atolls of the central Maldives surround a shallower (~550 m) Inner Sea (Betzler et al. 2013). Under the influence of the South Asian Monsoon, the monsoonal climate consists of the southwest monsoon *halhangu* (~May to September), the northeast monsoon *iruvai* (~November to February/March), and relatively short inter-monsoon periods in the spring (~March/April) and fall (~October) during which the wind speed decreases and changes direction (Table 1.1). The seasonally reversing monsoon winds and steep topography of the atoll system generate deep-water upwelling in this region, bringing nutrient-rich waters to surface waters (Preu and Engelbrecht 1991). With upwelling occurring the majority of the year, marine primary productivity associated with the monsoon seasons drives the shifting distribution of chlorophyll (Betzler et al., 2009; Kumar, Prakash, Ravichandran, & Narayana, 2016). There are high concentrations of surface chlorophyll during the monsoon seasons while chlorophyll concentrations are reduced during the brief inter-monsoon transition periods (de Vos et al. 2014). The strength of the monsoon winds thus affects the currents and the primary productivity in the region (Owen et al. 2011). Remote sensing satellites show chlorophyll plumes on the western sides of the atolls during the northeast monsoon season, with chlorophyll plumes recorded as far away as 400-500 kilometers west of the Maldives (Sasamal 2006). Primary productivity peaks at the end of the southwest monsoon season, with satellite maps showing large-scale flow of high chlorophyll concentrations to the east (Strutton et al. 2015). The seasonal shifts in primary productivity affect the distribution of marine megafauna including manta rays and blue whales in the Maldives (Anderson et al. 2011, 2012). However, it is unknown how primary productivity affects the trophic strategies of benthic organisms such as reef-building corals.

1.4 Climate-driven thermal stress and mass coral bleaching

Since the first documented occurrence in the early 1980s, the frequency and intensity of mass coral bleaching events has increased due to rising global sea temperature (Hoegh-Guldberg 1999; Hughes et al. 2018a). In the exceptionally warm year of 1998, coral mortality affected almost all coral reefs with some regions such as the reefs of the central Maldives experiencing mortality of more than 90% of shallow (5-10 m) coral reefs (Wilkinson et al. 1999). Coral communities recovered over the decades that followed 1998 although recovery varied across the Maldives with pronounced recovery

in the south (McClanahan 2000; Baker et al. 2008; Lasagna et al. 2010; Pisapia et al. 2016). In line with predictions, mass coral bleaching and mortality has occurred repeatedly across the Indian Ocean (Sheppard 2003). More recently, the unusual and anomalous El Niño associated with ocean warming patterns of 2015-2016 caused severe bleaching of corals worldwide (Hughes et al. 2018a). Across 11 atolls of the north, central, and south Maldives, widespread bleaching (>70%) was observed in shallow (0-13 m depth) reefs (Ibrahim et al. 2017). In the south, coral bleaching resulted in a 75% reduction in coral cover (Perry and Morgan 2017). However, the probability of coral bleaching was lower in deep reefs (59% at 24-30 m depth) compared to shallow reefs (95% at 3-5 m depth) (Muir et al. 2017).

The diverse nature of feeding patterns among reef-building corals underpins potential differences in the strategic response of corals to environmental change. Thermal stress elicits a physiological response in corals that disrupts the symbiosis and therefore symbiont autotrophy. However, some corals have the ability to increase heterotrophy during bleaching events to meet daily metabolic energy needs (Grottoli et al. 2006; Rodrigues and Grottoli 2006), with increased heterotrophic input maintained 11 months after bleaching (Hughes and Grottoli 2013). Understanding the range of heterotrophy for each species helps to evaluate the capacity of a coral to withstand and/or recover from bleaching events of varying intensities and duration (Grottoli et al. 2014).

1.5 The trophic ecology of coral reefs through the lens of isotope geochemistry

Natural abundances of stable isotopes are used to assess the source and abundance of assimilated nutrients (Fry 2006). Isotopes are chemical elements with different mass numbers. Carbon, for example, is principally composed of two stable isotopes: ^{12}C and ^{13}C. The superscript signifies the mass number, in which the number of neutrons varies. Heavier isotopes are generally rarer; the natural abundance of the lighter ^{12}C is 99.985% compared to the heavier ^{13}C isotope, which is present at 0.015%. The difference in the mass of isotopes results in different behaviors in chemical reactions and physical processes. Differences in fractionation – or the loss or retention of one isotope relative to the other – during physical processes creates variations in isotope values. Since lighter isotopes react more readily, the isotope composition changes during fractionation processes such as photosynthesis. This is due to the heavier isotope's lower mobility and higher binding energy. Natural abundances of stable isotopes are expressed using the δ (delta) notation with the isotope ratio expressed relative to a standard, such as the Pee Dee Belemnite for carbon isotopes or atmospheric N_2 for nitrogen isotopes. The δ notation (1) represents the ratio of the relative abundance of the sample (heavy to light isotope ratio, where R is the ratio of ^{13}C :^{12}C isotopes or ^{15}N :^{14}N isotopes) to the

relative abundance of the standard. Stable isotope ratios of tissue samples are measured using an elemental analyzer interfaced to an isotope ratio mass spectrometer.

(1) $\delta^{13}C$ or $\delta^{15}N = [(R_{sample} - R_{standard}) - 1] \times 1000 =$ *value in parts per thousand* (‰)

The $\delta^{13}C$ value of a sample is dependent both on the isotopic discrimination associated with the process(es) involved in the acquisition of carbon (e.g., Rubisco carboxylation) and the $\delta^{13}C$ value of the source carbon (Farquhar et al. 1989; Muscatine et al. 1989b). For example, in high light conditions of shallow water tropical coral reefs, the enzyme Rubisco incorporates all of the available carbon during photosynthesis therefore reducing discrimination against the heavy ^{13}C and resulting in a higher $\delta^{13}C$ for photosynthetically active symbionts (Farquhar et al. 1989). Across increasing reef depth, declines in $\delta^{13}C$ values of coral hosts are typically interpreted as a trophic shift from dependence on symbiont autotrophy to heterotrophically acquired carbon because symbiotic corals at depth often have $\delta^{13}C$ values that approach those of asymbiotic corals (Muscatine et al. 1989b). As discussed previously, particulate organic matter (POM) represent an important potential source for coral heterotrophic feeding. Due to the uptake of dissolved inorganic carbon, larger kinetic fractionation in planktonic photosynthesis results in typical $\delta^{13}C$ values of -19 to -24‰ of POM in the water column (Williams and Gordon 1970; Peterson and Fry 1987). Interestingly, $\delta^{13}C$ values of symbionts also may decrease with depth, which suggests that isotope discrimination associated with Rubisco carboxylation only activates as photosynthetic rates decline with a corresponding increase in the standing stock of CO_2 (Muscatine et al. 1989b). Alternatively, with the decrease in photosynthesis it is possible that mixotrophic endosymbiotic dinoflagellates also shift to a more heterotrophic lifestyle, living off organic carbon transferred from the host especially in nitrogen limited environments (Steen 1986; Dimond and Carrington 2008; Jeong et al. 2012).

Although the $\Delta^{13}C$ value (the difference between $\delta^{13}C_{coral\ host}$ and $\delta^{13}C_{symbiont}$) is often used as a proxy for heterotrophy (Muscatine et al. 1989b; Rodrigues and Grottoli 2006), several mechanisms that affect coral host and/or symbiont $\delta^{13}C$ values would inherently influence the resulting $\Delta^{13}C$ value. First, changes in symbiont photosynthesis (e.g., in low light deep reefs) are not necessarily concomitant with increased heterotrophic feeding (Alamaru et al. 2009). Second, coral $\delta^{13}C$ values reflect internal carbon cycling between the two symbiotic partners and carbon isotope fractionation including kinetic isotope effects related to CO_2 fixation and symbiont genotype (Farquhar et al. 1989; Einbinder et al. 2009; Leal et al. 2015). Indeed, symbiont genotype can affect the contribution of carbon derived from symbiont autotrophy (Starzak et al. 2014; Leal et al. 2015). Further, correlations

between coral tissue $\delta^{13}C$ values and coral lipid $\delta^{13}C$ values have been reported across depth gradients (Alamaru et al. 2009). Lipid assimilation and consumption can affect coral $\delta^{13}C$ values, with lipid catabolism affecting lipid $\delta^{13}C$ values in bleached coral (Grottoli et al. 2004; Grottoli and Rodrigues 2011). However, the proxy of $\Delta^{13}C$ for examining relative heterotrophy is useful when paired with environmental variables that are related to resource availability (e.g., chlorophyll concentrations and light availability) (Fox et al. 2018).

Nitrogen stable isotope ratios ($\delta^{15}N$) are used as tracers of oceanic nitrogen cycling, reflecting differences in nitrogen sources in the ocean. The local oceanography of a region influences the major source of biologically available nitrogen, which represents patterns of oceanic biogeochemical cycling (Sigman et al. 2009b). Major sources of nitrogen, such as that derived from nitrogen fixation or nitrate supplied from the deep ocean, have distinct isotopic signatures. The slight isotopic discrimination during nitrogen fixation causes organics to be slightly depleted (mean $\delta^{15}N$ value of -1 ± 1‰) relative to the $\delta^{15}N$ value of dissolved N_2 (0‰) (Minagawa and Wada 1986; Montoya et al. 2002). In contrast, nitrogen derived from deep-water nitrate has a global signature of +5-6‰ (Sigman et al. 2009a). The relative importance of these distinct nitrogen sources can be estimated by the $\delta^{15}N$ of POM, which in part reflects the primary nitrogen source. Differences in coral $\delta^{15}N$ values across regions and oceanographic settings are driven by global patterns of nitrogen isotopic fractionation during utilization of nitrate (Altabet 2001). Therefore, $\delta^{15}N$ values are useful for distinguishing major sources of marine nitrogen (Montoya 2007).

Coral tissue is generally enriched in $\delta^{15}N$ relative to the symbionts (Muscatine and Kaplan 1994; Alamaru et al. 2009; Lesser et al. 2010), which is expected given the recycling of nitrogen between the symbionts and the coral host (Tanaka et al. 2006). Reef-building corals acquire new nitrogen by feeding on particulates or through the uptake of nitrate, which is first reduced to ammonium and then assimilated via host and symbiont GS/GOGAT (glutamine and glutamate synthase) and host GDH (glutamate dehydrogenase) (Houlbrèque and Ferrier-Pagès 2009; Pernice et al. 2012). Recent studies suggest that ~80% of nitrogen metabolized by the host is recycled to the symbionts, which in turn provide nitrogen to the host through the release of organic matter or symbiont degradation (Tanaka et al. 2018). The amount of nitrogen provided by the host is likely sensitive to host feeding that often coincides with increased symbiont density and/or chlorophyll per symbiont cell (Houlbrèque and Ferrier-Pagès 2009). Coral heterotrophic feeding can affect nitrogen isotope values of both the coral host and symbionts, particularly for coral tissue at low light levels (e.g., <200 µmol photons m^{-2} s^{-1}; Reynaud et al. 2009). Laboratory studies have shown that heterotrophic feeding on plankton causes

both coral host and symbiont $\delta^{15}N$ values to change albeit the direction of change depends on the $\delta^{15}N$ value of the food source (Reynaud et al. 2009; Seemann 2013). Increased feeding would presumably cause an increase in $\delta^{15}N$ values of corals, but this ultimately depends on the $\delta^{15}N$ value of the particulate source being consumed. Decreases in symbiont $\delta^{15}N$ values can be caused by the assimilation of ^{15}N-depleted sources such as ammonium, which can benefit symbionts by increasing their population density (Muscatine et al. 1989a).

1.6 Fatty acid trophic biomarkers

In addition to carbon and nitrogen stable isotopes, other biochemical tracers including certain lipid classes can provide information about trophic ecology (Pethybridge et al. 2018). Specifically, the trophic interactions in marine ecosystems can be traced using fatty acid trophic biomarkers (Budge et al. 2006). Fatty acids, which are comprised of carbon chains with a methyl and carboxyl group, are a group of lipids that are critical for the storage and transport of energy, membrane structure, and gene regulation (Gurr et al. 2002). Fatty acid nomenclature is based on the number of carbon atoms (carbon chain length), the number of double bonds (degree of unsaturation), and the position of the first double bond relative to the methyl end. For example, 18:2n-6 (linoleic acid) has 18 carbon atoms and two unsaturated double bonds of which the first unsaturated bond is in the sixth position from the methyl end. Fatty acid composition is comprised of numerous individual fatty acids markers (e.g., 30 individual fatty acids), which can provide important insights into dietary inputs with fatty acids being widely used as trophic markers within aquatic food web studies (Iverson 2009).

In symbiotic reef-building corals, fatty acids can be derived from the coral host, their symbionts, and/or particulate resources from the water column (Bishop and Kenrick 1980; Al-Moghrabi et al. 1995; Imbs et al. 2014). The majority of coral total lipid includes triacylglycerols and wax esters, both of which are mainly comprised of fatty acids (Harland et al. 1993; Yamashiro et al. 1999). Fatty acid composition has been used to show differences among coral hosts (Latyshev et al. 1991) and among their symbionts (Zhukova and Titlyanov 2003), and thus has been used for coral chemotaxonomy (Imbs et al. 2007). The coral symbiosis has been generally considered as a classic animal versus plant dynamic with the photosynthetic symbionts providing polyunsaturated fatty acids (PUFA) to the coral host (Patton et al. 1977; Papina et al. 2003). However, coral hosts can also transfer PUFA to their symbionts (Imbs et al. 2014) and recent evidence shows that animals, including scleractinian corals, can synthesize PUFA *de novo* (Kabeya et al. 2018).

Figure 1.1. Species of reef-building coral a) *Pachyseris speciosa*, b) *Galaxea fascicularis*, and c) *Pocillopora verrucosa* from reefs of the central Maldives (Photo credit: Veronica Z. Radice).

1.7 Synopsis and thesis outline

This Ph.D. thesis investigates the trophic ecology of reef-building corals across environmental gradients. Three species of reef-building coral with diverse morphologies were chosen, including *Galaxea fascicularis* (encrusting/massive), *Pachyseris speciosa* (plating), and *Pocillopora verrucosa* (branching). These three species are common across the Indo-Pacific region and are common across outer reef slopes of the Maldives (Pichon and Benzoni 2007). *Pachyseris speciosa* (Dana, 1846) has a laminar or plating morphology, and has small polyps distributed among its continuous ridges (Fig. 1.1a; Veron 2000). *Pachyseris* can grow to >1 m in diameter, and often are found along steep slopes, walls, overhangs, and reef crevices that are sheltered from wave action. *Galaxea fascicularis* (Linnaeus, 1767), an encrusting or massive coral, has large polyps up to 10 mm in diameter with large tentacles lining the outer edge of the exsert septa (Fig. 1.1b; Veron 2000). *Pocillopora verrucosa* (Ellis and Solander, 1786) has knobby, short branches with notable bumps, or verrucae, covering the branches (Fig. 1.1c; Veron 2000). All three of these species are broadcast spawners (Madin et al. 2016a, 2016b).

Two research expeditions to the central Maldives were undertaken as part of the XL Catlin Seaview Survey, which explored the state of coral reefs across 22 countries (2012-2018). The first expedition to the Maldives took place in March-April 2015, and the second expedition took place in March-April 2017. Because of the shallow Inner Sea, the atolls of the central Maldives have different fore reef exposure to the local oceanography: oceanic fore reefs of atoll rims face the steep drop offs of the Indian Ocean while Inner Sea fore reefs face the shallower basin (Betzler et al. 2013). Corals were collected from shallow (10 m) and deep (30 m) oceanic and Inner Sea reefs across the central Maldives. This sampling design provided the opportunity to investigate the influence of upwelling on coral trophic ecology over depth in the Maldives.

Chapter 2 investigated the trophic strategies of three species of morphologically diverse reef-building corals across different environments. This study considered how the trophic strategies of reef-building corals may differ between shallow (10 m) and deep (30 m) reef slopes with different exposure (oceanic versus Inner Sea) to upwelling. Carbon and nitrogen natural abundance stable isotopes of the three coral host species (*G. fascicularis*, *P. speciosa*, and *P. verrucosa*) and their symbionts were analyzed, as well as particulate organic matter as a potential food source. The key question of this chapter was: How does the trophic behavior of corals vary in species inhabiting both shallow and deep reefs, and can this variability be explained by available resources across the Maldives archipelago?

Chapter 3 investigated how the thermal stress disturbance may have affected the trophic strategies of the same three species of coral. The ability of coral hosts to increase heterotrophic feeding is expected to be important during oceanic thermal stress events, such as those associated with global climate change. Temperature loggers deployed on shallow and deep reefs in April 2015 recorded seawater temperatures before, during, and after the thermal stress event that caused mass coral bleaching in 2016. Further, important data including particulate organic and inorganic nutrients of the reef water column were collected. Chapter 3 focused on the isotopic niches of the three species of coral hosts (*G. fascicularis*, *P. speciosa*, and *P. verrucosa*) and their associated symbionts and how these compared to isotopic niches from one year before the thermal stress event in the Maldives. The key question of this chapter was: Were there shifts in the trophic niches of corals from 2015 to 2017, and how did these relate to the impact of the thermal stress event of 2016 on the physiology and ecology of reef-building corals.

Chapter 4 further investigated the trophic strategies of the three species of corals and their symbionts using fatty acid trophic biomarkers. As important lipid components, fatty acids provide information about energy usage and storage. For a subset of samples that were analyzed for carbon and nitrogen isotope ratios (Chapter 3), the fatty acid composition of coral hosts (*G. fascicularis*, *P. speciosa*, and *P. verrucosa*) and their associated symbionts were characterized. This chapter investigated the role of coral heterotrophy by using fatty acid trophic biomarkers and examined how coral fatty acid composition related to potential sources of nutrition. The key question of this chapter was: Does coral fatty acid composition provide evidence of species-specific coral trophic strategies?

Chapter 5 encompasses a general discussion and synthesis of the three data chapters. Using the extensive isotopic data set presented in Chapters 2 and 3, several carbon isotope mixing models were considered in the estimation of autotrophy and heterotrophy for the three focal coral species.

Chapter 2:

Upwelling as the major source of nitrogen for shallow and deep reef-building corals across an oceanic atoll system

This chapter was published in Functional Ecology.

Radice VZ, Hoegh-Guldberg O, Fry B, Fox MD, and Dove S (2019). Upwelling as the major source of nitrogen for shallow and deep reef-building corals across an oceanic atoll system. *Functional Ecology*. DOI:10.1111/1365-2435.13314

2.1 Abstract

Oceanographic processes shape coral reefs worldwide by redistributing inorganic nutrients and particulate resources over depth. Deep-water upwelling occurs frequently in coral reef ecosystems but its impact on coral nutrition remains unclear. This study investigated the influence of upwelling on the trophic ecology of three common reef-building corals (*Galaxea fascicularis*, *Pachyseris speciosa*, *Pocillopora verrucosa*) from different reef depths (shallow reef, 10 m, versus deep reef, 30 m) and reef exposures (oceanic rim versus Inner Sea) across >250 km of the Maldives archipelago, Indian Ocean. Carbon and nitrogen stable isotope ratios ($\delta^{13}C$ and $\delta^{15}N$) of coral hosts, their symbionts, and particulate organic matter (POM) were used to characterize coral trophic strategies. Across the Maldives, consistent mean $\delta^{15}N$ values were recorded in hosts (5.5‰) and symbionts (5.2‰) of the three coral species from shallow and deep reefs of the oceanic and Inner Sea reef exposures. Coral hosts, symbionts, and POM from both depths had $\delta^{15}N$ values that were consistent with the isotopic signature of a deep-water nitrate source transported to surface waters via upwelling. In contrast, a wide range of $\delta^{13}C$ values (~10‰) revealed different trophic strategies and isotopic niches among the coral species. Different mean $\delta^{13}C$ values of *G. fascicularis* indicated greater symbiont autotrophy in corals from shallow (-15.5‰) compared to deep reefs (-17.6‰). Conversely, the mean $\delta^{13}C$ values of *P. speciosa* (-15.1‰) and *P. verrucosa* (-17.7‰) were not affected by reef depth. These corals maintained consistent trophic strategies over depth, with *P. speciosa* relying more on autotrophy compared to *P. verrucosa*. Despite different reef exposure to oceanic waters, coral host and POM $\delta^{15}N$ and $\delta^{13}C$ values did not differ between oceanic and Inner Sea reef exposures. Nutritional resources appear to be homogenous in the central Maldives due to atoll-wide water circulation. However, species-specific trophic strategies resulted in diverse patterns of $\delta^{13}C$ values over depth. Because heterotrophic feeding has been linked to coral host survival through coral bleaching events, understanding the trophic ecology of corals within the reef assemblage can provide insight into species resilience under ocean warming conditions. As a member of the typically competitive Pocilloporidae family, the dependence of *P. verrucosa* on heterotrophy may help this species be a future "winner" under sustained ocean warming.

2.2 Introduction

The function of coral reef ecosystems depends on the complex nutrient dynamics of ocean and reef processes (Lowe and Falter 2015), with resource availability across environmental gradients playing an important role in shaping the physiological niches of corals (Anthony and Connolly 2004). Nutrient fluxes in reef ecosystems have important implications for coral community structure and function (Roder et al. 2011; Schmidt et al. 2012). Deep-water upwelling and internal waves generate

fluxes of inorganic nutrients that increase reef-wide primary productivity and the availability of particulate resources, which can be an important factor for the growth of corals, especially in deep reefs (Leichter, Shellenbarger, Genovese, & Wing, 1998; Leichter & Genovese, 2006; Stuhldreier et al., 2015). Variation in nutrient and particulate concentrations can influence the trophic strategies of symbiotic corals, which obtain nutrients (carbon and nitrogen) from their photosynthetic algal endosymbionts (herein 'symbionts'; autotrophy) and from coral host feeding (heterotrophy) on organic resources such as particulate organic matter (POM; Porter 1976). While heterotrophic feeding provides an important input of carbon and nitrogen for corals (Goreau et al. 1971; Houlbrèque and Ferrier-Pagès 2009), feeding rates are species-specific and are influenced by local environmental conditions (Sebens, Vandersall, Savina, & Graham, 1996; Palardy, Grottoli, & Matthews, 2005). For example, spatial variation in the deep water delivery of nutrients and particulate resources can structure coral trophic strategies across regions and over depth within a single reef system (Fox et al. 2018; Williams et al. 2018). However, there is a limited understanding of how upwelling affects the trophic strategies of corals within different reef depths (shallow versus low-light deep reefs) and reef exposures (oceanic rim versus Inner Sea) in an oceanic atoll system.

Stable isotopes are commonly used to study nutrient dynamics in ecology given that isotope ratios (e.g. $\delta^{15}N$ and $\delta^{13}C$) provide insight into the source and relative abundance of assimilated nutrients (Peterson and Fry 1987) and are used to trace sources of carbon and nitrogen in symbiotic corals (reviewed in Maier, Weinbauer, & Pätzold, 2010). There are distinct isotopic signatures of primary sources of new nitrogen such as that derived from nitrogen fixation ($\delta^{15}N$ -2 to 0‰) versus deep-water nitrate ($\delta^{15}N$ +5 to 6‰; Sigman, Altabet, McCorkle, Francois, & Fischer, 2000; Montoya, Carpenter, & Capone, 2002). Because of the slow turnover (>300 days) of nitrogen in coral tissue (Tanaka et al. 2018), diverse $\delta^{15}N$ values of corals reflect regional primary nitrogen sources. For example, nitrogen fixation is an important source of nitrogen in the oligotrophic Red Sea (e.g., low $\delta^{15}N$ values; Kürten et al., 2014) while higher $\delta^{15}N$ values (e.g., >10‰) can result from incomplete nitrate uptake by phytoplankton and/or water-column denitrification (Altabet 2001; Wang et al. 2016). Reef-building corals acquire new nitrogen primarily by feeding on particulates and also through the uptake of dissolved inorganic nitrogen (DIN; Grover et al. 2003; Houlbrèque et al. 2004; Houlbrèque and Ferrier-Pagès 2009). In regard to sources of dissolved nitrogen, DIN can provide up to 75% of the daily coral nitrogen budget compared to dissolved organic nitrogen (DON); at high concentrations, DON sources such as dissolved free amino acids can contribute only up to 11-21% of the daily nitrogen budget (Hoegh-Guldberg and Williamson 1999; Grover et al. 2008). Overall, dissolved organic matter is typically less bioavailable than POM (Lønborg et al. 2018) and is found

in lower concentrations in oceanic seawater than in shallow lagoons (Tanaka et al. 2011). Therefore, our study focuses on POM and DIN as the major potential sources of nitrogen for corals in oceanic reef system (Wyatt et al. 2012). The Maldives archipelago in the Indian Ocean is subject to strong currents (Preu & Engelbrecht, 1991; Owen, Kruijsen, Turner, & Wright, 2011) and is dominated by the input of deep-water nutrients via upwelling while land-derived eutrophication is considered negligible (Jaleel 2013). Dissolved organic nitrogen is not considered a major source of nitrogen because macroalgal cover is generally very low in Maldives reefs and there is no evidence of macroalgal blooms that would create unfavorable conditions for coral growth (Brown et al. 2017). The monsoonal climate controls the spatial variation in resource delivery throughout the year (i.e., west versus east). The east-west shifting phytoplankton blooms affect seasonal manta ray distribution (Anderson et al. 2011), but the extent of the availability and use of upwelling resources by benthic reef-building corals across different reef exposures is unknown.

Corals from turbid reef environments, where photosynthesis may be impeded, have a greater ability to ingest POM compared to conspecifics from less turbid reefs (Anthony, 2000). To acclimate to different light environments, structural modifications by coral hosts and symbionts can modulate the light availability to symbionts (Kaniewska et al. 2011) while symbionts can increase light capture efficiency (Iglesias-Prieto and Trench 1994). Overall, the variation in $\delta^{13}C$ values among individual colonies of a given species is attributed to environmental conditions including light and water flow (Maier et al. 2010; Roder et al. 2010). The principal carbon source for autotrophy (symbiont photosynthesis) is seawater-derived dissolved inorganic carbon (DIC, $\delta^{13}C$~ +1‰) and dissolved CO_2 ($\delta^{13}C$~ -7‰), with host-respired CO_2 directed towards calcification (Furla et al. 2000). The apparent use of distinct DIC pools for calcification and photosynthesis by coral hosts and symbionts imply that a shift towards more negative $\delta^{13}C$ for symbionts is driven by reductions in the rate of photosynthesis (Alamaru et al. 2009). Generally, less negative $\delta^{13}C$ values (e.g., -11‰) of symbionts reflect carbon limitation in shallow reefs (i.e., high rates of photosynthesis maintain the discrimination against ^{13}C) compared to more negative $\delta^{13}C$ of symbionts in deeper reefs where light is limited (Farquhar et al. 1989; Muscatine et al. 1989b). As photosynthesis rates decline in some coral species in deep reefs, increased heterotrophic feeding can result in decreased $\delta^{13}C$ values that approach those of particulate sources such as POM (e.g., -21 to -26‰; Muscatine et al. 1989b; Einbinder et al. 2009; Soares et al. 2015). If population density is maintained across environmental gradients, then a reduction in one mechanism for acquiring energy would be presumably matched by an increase in another strategy. Because an organism's ecological niche is linked with resource availability and feeding strategies, the isotopic niche is used as a proxy for the ecological niche with $\delta^{13}C$ and $\delta^{15}N$ values revealing the

isotopic niche position in δ-space (Newsome et al. 2007). In order to evaluate species-specific trophic strategies and baseline resources, our study considers both $\delta^{13}C$ and $\delta^{15}N$ values that comprise the isotopic niche. A large isotopic niche would indicate the use of a wide variety of resources (more mixotrophic) while a small isotopic niche would indicate a more restricted use of resources.

There is great interest in the effects of upwelling on coral trophic strategies because coral heterotrophic feeding is typically considered facultative with species-specific patterns evident over depth (Palardy et al. 2005). Because the distribution of coral is largely affected by life history traits and resource use (Jackson, 1991), this chapter focuses on three species of coral with diverse life history strategies: the 'competitive' species *Pocillopora verrucosa*, the 'generalist' species *Pachyseris speciosa*, and the 'stress-tolerant' species *Galaxea fascicularis* (Darling et al. 2012; Madin et al. 2016a). This study investigates how trophic strategies of reef-building corals vary across gradients of light and resource availability (reef depth and reef exposure) in the Maldives. The project analyzed $\delta^{13}C$ and $\delta^{15}N$ values of POM (particulate food source) and coral host and symbiont tissue from these three morphologically distinct coral species (*G. fascicularis*, *P. speciosa*, and *P. verrucosa*) that are present between 10 and 30 m depth in the Maldives (Pichon and Benzoni 2007). To determine whether coral and POM $\delta^{15}N$ values reflect different sources of nitrogen across reef depth and reef exposure, corals and POM from reefs of the oceanic rim (facing the Indian Ocean; drop offs to 2000 m) were compared to reefs of the shallower Inner Sea (≤550 m) of the central Maldives (Betzler et al. 2013). Further, the relative coral colony abundance was estimated across reef depths and exposures and remotely sensed measurements of surface chlorophyll-*a* concentrations (chl-*a*) and *in situ* temperature sensors were used to investigate potential differences in species distribution and resource availability associated with upwelling. It was hypothesized that deep reef corals would have $\delta^{15}N$ values close to the isotopic signature of deep-water nitrate (expected for both hosts and symbionts) and more negative $\delta^{13}C$ values indicative of greater heterotrophy reflecting greater access to POM and deep-water nitrate via upwelling. It was expected that corals from exposed oceanic reefs would have $\delta^{15}N$ values that reflect greater access to deep-water nitrate and POM than reefs from the shallower Inner Sea (Sawall et al. 2014). Conversely, it was expected that corals would be more abundant in shallower reefs and have higher $\delta^{13}C$ values consistent with greater reliance on carbon from symbiont photosynthesis.

2.3 Materials and methods

2.3.1 Measurement of environmental variables

Variability in nearshore primary production (as a proxy for upwelling) was characterized in the central Maldives to examine seasonal shifts in primary production associated with the monsoon climate. Climatological means of surface chl-*a* concentrations were used as proxies for primary production in the central Maldives over the long-term (2004-2015) as well as the timeframe of the study in 2015 (Gove et al. 2013; Supplementary Information Methods S2.1). Temperature data were obtained from the oceanic reef environment by deploying loggers (HOBO Pendant, Onset, U.S.A.; 5 min recording interval) in shallow (10 m) and deep (30 m) reefs (31 March to 20 April 2015; sites 4-6) to monitor for cold-water pulses associated with upwelling and quantify patterns of temperature variability over depth. Concurrent deployments of light loggers, Odyssey PAR (Dataflow Systems, New Zealand; 10 s recording interval) and DEFI-L (JFE Advantech Co., Japan; 15 min recording interval; greater depth rating) were used to quantify differences in irradiance in shallow and deep reefs, respectively. Odyssey 2π PAR loggers were calibrated using DEFI-L calibration. The highest astronomical tide recorded in the Maldives (Malé) is 0.64 m (Owen et al. 2011).

2.3.2 Sample collection and processing

In March-April 2015 (spring inter-monsoon), fragments of corals *G. fascicularis*, *P. speciosa*, and *P. verrucosa* were collected by divers from shallow (10 m) and deep (30 m) fore reefs throughout the central Maldives (Fig. 2a, Tables S2.1 and S2.2), rinsed with filtered seawater, and frozen (-20°C shipboard then transferred to -80°C). Equal effort (time investment) was applied to the sampling of corals at each site and depth (target of nine colonies per species per depth at five oceanic reef sites and five Inner Sea reef sites), such that the number of sampled colonies can be used as a proxy for visible colony abundance. To examine the role of POM as a possible source of nutrition, seawater (10 L) was collected from each depth at all sites (except site 5) and filtered through pre-combusted (450°C, 5 h) 0.4 μm nominal pore size glass fiber filters (n=50; Machery-Nagel). Tissue was removed from coral skeletons using a pressurized airbrush with 0.22 μm filtered seawater, with symbionts (n=155) being separated from coral host tissue (n=161) by centrifugation (minimum 4 times each at 3000xg and subsequently resuspended in filtered seawater; Reynaud et al. 2002). Coral host tissue, symbiont tissue, and glass fiber filters were acidified briefly with 1 N HCl to remove any remaining carbonates, rinsed with MilliQ water, and freeze-dried prior to isotopic analysis. There were fewer symbiont samples analyzed due to insufficient dry weight of sample.

2.3.3 Isotopic analysis and isotopic niche estimates

Coral host and symbiont samples were analyzed ($\delta^{13}C$ and $\delta^{15}N$, shown as mean ± SD) with a PDZ Europa ANCA-GSL elemental analyzer and glass fiber filters (POM) were analyzed ($\delta^{13}C$ and $\delta^{15}N$)

with an Elementar Vario EL Cube elemental analyzer (Elementar Analysensysteme GmbH, Hanau, Germany), each interfaced to a PDZ Europa 20-20 isotope ratio mass spectrometer (Sercon Ltd., Cheshire, U.K.), at the University of California Davis, U.S.A. Stable isotope ratios are reported in the delta (δ) notation, which is expressed in per mil (‰):

$\delta^{13}C$ or $\delta^{15}N = [(R_{sample} / R_{standard}) -1] \times 1000$

where R represents the ratio of the heavy to light isotope (i.e. $^{13}C/^{12}C$ or $^{15}N/^{14}N$). A subset of samples (n=40) were measured in duplicate or triplicate and resulted in isotope values typically differing by ≤0.2‰. Repeated measurements of six internal standards (G-7: Peach leaves, G-13: Bovine liver, G-17: USGS-41 Glutamic Acid, G-18: Nylon 5, G-20: Glutamic acid, G-21: Enriched alanine) resulted in precision of ≤0.13‰ for $\delta^{13}C$ and ≤0.15‰ for $\delta^{15}N$. To compare isotopic niche position among coral species (Newsome et al. 2007), maximum likelihood standard ellipses were fitted to $\delta^{13}C$ and $\delta^{15}N$ data. Species-specific coral host and symbiont standard ellipse areas ($‰^2$), representing individual isotopic niche size, were estimated by Bayesian modeling ($2x10^6$ posterior draws with 10^4 burn-in) using the SIBER package in R (Stable Isotope Bayesian Ellipses in R; Jackson et al., 2011; R Core Team, 2017). Credibility intervals of model solutions are presented in probability density distribution plots.

2.3.4 Statistical analysis

A linear mixed effects model was used to examine $\delta^{13}C$ and $\delta^{15}N$ of coral hosts and symbionts in regard to the factors coral host species (*G. fascicularis*, *P. speciosa*, and *P. verrucosa*), reef depth (shallow versus deep), and reef exposure (oceanic rim versus Inner Sea) with indivudal coral colony and site treated as random effects. Because a major change in POM $\delta^{15}N$ values was observed between two consecutive time periods of the survey (Period 1: sites 1-14, 29 March to 8 April 2015 and Period 2: sites 15-27, 8-16 April 2015), the effect of sampling period was considered in the analysis of POM isotopic data. We used a linear mixed effects model, with POM sample (individual glass fiber filter) and site included as random effects, to assess the effect of reef depth (shallow versus deep), reef exposure (oceanic versus Inner Sea), and sampling period (Period 1 versus 2) on POM $\delta^{13}C$ and $\delta^{15}N$ values. The linear mixed effects model was fit using the function 'lme' from the 'nlme' package (Pinheiro, Bates, DebRoy, Sarkar, & R Core Team, 2018). Data met assumptions of normality (QQ-plots and residual plots) and homogeneity of variance (Levene's test). Statistical significance was determined with an α value of 0.05.

2.4 Results

2.4.1 Variability of environmental parameters across sites in the Maldives

Climatological maps of chl-*a* (12-year mean) from the central atolls show seasonal east-west shifts in the concentration of chl-*a* (Fig. 2.1). Increased chl-*a* concentrations occur downwind in the west during the NE monsoon when winds are from the east, whereas plumes develop downwind in the east during the SW monsoon when winds are from the west. At monthly intervals, for example the year (2015) when the study took place, chl-*a* concentrations reflected changes in the monsoon seasons with elevated chl-*a* downwind as a consistent upwelling signal (Figs. 2b-c and S2.1). During the study period, wind direction switched abruptly with the change in monsoon season (Fig. S2.2).

Temperature and light were measured in shallow and deep reefs during the expedition (Fig. S2.3). Temperature records from a 3-week period during the inter-monsoon revealed fluxes of cooler water (minimum 26.68°C) in deep (30 m) but not shallow (10 m) reefs (Fig. S2.3a-c). Over this period, the daily average seawater temperature was 29.77°C and 29.47°C in shallow and deep reefs, respectively. In the third week, daily seawater temperatures increased and exceeded the long-term maximum monthly mean temperature in both shallow and deep reefs but this was then followed by a temperature decline (Fig. S2.3d). Light loggers recorded an average day-time (0600-1800 h) irradiance of 160.43 μmol quanta m^{-2} s^{-1} in shallow reefs and 60.44 μmol quanta m^{-2} s^{-1} in deep reefs. Surface light averaged about 1500 µmol quanta m^{-2} s^{-1}, so light levels in shallow and deep reefs were about 10% and 4%, respectively.

2.4.2 Isotope ratios of particulate organic matter, coral hosts, and symbionts

POM $\delta^{15}N$ and $\delta^{13}C$ values were measured to estimate potential differences in nitrogen and carbon sources between shallow and deep reefs and between oceanic and Inner Sea reefs, with the major available nitrogen source for corals inferred from POM $\delta^{15}N$ values. POM isotope ratios did not differ by reef depth (Table S2.3). POM $\delta^{15}N$ values significantly decreased from 5.3 ± 1.1‰ in Period 1 to -1.2 ± 2.4‰ in Period 2 (Figs. 2.3 and S2.4; Table S2.3). There was also a shift in POM $\delta^{13}C$ values between Period 1 (-25.2 ± 1.0‰) and Period 2 (-23.8 ± 1.0‰) although the change was not significant (Table S2.3). The magnitude of the shift between Period 1 and 2 was smaller for $\delta^{13}C$ (1.4‰) than for $\delta^{15}N$ (6.5‰; Figs. 2.3 and S2.4). There were large changes in POM $\delta^{15}N$ and $\delta^{13}C$ values at the same site sampled at the start and end of the survey (Fig. S2.4). The shift in POM $\delta^{15}N$ and $\delta^{13}C$ values between Period 1 and 2 supports the existence of two different water masses sampled during the survey (Figs. 2.3 and S2.4).

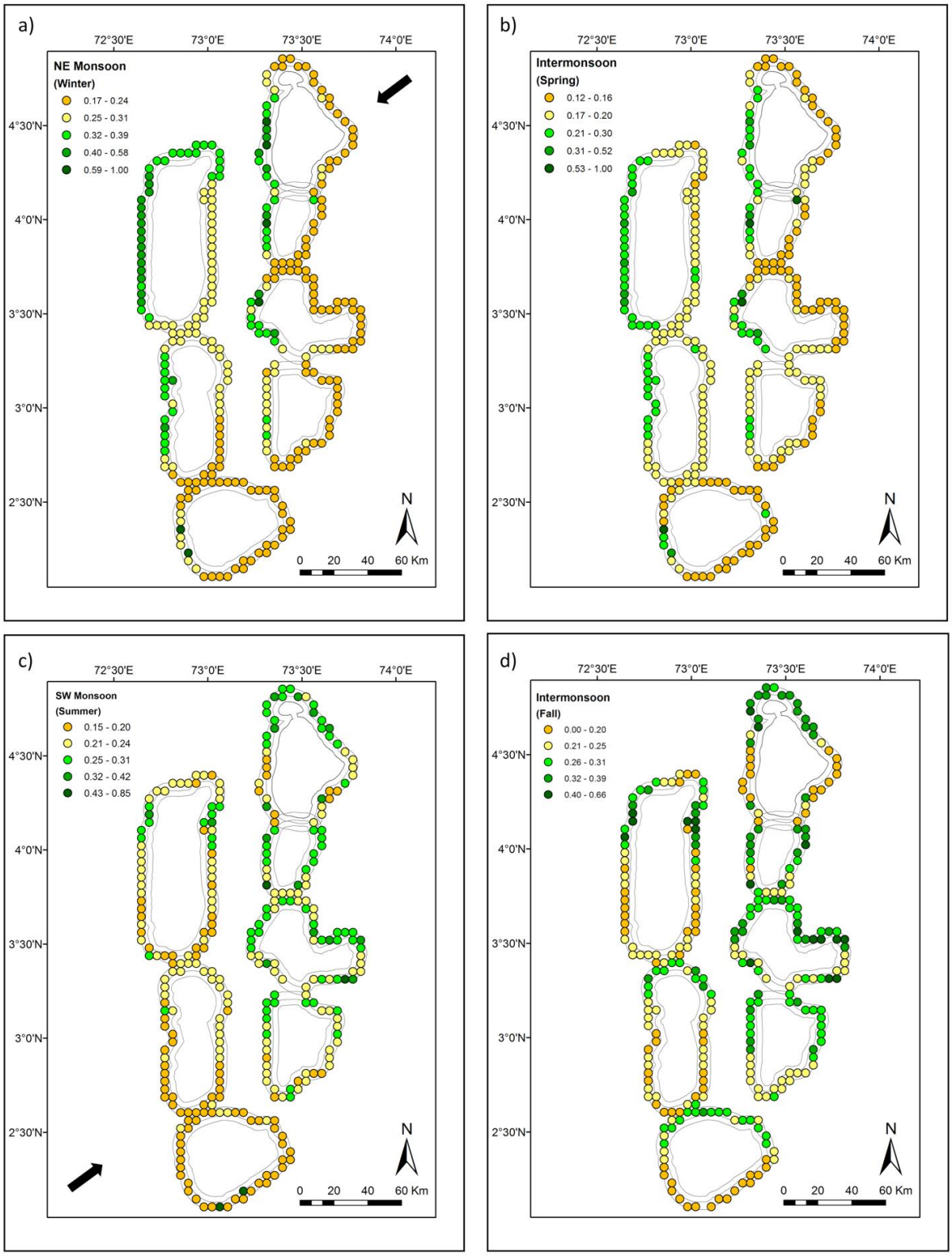

Figure 2.1. Mean surface chlorophyll-*a* concentrations (2004-2015; mg m^{-3}) during the a) northeast (NE; winter) and c) southwest (SW; summer) monsoon seasons and the b) spring and d) fall inter-monsoon periods show shifts in primary productivity in the central Maldives. Maps are shown in chronological order, with arrows indicating monsoon wind direction.

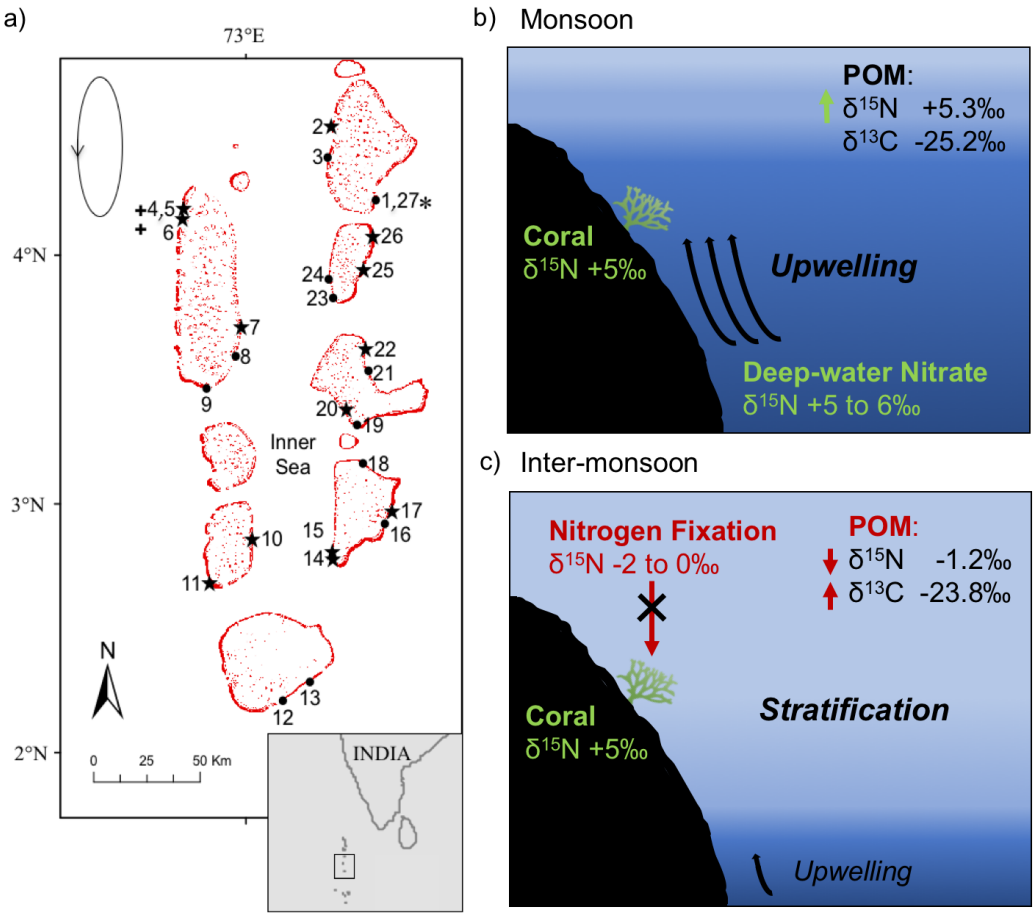

Figure 2.2. a) Map of the central Maldives atolls with sampling sites shown in chronological order of the survey (sampling: ●=particulate organic matter (POM) only, ★=POM and corals; ✚= temperature and light loggers). Site 1/27, which is noted by an asterisk (*), represents the start and end of the survey with the arrow on the oval (top left) showing survey direction. The Maldives climate is characterized by b) monsoon seasons and c) brief inter-monsoon periods, with POM carbon ($\delta^{13}C$) and nitrogen isotope values ($\delta^{15}N$) reflecting the dominant sources available ($\delta^{15}N$ isotopic signatures for nitrogen fixation and deep-water nitrate obtained from the literature cited within the Introduction). POM and coral isotope ratios are results from this study. Nitrogen fixation is not depicted during the b) monsoon season due to the strong upwelling and water column mixing while nitrogen fixation represents a potential nitrogen source during the c) brief inter-monsoon when water stratification occurs. However, a potential nitrogen source derived from nitrogen fixation appears insignificant for overall coral nutrition due to predominant upwelling of deep-water nitrate in this reef system.

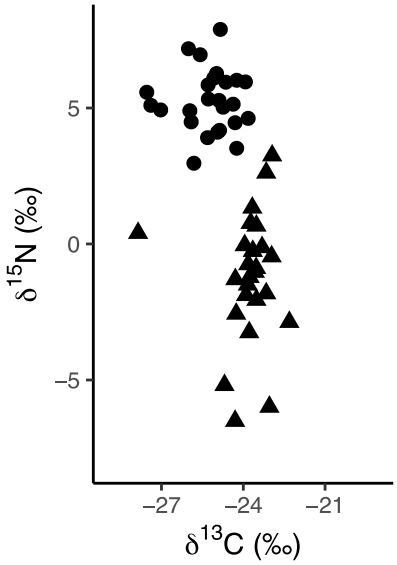

Figure 2.3. Particulate organic matter (POM) from coral reef waters show changes in nitrogen isotope ratios ($\delta^{15}N$) but not carbon isotope ratios ($\delta^{13}C$) during the brief inter-monsoon period in the Maldives. POM samples are grouped by (consecutive) sampling periods: Period 1 (circle) represents POM from the first part of the survey (29 March to 8 April 2015) and Period 2 (triangle) shows POM from the second part of the survey (8-16 April 2015). Data are shown from both shallow and deep reefs because reef depth did not affect POM isotopic ratios.

Despite extensive plumes of chl-*a* moving westward in the months preceding the survey (Fig. S2.1), coral host $\delta^{13}C$ and $\delta^{15}N$ values did not differ between oceanic and Inner Sea reefs (Table 2.1, Fig. 2.4). There was a narrow range of $\delta^{15}N$ values (means of 5.2 to 5.8‰) of all three coral species from both depths (Table S2.4). The significant interaction between coral species and depth explained the variability among coral host $\delta^{13}C$ values (Tables 2.1 and S2.4). Mean $\delta^{13}C$ values of host *G. fascicularis* differed significantly between shallow (-15.5 ± 1.2‰) and deep reefs (-17.6 ± 0.8%), resulting in the widest isotopic range observed among the coral species. Irrespective of depth, host *P. speciosa* had significantly higher mean $\delta^{13}C$ values (shallow -15.2 ± 1.4‰, deep -15.1 ± 1.0‰) than host *P. verrucosa* (shallow -17.4 ± 1.1‰, deep -18.0 ± 0.8‰) and deep host *G. fascicularis* (-17.6 ± 0.8%).

The variation in symbiont $\delta^{13}C$ values was due to the interaction among the factors coral host species, reef depth, and reef exposure (Table 2.1). The interaction was driven by lower $\delta^{13}C$ values of *P. speciosa* symbionts from shallow oceanic reefs (-15.4 ± 1.5‰) compared to shallow Inner Sea reefs (-13.4 ± 2.1‰) and deep oceanic reefs (-13.7 ± 2.0‰) (Fig. 2.5). *Pachyseris speciosa* (shallow -14.0

± 2.1‰, deep 14.1 ± 1.6‰) and *P. verrucosa* (shallow -16.3 ± 1.3‰, deep -17.0 ± 0.9‰) symbionts each had similar mean $\delta^{13}C$ values between depths, reflecting patterns of the coral host. *Galaxea fascicularis* symbiont $\delta^{13}C$ values were significantly lower in deep reefs (-17.2 ± 1.0‰) compared to its symbionts from shallow reefs (-15.0 ± 1.3‰; Table 2.1). Mean $\delta^{15}N$ values of each species' symbionts were also within a narrow range (4.3 to 5.7‰; Table S2.4). Coral species and reef depth had an effect on symbiont $\delta^{15}N$ values, with significantly lower mean $\delta^{15}N$ values of *G. fascicularis* symbionts in shallow reefs (4.3 ± 0.5‰) compared to deep reefs (4.9 ± 0.7‰; Table 2.1), with *G. fascicularis* symbionts from both depths differing from shallow *P. verrucosa* symbionts (5.4 ± 0.6‰) (Table 1). Overall, *G. fascicularis* symbionts (4.6 ± 0.7‰) had lower mean $\delta^{15}N$ values compared to those of *P. speciosa* (5.5 ± 0.6‰). There was a significant effect of reef exposure, which was attributed to the lower $\delta^{15}N$ values of *G. fascicularis* symbionts compared to the symbionts of the other coral species (e.g., Inner Sea *G. fascicularis* 4.8 ± 0.6‰ versus Inner Sea *P. speciosa* 5.7 ± 0.6‰) (Fig. 2.5).

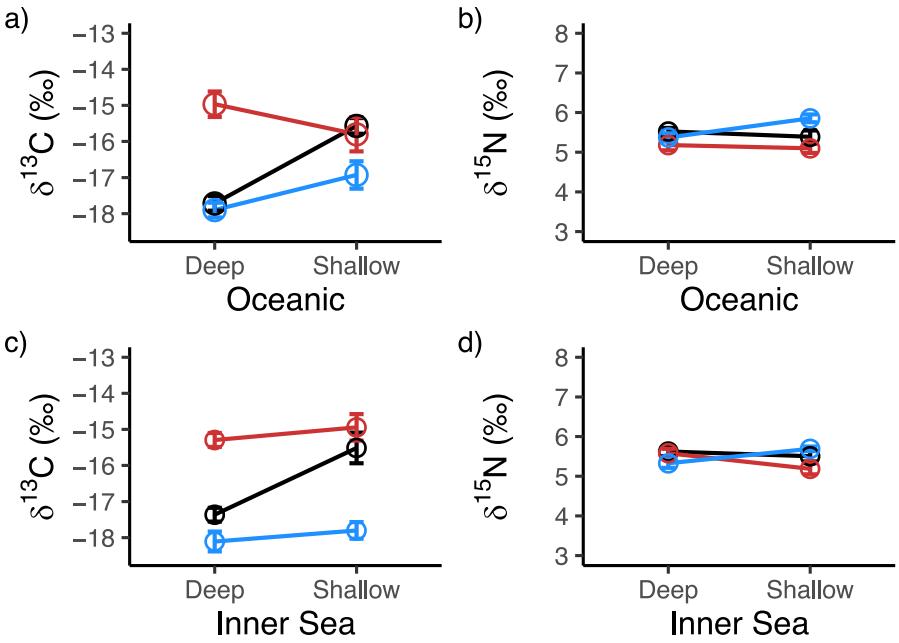

Figure 2.4. Coral host carbon ($\delta^{13}C$) and nitrogen ($\delta^{15}N$) isotope ratios by coral species, reef depth (shallow versus deep), and reef exposure (oceanic versus Inner Sea). The three species of reef-building corals (*Galaxea fascicularis*- black, *Pachyseris speciosa*- red, *Pocillopora verrucosa*- blue) were collected from shallow (10 m) and deep (30 m) reefs in the central Maldives. Coral host $\delta^{13}C$ and $\delta^{15}N$ values (mean ± SE) are grouped by oceanic reef exposure (a and b, respectively) and by Inner Sea reef exposure (c and d, respectively).

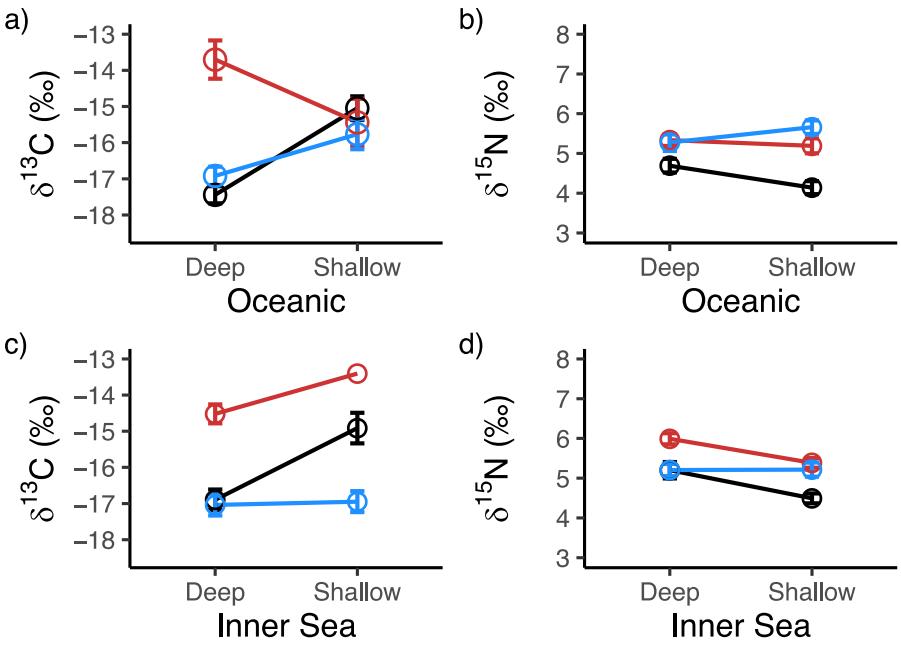

Figure 2.5. The effect of coral host species, reef depth, and reef exposure on symbiont carbon ($\delta^{13}C$) and nitrogen ($\delta^{15}N$) isotope ratios. Symbionts were isolated from three species of reef-building corals (*Galaxea fascicularis*- black, *Pachyseris speciosa*- red, *Pocillopora verrucosa*- blue) collected from shallow (10 m) and deep (30 m) reefs in the central Maldives. Symbiont $\delta^{13}C$ and $\delta^{15}N$ values (mean ± SE) are grouped by oceanic reef exposure (a and b, respectively) and by Inner Sea reef exposure (c and d, respectively).

2.4.3 Coral colony abundance between shallow and deep reefs

The number of colonies of each species collected with equal sampling effort revealed differences in species abundance between shallow and deep reefs (Table S2.4). There was a significant effect of coral species and depth on coral colony abundance (ANOVA, $F_{2,48}$= 10.453, p<0.001) but no effect of reef exposure. *Pachyseris speciosa* was significantly less abundant in shallow compared to deep reefs (Tukey p=0.009), while *G. fascicularis* was significantly more abundant than *P. speciosa* in shallow reefs (Tukey p=0.012).

2.4.4 Coral isotopic niches

The isotopic niches of three species of coral hosts from shallow and deep reefs revealed distinct species-specific patterns (Fig. 2.6a). The shallow isotopic niche (1.6‰^{2}) of coral host *G. fascicularis* was more than twice the size of its deep isotopic niche (0.7‰^{2}), with no overlap between the two niches (Figs. 2.6a and S2.5, Table S2.4). The shallow (1.7‰^{2}) and deep (1.8‰^{2}) isotopic niches of host *P. speciosa* were similar in size and position while the smaller isotopic niches (shallow 1.0‰^{2}, deep 0.8‰^{2}) of host *P. verrucosa* had marginal overlap. The isotopic niche of shallow host *G.*

fascicularis overlapped with the niches of shallow and deep host *P. speciosa* while the niche of deep host *G. fascicularis* overlapped with those of shallow and deep host *P. verrucosa*. The symbionts of shallow *G. fascicularis* showed the most distinct isotopic niche among all species due to lower $\delta^{15}N$ values (Fig. 2.6b). In contrast, symbionts of deep *G. fascicularis* had similar isotopic niches to *P. verrucosa* symbionts across both depths but remained distinct from *P. speciosa* symbionts. The isotopic niche sizes of symbionts were generally larger than those of their coral hosts (Table S2.4, Figs. S2.5 and S2.6).

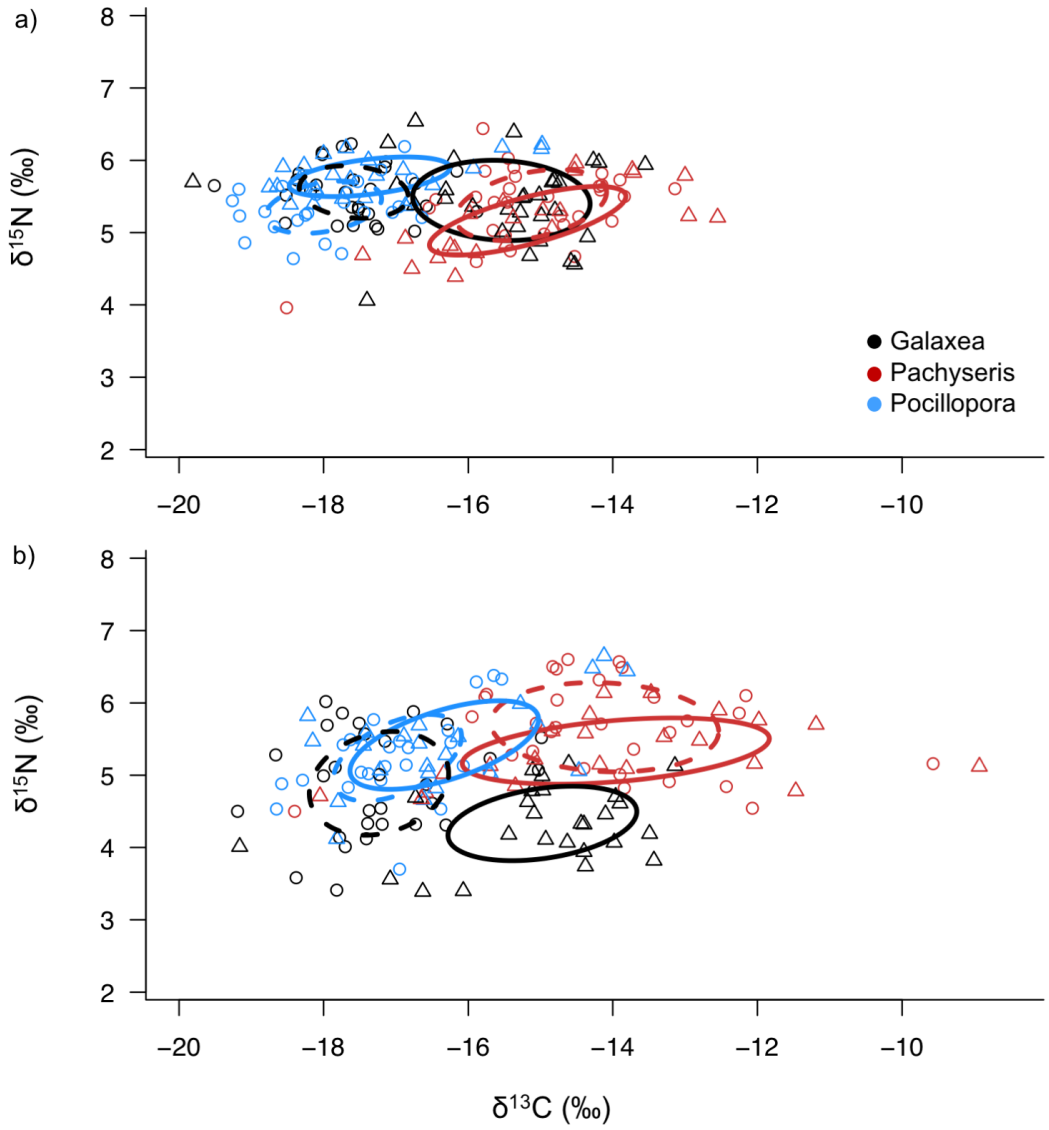

Figure 2.6. Isotopic niches of shallow (solid line, △) and deep (dash line, ○) reef-building corals from the central Maldives. Carbon ($\delta^{13}C$) and nitrogen ($\delta^{15}N$) isotope ratios of a) coral hosts *Galaxea fascicularis*, *Pachyseris speciosa*, and *Pocillopora verrucosa* and b) their symbionts are shown with maximum likelihood standard ellipses representing isotopic niches.

Table 2.1. A linear mixed effects model was used to test the variables coral species (*Galaxea fascicularis*, *Pachyseris speciosa*, *Pocillopora verrucosa*), reef depth (shallow or deep), and reef exposure (oceanic or Inner Sea) on coral host and symbiont carbon ($\delta^{13}C$) and nitrogen ($\delta^{15}N$) isotope ratios (DF- degrees of freedom; SE- standard error).

Coral Host	$\delta^{13}C$					$\delta^{15}N$				
Variable	DF	Estimate	SE	t-value	p-value	DF	Estimate	SE	t-value	p-value
(Intercept)	149	-17.4	0.3	-54.62	**<0.001**	149	5.6	0.1	43.04	**<0.001**
Oceanic		-0.4	0.4	-0.87	0.385		-0.1	0.2	-0.61	0.545
Pachyseris		2.1	0.4	4.95	**<0.001**		0.0	0.2	-0.25	0.802
Pocillopora		-0.7	0.4	-1.69	0.094		-0.3	0.2	-1.65	0.102
Shallow		1.9	0.4	4.42	**<0.001**		-0.1	0.2	-0.69	0.490
Oceanic: Pachyseris		0.7	0.6	1.22	0.226		-0.3	0.2	-1.30	0.196
Oceanic: Pocillopora		0.6	0.6	0.96	0.339		0.1	0.2	0.62	0.539
Oceanic: Shallow		0.3	0.6	0.54	0.591		0.0	0.2	-0.06	0.949
Pachyseris: Shallow		-1.5	0.6	-2.66	**0.009**		-0.3	0.2	-1.18	0.242
Pocillopora: Shallow		-1.5	0.6	-2.57	**0.011**		0.5	0.2	1.96	0.052
Oceanic: Pachyseris: Shallow		-1.5	0.8	-1.76	0.081		0.3	0.3	0.94	0.351
Oceanic: Pocillopora:Shallow		0.4	0.8	0.45	0.655		0.1	0.3	0.39	0.698
Symbiont	$\delta^{13}C$					$\delta^{15}N$				
Variable	DF	Estimate	SE	t-value	p-value	DF	Estimate	SE	t-value	p-value
(Intercept)	142	-16.9	0.4	-41.59	**<0.001**	143	5.2	0.2	30.35	**<0.001**
Oceanic		-0.5	0.5	-1.06	0.291		-0.5	0.2	-2.34	**0.021**
Pachyseris		2.4	0.5	4.44	**<0.001**		0.8	0.2	3.50	**0.001**

Pocillopora	-0.1	0.6	-0.26	0.796	0.0	0.2	0.02	0.987
Shallow	2.0	0.5	3.65	**<0.001**	-0.7	0.2	-3.09	**0.002**
Oceanic:Pachyseris	1.4	0.7	1.92	0.057	-0.1	0.3	-0.49	0.626
Oceanic: Pocillopora	0.7	0.8	0.89	0.376	0.6	0.3	1.82	0.071
Oceanic: Shallow	0.4	0.7	0.56	0.575	0.2	0.3	0.50	0.617
Pachyseris:Shallow	-0.9	0.7	-1.19	0.236	0.1	0.3	0.34	0.736
Pocillopora: Shallow	-1.9	0.8	-2.42	**0.017**	0.7	0.3	2.21	**0.029**
Oceanic:Pachyseris: Shallow	-3.3	1.1	-2.97	**0.003**	0.3	0.5	0.66	0.513
Oceanic: Pocillopora:Shallow	0.6	1.1	0.60	0.551	0.2	0.5	0.48	0.632

2.5 Discussion

2.5.1 Nitrogen isotope ratios indicate importance of deep-water nitrate and water column mixing

In the Maldives, prevailing wind-driven upwelling associated with the monsoon seasons (~10 months of the year) has a greater impact on nutrient and particulate availability than the short inter-monsoon transition periods (~2 months) (Fig. 2.2b-c). Despite fluxes of cooler seawater recorded in deep (30 m) but not shallow (10 m) reefs, reef depth did not affect the $\delta^{15}N$ and $\delta^{13}C$ values of POM. Nutrients are likely distributed across the double atoll chain of the central Maldives via strong currents within and between the atolls (Preu & Engelbrecht, 1991; Owen, Kruijsen, Turner, & Wright, 2011). The results showed that POM and coral hosts from both oceanic and Inner Sea reef exposures had similar $\delta^{15}N$ values. Similar mean $\delta^{15}N$ values of three species of coral hosts (range between 5.2 and 5.8‰), their symbionts (range between 4.3 and 5.7‰), and POM (5.3‰, Period 1) from both shallow and deep reefs are consistent with a well-mixed water column supplied with deep-water nitrate as the major nitrogen source. Previous records of bulk coral (combined host and symbiont tissue of *Porites lobata*) from the Maldives showed similar mean $\delta^{15}N$ values (5.8‰), with the exception of coral collected from sites potentially affected by sewage disposal (Risk et al. 1993). The long-term retention and recycling of nitrogen between coral hosts and symbionts indicates that Maldives coral $\delta^{15}N$ values of ~5‰ reflect a time-integrated signal of nitrogen principally derived from deep-water nitrate (Tremblay, Maguer, Grover, & Ferrier-Pagès, 2015; Tanaka et al., 2018). In other regions subject to upwelling of deep-water nitrate, such as the Florida Keys reef tract, regional oceanography also appears to influence coral $\delta^{15}N$ values (Swart, Saied, & Lamb, 2005; Leichter et al., 2007).

Although the $\delta^{15}N$ values of corals in the Maldives indicate community- and reef-wide reliance on an upwelled nitrate source, nitrogen fixation can provide an important source of new nitrogen for some coral species and reef ecosystems (Cardini et al. 2015). Despite consistent $\delta^{15}N$ values among the majority of the coral host species (5.5‰) and symbionts (5.3‰) from Maldives reefs, the symbionts of *G. fascicularis* from shallow reefs (4.3‰) occupied a unique isotopic niche due to lower $\delta^{15}N$ values (Fig. 6). Because symbionts, rather than the host, preferentially use nitrogen derived from nitrogen fixation (Lesser et al. 2007), the lower $\delta^{15}N$ values of shallow *G. fascicularis* symbionts could be due to a small proportion of nitrogen derived from nitrogen-fixing bacteria (Rädecker et al. 2015). Further investigation into the potential role of nitrogen fixing bacteria and its association with symbionts of *G. fascicularis* is required (Li et al. 2013). However, based on the $\delta^{15}N$ values from the Maldives, the potential input of nitrogen derived from nitrogen fixation would be minimal. *Galaxea fascicularis* host and symbionts from the Maldives did not have particularly low $\delta^{15}N$ values as corals

from other regions, which have $\delta^{15}N$ values reflecting the distinct isotopic signature of nitrogen fixation (Lesser et al., 2007; Alamaru et al., 2009).

Spatiotemporal sampling during our survey revealed a significant shift in mean $\delta^{15}N$ values of POM between the consecutive Period 1 (5.3‰) and Period 2 (-1.2‰). This change in isotopic ratios of POM likely reflected the variation in the primary nitrogen source during the shift from the dominant upwelling system (deep-water nitrate) to a stratified water column (nitrogen fixation) during the brief inter-monsoon transition period (Figs. 2.2, 2.3, S2.4; Qasim, 1970). The slight increase in $\delta^{13}C$ values of POM in Period 2 (from -25.2‰ to -23.8‰) possibly reflects an increase in the abundance of *Trichodesmium* (higher $\delta^{13}C$) and/or ^{13}C-rich diatoms within the phytoplankton community, which can contain cyanobacteria (Fry & Wainright, 1991; Carpenter et al., 1999; Tchernov & Lipschultz, 2008). During the inter-monsoon period in the Maldives, lower concentrations of chl-*a* and blooms of nitrogen-fixing *Trichodesmium* provide support for the hypothesis that POM from Period 2 reflected increased nitrogen fixation in the water column (Gower and King 2011; Kumar et al. 2016). Alternatively, a decrease in $\delta^{15}N$ values (e.g., POM) can result from fractionation under high (e.g., >15 µM) nitrate concentrations (Montoya, 2008). However, the latter is unlikely given that seawater temperatures increased and satellite maps showed relatively low concentrations of surface chl-*a* (a proxy for low upwelling), all of which are consistent with low-nutrient, stratified waters as winds subsided and shifted direction during the inter-monsoon period (Figs. S2.1-S2.4). Changes in POM $\delta^{15}N$ and $\delta^{13}C$ values from the same site sampled at the start and end of the survey indicate that the isotopic differences reflected temporal shifts in water mass rather than regional east-west differences (Figs. 2.3 and S2.4). In regions where the Island Mass Effect or oceanographic processes generate localized upwelling, deep-water nitrate can have a greater role than nitrogen fixation in supplying nitrogen to the reef and can support an increased abundance of plankton that can be beneficial for coral heterotrophic feeding (Yamazaki et al., 2011; Gove et al., 2016).

2.5.2 Species-specific trophic strategies reveal distinct isotopic niches across shallow to deep reefs

Despite similar particulate resources over depth (e.g., POM $\delta^{13}C$ and $\delta^{15}N$) and water column mixing supporting consistent coral host $\delta^{15}N$ values, host $\delta^{13}C$ values reflected differentiation in the physiology of the coral host species and their symbionts. Different $\delta^{13}C$ values resulting in distinct shallow and deep isotopic niches of host *G. fascicularis* indicates a difference in carbon resources due to decreased photosynthesis and/or greater heterotrophic feeding with increasing depth (Muscatine et al., 1989). Although *G. fascicularis* has been shown to have a lower feeding rate and requirement for heterotrophic carbon relative to other species when grown in aquaria (van Os et al.,

2012; Hoogenboom, Rottier, Sikorski, & Ferrier-Pagès, 2015), the external digestion of particulate prey via mesenterial filaments is a mechanism by which *G. fascicularis* can obtain carbon and nitrogen (Wijgerde et al. 2011). While the feeding rate of *G. fascicularis* does not appear to be affected by light availability (Hii et al. 2009), changes in *G. fascicularis* skeleton structure may help to optimize photosynthesis in shallow reefs where light is not limiting (Crabbe and Smith 2006). Indeed, skeletal growth of *G. fascicularis* is greatest at high irradiance (Schutter et al. 2008). As corals can depend more on heterotrophy in regions of high primary productivity (Fox et al. 2018), the 2-fold difference in isotopic niche size of shallow versus deep *G. fascicularis* from a well-mixed water column is likely due to changes in symbiont autotrophy over depth. Because symbiont physiology and irradiance can affect carbon acquisition (Ezzat et al. 2017), future work could examine carbon isotope fractionation in relation to DIC fluxes in symbionts especially since *G. fascicularis* can associate with two symbiont clades (Dong, Huang, Huang, & Li, 2009; Maier et al., 2010; Hoins et al., 2016).

Coral host *P. speciosa* showed consistent $\delta^{13}C$ values over depth, resulting in an overlap of both its isotopic niches with that of host *G. fascicularis* from shallow reefs. Although the isotopic niche size and position of shallow and deep *P. speciosa* did not differ with depth, *P. speciosa* colony abundance was greater in deep reefs. The 2-dimensional plating morphology of this coral species and symbiont photobiological acclimation to reduced irradiance due to increasing depth and/or turbidity help to explain the apparent cryptic nature of *P. speciosa* in shallow reefs and its greater abundance in reef cavities and lower-light upper mesophotic reefs of the Maldives (4% of surface irradiance at 30 m; Ciarapica & Passeri, 1993; Cooper et al., 2011; Browne, Smithers, & Perry, 2012). Indeed, *P. speciosa* symbionts are efficient autotrophs over large depth ranges (i.e., 0-60 m), with the coral host showing a consistent association with one clade of symbionts across shallow to deep mesophotic reefs of different oceans (Bongaerts et al. 2011b; Cooper et al. 2011; Ziegler et al. 2015b). In addition to our findings from the Maldives, a previous study also observed a decreased abundance of *P. speciosa* colonies in shallow reefs compared to deep reefs of the upper mesophotic zone (Ziegler, Roder, Büchel, & Voolstra, 2015). Therefore, the similar, more positive values of $\delta^{13}C$ of *P. speciosa* from shallow and deep reefs is likely related to a dependence on symbiont autotrophy over depth. The heterotrophic feeding capacity of *P. speciosa* is possibly limited to fine organic matter due to an absence of tentacles although it can feed using mesenterial filaments (Goreau et al. 1971).

Compared to other more oligotrophic reef systems, the relatively high primary productivity in the Maldives is tightly coupled with coral heterotrophy especially for *P. verrucosa* (Fox et al. 2018).

Colonies of the typically competitive branching coral *P. verrucosa* showed similar abundance and consistent $\delta^{13}C$ and $\delta^{15}N$ values in shallow and deep reefs, which indicates that *P. verrucosa* maintains the same trophic strategy independent of reef depth. Within the Pocilloporidae family, the focal species *P. verrucosa* is known to be an effective heterotroph with high phenotypic plasticity (Séré, Massé, Perissinotto, & Schleyer, 2010; Ziegler, Roder, Büchel, & Voolstra, 2015) while its congener *Pocillopora meandrina* is also dependent on heterotrophy (Roder et al., 2010; Fox et al., 2018). The more negative $\delta^{13}C$ values of *P. verrucosa* recorded in this study provide evidence for its dependence on heterotrophy in both shallow and deep reefs in the Maldives. The ability to obtain nutrients through coral host heterotrophy likely supports the lower levels of coral bleaching and coral loss observed for Pocilloporid corals, including *P. verrucosa* (Grottoli, Rodrigues, & Palardy, 2006; Muir, Marshall, Abdulla, & Aguirre, 2017; Hughes et al., 2018). However, if a coral bleaching event would occur during an inter-monsoon period when water column mixing is reduced, then coral feeding capacity and survival rates may be affected (Palardy et al. 2008). Further work defining the trophic niches of individual coral species is needed to understand coral community and reef ecosystem function, especially because coral reef assemblages are changing due to the increased frequency of climate-driven oceanic thermal stress conditions.

2.6 Acknowledgements

We thank Dominic Bryant, Craig Heatherington, Kelly Latijnhouwers, the Seaview Survey Maldives team, the Maldives Marine Research Centre, especially Shiham Adam and Nizam Ibrahim, the Ministry of Fisheries and Agriculture, the Environmental Protection Agency, the M/V Emperor Voyager crew, and Casa Mia staff for their research support in the Maldives. We thank three anonymous reviewers and associate editor for valuable comments on this manuscript and thank Michael Brett and William Skirving for helpful discussions. We also thank the Stable Isotope Facility at the University of California Davis. MODIS Aqua chl-*a* data were obtained from the NASA EOSDIS Physical Oceanography Distributed Active Archive Center. This study was accomplished as part of the XL Catlin Seaview Survey, designed and undertaken by the Global Change Institute, and funded by XL Catlin in partnership with The Ocean Agency and The University of Queensland. This work was also supported by the Australian Research Council (ARC) Centre of Excellence for Coral Reef Studies (SD and OHG), an ARC Laureate Fellowship (OHG), the University of Queensland Research Training Tuition Fee Scholarship (VZR), and a NOAA Nancy Foster Scholarship (MDF).

2.7 Supplementary Information

Methods S2.1. To visualize seasonal patterns associated with the monsoon climate of the Maldives, the climatological means are divided into the primary seasons of the South Asian Monsoon: northeast (NE) monsoon from ~November to March and southwest (SW) monsoon from ~May-September. Inter-monsoon periods occur during the spring (~April) and fall (~October). We used the eight-day 0.0417° (4 km) spatial resolution product of surface chlorophyll-*a* (mg m^{-3}) derived from the NASA Moderate Resolution Imaging Spectroradiometer (MODIS; https://modis.gsfc.nasa.gov/). Briefly, pixels that fell within ~3.27 km of the 30 m isobath of the atoll fore reefs were excluded to avoid data confounded by optically shallow water (Carder et al. 2003; Gove et al. 2013). To identify the next closest pixels to the atoll exterior, a full pixel width (4.4 km) buffer region was extended beyond the 3.27 km exclusion zone and used to select a single band of pixels around each atoll. MODIS Aqua (Level 3, 4 km) monthly chlorophyll-*a* maps were also obtained for the months directly preceding and following the survey (January-June 2015) to evaluate possible variability in the annual monsoon weather patterns at the time of our study (http://podaac.jpl.nasa.gov/, Hu et al. 2012).

Table S2.1. Life history strategies of the three scleractinian symbiotic coral species in this study (Darling et al. 2012; Madin et al. 2016a, 2016b).

	Coral Traits Database:		This study:
Coral species	Life history strategy	Description	Maldives Observation (2015)
Galaxea fascicularis	Stress-tolerant	Advantageous traits in chronically harsh environments	Generalist: Flexible trophic strategy
Pachyseris speciosa	Generalist	Does well in habitats where competition is limited by low levels of stress and disturbance	Specialist: Low-light specialist found on deep or turbid reefs and/or in shaded reef cavities
Pocillopora verrucosa	Competitive	Efficient at using resources and can dominate communities in productive environments	Competitive: Efficient resource use (heterotroph)

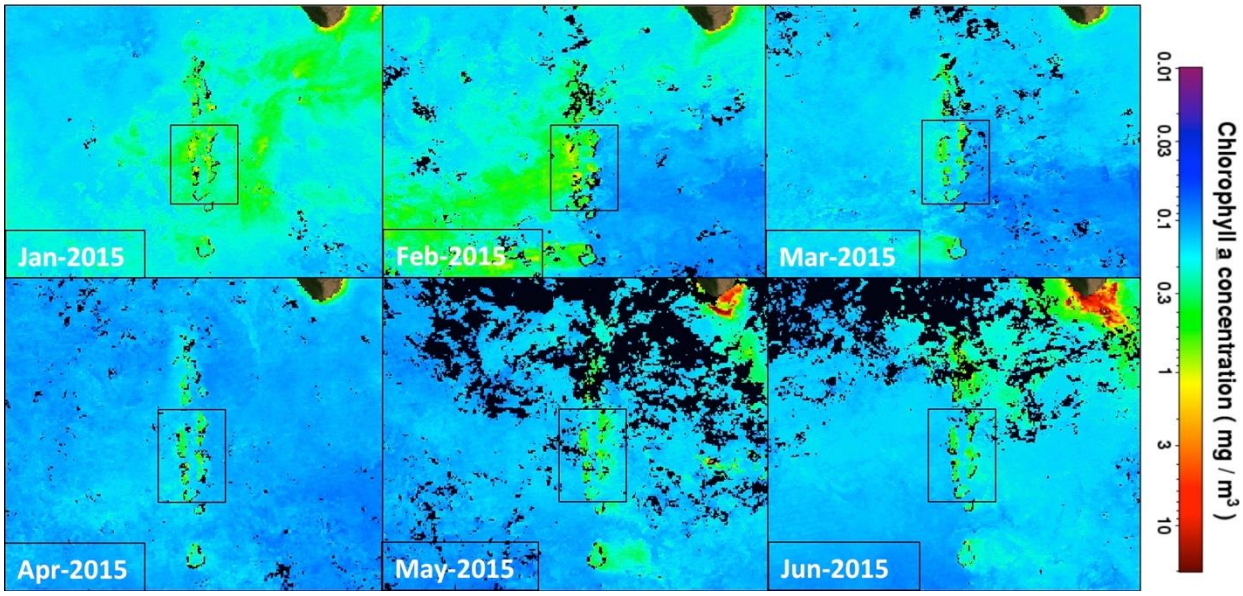

Figure S2.1. Monthly average chlorophyll-*a* concentrations in the central Indian Ocean (mg m^{-3}; 4-km MODIS-Aqua satellite) during the months preceding and following the survey (March-April 2015). The black box outlines the central Maldives atolls that were surveyed.

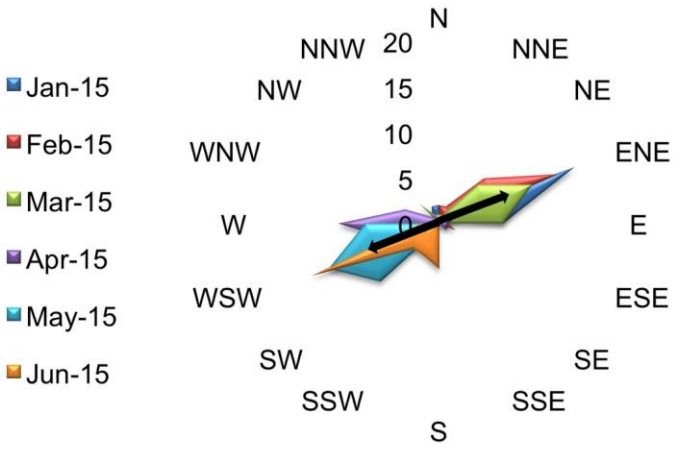

Figure S2.2. Monthly sums of daily wind direction counts (numbered) for the months preceding and following the survey period (March-April 2015). Wind direction changes according to the monsoon seasons, from the NE (Jan-Mar; NE monsoon) to the SW (Apr-Jun; SW monsoon). Wind data are from site 1/27 (Hulhumale, North Malé; see map in Fig. 2a) obtained from the Maldives Meteorological Service (www.meteorology.gov.mv/).

Table S2.2. Summary of reef sites surveyed during a 19-day cruise (inter-monsoon period; 29 March to 16 April 2015) in the central Maldives, as marked in the map (Fig. 2a) created in ArcMap 10.3.1 using the layer *Global Distribution of Coral Reefs* (2010) from the UNEP-WCMC Millennium Coral Reef Mapping Project (UNEP-WCMC et al. 2010). Yes/No (Y/N) designation indicates whether particulate organic matter (POM) or coral were sampled at a site.

Date	Atoll	Site name	Site number	Latitude	Longitude	POM	Coral
29/03/2015	N. Male	Hulhumale	1	4.215	73.549	Y	N
30/03/2015	N. Male	Reethi Rah	2	4.521	73.362	Y	Y
30/03/2015	N. Male	Rasfari	3	4.398	73.347	Y	N
1/04/2015	N. Ari	Mathiveri	4	4.191	72.737	Y	Y
1/04/2015	N. Ari	Fattaru Faru	5	4.205	72.733	N	N
1/04/2015	N. Ari	Dinoluga	6	4.151	72.732	Y	Y
3/04/2015	S. Ari	Dhiggaru Falhu	7	3.714	72.981	Y	Y
3/04/2015	S. Ari	Dhangethi	8	3.596	72.957	Y	N
4/04/2015	S. Ari	Maamigilli	9	3.467	72.835	Y	N
5/04/2015	Dhaalu	Hulhuvehi	10	2.862	73.029	Y	Y
5/04/2015	Dhaalu	Maafushi	11	2.683	72.847	Y	Y
6/04/2015	Thaa	Thimarufushi	12	2.209	73.156	Y	N
6/04/2015	Thaa	Fenfushi	13	2.287	73.272	Y	N
8/04/2015	Meemu	Kurali	14	2.782	73.369	Y	Y
8/04/2015	Meemu	Bodu Hura	15	2.811	73.366	Y	Y
9/04/2015	Meemu	Muli	16	2.922	73.588	Y	N
9/04/2015	Meemu	Veyvah	17	2.975	73.620	Y	Y

10/04/2015	Meemu	Kuvali	18	3.163	73.495	Y	N
11/04/2015	Vaavu	Kuda Aanuvari Falhu	19	3.321	73.471	Y	N
12/04/2015	Vaavu	Kandimma Falhu	20	3.385	73.426	Y	Y
12/04/2015	Vaavu	Maadhiggaru Falhu	21	3.539	73.520	Y	N
13/04/2015	Vaavu	Medhu Faru	22	3.626	73.509	Y	Y
14/04/2015	S. Male	Tholimaraahuraa	23	3.831	73.370	Y	N
14/04/2015	S. Male	Ranalhi	24	3.907	73.351	Y	N
15/04/2015	S. Male	Maafushi S. Male	25	3.945	73.500	Y	Y
15/04/2015	S. Male	Fushidiggaru Falhu	26	4.079	73.539	Y	Y
16/04/2015	N. Male	Hulhumale	27	4.225	73.551	Y	N

Table S2.3. A linear mixed effects model was used to test the variables reef depth (shallow or deep), reef exposure (oceanic or Inner Sea), and sampling period (Period 1 or Period 2) on the carbon ($\delta^{13}C$) and nitrogen ($\delta^{15}N$) isotope ratios of particulate organic matter sampled from the reef water column.

	$\delta^{13}C$					$\delta^{15}N$				
Variable	DF	Estimate	Std. Error	t-value	p-value	DF	Estimate	Std. Error	t-value	p-value
(Intercept)	34	-25.0	0.4	-63.20	**<0.001**	34	5.0	0.8	6.53	**<0.001**
Oceanic		0.7	0.7	1.05	0.300		0.5	1.3	0.36	0.722
Period 2		0.9	0.6	1.47	0.152		-6.9	1.1	-6.09	**<0.001**
Shallow		-1.0	0.6	-1.84	0.074		0.8	1.1	0.78	0.439
Oceanic:Period 2		-0.1	0.9	-0.07	0.947		-0.3	1.7	-0.19	0.852
Oceanic:Shallow		-0.1	0.9	-0.10	0.923		-0.2	1.8	-0.09	0.930
Period 2:Shallow		0.5	0.9	0.61	0.548		1.4	1.7	0.85	0.403
Oceanic:Period 2:Shallow		0.6	1.2	0.52	0.607		-1.9	2.4	-0.78	0.439

Table S2.4. Summary of carbon and nitrogen isotope ratios ($\delta^{13}C$ and $\delta^{15}N$; mean ± SD), molar C:N ratio (± SD), isotopic niche size (Bayesian standard ellipse area), and colony abundance (mean number of colonies ± SD, sampled with equal sampling effort from each depth and reef exposure) for three species of corals and their symbionts.

Species	Depth	n	$\delta^{13}C$ (‰)	$\delta^{15}N$ (‰)	C:N	Isotopic niche size (‰^{2})	Colony abundance	
							Inner Sea	Oceanic
Galaxea fascicularis								
Host	Shallow	31	-15.5 ± 1.2	5.4 ± 0.6	6.3 ± 0.6	1.6	8 ± 1	8 ± 1
	Deep	29	-17.6 ± 0.8	5.6 ± 0.4	6.1 ± 0.5	0.7	4 ± 3	6 ± 3
Symbiont	Shallow	26	-15.0 ± 1.3	4.3 ± 0.5	7.9 ± 1.0	2.0	-	-
	Deep	29	-17.2 ± 1.0	4.9 ± 0.7	8.1 ± 1.3	2.3	-	-
Pachyseris speciosa								
Host	Shallow	22	-15.2 ± 1.4	5.2 ± 0.5	6.4 ± 0.4	1.7	6 ± 3	1 ± 3
	Deep	30	-15.1 ± 1.0	5.4 ± 0.5	6.4 ± 0.2	1.8	9 ± 1	8 ± 2
Symbiont	Shallow	22	-14.0 ± 2.1	5.3 ± 0.5	9.7 ± 1.5	2.8	-	-
	Deep	30	-14.1 ± 1.6	5.7 ± 0.6	9.8 ± 1.6	2.6	-	-
Pocillopora verrucosa								
Host	Shallow	24	-17.4 ± 1.1	5.8 ± 0.3	5.7 ± 0.3	1.0	6 ± 3	7 ± 4
	Deep	25	-18.0 ± 0.8	5.4 ± 0.4	6.0 ± 0.4	0.8	4 ± 3	5 ± 5
Symbiont	Shallow	24	-16.3 ± 1.3	5.4 ± 0.6	7.1 ± 1.1	1.7	-	-
	Deep	24	-17.0 ± 0.9	5.2 ± 0.6	6.8 ± 0.9	1.3	-	-

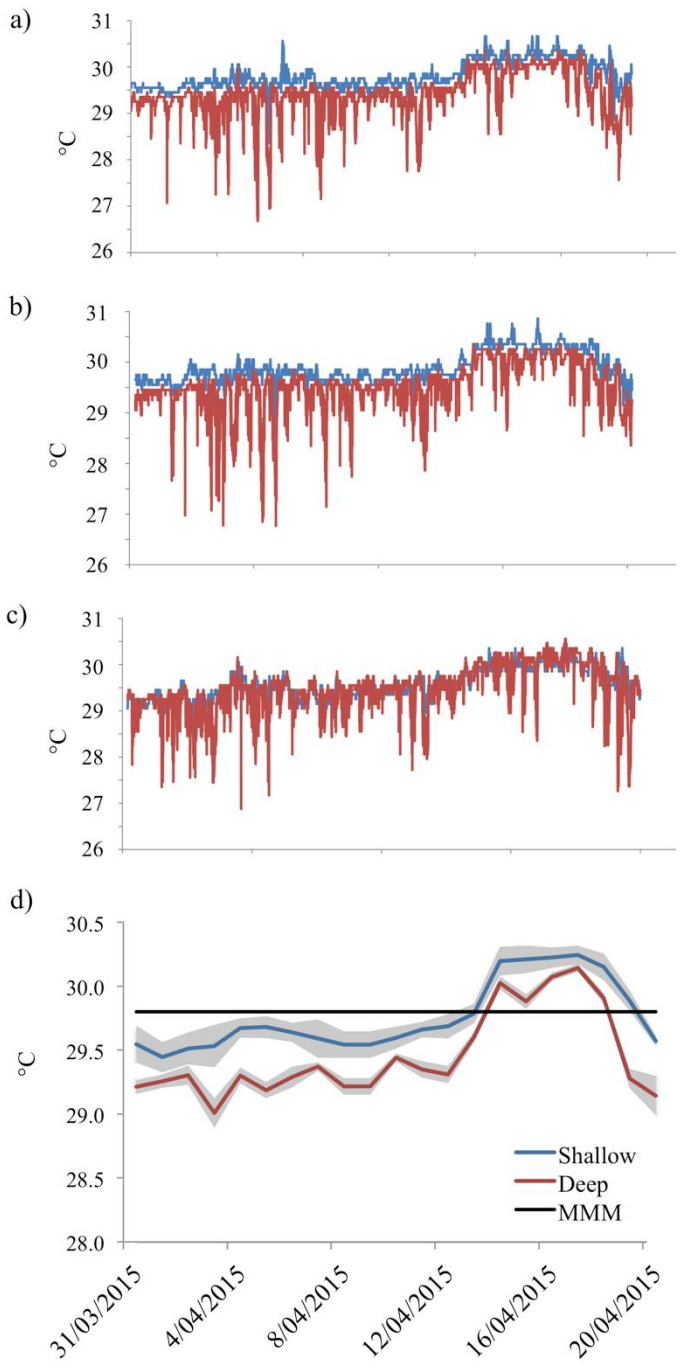

Figure S2.3. Variability in seawater temperature (5 min interval; March-April 2015) from shallow (10 m) and deep (30 m) reefs at three locations (a, b, and c) on the western oceanic rim of the Maldives archipelago (sites 4, 5, and 6 shown on map in Fig. 4a). d) Average daily seawater temperatures from shallow and deep reefs (average of three sites shown in a, b, and c) with standard error (grey scale shading) and maximum monthly mean (MMM) sea surface temperature (NOAA Coral Reef Watch; Malé, Maldives).

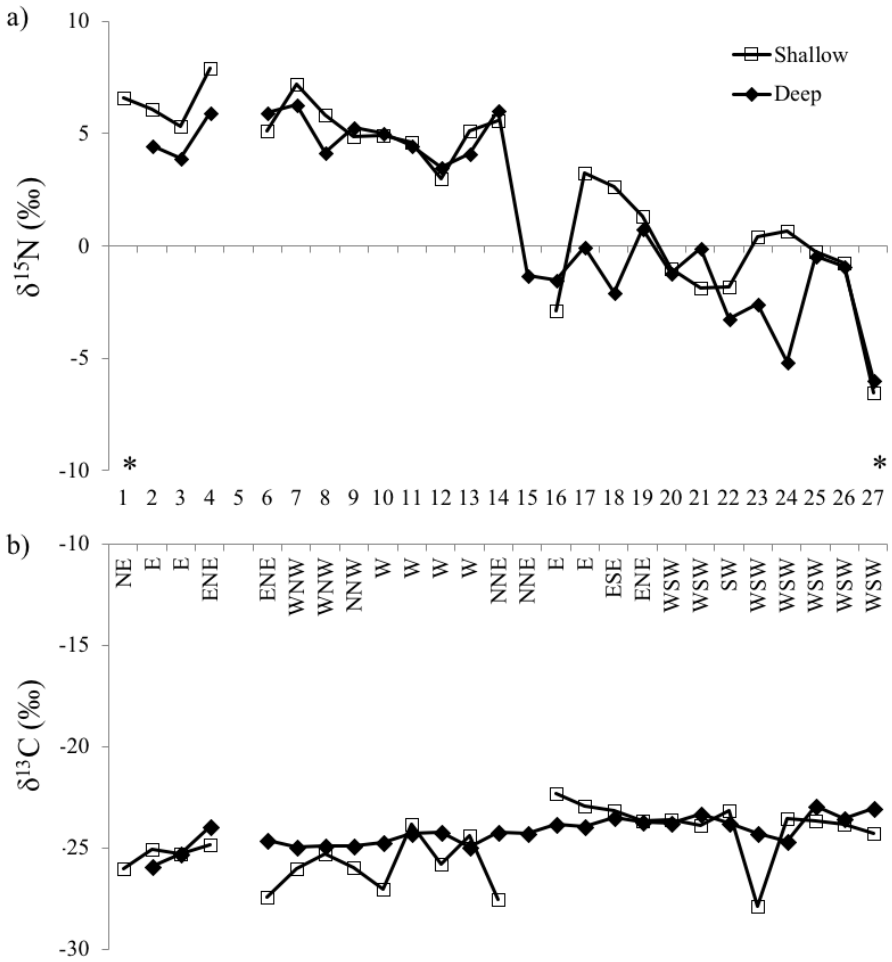

Figure S2.4. Particulate organic matter (POM) and daily wind direction from coral reefs across the central Maldives (numbers along x-axis indicate coral reef site, see map in Fig. 2.2a). a) POM nitrogen isotope ratios ($\delta^{15}N$) from shallow (10 m) and deep (30 m) reefs and b) carbon isotope ratios ($\delta^{13}C$) from shallow and deep reefs shown in chronological order of the survey. The same site, represented by the asterisk (*), was visited at the start and the end of the survey.

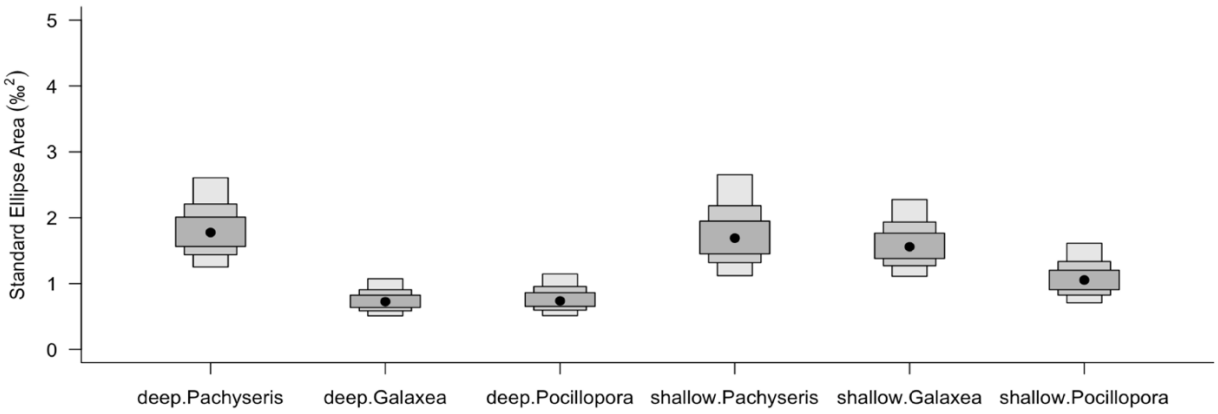

Figure S2.5. Isotopic niche sizes of coral hosts represented by Bayesian standard ellipse areas (black circle) of three species of coral (*Galaxea fascicularis*, *Pachyseris speciosa*, *Pocillopora verrucosa*) from shallow (10 m) and deep (30 m) reefs in the Maldives. Posterior distribution credibility intervals (50%, 75%, and 95%) shown in grey scale.

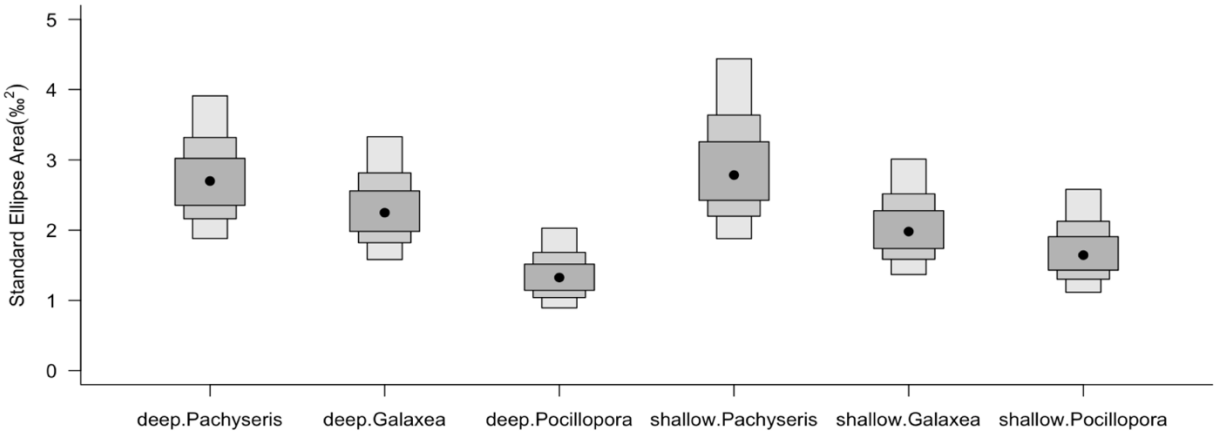

Figure S2.6. Isotopic niche sizes of symbionts represented by Bayesian standard ellipse areas (black circle) of symbionts isolated from three species of coral (*Galaxea fascicularis*, *Pachyseris speciosa*, *Pocillopora verrucosa*) from shallow (10 m) and deep (30 m) reefs in the Maldives. Posterior distribution credibility intervals (50%, 75%, and 95%) shown in grey scale.

Chapter 3:

Coral isotopic niches indicate trophic shift following a thermal stress event

3.1 Abstract

The visible symptom of anthropogenic ocean warming on coral reef ecosystems is a drastic loss of autotrophic symbionts by reef-building corals. However, corals subject to thermal stress conditions show differential survival that is not necessarily related to coral bleaching susceptibility alone but is also related to heterotrophic feeding. Heterotrophy can support coral survival through thermal events by either providing the host with an alternate source of energy and/or supplying the coral with the energy required to sustain symbiont autotrophy. In 2016, global oceanic thermal stress resulted in severe mass coral bleaching and mortality worldwide including the Maldives, Indian Ocean. In the reefs of the Maldives, in situ seawater temperatures recorded for 1.5 years through the thermal stress event recorded temperatures exceeding local monthly maximum means in both shallow (10 m) and deep (30 m) reefs. To better understand the different susceptibility of corals to thermal stress over depth, we investigated the response of three species of reef-building coral with diverse trophic strategies (*Galaxea fascicularis*, *Pachyseris speciosa*, and *Pocillopora verrucosa*). Eight months following the thermal stress event, carbon and nitrogen isotope ratios showed changes in coral trophic strategies. Increases in isotopic niche size indicated that increased heterotrophy likely helped to maintain autotrophy in the more autotrophic coral *P. speciosa*. In contrast, a reduced isotopic niche size of shallow populations of *G. fascicularis* indicated that an increase in heterotrophy may have mostly supported the host without a concomitant support of autotrophy. The isotopic niche size of shallow *P. verrucosa* increased following the thermal stress event although the isotopic niche size did not change in deep reefs, indicating that *P. verrucosa* maintained a consistent trophic strategy and was apparently less susceptible to thermal stress in deep reefs of the Maldives. These trends and trophic mechanisms that supported the survival of these corals provides insight into how reef-building corals are likely to respond to global climate change.

3.2 Introduction

In 2016, a global mass coral bleaching event affected at least 75% of the world's coral reefs (Hughes et al. 2018a). Coral 'bleaching', or the breakdown of symbiosis between corals and their endosymbiotic dinoflagellates of the genus *Symbiodinium* (herein 'symbionts'), occurs during anomalous changes in seawater temperature (Hoegh-Guldberg 1999; Hoegh-Guldberg et al. 2005; Weis 2008). If anomalous thermal stress persists, high rates of coral mortality are likely to occur (Williams and Bunkley-Williams 1990; Baker et al. 2008). In the central Indian Ocean, the reefs of the Maldives archipelago have endured several mass coral bleaching events (McClanahan 2000; Pisapia et al. 2016). A prolonged thermal stress event in 2016 exceeded the temperature-related coral bleaching threshold, causing greater than 70% of corals to bleach between 0 and 13 m depth across

11 atolls of the Maldives (Ibrahim et al. 2017). However, the probability of moderate to severe coral bleaching was reduced (60%) on deep reefs (24-30 m depth) compared to shallow reefs (85%) of 10 m depth (Muir et al. 2017). Corals are differentially susceptible to bleaching (Marshall and Baird 2000), with bleaching susceptibility among taxa not necessarily correlated with susceptibility to mortality (Hughes et al. 2018b). Reef surveys following the 2016 mass bleaching event in the Maldives provide clear evidence of mass mortality among certain genera of corals, such as the >80% reduction of corals within the genus *Acropora* but less than 10% of the genus *Porites* (Ibrahim et al. 2017). However, there is little to no information on the impact and outcome of the thermal stress event on other genera or specific species.

As mixotrophic organisms, reef-building corals depend on organic resources from their symbionts (autotrophy) as well as from heterotrophic feeding on particulate organic matter (POM) in the water column (Goreau et al. 1971; Houlbrèque and Ferrier-Pagès 2009). Corals that survive a thermal event may do so either because symbiont autotrophy was not significantly impeded and/or because host heterotrophic feeding on particulate organic material increases to compensate for affected autotrophy (Grottoli et al. 2006) or by consuming stored energy reserves of lipids, proteins, and carbohydrates (Grottoli et al. 2004; Rodrigues and Grottoli 2007). Since coral species show different capacities with respect to heterotrophic feeding, the contribution of heterotrophy to coral metabolism and the potential role of feeding in coral species response to bleaching greatly varies (Grottoli et al. 2006; Palardy et al. 2008). Because some corals can increase heterotrophic feeding in reefs with high particulate concentrations (Anthony 2000), potential heterotrophy also depend on the availability of particulate organic sources in the water column (Fox et al. 2018). Upwelling of nutrients to surface waters in the Maldives increases primary productivity and particulate organics present in the water column (Sasamal 2007; de Vos et al. 2014). Water column properties after the thermal stress event could be different to those observed before the mass coral bleaching, due to either prolonged changes associated with a significantly degraded coral reef (Morillo-Velarde et al. 2018) or random temporal variability. As the heat content of the ocean rises, increased seawater stratification may restrict upwelling and in turn affect zooplankton populations (Roemmich and McGowan 1995) although climate change may have differential impacts on regional water circulation (Sydeman et al. 2014; Karnauskas et al. 2016). Alternatively, as thermal events increase the death and decay of reef organisms, an invigorated detrital cycle may increase the availability of POM as a major source of carbon for consumers in degraded reefs (Morillo-Velarde et al. 2018).

Coral host heterotrophic feeding is especially important under thermal stress conditions as external food supply provides essential nutrients to the host and, in some cases, also helps to prevent damage to symbiont photosynthetic processes (Borell et al. 2008; Ferrier-Pagès et al. 2010; Hoogenboom et al. 2012). Patterns of resource use can be evaluated using carbon and nitrogen stable isotope ratios ($\delta^{13}C$ and $\delta^{15}N$), which provide time-integrated insight into nutrient abundance and assimilation (Peterson and Fry 1987). Increased heterotrophy by bleached corals is associated with an increase in host $\delta^{15}N$ values and a reduction in host $\delta^{13}C$ values (Rodrigues and Grottoli 2006; Bessell-Browne et al. 2014; Schoepf et al. 2015). These isotopic differences have been observed at least 1.5 to 4 months following the dissipation of the thermal event, while 11 months into recovery there is variation in the isotopic signal among coral species but isotopic changes can still be detected (Rodrigues and Grottoli 2006; Levas et al. 2013; Bessell-Browne et al. 2014; Schoepf et al. 2015). For fed corals, there is the potential for the isotopic signal of heterotrophy to last almost one year after the dissipation of a thermal event, and at least seven months after the reestablishment of symbiont autotrophy (Hughes and Grottoli 2013). Despite the relatively rapid turnover of symbionts within the coral host (~1 month), host nitrogen turnover is relatively slow (370 days to turnover 63% of nitrogen) because the symbionts act as a sink for host metabolized nitrogen that leads to a large proportion of recycled nitrogen in the coral holobiont (Tanaka et al. 2015, 2018). If a significant reduction in the population of symbionts impedes autotrophy, then nitrogen turnover accelerates (56 days; Tanaka et al. 2018) because host metabolized nitrogen is excreted rather than cycled to the symbiont (Rahav et al. 1989). Non-symbiotic corals, which depend exclusively on heterotrophic feeding, typically have higher $\delta^{15}N$ values than symbiont-associated corals (Muscatine et al. 2005), but the realized $\delta^{15}N$ value would depend on the $\delta^{15}N$ of resources available in the water column (Chapter 2). As autotrophy is re-established following the dissipation of the thermal stress event, then the relative input of recycled to new nitrogen will increase and, overtime, would likely re-establish the pre-bleaching status quo. Coral holobiont carbon pools turn over at greater rates than nitrogen, with the host carbon pool experiencing 100% turnover within 40 days, and symbiont carbon pools turning over at even faster rates (Tanaka et al. 2018). Eight months following the thermal stress event, decreased $\delta^{13}C$ values of coral hosts may indicate whether the host has increased heterotrophic feeding in response to the thermal event, with the proviso that potential temporal changes to water column POM concentrations and $\delta^{13}C$ values are not identified as drivers to changes in host $\delta^{13}C$ values.

Based on the mechanisms associated with how heterotrophy can help corals survive thermal stress events, bivariate isotopic niches ($\delta^{13}C$ and $\delta^{15}N$) can be used to investigate shifts in the ecological

niches of reef organisms due to reef disturbance (Letourneur et al. 2017; Plass-Johnson et al. 2018). Although an isotopic niche is not a direct measurement of a species ecological niche, trophic strategy and resource use of an organism plays a profound role in influencing the isotopic niche (Newsome et al. 2007). Following ecological niche theory, an environmental disturbance can negatively or positively affect an organism's niche by either restricting or expanding the niche depending on a species' response to the impact of the disturbance (Letourneur et al. 2017). For example, a thermal stress event may decrease the size of an isotopic niche of a coral due to reductions in symbiont autotrophy (Jones et al. 1998). Alternatively, a thermal stress event may increase the size of a coral's isotopic niche if a coral can increase heterotrophic feeding that in turn supports autotrophy (Tremblay et al. 2016). If a coral shifts to alternate energy resources such as by increasing heterotrophic feeding to compensate for reduced symbiont autotrophy (Grottoli et al. 2006), the position of the isotopic niche of a coral can shift in isotopic space to reflect a change in resource use. Therefore, potential shifts in the sizes and position of isotopic niches can provide insight into changes in coral trophic ecology. Coral bleaching surveys in the Maldives showed that *Galaxea* were more susceptible to bleaching than *Pachyseris*, which in turn were more susceptible than *Pocillopora* (Ibrahim et al. 2017). However, it is unknown how coral susceptibility to the thermal stress event translated into coral survival for these genera.

In situ seawater temperature was recorded in shallow (10 m) and deep (30 m) reefs in the year prior to and following the thermal stress event. Because species-specific coral bleaching susceptibility can change as a function of depth (Baird et al. 2018), an adjusted maximum monthly mean temperature was calculated for shallow and deep reefs to investigate the severity of the thermal stress event. Eight months after the extraordinary thermal stress event and mass coral bleaching in the Maldives, we investigated the colony abundance and $\delta^{13}C$ and $\delta^{15}N$ values of three species of coral hosts (*Galaxea fascicularis, Pachyseris speciosa*, and *Pocillopora verrucosa*) and their symbionts to evaluate the effect of a thermal stress event on surviving coral colonies from shallow and deep reefs. Under thermal stress conditions, *P. verrucosa* can utilize lipid reserves (Rodríguez-Troncoso et al. 2016) while *G. fascicularis* can increase heterotrophic feeding (Borell et al. 2008; Ferrier-Pagès et al. 2010). The heterotrophic feeding capability of the species *Pachyseris speciosa* is unknown, but *P. speciosa* does have active mesenterial filaments that can aid in ingesting small particles (Goreau et al. 1971; Stafford-Smith and Ormond 1992; Browne et al. 2012). It was hypothesized that, eight months after the thermal stress, the relatively rapid carbon turnover of symbionts would result in symbiont $\delta^{13}C$ values that reflect normal (unimpeded autotrophy) species-specific trophic strategies as characterized one year before the thermal stress event (Chapter 2). If symbiont autotrophy was impeded during the

thermal stress event, lower $\delta^{13}C$ values and higher $\delta^{15}N$ values of coral hosts were expected due to increased heterotrophy, potentially driven by the thermal stress related disruption to the coral symbiosis. Further, it was hypothesized that host $\delta^{13}C$ values would be more negative in coral species that depended on prolonged heterotrophic feeding during recovery (Hughes and Grottoli 2013). Although symbiont $\delta^{13}C$ and $\delta^{15}N$ values are unlikely retain a bleaching signal due to the turnover of symbionts, it is possible that increased symbiont $\delta^{15}N$ values could reflect increased host $\delta^{15}N$ values since symbionts acquire the majority of their nitrogen from host-derived nitrogen cycling (Tanaka et al. 2015, 2018). It was expected that coral isotopic niches would change in response to the impact of the thermal stress event on normal symbiont autotrophy, and that an increase in heterotrophy would result in a shift in the isotopic niche with a shift to relatively higher $\delta^{15}N$ values and relatively lower $\delta^{13}C$ values. However, if autotrophy was consequently supported by increased heterotrophy, a larger isotopic niche reflecting the wider range of $\delta^{13}C$ and $\delta^{15}N$ values would be expected. Finally, if symbiont autotrophy was not impeded during the thermal stress event that resulted in mass coral bleaching (West and Salm 2003; Sampayo et al. 2008), it was expected that $\delta^{13}C$ and $\delta^{15}N$ values of coral hosts and symbionts would be similar to values recorded one year before the thermal stress in the Maldives unless water column POM signatures have changed significantly over the study period. To investigate potential changes in particulate organic availability in the water column (10-50 m depth), $\delta^{13}C$ and $\delta^{15}N$ values of POM were compared one year before and one year after the onset of the thermal stress event. In our survey eight months after the cessation of the thermal stress event, inorganic nutrients were measured (nitrate, $\delta^{15}N$-nitrate and $\delta^{18}O$-nitrate) to investigate nitrate sources and the oligotrophic status of the water column (Kendall et al. 2008; Casciotti 2016).

3.3 Materials and methods

3.3.1 Sample collection

Coral fragments (*Galaxea fascicularis*, *Pachyseris speciosa*, and *Pocillopora verrucosa*) were collected from shallow (10 m) and deep (30 m) reefs by divers across oceanic and Inner Sea reefs of the central Maldives on an expedition between 20 March and 1 April 2017 (Supplementary Information Table S3.1). Following up on an expedition from March-April 2015, we resurveyed 19 sites and surveyed three new sites (Table S3.1). Because equal effort (time investment) was applied to coral collections at each site and depth (target of nine colonies/species/depth), the number of collected coral fragments was assessed as a proxy for the visible abundance of colonies across shallow and deep reefs before (2015) and after (2017) the thermal stress event in the Maldives. Plankton were collected at dusk by towing mesh nets (53 and 250 μm) submerged below the surface for 10 minutes at a speed of 2-3 knots (Table S3.1).

Seawater samples (10 L) were collected by divers on the reef (10 and 30 m) and by a hand pump from the surface (target depth of 10, 30, and 50 m). Actual depth of seawater collected by pump was recorded using a Sensus Ultra (ReefNet Inc.). Depth of seawater samples was subsequently categorized into four depth zones: 10 m, 20-29 m, 30-39 m, 40-50 m. Seawater for nutrient analysis was filtered through 0.22 μm polyethersulfone syringe filters (Millex-GP, Merck). Seawater for isotopic analysis of particulate organic matter (POM) was filtered through pre-combusted (450°C, 5 h) 0.4 μm nominal pore size glass fiber filters (Machery-Nagel). The particulate organic nitrogen (PON) concentration was calculated as the micrograms of nitrogen per liter of seawater.

Temperature was recorded in shallow (10 m) and deep (30 m) reefs at three sites (see Chapter 2, Fig. 2.4a: sites 1/27, 4 and 6) between April 2015 and October 2016 (HOBO Pendant, Onset, U.S.A.; 15 min interval). In addition, remotely sensed sea surface temperatures (SST) and maximum monthly mean (MMM) SST climatology were obtained for the Maldives NOAA Virtual Station (Liu et al. 2014). Degree Heating Weeks (DHW) for *in situ* temperature data were calculated from 12 week accumulated +1°C Hotspots (daily temperature minus MMM climatology) based on NOAA methodology and compared to DHW of 5-km SST products from the Maldives virtual station (NOAA Coral Reef Watch 2013). Because of differences between SST and temperatures at 10 m and 30 m depth, we used an adjusted MMM for *in situ* seawater temperatures. For the period preceding, during, and following the thermal stress event in the Maldives (January through September 2016), we calculated the difference between the daily SST of the Maldives NOAA Virtual Station and the average *in situ* temperatures recorded at 10 m and 30 m depth (each an average of three sites). $MMM_{adjusted}$ was the difference between the SST MMM and the average of the difference between SST and temperatures at 10 or 30 m depth, respectively. The NOAA Bleaching Alert Level designations were used to describe the DHW data as the following: significant bleaching is expected within a few weeks of Bleaching Alert Level 1 ($4 \leq DHW < 8$) and widespread bleaching and significant mortality are likely during Bleaching Alert Level 2 ($DHW \geq 8$).

3.3.2 Inorganic nutrient and isotopic analyses

Seawater inorganic nutrients (NO_3^-, NH_4^+, PO_4^{-3}) were determined by flow injection analysis at the Advanced Water Management Centre, University of Queensland and at Queensland Health. The Redfield ratio (average ± SD) of seawater were calculated (($[NO_3^-]+[NH_4^+]$)/$[PO_4^{-3}]$) to estimate potential nutrient limitations in the water column (Redfield 1958, 1963). Nitrogen and oxygen isotope ratios ($\delta^{15}N$ and $\delta^{18}O$) of seawater NO_3^- (n=21) were analyzed by a bacterial denitrification assay at

the Woods Hole Oceanographic Institute (Sigman et al. 2001; Casciotti et al. 2002). Repeated measurements of three references resulted in analytical precision of <0.001. Coral host and symbiont tissue and POM were prepared as described in Chapter 2. Isotope ratios ($\delta^{13}C$ and $\delta^{15}N$) of coral host (n=238) and symbiont (n=238) tissue and plankton (n=30) were analyzed with a PDZ Europa ANCA-GSL elemental analyzer. Glass fiber filters (POM; n=112) were analyzed with an Elementar Vario EL Cube elemental analyzer (Elementar Analysensysteme GmbH, Hanau, Germany). Analyzers were interfaced to a PDZ Europa 20-20 isotope ratio mass spectrometer (Sercon Ltd., Cheshire, U.K.), at the University of California Davis, U.S.A. Repeated measurements of internal standards (G-6: Nylon 6, G-13: Bovine liver, G-20: Glutamic acid, G-21: Enriched alanine) resulted in precision of ≤0.14‰ for $\delta^{13}C$ and ≤0.15‰ for $\delta^{15}N$. Stable isotope ratios are reported in the delta (δ) notation, which is expressed in per mil (‰): $\delta^{13}C$ or $\delta^{15}N = [(R_{sample} / R_{standard}) -1] \times 1000$ where R represents the ratio of the heavy to light isotope (i.e. $^{13}C/^{12}C$ or $^{15}N/^{14}N$). A subset of samples (n=25) run in triplicate showed that the analytical precision of the isotopic analyses was within ±0.1‰ for both $\delta^{13}C$ and $\delta^{15}N$.

3.3.3 Statistical analyses

POM samples with very low nitrogen (<10 µg) were removed (n=21) from analyses due to analytical detection limitations. Statistical analyses and visualization were conducted using the R computing environment (Wickham 2009; Wilke 2017; R-Core-Team 2018). Stable isotope ratios (average ± SD) of coral hosts, symbionts, and POM were analyzed for the factors depth (shallow versus deep reefs) and year before (2015) versus after (2017) the thermal stress event in 2016. Since previous coral $\delta^{13}C$ and $\delta^{15}N$ results (Chapter 2) showed species-specific differences, individual ANOVA were applied for each coral species with post hoc Tukey HSD tests used to further explore significant species or interactive effects. Isotopic ratios were not transformed (Dorado et al. 2012), and the α value adjusted following a Bonferroni correction for multiple tests ($\alpha = 0.05/6$) was 0.008. To examine variation in the isotopic niche sizes and relative position among coral species host and symbionts before and after the thermal stress event (2015 isotopic data from Chapter 2), maximum likelihood standard ellipses were fitted to $\delta^{13}C$ and $\delta^{15}N$ data with the standard ellipse area (SEA) representing the isotopic niche (Newsome et al. 2007). Bayesian multivariate normal distributions were fitted to the data ($2x10^6$ posterior draws with 10^4 burn-in) and the SEA-B (Bayesian SEA) were calculated on the posterior distribution (Jackson et al. 2011). Credibility intervals of model solutions (SEA-B) are presented in probability density distribution plots with SEA shown (SEA and SEA-c yielded similar values because of our large sample sizes; see Table S3.3). To examine the effect of the thermal stress event on coral isotopic niches, potential changes in the isotopic niche size (SEA-B) associated with each

coral species' host or symbionts were calculated using the probability of the posterior distribution. The posterior draws were compared for each group (host or symbiont) per reef depth (shallow or deep) relative to the thermal stress event (pre- or post-thermal stress event). Groups are only compared across the same reef depth (e.g., shallow *G. fascicularis* pre-thermal stress versus shallow *G. fascicularis* post-thermal stress). The magnitude of the proportion of draws is used as a proxy for the probability that one group's posterior distribution (of isotopic niche size) is smaller than that of the other group. A probability of >90% was considered a significant change in isotopic niche size and is marked with an asterisk (*) in the probability density distribution plots.

3.4 Results

3.4.1 Seawater temperature and inorganic nutrients

Seawater temperature was measured in shallow (10 m) and deep (30 m) reefs between April 2015 and October 2016 (Fig. 3.1, Table S3.1). The maximum daily temperatures recorded in shallow and deep reefs were 31.98°C and 31.88°C (April-May 2016) while minimum daily temperatures reached 26.68°C and 25.81°C in January and September 2016, respectively. For oceanic reefs on the west side of the double atoll chain (Dinoluga and Mathiveri), the lowest monthly average temperature was in January (28.33-28.55°C) during the northeast monsoon when the wind direction is from the east (Fig. 3.1a; Table S3.2). For the oceanic reef on the east side of the central atoll chain (Hulhumale), the lowest monthly average temperature (28.22°C) was in September during the southwest monsoon when wind direction is from the west (Fig. 3.1a; Table S3.2). Between April and July 2016, NOAA Coral Reef Watch SST data recorded 44 days at Bleaching Alert Level 1 ($4 \leq DHW < 8$) and 59 days at Bleaching Alert Level 2 ($DHW \geq 8$), with a maximum of 10 DHW. Using the $MMM_{adjusted}$, our *in situ* temperature data from shallow reefs (10 m depth) recorded 44 days at Bleaching Alert Level 1 ($4 \leq DHW < 8$) and 72 days at Bleaching Alert Level 2 ($DHW \geq 8$), with a maximum of 12 DHW. Also using the $MMM_{adjusted}$, temperature on deep reefs (30 m depth) sustained 55 days at Bleaching Alert Level 1 ($4 \leq DHW < 8$) and 62 days at Bleaching Alert Level 2 ($DHW \geq 8$), with a maximum of 10 DHW. Shallow and deep reefs' DHW remained at Bleaching Alert Level 1 ($4 \leq DHW < 8$) until early August 2016, despite temperatures declining below Hotspot thresholds by early July 2016. The offset (average ± SE) between satellite SST and temperatures from 10 m and 30 m depth were 0.36 ± 0.01 and 0.46 ± 0.02, respectively (Fig. 3.1b).

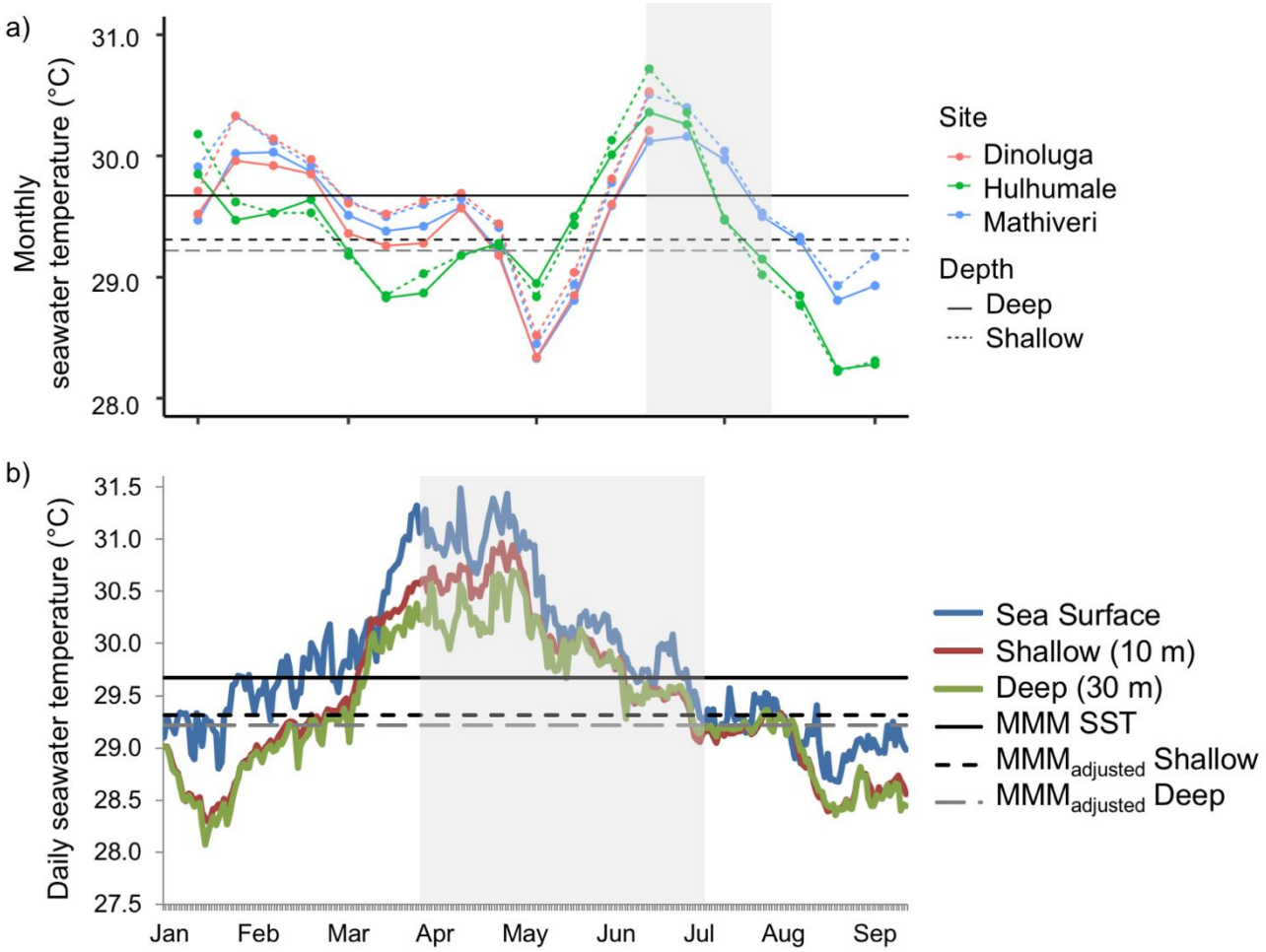

Figure 3.1. Seawater temperature from shallow (10 m) and deep (30 m) reefs in the central Maldives. a) Monthly seawater temperature (April 2015 to October 2016) from shallow and deep reefs of three sites. b) Daily sea surface temperature (SST; NOAA Coral Reef Watch Virtual Station) and shallow reef and deep reef seawater temperature (average of three sites shown in 2a) between January and September 2016. Monthly maximum mean (MMM) of SST and $MMM_{adjusted}$ (adjusted relative to SST) of shallow and deep reefs are shown. Shading indicates the mass coral bleaching event in the Maldives (April through July 2016; Ibrahim et al. 2017).

There were significant differences in the nitrate and phosphate concentrations among seawater samples collected (2017) from different reef depths (ANOVA, $F_{3,89}$=9.276, $p<0.001$ and $F_{3,89}$=8.18, $p<0.001$, respectively), with a range of 0.30-2.47 µM for nitrate and 0.01-0.29 µM for phosphate. The mean concentration of nitrate was greatest (1.40 µM) in seawater samples from mesophotic (40-50 m) depths compared to other reef depths (Tukey $p \leq 0.001$), and included the three highest concentrations >2.00 µM recorded (Fig. S3.1). Average phosphate concentrations were highest (0.13 µM) at mesophotic depths of 40-50 m compared to all other shallower depths (Tukey $p<0.004$). The concentration of ammonium did not differ between depths (ANOVA, $F_{3,92}$=2.154,

p=0.099) although there was a substantial range in the concentration (0.18-2.33 μM). Low nutrient concentrations resulted in variable Redfield ratios of 21.85 ± 14.18, with a range between 6.21 and 100.00.

The depth from which seawater was sampled (2017) did not affect $\delta^{15}N$ or $\delta^{18}O$ values of nitrate ($F_{2,18}$=0.492, p=0.620 and $F_{2,18}$=3.368, p=0.057, respectively). The $\delta^{15}N$ and $\delta^{18}O$ values of seawater nitrate revealed substantial variability within depths for each isotope, with nitrate across all depths likely to have been derived from both marine and atmospheric sources (Fig. S3.2 and S3.3). The $\delta^{18}O$ values of nitrate were particularly high, with an average of 40.8 ± 21.0‰ in shallow reefs (10 m), an average of 32.5 ± 22.7‰ in deep reefs at 30-39 m depth, and an average of 14.2 ± 13.9‰ at mesophotic depths (40-50 m). The average $\delta^{15}N$ of nitrate was also highest (10.8 ± 4.2‰) in shallow (10 m) reefs but was lower at increasing depths of 30-39 m (8.5 ± 3.0‰) and 40-50 m (8.4 ± 6.9‰). With an average $\delta^{15}N$ of 9.7 ± 3.6‰ and $\delta^{18}O$ of 50.0 ± 13.5‰, Group 1 represents atmospheric-derived nitrate that is characterized by enriched $\delta^{18}O$ values. In contrast, Group 2 had an average $\delta^{15}N$ of 10.0 ± 6.2‰ and $\delta^{18}O$ of 18.2 ± 6.9‰ and represents marine-derived nitrate (Fig. S3.3).

3.4.2 Isotope ratios of plankton and particulate organic matter

Net mesh size (53 μm and 250 μm) did not affect surface plankton $\delta^{13}C$ and $\delta^{15}N$ values in 2017 ($F_{1,28}$=0.288, p=0.596 and $F_{1,28}$=0.521, p=0.477, respectively). Plankton had an average $\delta^{13}C$ value of -21.5 ± 0.4‰ and an average $\delta^{15}N$ value of 6.4 ± 0.8‰. POM was filtered from seawater collected from 10, 20-29, 30-39, and 40-50 m depths to investigate the isotope ratios of organic sources. Reef depth did not affect the isotope ratios of POM so data from all depths were grouped together for analysis (ANOVA $\delta^{13}C$ $F_{3,87}$=0.769, p=0.515; $\delta^{15}N$ $F_{3,87}$=0.937, p=0.426). The average $\delta^{13}C$ of POM was -21.4 ± 2.4‰ with a range of -25.8 to -15.7‰, and the average $\delta^{15}N$ of POM was 6.5 ± 1.2‰, with a range of 3.3‰ to 8.8‰. When POM sampled from the year prior to thermal stress event (2015) was compared to the year after (2017), a significant change in $\delta^{13}C$ values (ANOVA $F_{1,139}$=70.27, p<0.001) and $\delta^{15}N$ values was observed (ANOVA $F_{1,139}$=112.4, p<0.001; Fig. S3.4). Further, there was a lower concentration of particulate organic nitrogen following the thermal stress event (ANOVA $F_{1,138}$=83.84, p<0.001; Fig. S3.4).

Table 3.1. Carbon and nitrogen ($\delta^{13}C$ and $\delta^{15}N$) stable isotope ratios and C:N ratios (mean ± SD) of three coral host species and their symbionts collected from shallow (10 m) and deep (30 m) reefs in the year before (2015) and after (2017) the thermal stress event in the Maldives.

	2015				2017			
Coral Host	n	$\delta^{13}C$	$\delta^{15}N$	C:N	n	$\delta^{13}C$	$\delta^{15}N$	C:N
Galaxea fascicularis								
Shallow	31	-15.5 ± 1.2	5.4 ± 0.6	6.3 ± 0.6	41	-16.7 ± 1.1	6.0 ± 0.5	5.4 ± 0.4
Deep	29	-17.6 ± 0.8	5.6 ± 0.4	6.1 ± 0.5	39	-17.6 ± 0.6	6.1 ± 0.6	5.3 ± 0.4
Pachyseris speciosa								
Shallow	22	-15.2 ± 1.4	5.2 ± 0.5	6.4 ± 0.4	31	-15.5 ± 1.5	6.0 ± 0.6	5.9 ± 0.6
Deep	30	-15.1 ± 1.0	5.4 ± 0.5	6.4 ± 0.2	47	-15.5 ± 1.3	5.9 ± 0.6	6.0 ± 0.6
Pocillopora verrucosa								
Shallow	24	-17.4 ± 1.1	5.8 ± 0.3	5.7 ± 0.3	41	-17.6 ± 0.8	6.1 ± 0.5	5.2 ± 0.4
Deep	25	-18.0 ± 0.8	5.4 ± 0.4	6.0 ± 0.4	39	-18.5 ± 0.8	5.9 ± 0.4	5.2 ± 0.4
Symbionts								
Galaxea fascicularis								
Shallow	26	-15.0 ± 1.3	4.3 ± 0.5	7.9 ± 1.0	41	-15.6 ± 1.7	4.6 ± 0.6	9.6 ± 1.5
Deep	29	-17.2 ± 1.0	4.9 ± 0.7	8.1 ± 1.3	39	-16.6 ± 1.7	4.8 ± 0.5	9.3 ± 1.3
Pachyseris speciosa								
Shallow	22	-14.0 ± 2.1	5.3 ± 0.5	9.7 ± 1.5	31	-14.4 ± 1.9	5.4 ± 0.8	11.8 ± 2.9
Deep	30	-14.1 ± 1.6	5.7 ± 0.6	9.8 ± 1.6	47	-14.0 ± 1.7	5.4 ± 0.8	10.8 ± 2.1
Pocillopora verrucosa								

Shallow	24	-16.3 ± 1.3	5.4 ± 0.6	7.1 ± 1.1	41	-16.6 ± 1.1	5.2 ± 0.5	8.8 ± 1.2
Deep	24	-17.0 ± 0.9	5.2 ± 0.6	6.8 ± 0.9	39	-17.8 ± 1.0	4.4 ± 0.6	9.1 ± 1.5

3.4.3 Coral colony abundance

The number of coral fragments collected was assessed as a proxy for the visible abundance of coral colonies over depth because equal effort was applied to sample the target number of colonies (Table S3.2). There was a significant interaction of coral species and reef depth on the visible abundance of coral colonies (ANOVA, $F_{2,108}$=21.636, p<0.001) but no effect of sampling year. Differences in coral abundances over depth included: greater abundance of *P. speciosa* (p<0.001) in deep reefs compared to shallow reefs; greater abundance of *G. fascicularis* in shallow reefs compared to deep reefs (p=0.011); greater abundance of *P. speciosa* in deep reefs compared to *G. fascicularis* (p=0.002) and *P. verrucosa* (p=0.016) in deep reefs; and lower abundance of *P. speciosa* in shallow reefs compared to *G. fascicularis* (p<0.001) and *P. verrucosa* (p=0.007) in shallow reefs (Fig. S3.5).

3.4.4 Isotopic ratios of coral hosts and symbionts

The δ^{13}C values of the host tissues of *G. fascicularis* were significantly different before and after the 2016 thermal stress event (2015 versus 2017 sampling years) and between depths (10 versus 30 m; Tables 3.1 and 3.2). Shallow reef host *G. fascicularis* δ^{13}C values significantly decreased between sampling years (from -15.5‰ to -16.7‰ before and after the thermal stress, respectively; Tukey p<0.001). After the thermal stress event, δ^{13}C values of shallow (-16.7‰) and deep (-17.6‰) colonies of host *G. fascicularis* were significantly different (Tukey p=0.001). Depth, but not sampling year, was a significant factor affecting the δ^{13}C values of host *P. verrucosa* (Table 3.2). In contrast, neither sampling year nor reef depth affected host *P. speciosa* δ^{13}C values (Table 3.2). All coral host species' δ^{15}N values significantly increased following the thermal stress event, with each species mean δ^{15}N around 6‰. Reef depth only affected δ^{15}N values of host *P. verrucosa*, with lower δ^{15}N values recorded in deep reef colonies prior to the thermal stress (Tables 3.1 and 3.2).

The symbionts of *G. fascicularis* and *P. verrucosa* had δ^{13}C values which reflected those of their hosts, with significant differences (~1‰) between shallow and deep symbionts (Tables 3.1 and 3.2). In contrast, *P. speciosa* symbiont δ^{13}C values were similar between depths and before and after the thermal stress event (Table 3.1). Average δ^{15}N values of *G. fascicularis* symbionts were consistently the lowest among the three species (<5‰) and were significantly affected by reef depth (Tables 3.1 and 3.2). Sampling year and reef depth significantly affected δ^{15}N values of *P. verrucosa* symbionts, which was primarily due to the lower mean δ^{15}N value (4.4‰) of deep symbionts after the thermal stress in contrast to the higher δ^{15}N (≥5.2‰) from other depths/years (Tables 3.1 and 3.2).

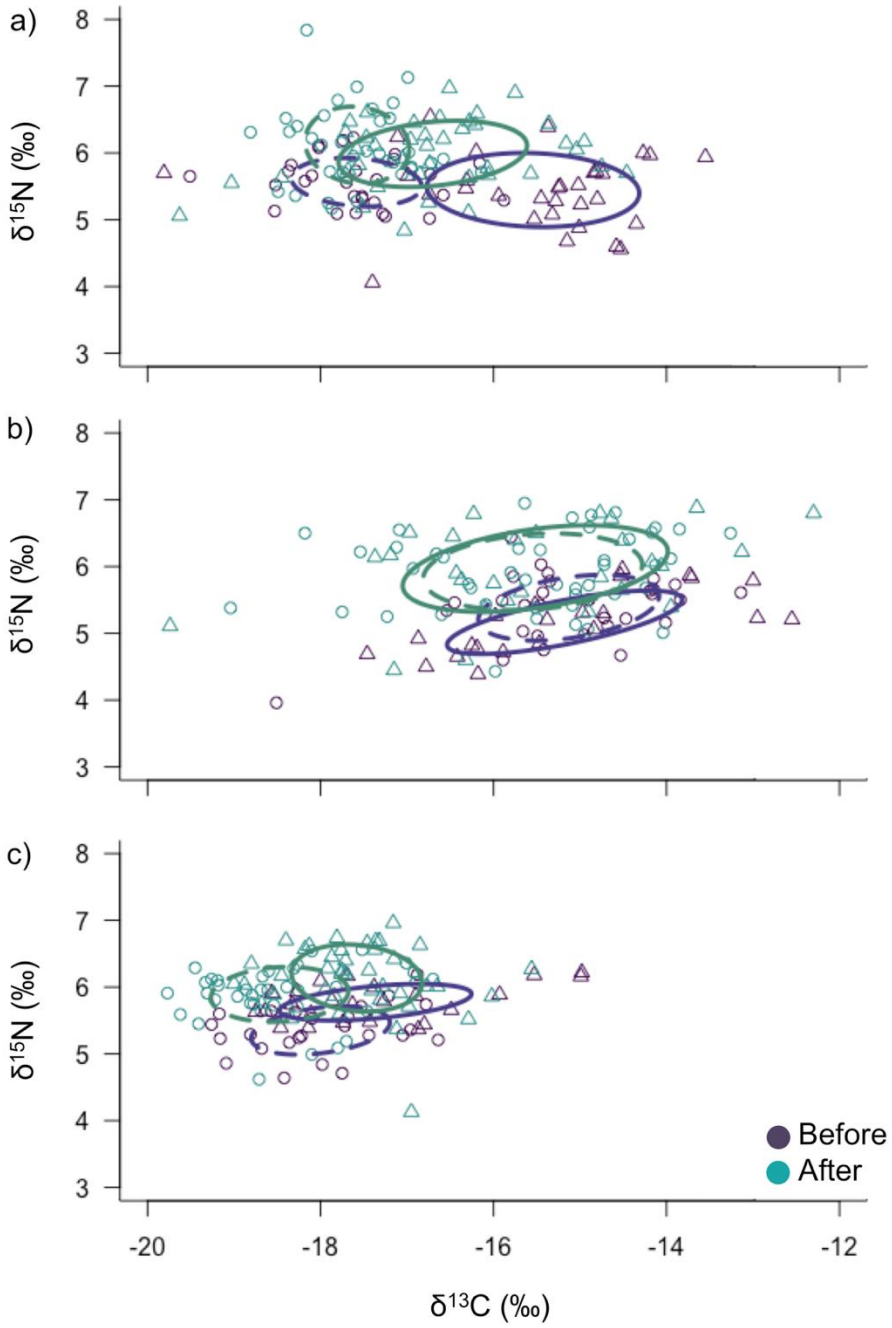

Figure 3.2. Isotopic niches of shallow (10 m: △, solid line ellipse) and deep (30 m: ○, dashed line ellipse) coral hosts a) *Galaxea fascicularis*, b) *Pachyseris speciosa*, and c) *Pocillopora verrucosa* one year before (2015) and eight months after (2017) the thermal stress event in the Maldives. Maximum likelihood standard ellipses were fitted to multivariate isotopic data ($\delta^{15}N$ and $\delta^{13}C$) with variation of individual samples shown.

3.4.5 Isotopic niches

Maximum likelihood standard ellipses fitted to coral host $\delta^{13}C$ and $\delta^{15}N$ data from before (2015) and after (2017) the thermal stress event revealed shifts in the isotopic niches of each coral host species

that were largely due to increased $\delta^{15}N$ values (Fig. 3.2). After the thermal stress, significant changes in the $\delta^{13}C$ and $\delta^{15}N$ values of shallow host *G. fascicularis* resulted in a shift in the position of its isotopic niche, which converged with the isotopic niche of host *G. fascicularis* from deep reefs (Fig. 3.2a). Prior to the 2016 thermal stress event, the size of the isotopic niche of host *G. fascicularis* differed between shallow (2.1‰^{2}) and deep (0.8‰^{2}) reefs (Fig. 3.4a, Table S3.3). However, the isotopic niche size of host *G. fascicularis* from shallow reefs decreased (probability 92%) while the isotopic niche of deep *G. fascicularis* increased (probability 91%) after the thermal stress (Fig. 3.4a, Table S3.3). Similarly, there were distinct isotopic niche positions of the symbionts of shallow and deep *G. fascicularis* before the thermal stress event. However, *G. fascicularis* symbiont isotopic niches overlapped after the thermal stress due to converging $\delta^{13}C$ values (Fig. 3.3a). The shift in the isotopic niche position of symbionts of shallow *G. fascicularis* reflected the increased isotopic niche size after the thermal stress event (probability 99%; Fig. 3.4b, Table S3.3).

Host *P. speciosa* showed a clear shift in the position of both its shallow and deep isotopic niches due to increased $\delta^{15}N$ values (Fig. 3.2b). The isotopic niche sizes of both shallow and deep host *P. speciosa* were larger post-thermal stress (probability 91% and 92%, respectively), with the shallow isotopic niche doubling in size (1.4‰^{2} to 2.9‰^{2}) (Fig. 3.4c, Table S3.3). In contrast, the isotopic niches of *P. speciosa* symbionts largely overlapped before and after the thermal stress (Fig. 3.3b). After the thermal stress event, there were shifts in the positions of the shallow and deep isotopic niches of host *P. verrucosa* although the niches showed overlap between the two time points (Fig. 3.2c). The isotopic niche size of shallow host *P. verrucosa* increased post-thermal stress (probability 99%) but there was no change in the size of its isotopic niche in deep reefs (probability 25%) (Fig. 3.4e). Following the thermal stress, deep reef *P. verrucosa* symbionts showed a clear shift in isotopic niche position due to decreased $\delta^{15}N$ values (Fig. 3.3c). However, the shift in niche position did not reflect a change in isotopic niche size (Fig. 3.4). Overall, symbiont isotopic niches from both years were constrained to $\delta^{15}N$ values between +4 and 6‰. The isotopic niches of symbionts were generally larger than host isotopic niches, in some cases symbiont isotopic niches were ~two-fold greater in size (Fig. 3.3, Table S3.3).

Further, the $\Delta^{13}C$ proxy for coral heterotrophy ($\delta^{13}C_{host}$ - $\delta^{13}C_{symbiont}$) and $\Delta^{15}N$ proxy for nitrogen recycling was evaluated for each species before and after the thermal stress event. All three species had an increase in $\Delta^{15}N$ driven by the change in $\delta^{15}N$ values of all coral hosts (Figs. 3.2 and 3.5). Among the three species, shallow and deep *G. fascicularis* and deep *P. speciosa* showed a decrease in $\Delta^{13}C$ but deep *P. verrucosa* had an increase in $\Delta^{13}C$ following the thermal stress event (Fig. 3.5).

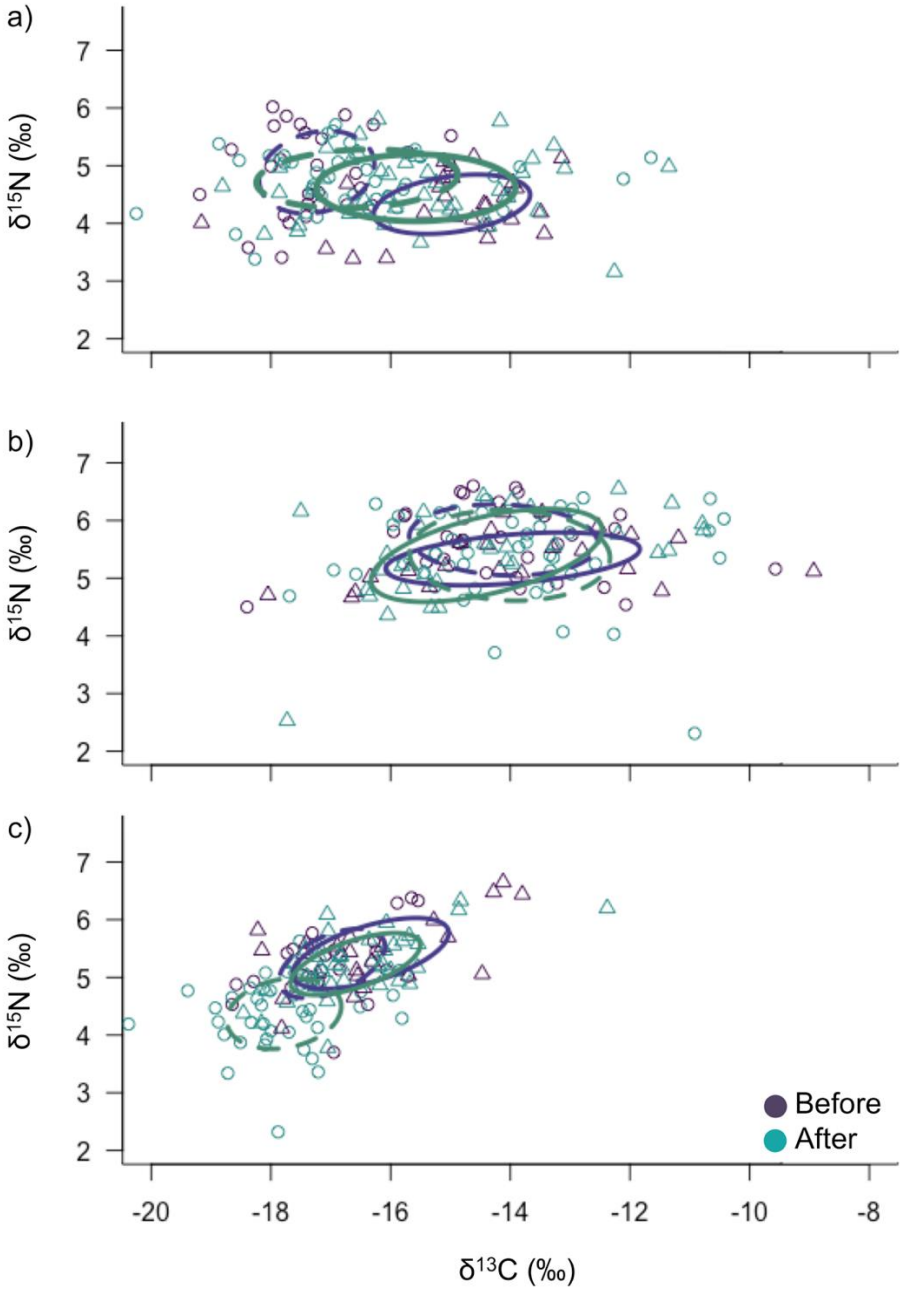

Figure 3.3. Isotopic niches of shallow (10 m: △, solid line ellipse) and deep (30 m: ○, dashed line ellipse) symbionts of a) *Galaxea fascicularis*, b) *Pachyseris speciosa*, and c) *Pocillopora verrucosa* one year before (2015) and eight months after (2017) the thermal stress event in the Maldives. Maximum likelihood standard ellipses were fitted to multivariate isotopic data ($\delta^{15}N$ and $\delta^{13}C$) with variation of individual samples shown.

Table 3.2. Multi-factorial analysis of variance (ANOVA) tested the effect of sampling year (2015 versus 2017) relative to the 2016 thermal stress event and reef depth (10 m versus 30 m) on the carbon ($\delta^{13}C$) and nitrogen ($\delta^{15}N$) isotope values of three species of coral hosts and their symbionts.

		Coral Host			Symbiont		
		df	F	p	df	F	p
$\delta^{13}C$	*Galaxea fascicularis*						
	Year	1,132	12.15	**0.001**	1,131	0.18	0.672
	Depth	1,132	71.51	**<0.001**	1,131	34.72	**<0.001**
	Year*Depth	1,132	12.42	**0.001**	1,131	6.04	0.015
	Pachyseris speciosa						
	Year	1,121	2.66	0.106	1,126	0.13	0.722
	Depth	1,121	0.00	0.990	1,126	0.28	0.600
	Year*Depth	1,121	0.03	0.875	1,126	0.68	0.411
	Pocillopora verrucosa						
	Year	1,124	4.25	0.041	1,123	6.84	0.010
	Depth	1,124	28.47	**<0.001**	1,123	27.92	**<0.001**
	Year*Depth	1,124	0.90	0.344	1,123	1.97	0.163
$\delta^{15}N$	*Galaxea fascicularis*						
	Year	1,134	35.27	**<0.001**	1,131	0.46	0.497
	Depth	1,134	1.28	0.260	1,131	10.10	**0.002**
	Year*Depth	1,134	0.03	0.866	1,131	3.83	0.053
	Pachyseris speciosa						
	Year	1,121	41.14	**<0.001**	1,126	0.99	0.321
	Depth	1,121	0.40	0.529	1,126	1.13	0.290
	Year*Depth	1,121	1.65	0.202	1,126	1.60	0.208
	Pocillopora verrucosa						
	Year	1,124	37.45	**<0.001**	1,124	24.10	**<0.001**
	Depth	1,124	18.30	**<0.001**	1,124	34.53	**<0.001**
	Year*Depth	1,124	1.38	0.242	1,124	9.46	**0.003**

Significant p-values are in bold. Due to multiple testing, the adjusted α value following a Bonferroni correction was $\alpha=0.008=0.05/6$.

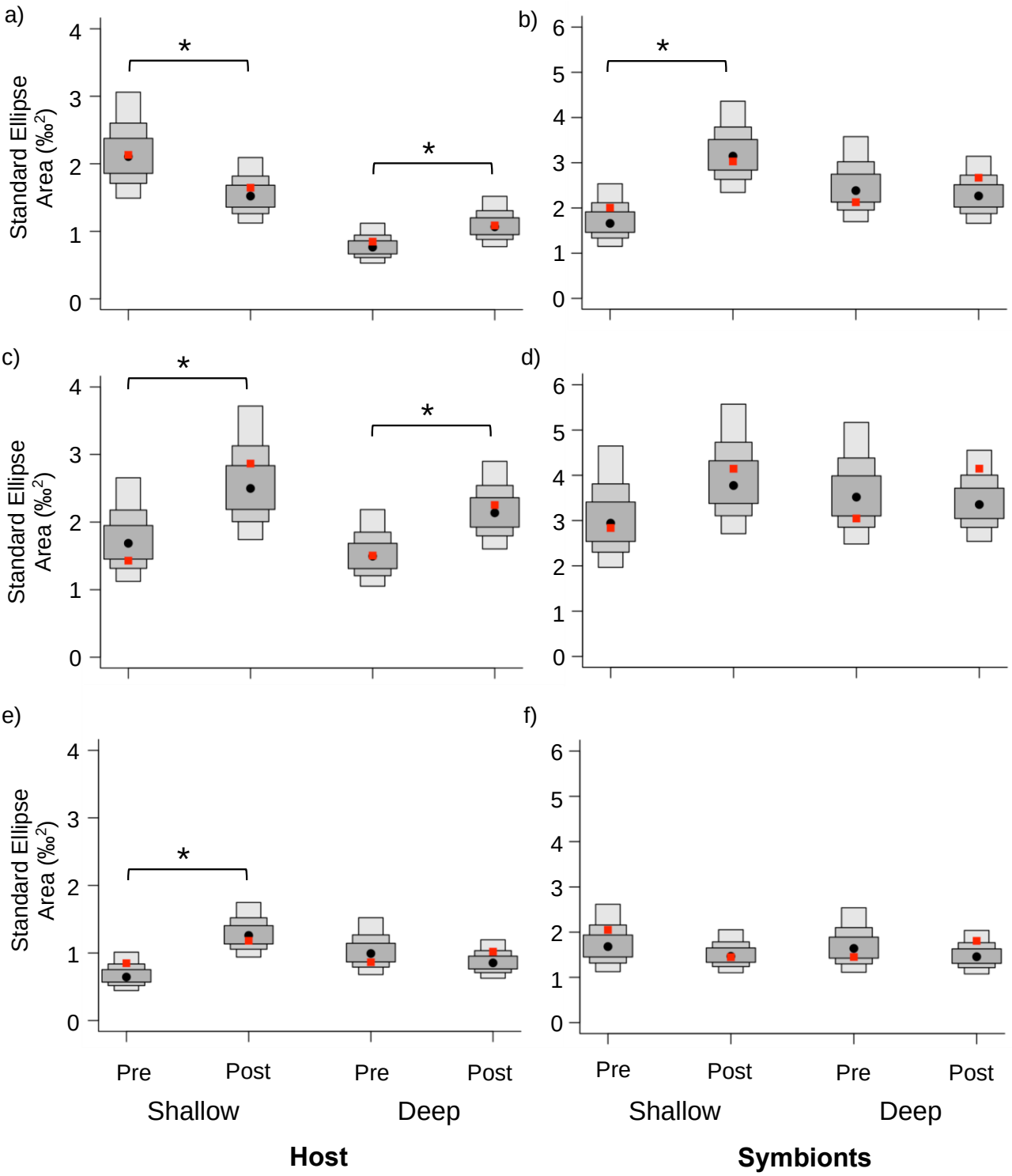

Figure 3.4. Isotopic niche sizes of coral hosts and their symbionts from shallow (10 m) and deep (30 m) reefs before ('Pre') and after ('Post') thermal stress event in the Maldives in 2016. Standard ellipse area and Bayesian standard ellipse area (SEA and SEA-B, respectively) of a) *Galaxea fascicularis* coral hosts and b) symbionts, c) *Pachyseris speciosa* coral hosts and d) symbionts, e) *Pocillopora verrucosa* coral hosts and f) symbionts. The SEA (red square) and mode of SEA-B (black circle) are plotted on top of grey scale shading indicating posterior distribution credibility intervals (50%, 75%,

and 95%). For a given species/tissue type/depth, a change in isotopic niche size after the thermal stress event is signified with an asterisk (*) in the plots (probability of >90%). Note different scale of y-axis between hosts (left panel) and symbionts (right panel).

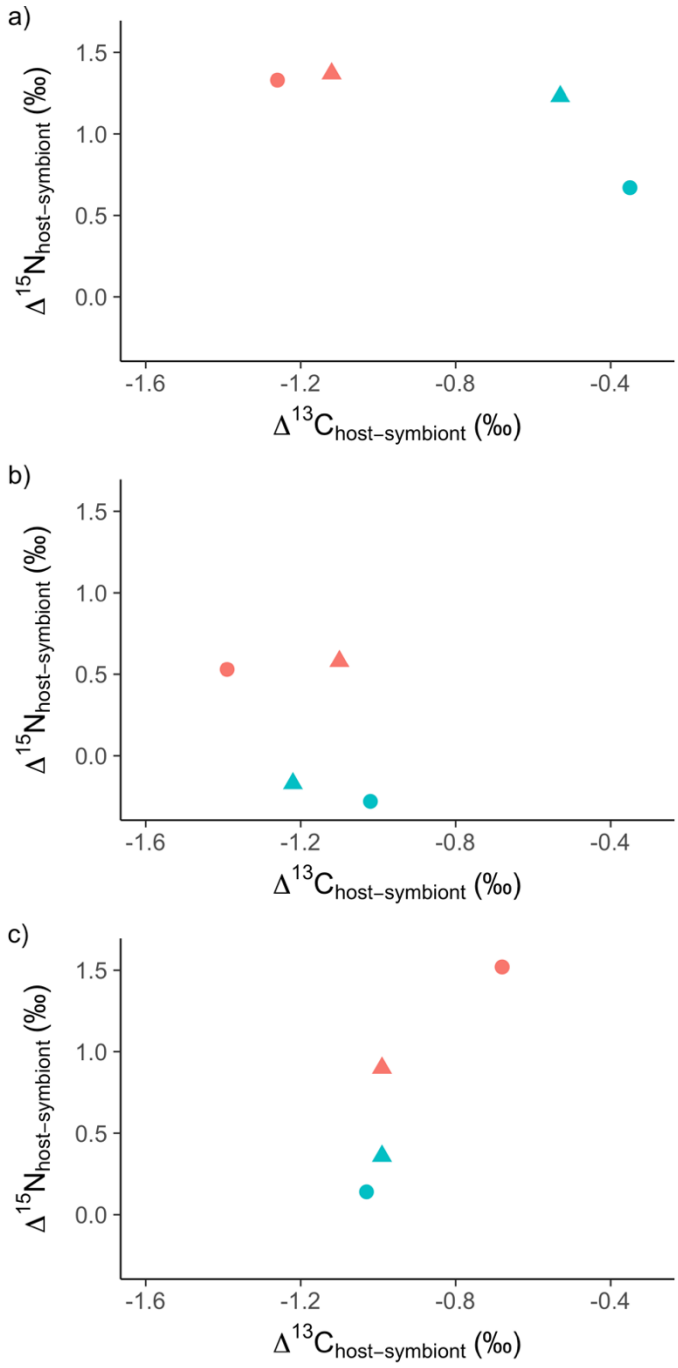

Figure 3.5. Comparisons of carbon and nitrogen cycling between coral hosts and their symbionts a) *Galaxea fascicularis*, b) *Pachyseris speciosa*, and c) *Pocillopora verrucosa* before (green) and after (red) the thermal stress event. For example, $\Delta^{13}C$ is the difference between $\delta^{13}C_{Host}$ and $\delta^{13}C_{Symbionts}$ for a given species from shallow (triangle) or deep (circle) reefs.

3.5 Discussion

The trophic ecology of coral communities is sensitive to environmental conditions (Williams et al. 2018), with diverse morphologies and life history strategies associated with different responses by reef-building corals to disturbance events such as thermal stress and resulting mass coral bleaching (Darling et al. 2013). Degree heating weeks calculated from *in situ* seawater temperatures from shallow and deep reefs in the central Maldives show that the thermal stress (Bleaching Alert Level 1 or 2) lasted nearly four months in 2016. Although the bleaching history of the specific coral colonies was unknown, *in situ* seawater temperature and isotopic results indicated that both shallow and deep reefs experienced severe thermal stress (12 and 10 maximum DHW, respectively). Indeed, mass coral bleaching was prevalent across the central and southern atolls of the Maldives (Ibrahim et al. 2017; Perry and Morgan 2017). The isotopic shifts in coral tissue observed eight months after the thermal stress event in the Maldives provides evidence for prolonged changes in coral trophic strategy (Baumann et al. 2014). The photosynthetic efficiency of the symbiont populations presumably recovered during this period, given that we sampled apparently healthy (i.e., non-bleached) colonies of the three coral species eight months after the thermal stress event that caused mass coral bleaching (Ibrahim et al. 2017). The two mechanisms of survival include (1) maintenance of symbiont autotrophy through the thermal stress via increased host heterotrophy (Borell et al. 2008; Ferrier-Pagès et al. 2010; Hoogenboom et al. 2012), and (2) host heterotrophy increased to compensate for reduced symbiont autotrophy (Grottoli et al. 2006). These mechanisms exist along a continuum, with corals being able to employ both trophic strategies to a greater or lesser extent. Although changes in $\delta^{15}N$ values of coral hosts that may be linked to heterotrophy were not uniformly matched by expected shifts to more negative $\delta^{13}C$ values, changes in the position and/or size of isotopic niches provide insight into the survival mechanisms employed by the focal species.

Although the probability of severe coral bleaching in the Maldives was reduced in deep reefs (Muir et al. 2017), there was a change in the isotopic niches of both shallow and deep reef corals (Fig. 3.4). After the thermal stress event, increased $\delta^{15}N$ values in coral hosts provide insight into changes in coral trophic strategy while decreased $\delta^{13}C$ values of shallow *G. fascicularis* and deep *P. verrucosa* indicate that these two species had the ability to increase heterotrophic feeding. The reduced size of the isotopic niche of host *G. fascicularis* from shallow reefs and the change in host $\delta^{13}C$ and $\delta^{15}N$ values indicates a decline in symbiont autotrophy and an increase in host heterotrophy. One year after the thermal stress event, *P. verrucosa* from deep reefs had the most negative $\delta^{13}C$ values and the largest difference between host and symbiont $\delta^{15}N$ values, which is consistent with this species being the most heterotrophic among the species in this study. The similar sized isotopic niche of deep host

P. verrucosa before and after the thermal stress event indicates that the deep reef population apparently did not require a shift in trophic strategy in response to the thermal stress event. In contrast, larger isotopic niche sizes of *P. speciosa* indicate that this species was least capable in handling thermal stress. However, despite the increased $\delta^{15}N$ values of host *P. speciosa*, the consistent, more positive $\delta^{13}C$ values between sampling years and depths indicates that this species is dependent on symbiont autotrophy. Despite its greater abundance in deep reefs, the more autotrophic *P. speciosa* appeared to depend on the first mechanism as did shallow populations of the generally more heterotrophic *P. verrucosa* (Chapter 2). By contrast, *G. fascicularis*, which depends more on autotrophy in shallow reefs than deep reefs (Chapter 2), appeared to depend on the second survival mechanism.

The strong oligotrophic signature of the water column post-thermal stress suggests that, if reef-wide mortality had shifted the system to a more eutrophic environment following the thermal event (Morillo-Velarde et al. 2018), this shift was not maintained over the long-term. However, the C:N molar ratios of POM (3.5 before thermal stress) increased eight months after the thermal stress event (C:N 10.1), which may reflect increased levels of ultraviolet radiation (Courtial et al. 2018). The oligotrophic status of the water column also indicates that evidence for increased heterotrophy following the thermal stress event is not simply a function of a greater availability of food in the water column but also may be dictated by long term history of particulate resource availability (Anthony 2000). When increased heterotrophy occurs, it most likely reflects a need for greater energy inputs to repair long-term damage caused by the thermal stress event (Hughes and Grottoli 2013). Overall, low concentrations of PON, high $\delta^{18}O\text{-}NO_3^-$ values, and high Redfield ratios provide evidence for a phosphate-limited oligotrophic water column after the thermal stress event in the Maldives (Figs. S3.2, S3.3, and S3.4; Tyrrell 1999). There were some minor differences in POM $\delta^{13}C$ and $\delta^{15}N$ values before and after the thermal stress event, including a wider range of $\delta^{13}C$ values post-thermal stress but, overall, similar $\delta^{15}N$ values (Fig. S3.4). The more positive $\delta^{13}C$ values of POM recorded post-thermal stress may reflect sampling of degraded cyanobacteria (Fry et al. 1984; Tchernov and Lipschultz 2008; Dorado et al. 2012). Because cyanobacterial metabolites can deter consumption by marine organisms (Nagle and Paul 1998), it is unlikely that these differences in POM would influence the isotopic ratios of coral holobionts.

3.5.1 Response of P. speciosa

The increased size of the isotopic niches of both shallow and deep host *P. speciosa* following the thermal stress event indicated a stress response to the thermal event (Fig. 3.4). Under thermal stress

conditions, heterotrophic feeding can help sustain and/or restore symbiont density and autotrophy (Borell et al. 2008; Ezzat et al. 2016; Tremblay et al. 2016). As *P. speciosa* is dependent on symbiont autotrophy (Chapter 2), the larger isotopic niche sizes due to increased $\delta^{15}N$ values observed after the thermal stress is consistent with increased heterotrophy supporting symbiont autotrophy. Further, the $\Delta^{13}C$ proxy for heterotrophy supports an increase in heterotrophy in deep *P. speciosa* following the thermal stress event while the $\Delta^{13}C$ value of shallow populations of *P. speciosa* was indicative of heterotrophy (Rodrigues and Grottoli 2006).

3.5.2 Response of G. fascicularis

After the thermal stress event, changes in the isotopic niche sizes of host *G. fascicularis* provides additional evidence of the different trophic strategies between shallow and deep reef populations (Chapter 2). For the autotrophy-dependent *G. fascicularis* from shallow reefs, the decreased size of the host isotopic niche after the thermal stress event indicates reduced autotrophy with decreased $\delta^{13}C$ values (-1.2‰) shifting towards the more negative $\delta^{13}C$ values of deep reef *G. fascicularis*. Because *G. fascicularis* can feed heterotrophically and increase heterotrophic feeding under conditions of thermal stress (Borell et al. 2008; Ferrier-Pagès et al. 2010; Wijgerde et al. 2011), the decrease in $\delta^{13}C$ values and increase in $\delta^{15}N$ values of host *G. fascicularis* supports a shift to heterotrophic feeding (Hoogenboom et al. 2015). The isotopic niche size of deep populations of host *G. fascicularis* slightly increased following the thermal stress event, supporting a generally greater dependence on heterotrophic feeding in lower light deep reefs. The relatively high proportion of lipids (>35%) in host *G. fascicularis* suggests that this species may retain energy in favor of an allocation to its symbionts (Yamashiro et al. 1999; Borell et al. 2008). Because symbionts of shallow *G. fascicularis* showed a decrease in isotopic niche size, the decreased isotopic niche size of shallow host *G. fascicularis* is consistent with a bleaching-induced reduction in autotrophy with a concurrent increase in heterotrophy under thermal stress conditions (Ferrier-Pagès et al. 2010).

3.5.3 Response of P. verrucosa

Relative to the other coral genera in this study, *Pocillopora* was the least susceptible to mass coral bleaching in the Maldives in 2016 (Ibrahim et al. 2017) with a lower proportion of bleached *P. verrucosa* colonies observed especially in deep reefs (24-30 m; Muir et al. 2017). Although *P. verrucosa* is relatively more heterotrophic compared to the other species, its shallow host isotopic niche also showed an increase in size following the thermal stress event (Fig. 3.4). After the thermal stress, the isotopic niche of shallow host *P. verrucosa* became similar in size to that of deep host *P. verrucosa*. The isotopic niches of *P. verrucosa* symbionts were consistent before and after the thermal

stress event, which indicates that a shift in autotrophy likely did not occur. The consistent $\delta^{13}C$ values and generally similar isotopic niches of *P. verrucosa* support a dependence on one main trophic strategy over depth (Maritorena et al. 2002). Overall, the minimal changes in the isotopic niches of *P. verrucosa* is consistent with relatively lower bleaching-related physiological stress and the ability to maintain or, in the case of shallow host populations, increase heterotrophy (Fig. 3.4).

3.5.4 Nitrogen isotope ratios provide insight into changes in coral nitrogen cycling

The largest difference between the average $\delta^{15}N$ values of a coral host species and its symbionts was between *P. verrucosa* hosts and symbionts (1.5‰). After the thermal stress event, $\delta^{15}N$ values decreased only in the symbionts of deep *P. verrucosa* colonies (5.2 to 4.4‰). We hypothesize that decreased $\delta^{15}N$ values of deep *P. verrucosa* symbionts after the beaching event could be explained by the assimilation and fractionation of a greater abundance of ^{15}N-depleted nitrogen sources such as ammonium (host waste product) and/or diazotroph-derived nitrogen (Reynaud et al. 2009; Pogoreutz et al. 2017). A recent study showed that the degree of heterotrophy by corals from deep reefs correlates with the rate at which diazotroph-derived nitrogen is assimilated (Bednarz et al. 2017). However, low $\delta^{15}N$ values (-2 to 0‰) that are characteristic of diazotroph-derived nitrogen were not recorded in POM $\delta^{15}N$ values in 2017 (Montoya et al. 2002). Relative to the other two coral species, host *P. verrucosa* had the most negative $\delta^{13}C$ values indicative of heterotrophy, especially in deep host colonies after the thermal stress (Muscatine et al. 1989b). Therefore, a greater dependence on heterotrophy may have resulted in the lower $\delta^{15}N$ values of *P. verrucosa* symbionts due to the recycling of host nitrogen waste products such as ^{15}N-depleted ammonium (Reynaud et al. 2009).

Overall, the significant increase in average $\delta^{15}N$ values across all three coral host species indicates that there was a change in the source(s) and/or abundance of nitrogen available and/or assimilated by the corals. Although the turnover of nitrogen in corals is slow under normal symbiosis (~ one year), nitrogen turnover is faster (~ 56 days) in corals that have lost their symbionts such as during mass coral bleaching (Tanaka et al. 2018). An increase in host $\delta^{15}N$ values but an absence of a change in symbiont $\delta^{15}N$ values could be a result of two scenarios. First, a loss of symbionts during coral bleaching would suggest that, eight months after the thermal stress event, host $\delta^{15}N$ values could retain a signal of a change in trophic strategy if increased heterotrophy is maintained while symbiont $\delta^{15}N$ values represent a more recent, post-thermal stress symbiont community. The recycling of nitrogen between the host and symbionts would be affected by impeded autotrophy during thermal stress and coral bleaching because nitrogen recycling by the coral host is dependent on carbon translocated from the symbionts (Wang and Douglas 1998; Reynaud et al. 2009). Under elevated

seawater temperature, the uptake of both nitrate and ammonium is reduced in some coral species (Godinot et al. 2011). Alternatively, because coral hosts and symbionts recycle nitrogen and symbiont autotrophy can be maintained by heterotrophic feeding during elevated seawater temperature (Wang and Douglas 1998; Ezzat et al. 2016; Tremblay et al. 2016), symbiont $\delta^{15}N$ values may reflect host-dependent regulation of nitrogen available to the symbiont (Falkowski et al. 1993; Cui et al. 2018). Reduced nitrate assimilation by the host and symbionts has been observed in thermally acclimated corals, which may represent nitrogen limitation by the host or a change in nitrogen cycling (Gibbin et al. 2018). Nitrogen limitation is capable of inducing lipid synthesis in symbionts (Weng et al. 2014), and increased C:N of symbionts from all three species could be due to increased lipid synthesis, nitrogen limitation, or both (Table 3.1). However, considering the short turnover time of symbiont populations (Wilkerson et al. 1983; Hoegh-Guldberg and Smith 1989; Tanaka et al. 2006), symbiont $\delta^{15}N$ and $\delta^{13}C$ values likely represent an eight months post-thermal stress symbiont community in which autotrophy was reestablished. A semi-qualitative assessment of the visible abundance of coral colonies of *G. fascicularis*, *P. speciosa*, and *P. verrucosa* indicated that coral colony abundance did not change between 2015 and 2017, suggesting that at least a proportion of colonies were able to survive the thermal stress event. Although more robust benthic surveys are needed to quantify coral community compositions before and after the 2016 thermal stress event, the survival of the focal species in this study indicates that the corals employed trophic strategies that enabled them to survive the thermal stress event. Indeed, particulate resource availability has been linked with coral heterotrophy given the oceanic primary productivity throughout the atolls of the Maldives (Fox et al. 2018). In the upwelling region of the Maldives, coral heterotrophy may play an important role in coral resilience in a rapidly changing climate.

3.6 Acknowledgements

We thank Kristen Brown, Dominic Bryant, Mary Bryant, Pete Dalton, Susie Green, Chris Hoegh-Guldberg, the Seaview Survey team, the Maldives Marine Research Centre, especially Shiham Adam and Nizam Ibrahim, the Ministry of Fisheries and Agriculture, the Environmental Protection Agency, the crew of the MV Emperor Atoll, Stina Boman, and Sébastien Pauner for their invaluable assistance during field work in the Maldives. We also would like to thank Scott Wankel and Jen Karolewski (Woods Hole Oceanographic Institution), Joy Matthews (University of California Davis), and Beatrice Keller-Lehmann (University of Queensland) for sample analysis and Martin Wynne, Sarah Pausina, Alexa Grutter, and Frank Coman for advice regarding plankton sampling and for lending equipment. This study was accomplished as part of the XL Catlin Seaview Survey, designed and undertaken by the Global Change Institute, and funded by XL Catlin in partnership with The

Ocean Agency and The University of Queensland. This study was also supported by the Australian Research Council (ARC) Centre of Excellence for Coral Reef Studies (SD and OHG), an ARC Laureate Fellowship (OHG), and the University of Queensland Research Training Tuition Fee Scholarship (VZR).

3.7 Supplementary Information

Table S3.1. Coral reefs surveyed across the central Maldives in 2017. POM was sampled at each site. All sites except those marked with an asterisk (*) were previously surveyed in 2015. Seawater temperature was measured at three sites (‡) between April 2015 and October 2016. Plankton tows (†) were conducted in 2017.

Date	Atoll	Site	Latitude	Longitude	Coral sampled	Reef Exposure
20/3/17	North Male	Hulhumale ‡	4.225	73.551	No	Oceanic
20/3/17	North Male	Lankan Faru*	4.281	73.559	No	Oceanic
21/3/17	North Male	Rasfari	4.398	73.345	No	Inner Sea
21/3/17	North Male	Reethi Rah	4.511	73.361	Yes	Inner Sea
22/3/17	North Ari	Mathiveri † ‡	4.18	72.745	Yes	Oceanic
22/3/17	North Ari	Dinoluga ‡	4.151	72.732	Yes	Oceanic
24/3/17	South Ari	Dhiggaru Falhu†	3.714	72.981	Yes	Inner Sea
24/3/17	South Ari	Dhangethi	3.596	72.957	Yes	Inner Sea
25/3/17	Dhaalu	Maadheli*	2.88	72.829	Yes	Oceanic
25/3/17	Dhaalu	Maafushi	2.683	72.847	Yes	Oceanic
26/3/17	Dhaalu	Naibukaloabodufushi*	2.774	73.027	Yes	Inner Sea
26/3/17	Dhaalu	Hulhuvehi†	2.862	73.029	Yes	Inner Sea
27/3/17	Meemu	Kurali	2.782	73.369	Yes	Inner Sea
27/3/17	Meemu	Bodu Hura	2.811	73.366	Yes	Inner Sea
28/3/17	Meemu	Muli	2.923	73.588	No	Oceanic
28/3/17	Meemu	Veyvah†	2.975	73.62	Yes	Oceanic
29/3/17	Vaavu	Kuda Aanuvari Falhu	3.385	73.426	No	Inner Sea
29/3/17	Vaavu	Kandimma Falhu	3.42	73.375	Yes	Inner Sea
30/3/17	Vaavu	Maadhiggaru Falhu	3.539	73.52	No	Oceanic
30/3/17	Vaavu	Medhu Faru†	3.626	73.509	Yes	Oceanic
31/3/17	South Male	Tholhimaraahuraa	3.831	73.37	Yes	Inner Sea
31/3/17	South Male	Fushidiggaru Falhu†	4.079	73.539	Yes	Oceanic
1/4/17	South Male	Hulhumale	4.227	73.554	No	Oceanic

Table S3.2. The visible abundance of sampled coral colonies (mean ± SD) was used to estimate the distribution of coral species across depths (shallow 10 m versus deep 30 m) and reef exposures between sampling years (5 reefs in the Inner Sea and 5 Oceanic reefs surveyed in 2015 and 2017).

	Pre-Thermal stress (2015)		Post-thermal stress (2017)	
	Inner Sea	Oceanic	Inner Sea	Oceanic
Galaxea fascicularis				
Shallow	8 ± 1	8 ± 1	8 ± 1	7 ± 3
Deep	4 ± 3	6 ± 3	4 ± 2	4 ± 4
Pachyseris speciosa				
Shallow	6 ± 3	1 ± 3	6 ± 4	0 ± 0
Deep	9 ± 1	8 ± 2	9 ± 1	8 ± 2
Pocillopora verrucosa				
Shallow	6 ± 3	7 ± 4	6 ± 4	8 ± 1
Deep	4 ± 3	5 ± 5	7 ± 4	4 ± 4

Table S3.3. Isotopic niche metrics for three species of coral hosts and their symbionts from shallow (10 m) and deep (30 m) reefs sampled before (2015) and after (2017) the thermal stress event in the Maldives in 2016. Standard ellipse area (SEA) and small sample size corrected standard ellipse area (SEAc) are shown along with carbon isotope ($\delta^{13}C$) and nitrogen isotope ($\delta^{15}N$) ranges (minimum to maximum isotopic value for given isotopic ratio).

	Thermal	$\delta^{13}C$ Range		$\delta^{15}N$ Range		SEA ($‰^2$)		SEA-c ($‰^2$)	
	Stress	Shallow	Deep	Shallow	Deep	Shallow	Deep	Shallow	Deep
Coral host									
Galaxea fascicularis	Before	-19.8 to -13.6	-19.5 to -15.9	4.6 to 6.5	5.0 to 6.2	2.1	0.8	2.2	0.9
	After	-19.6 to -14.5	-18.8 to -16.1	4.8 to 7.0	5.1 to 7.8	1.6	1.1	1.7	1.1
Pachyseris speciosa	Before	-17.5 to -12.6	-18.5 to -13.1	4.4 to 6.0	4.0 to 6.4	1.4	1.5	1.5	1.6
	After	-19.7 to -12.3	-19.0 to -13.3	4.5 to 6.9	4.4 to 7.0	2.9	2.3	3.0	2.3
Pocillopora verrucosa	Before	-18.8 to -15.0	-19.3 to -16.6	5.4 to 6.2	4.6 to 6.2	0.8	0.9	0.9	0.9
	After	-19.0 to -15.6	-19.8 to -16.7	4.1 to 7.0	4.6 to 6.6	1.2	1.0	1.2	1.0
Symbionts									
Galaxea fascicularis	Before	-19.2 to -13.1	-19.2 to -15.0	3.4 to 5.2	3.4 to 6.0	2.0	2.1	2.1	2.2
	After	-18.8 to -11.4	-20.3 to -11.7	3.2 to 5.8	3.4 to 5.7	3.0	2.7	3.1	2.7
Pachyseris speciosa	Before	-18.1 to -8.9	-18.4 to -9.6	4.7 to 6.1	4.5 to 6.6	2.8	3.0	3.0	3.2
	After	-17.7 to -10.8	-17.7 to -10.4	2.5 to 6.6	2.3 to 6.4	4.1	4.1	4.3	4.2
Pocillopora verrucosa	Before	-18.2 to -13.8	-18.7 to -15.5	4.1 to 6.7	3.7 to 6.4	2.0	1.5	2.1	1.5
	After	-18.5 to -12.4	-20.4 to -15.8	3.8 to 6.3	2.3 to 5.6	1.4	1.8	1.5	1.9

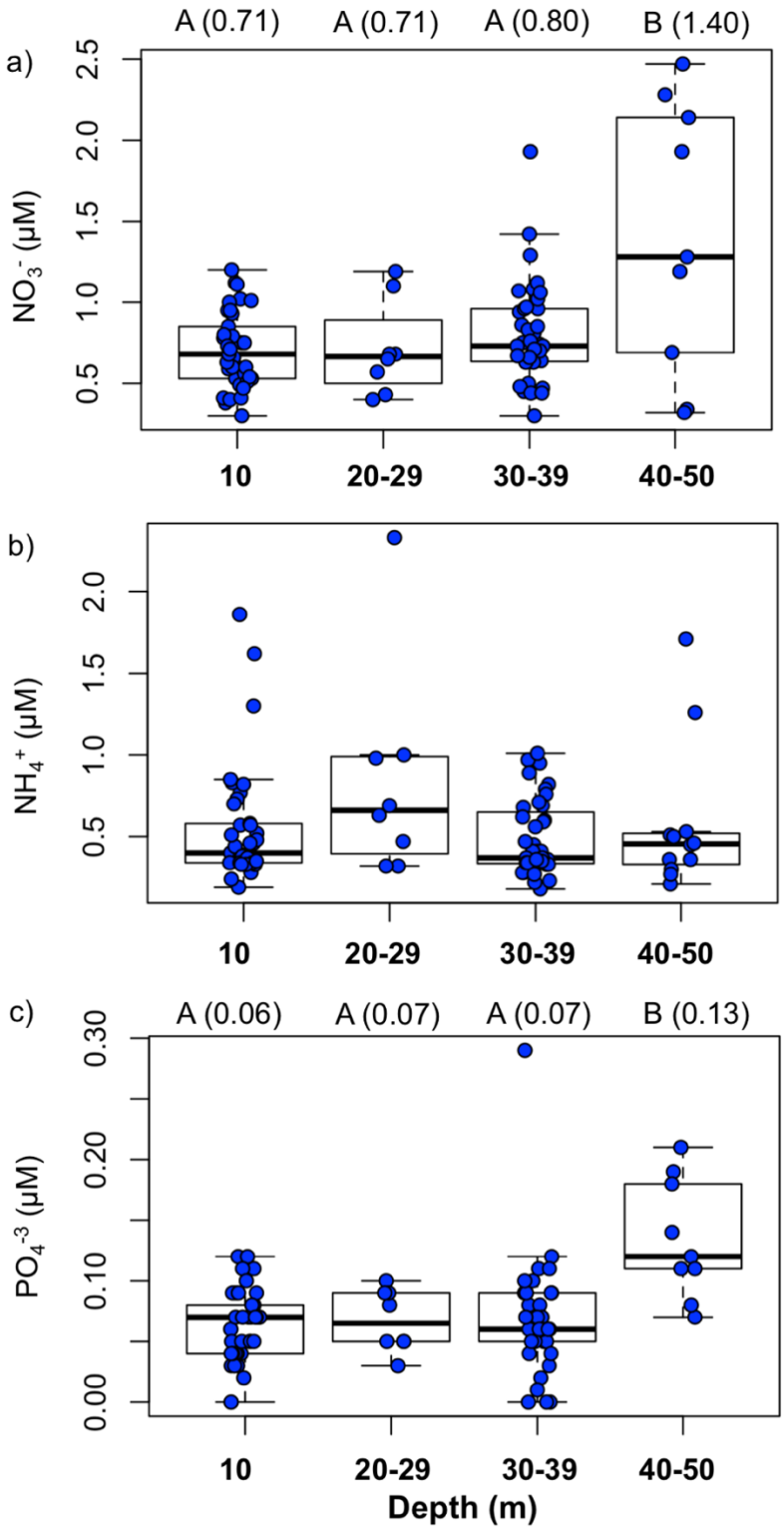

Figure S3.1. Inorganic nutrients of seawater collected in the central Maldives. Nitrate (NO_3^-), ammonium (NH_4^+), and phosphate (PO_4^{-3}) concentrations were measured in seawater collected from 10 m, 20-29 m, 30-39 m, and 40-50 m reef depth (boxplot shows the median). Nitrite was undetectable for a majority of the samples. Letters denote statistical difference with mean concentration shown in parentheses.

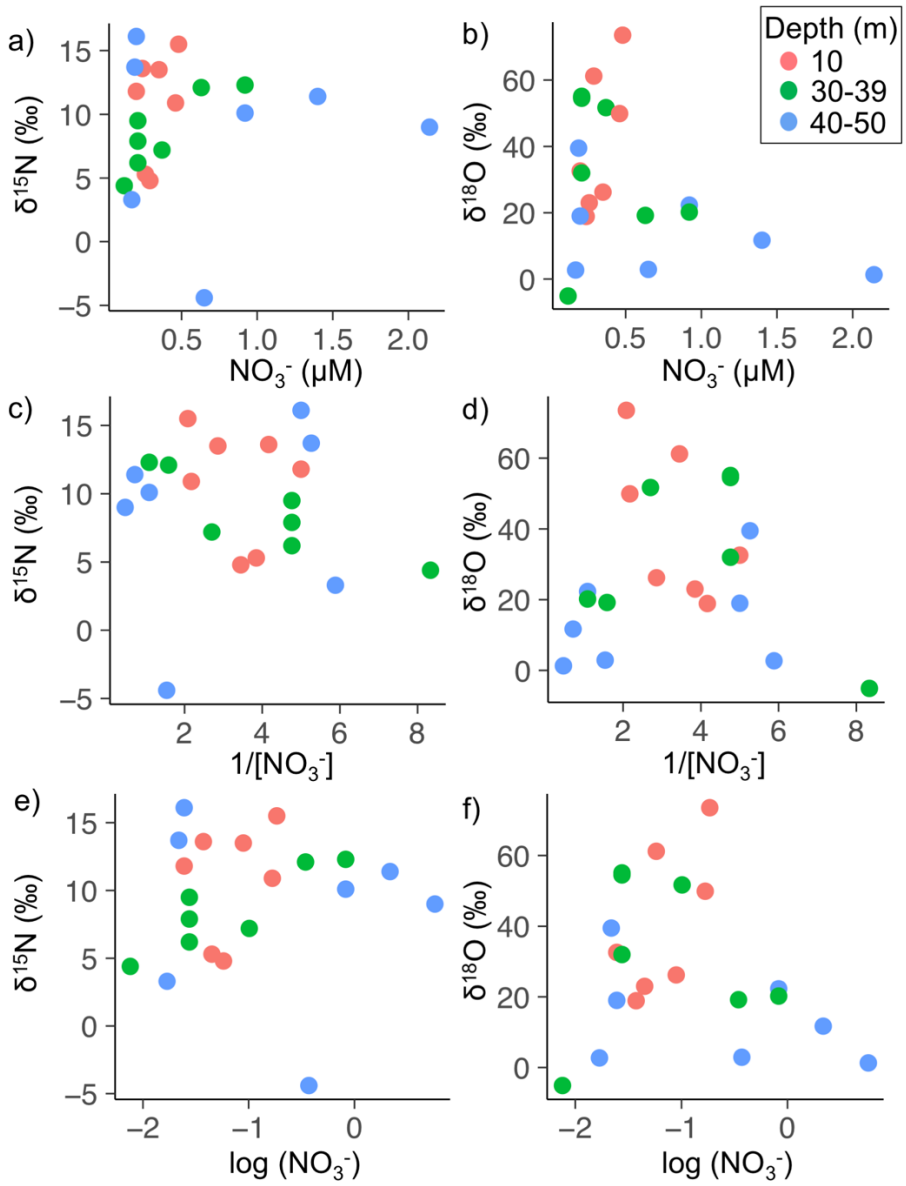

Figure S3.2. The nitrogen isotope ratios ($\delta^{15}N$) and oxygen isotopic ratios ($\delta^{18}O$) of dissolved nitrate (NO_3^-) in seawater collected from 10 m, 30-39 m, and 40-50 m reef depth in the central Maldives. The $\delta^{15}N$-NO_3^- values and $\delta^{18}O$-NO_3^- values are shown in relation to NO_3^- concentration (a, b), the inverse of the NO_3^- concentration (c, d), and the log of the NO_3^- concentration (e, f).

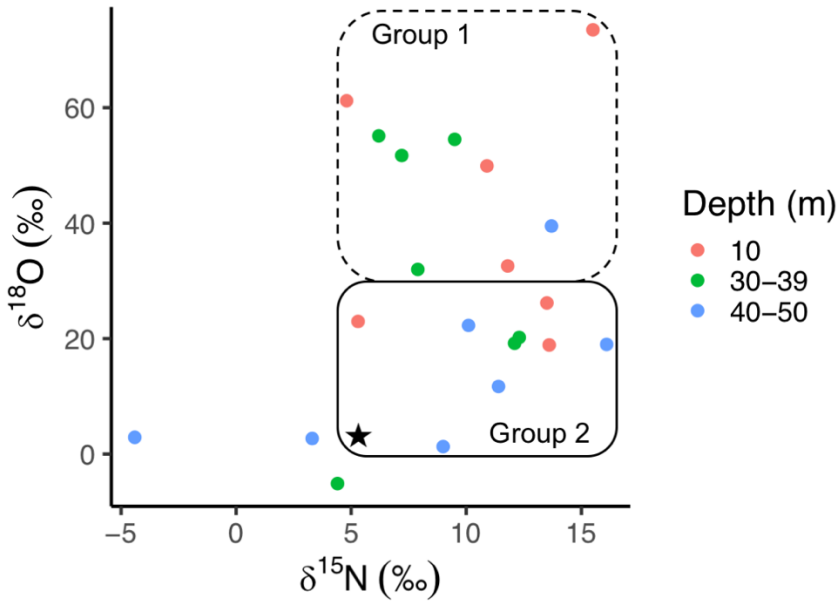

Figure S3.3. Nitrogen and oxygen isotopic ratios ($\delta^{15}N$ and $\delta^{18}O$, respectively) of dissolved nitrate from the reef water column in the Maldives. Group 1 (dashed line) represents sources of atmospheric nitrate characterized by enriched $\delta^{18}O$ values, while Group 2 (solid line) represents nitrate derived from marine sources. The star symbol indicates the isotopic signature of deep-water nitrate with $\delta^{15}N$ around +5‰ and $\delta^{18}O$ around +3‰.

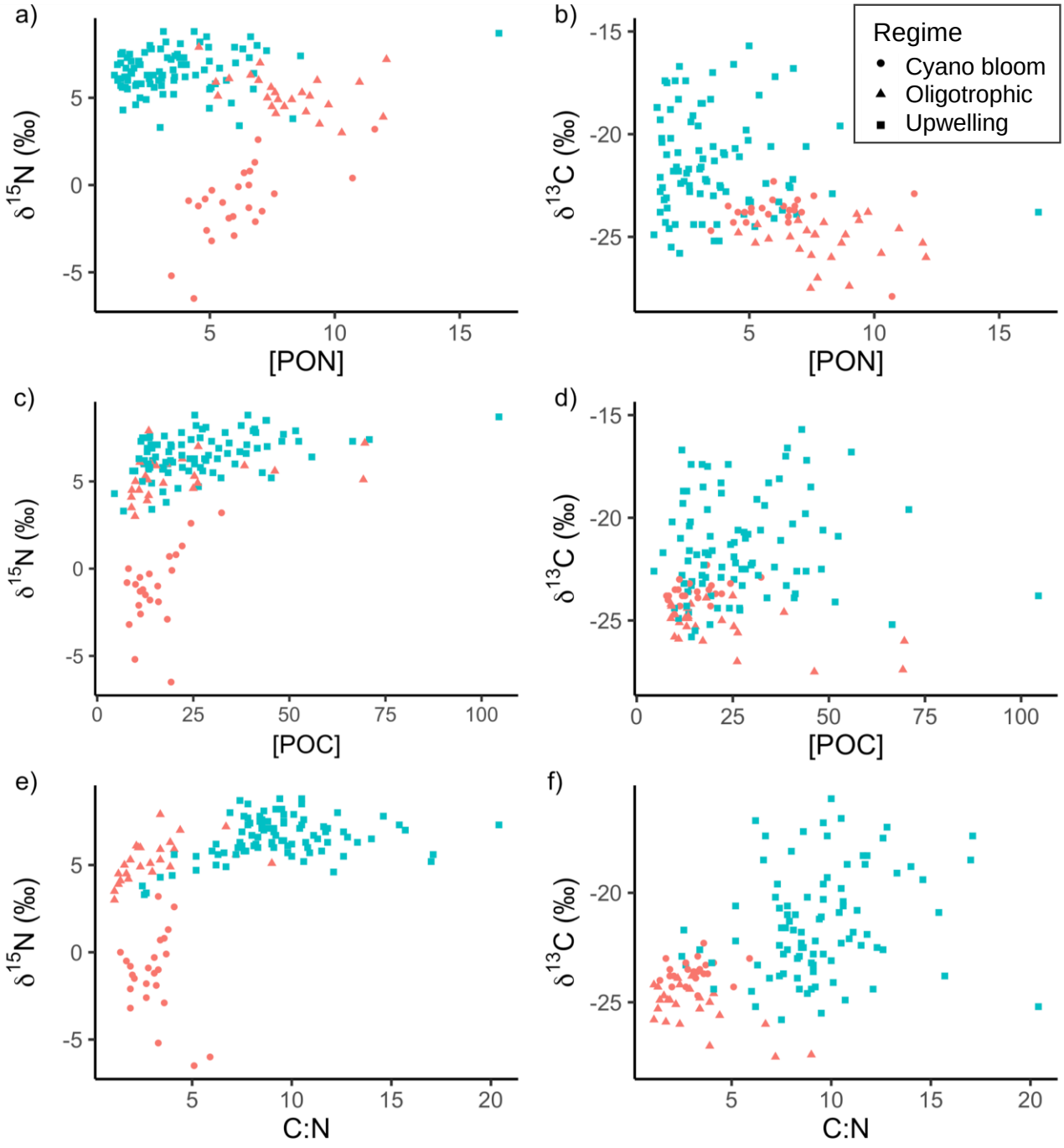

Figure S3.4. Different regimes of the reef water column are characterized by the isotopic variability of particulate organic matter (POM) collected before and after the 2016 thermal stress event in the Maldives. The concentration of particulate organic nitrogen (PON) is shown in relation to a) POM nitrogen isotope ratios ($\delta^{15}N$) and b) POM carbon isotopes ratios ($\delta^{13}C$); the concentration of particulate organic carbon (POC) is shown in relation to c) POM $\delta^{15}N$ values and d) POM $\delta^{13}C$ values; POM molar C:N ratios are shown in relation to e) POM $\delta^{15}N$ values and f) POM $\delta^{13}C$ values.

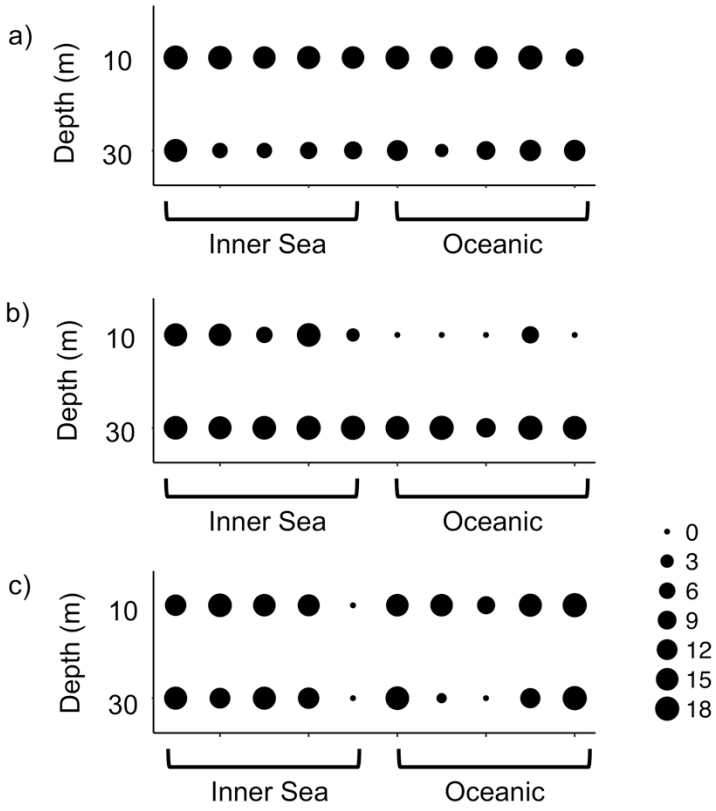

Figure S3.5. Total number of colonies sampled in 2015 and 2017 as a proxy for the visible abundance of coral species a) *Galaxea fascicularis*, b) *Pachyseris speciosa*, and c) *Pocillopora verrucosa* across shallow (10 m) to deep (30 m) reef slopes. Sum of colony fragments shown only for reefs that were surveyed both years, with a sampling target of a maximum of nine colonies per species per depth per year from five Inner Sea sites (Bodu Hura, Dhiggaru Falhu, Hulhuvehi, Kandimma Falhu, and Reethi Rah) and five Oceanic reef sites (Dinoluga, Maafushi, Mathiveri, Medhu Faru, and Veyvah; see Table S3.1).

Chapter 4:

Evaluating coral trophic strategies using fatty acid composition and indices

4.1 Abstract

The ecological success of shallow reef-building corals has been linked to the symbiosis between the coral host and its dinoflagellate symbionts (herein 'symbionts'). As mixotrophs, symbiotic corals depend on nutrients 1) transferred from their photosynthetic symbionts (autotrophy) and 2) acquired by host feeding on particulate organic resources (heterotrophy). However, coral species differ in the extent to which they depend on heterotrophy for nutrition and these differences are typically poorly defined. Here, a multi-tracer approach was used to investigate the role of heterotrophy in three species of common reef-building coral (*Galaxea fascicularis*, *Pachyseris speciosa*, and *Pocillopora verrucosa*). The composition and various indices of fatty acids were compared among the three coral host species and their symbionts. Established indices used to examine the input of fatty acids derived from photosynthesis or animals were applied in a novel context to examine the relative contribution of autotrophy and heterotrophy in corals. Further, a linear discriminant analysis (LDA) was used to estimate the contribution of polyunsaturated fatty acids (PUFA) derived from various potential sources (symbionts and a diverse taxonomic range of plankton) to the three species of corals. The total fatty acid composition and various fatty acid indices revealed differences between the more heterotrophic (*P. verrucosa*) and more autotrophic (*P. speciosa*) coral hosts, with the coral host *G. fascicularis* showing overlap with the other two species and greater variability overall. The symbionts of *P. verrucosa* showed distinct separation from *G. fascicularis* and *P. speciosa* symbionts, with the latter two also showing differences in fatty acid composition. Despite the depth gradient across which the corals were collected (10 and 30 m), fatty acid composition was not affected by reef depth. The application of three fatty acid indices proved to be informative in characterizing relative autotrophy and heterotrophy among the three species of coral. For the more heterotrophic coral *P. verrucosa*, the fatty acid indices and LDA results both indicated a greater proportion of copepod-derived fatty acids compared to the other coral species. Overall, the LDA estimated that PUFA derived from potential particulate resources (copepods and diatoms) comprised a greater proportion (mean 88%) of coral host PUFA in contrast to the lower proportion of symbiont-derived PUFA (mean 12%). These estimates provide insight into the importance of heterotrophy in coral nutrition, especially in productive reef systems. This study provides extensive evidence of the utility of fatty acids in characterizing coral trophic strategies.

4.2 Introduction

The evolutionary success of symbiotic reef-building corals in typically nutrient-poor oceans is attributed to the coral-dinoflagellate symbiosis (Frankowiak et al. 2016). As mixotrophic organisms, the different trophic strategies of symbiotic reef-building corals allows corals to adapt to a wide range

of environmental conditions (Porter 1976; Muscatine and Porter 1977). Although autotrophic dinoflagellate symbionts (herein 'symbionts') contribute significantly to coral host nutrition, external food sources are an important component of coral nutrition especially in reefs with high food availability and/or under low-light conditions of shaded or deep reefs (Falkowski et al. 1984; Muscatine et al. 1989b). Symbiotic corals obtain nutrients from their symbionts (autotrophy) as well as from feeding on particulate resources available in the water column (heterotrophy; Houlbrèque and Ferrier-Pagès 2009). Potential particulate resources for heterotrophic feeding include bacteria, detritus, flagellates, phytoplankton, and zooplankton (Houlbrèque and Ferrier-Pagès 2009; Leal et al. 2014; Levas et al. 2016). The contribution of heterotrophy to coral metabolism greatly varies because symbiotic coral species show different capacities to feed via heterotrophy, with heterotrophic carbon accounting for up to 46% of daily requirements in some species of coral (Palardy et al. 2008). Host heterotrophic feeding has a positive feedback on symbiont autotrophy (Tremblay et al. 2016; Lim et al. 2017), with a positive correlation between symbiont density and lipid content (Yamashiro et al. 2005). However, the ability of corals to increase heterotrophy and assimilate different lipids tends to be species specific (Rodrigues et al. 2008). Lipids are important for energy storage and comprise a major constituent of coral carbon content and overall dry weight (Harland et al. 1993), with particular reproductive strategies and timing (e.g., spawning) affecting lipid content (Ward 1995). However, total lipid content varies among species. For example, the coral *Galaxea fascicularis* has a relatively high proportion of lipids (>35% tissue dry weight) while the coral *Pocillopora verrucosa* has a relatively low lipid content of ~11-14% (Harland et al. 1993; Yamashiro et al. 1999, 2005) compared to its congeners (30-41%; Patton et al. 1977; Stimson 1987). Lipid assimilation and trophic strategy are important components of coral metabolism and ecology, especially under anomalously warm seawater conditions that compromise the coral symbiosis and cause coral bleaching (Rodrigues et al. 2008).

Fatty acids are essential for energy use and storage, cell membrane structure, and gene regulation (Gurr et al. 2002), with fatty acid composition showing consistent patterns related to taxonomy (Galloway and Winder 2015). As the major component of coral lipids (up to 73%; Treignier et al. 2008; Tolosa et al. 2011), fatty acids reflect patterns in coral nutrition and have been used in various ways as trophic markers to assess autotrophic versus heterotrophic feeding strategies of corals (Teece et al. 2011; Seemann et al. 2013). Due to the carbon exchange between coral hosts and symbionts (Patton et al. 1977), the fatty acid composition of cultured symbionts differ from those of coral-associated symbionts (Chen et al. 2015; Wang et al. 2015). Experimental feeding studies have shown variable effects of food availability on coral host fatty acid composition, specifically for

monounsaturated fatty acids (MUFA; Tolosa et al. 2011; Tagliafico et al. 2017). Certain MUFA are important precursors for the synthesis of polyunsaturated fatty acids (PUFA; Gurr et al. 2002). Fatty acid indices are commonly used in marine ecology to evaluate trophic strategies but the following three indices have yet to be tested for corals (Dalsgaard et al. 2003). First, the ratio of fatty acids 18:1n-7 to 18:1n-9 is used to evaluate relative herbivory versus carnivory because 18:1n-9 is a major fatty acid in marine animals and 18:1n-7 is produced by the elongation of 16:1n-7 that is derived from photosynthesis (Graeve et al. 1997; Schukat et al. 2014). A correlated fatty acid index is used to characterize the ratio of photosynthetic input (sum of fatty acids 16:1n-7 and 18:1n-7) to animal dietary input (sum of fatty acids 18:1n-9, 20:1n-9, and 22:1n-11; Sargent and Falk-Petersen 1981). The sum of long-chain MUFA (LC-MUFA, ∑20:1 and ∑22:1) is used to evaluate potential feeding on copepods because herbivorous marine copepods, including tropical copepods, have elevated concentrations of LC-MUFA (Dalsgaard et al. 2003; Brett et al. 2009; Kattner and Hagen 2009). This index has been previously applied to cold-water corals and subtropical symbiotic jellyfish to investigate feeding on copepods (Dodds et al. 2009; Mortillaro et al. 2009). Tropical symbiotic reef-building corals (e.g. Goniopora) and hydrocorals (e.g. Millepora), which can feed extensively on plankton, have high proportions (~5-6%) of LC-MUFA (Latyshev et al. 1991; Lewis 2006; Imbs 2013). Indeed, symbiotic reef-building coral hosts that are fed show higher proportions of LC-MUFA than starved corals but these fatty acids can be negligible in symbionts (Al-Moghrabi et al. 1995; Tolosa et al. 2011). Further, the composition of PUFA has been used in chemotaxonomy to distinguish among phytoplankton groups (Galloway and Winder 2015) and between symbiotic corals, asymbiotic corals, hexacorals, and octocorals (Imbs et al. 2007, 2010a; Figueiredo et al. 2017). Coral PUFA composition is also useful to consider in the context of trophic ecology including coral feeding on plankton (Meyers 1979).

While much of the literature on coral fatty acids has assumed that corals, as animals, lack certain desaturases (i.e., Δ12 and Δ15) required for the synthesis of metabolically active PUFA, a recent study has shown that cnidaria, including Scleractinian corals, have genes for *de novo* synthesis of n-3 PUFA (Kabeya et al. 2018). In addition, desaturase activity has been functionally characterized for a variety of invertebrates including the nematode *Caenorhabditis elegans* (Spychalla et al. 1997; Peyou-Ndi et al. 2000; Zhou et al. 2011), a sea urchin (Kabeya et al. 2017), and cnidaria (Kabeya et al. 2018). Besides the transfer of fatty acids from the symbionts to the coral host (Papina et al. 2003), the evidence for cnidarian desaturases that can synthesize n-3 PUFA de novo (Kabeya et al. 2018) supports the idea that coral hosts can also transfer PUFA to their symbionts (Imbs et al. 2014). Indeed, certain long-chain fatty acids (i.e., C_{22}) appear to be host-derived rather than symbiont-derived (Dunn

et al. 2012). The ability of both symbiotic partners to synthesize and transfer fatty acids, including PUFA, complicates the delineation between each partner's biosynthetic pathways and hinders the use of individual fatty acids as trophic biomarkers (Dalsgaard et al. 2003; Mocking et al. 2012; Monroig et al. 2013). Further, experimental feeding studies typically focus on one potential particulate food source (e.g., most often Artemia nauplii) while the taxonomic diversity of planktonic food sources in reef systems has not been considered in the context of fatty acids and coral trophic ecology. The use of multiple tracers (i.e., 30 individual fatty acids), fatty acids indices, and comparison among taxonomic groups of different trophic levels allows for a robust evaluation of diverse coral trophic strategies.

To evaluate the use of fatty acid biomarkers in characterizing coral trophic strategies, the coral fatty acid composition of three species of reef-building corals (*Galaxea fascicularis, Pachyseris speciosa,* and *Pocillopora verrucosa*) and their associated symbionts were investigated. Because dietary fatty acids can be modified in consumers, this study focuses on corals for which prior knowledge of species-specific trophic strategies is available (Chapter 2). The fatty acid composition of coral hosts and symbionts from different reef depths (10 and 30 m) were investigated because reef depth has been shown to have different effects on the fatty acid composition of corals (Meyers et al. 1978; Latyshev et al. 1991) and previous research in the same reef system showed differential $\delta^{13}C$ values of *G. fascicularis* over depth (Chapter 2). This study provides a comprehensive evaluation of the trophic strategies of symbiotic corals by 1) examining the composition of multiple tracers (i.e., 30 individual fatty acids), 2) applying three established fatty acid indices in the novel context of coral trophic ecology, and 3) estimating the contribution of various sources of PUFA using a linear discriminant analysis. Total fatty acid compositions are used to evaluate patterns in coral trophic strategies while the relationship between host and symbiont proportions of individual fatty acids is used to investigate nutritional cycling between the symbiotic partners. Established fatty acid indices are applied in a novel context to examine relative autotrophy and heterotrophy among different coral species from the same reef system. Two different fatty acid indices were used to evaluate nutritional input from photosynthetic- versus animal-derived sources while another index tested for potential feeding on copepods. Further, a linear discriminant analysis was employed to estimate the relative contribution of different sources (symbionts and diverse plankton groups) to coral host PUFA composition to investigate the role of symbiont autotrophy and host heterotrophy. It was hypothesized that the relatively more autotrophic coral species *P. speciosa* would have a total fatty acid composition that differed from the more heterotrophic coral *P. verrucosa*. Because *G. fascicularis* can shift its trophic strategy as a function of environmental conditions, it was expected that this

species would have a fatty acid composition that was similar to both *P. speciosa* and *P. verrucosa*. It was expected that the different fatty acid indices would show a greater fatty acid input from symbiont autotrophy for *P. speciosa* and less for *P. verrucosa* and *G. fascicularis*. Further, it was hypothesized that the more heterotrophic coral *P. verrucosa* would have a PUFA composition that was more similar to the plankton prey groups compared to the other two coral species. Using multiple biochemical tracers, this study evaluates trophic strategies among three morphologically diverse species of coral and considers potential sources for coral heterotrophic feeding.

4.3 Methods

4.3.1 Sample collection

Fragments of three species of corals (*Galaxea fascicularis*, *Pachyseris speciosa*, and *Pocillopora verrucosa*) were collected by scuba divers from shallow (10 m depth) and deep (30 m depth) reefs in the central Maldives, Indian Ocean, in March-April 2017 (Chapter 3). Coral fragments were rinsed with filtered (0.4 μm) seawater and immediately frozen until analysis. Briefly, tissue was removed from the coral skeleton by a pressurized airbrush with 10 mL filtered (0.22 μm) seawater, host tissue was separated from symbionts by centrifugation, samples were acidified to remove any carbonates and then freeze-dried prior to fatty acid analysis (Chapter 2).

4.3.2 Extraction and analysis of fatty acids

Using a modified Folch method (Folch et al. 1957) following Taipale et al. (2013), fatty acids were extracted from freeze-dried coral host (n=30) or symbiont (n=30) tissue (mean 5.2 mg ± 0.1 SD) weighed into a glass culture tube (pre-combusted at 450°C for 4 h, twice rinsed with 2:1 $CHCl_3$:MeOH). In a fume hood, 4 mL of 2:1 (by volume) $CHCl_3$:MeOH was added to each tube, followed by 1 mL Milli-Q water. Tubes were flushed and capped under a stream of N_2 gas (Nitrogen Evaporator N-EVAP 111, Organomation, U.S.A.) for 10-20 seconds to displace air from tube in order to preserve fatty acids, which are sensitive to oxidation. This mixture was sonicated in a water bath with ice for 10 minutes, mixed for 10 seconds using a vortex, and centrifuged for 5 minutes at 483xg (10°C) to separate the phases. The resulting lower organic phase was transferred into a separate culture tube using a sterile glass Pasteur pipette, and immediately flushed with N_2 gas. Fatty acids were extracted a second time by adding 2 mL $CHCl_3$ to the original tube, and the tube was immediately flushed with N_2 gas. This mixture (original tube) was sonicated in a water bath with ice for 10 minutes, mixed for 10 seconds using a vortex, and centrifuged for 5 minutes at 483xg (10°C). The resulting lower organic phase of this tube was transferred and combined with the first lower phase (which combined two extractions of the lower organic phase). The combined organic phases

were evaporated under a constant stream of N_2 gas. Once evaporated, 1.3 mL of toluene followed by 2 mL 1% H_2SO_4 in methanol were added to resuspend the fatty acids. The extraction was flushed with N_2 gas and then heated in a 90°C water bath for 90 minutes to methylate the fatty acids. Then, 1.5 mL of Milli-Q water was added to each tube, followed by 4 mL of n-Hexane. The extraction was immediately flushed with N_2 gas, mixed using a vortex, and centrifuged for 2 minutes at 483xg. The resulting upper (organic) phase was transferred to a new tube, which was flushed with N_2 gas. To remove all of the fatty acid methyl esters, an additional 4 mL n-Hexane was added to the tube where the lower phase remained. Again, the tubes were flushed with N_2 gas, mixed, and centrifuged (2 minutes, 483xg). The final resulting upper phase was transferred and combined with the previously extracted upper phase. The combined organic extractions were then evaporated under a constant stream of N_2 gas. In the tubes where the hexane was evaporated, the fatty acid methyl esters were dissolved in a known volume of n-hexane (0.5-1.5 mL) for gas chromatography analysis.

The fatty acid methyl esters were analyzed using a Gas Chromatograph coupled with a Flame Ionization Detector (GC-FID, Hewlett Packard HP6890) with an Agilent DB-23 column (Heater 300°C, H_2 flow 40.0 mL/min, N_2 flow 30.0 mL/min, air flow 450 mL/min). An 85-minute run time was used to achieve optimal separation of the monounsaturated and polyunsaturated fatty acids (Taipale et al. 2011). Fatty acid peaks on the chromatographs were identified by comparing retention times as well as peak area with several reference standards (FAME 37 mix and oyster *Ostrea lurida*) and a subset of samples run on a gas chromatograph mass spectrometer (GC-MS QP2010 Plus) under the same method and analytical conditions. Sample fatty acid concentrations were quantified using a dilution of the GLC-68D standard (Nu-Check-Prep) that was quantified with the GC-FID. The total mass of fatty acids of each coral species and tissue type was quantified using a concentration conversion factor that was generated with a standard curve method for different concentrations of the GLC-68D standard (Lowe 2018). Comparing fatty acid peak area versus mass, the slopes of the linear regressions were consistent among fatty acid standards and the calculated fatty acid concentration was within an average of 1.4% (Lowe 2018). Using the derived average slope, the mass of each fatty acid per dry weight tissue was calculated using the mass of the tissue sample, volume of hexane, and peak area of a fatty acid.

4.3.3 Statistical analysis

Because of the variability of fatty acid composition, data were not transformed in order to avoid falsely inflating the contribution of minor fatty acids (Howell et al. 2003). Non-parametric PERMANOVA analyses were used to test whether the relative fatty acid compositions (% total fatty

acids) were similar among the hosts and symbionts of the three coral species from shallow and deep reefs (9999 permutations; PRIMER-E version 6 with PERMANOVA add-on, Plymouth, U.K.). PERMDISP, used to test the homogeneity of multivariate dispersion for the significant interaction observed in the PERMANOVA result, showed that the data were homogeneous. To investigate the potential relationship of fatty acid composition between coral host and symbionts, linear regressions were fitted to compare symbiont and host proportions of individual fatty acids.

To assess coral trophic strategies, established fatty acid indices including 1) the ratio of 18:1n-7 to 18:1n-9 fatty acids, 2) the ratio of photosynthetic- (the sum of fatty acids 16:1n-7 and 18:1n-7) versus animal-derived input (the sum of fatty acids 18:1n-9, 20:1n-9, and 22:1n-11), and 3) the sum of long-chain MUFA (20:1n-11, 20:1n-9, 20:1n-7, 22:1n-11, 22:1n-9, and 22:1n-7), a trophic index for herbivorous copepod consumption, were analysed using analysis of variances (ANOVA) with TukeyHSD post-hoc tests where applicable (R-Core-Team 2018).

Principal Component Analysis (PCA), which reduces the dimensionality of data and identifies correlated variables, was used to separately analyze coral hosts and symbionts fatty acid composition for the full suite of 30 fatty acids as well as for PUFA (Imbs et al. 2007; Le et al. 2008; Kassambara and Mundt 2017). For the PUFA analysis, the PCA included all (12) PUFA in the samples: 18:2n-6, 18:3n-3, 18:3n-6, 18:4n-3, 20:2n-6, 20:3n-6, 20:4n-3, 20:4n-6, 20:5n-3, 22:4n-6, 22:5n-3, and 22:6n-3. Next, the compositions of metabolically important PUFA (18:2n-6, 18:3n-3, 18:3n-6, 18:4n-3, 18:5n-3, 20:4n-6, 20:5n-3, 22:6n-3) were compared among coral hosts, symbionts, and various potential prey sources including diatoms (n=58, phylum Ochrophyta), cyanobacteria (n=12, phylum Cyanophyceae), dinoflagellates (n=16, phylum Dinophyceae), cryptophytes (n=25, phylum Cryptophyceae), and tropical copepods (n=47) (Schnack-Schiel et al. 2008; Treignier et al. 2008; Kattner and Hagen 2009; Schukat et al. 2014; Teuber et al. 2014; Bode et al. 2015; Galloway and Winder 2015; Fay et al. 2017). From a database of phytoplankton fatty acids, selected data i) were presented as proportions (percent of total fatty acids), ii) consisted of more than three individual fatty acids, iii) were of marine origin, iv) were not from polar regions, and v) were not subject to experimental treatments (Galloway and Winder 2015). Dinoflagellates were further filtered according to phytoplankton community composition recorded in reefs of the Maldives (Stanca et al. 2013). To estimate the relative contribution of different sources of PUFA to each coral host species, a linear discriminant analysis (LDA) (MASS package) was used to investigate the proportion of sources contributing to coral host PUFA composition (Venables and Ripley 2002). Using a leave-one-out cross-validation approach to evaluate the classification of potential sources of PUFA, sources with a

classification rate <70% (i.e., cyanobacteria and dinoflagellates) were removed from the analysis (Table S4.2). Further, cryptophytes were removed because this group showed no overlap with coral hosts (Fig. S4.5). The fatty acid 18:5n-3 was removed from the analysis because it was not present in the potential sources (copepods, diatoms, symbionts) used in the final model. A training data set was used to predict the contributions of various PUFA sources to coral host PUFA composition. A bootstrap approach was used to account for the within group variation in PUFA composition and to generate confidence estimates for the contribution of each group to coral host PUFA composition in the final model (Fox et al. *In revision*). PUFA were re-sampled from each group (with replacement) and a LDA was used to classify coral host samples of each species with each unique permutation of the raw data (n=10,000). This approach allowed us to maximize the variation in each putative source (copepods, diatoms, symbionts) and generate a distribution of possible contributions to the diet of each coral species. This distribution of all possible diet combinations was used to determine the proportional contribution of copepods, diatoms, and symbionts to each coral species, which are reported as the mean and 95% confidence interval. To acknowledge that PUFA composition from pure autotrophy (photosynthesis-derived) may differ from host-associated symbiont PUFA composition due to carbon cycling between coral hosts and their symbionts, an additional model including published data from cultured symbionts was considered (Wang et al. 2015). Although the small sample size of cultured symbiont data precludes using a LDA to classify coral host samples, the cultured symbiont samples appear to comprise a separate group from the host-associated symbionts (Fig. S4.6). Therefore, results are discussed in terms of symbiont-derived PUFA rather than autotrophy-derived PUFA.

4.4 Results

4.4.1 Coral host and symbiont fatty acid compositions

The composition of coral host and symbiont fatty acids were analyzed as proportions of total (30) fatty acids (Table S4.1 and Fig. S4.1). PERMANOVA results revealed that depth was not a significant factor affecting coral host and symbiont fatty acid profiles (Pseudo-$F_{1,48}$=0.687, P(perm) = 0.542). Therefore, data from both depths were combined for all analyses. Fatty acid composition was significantly affected by the interaction between tissue type (host versus symbiont) and the three coral species (Pseudo-$F_{2,48}$=2.952, P(perm) = 0.019). PERMANOVA pairwise comparisons showed that the fatty acid composition of coral host and symbiont tissue were significantly different (P(perm)<0.001). For the fatty acid composition of host tissue, *P. speciosa* was significantly different than *P. verrucosa* (P(perm)<0.001) while *G. fascicularis* was significantly different than *P. speciosa* (P(perm)=0.008) and *P. verrucosa* (P(perm)=0.019). The fatty acid composition of *P. speciosa*

symbionts was significantly different than *P. verrucosa* symbionts (P(perm)=0.001) while *G. fascicularis* symbiont fatty acid composition was significantly different than that of *P. speciosa* symbionts (P(perm)=0.020) and *P. verrucosa* symbionts (P(perm)=0.021).

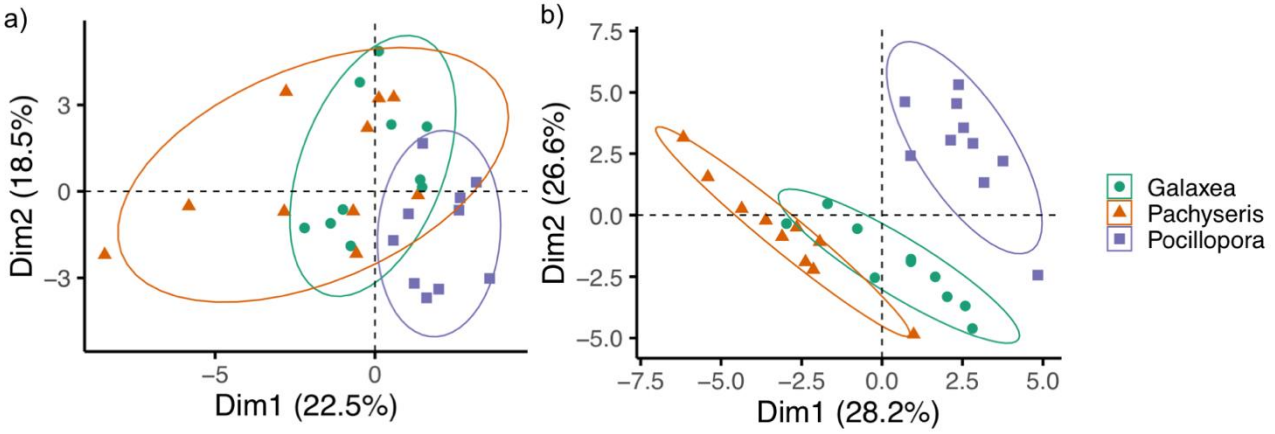

Figure 4.1. Principal component analysis based on the composition of total (30) fatty acids in a) coral hosts *Galaxea fascicularis*, *Pachyseris speciosa*, and *Pocillopora verrucosa* and b) their associated symbionts with 80% concentration ellipses shown.

PCA were used to reduce the dimensionality of the data and compare fatty acid composition among the species of coral hosts or symbionts, with the most important variables listed in order of higher to lower contribution. In the PCA of host total fatty acid composition, there was a difference between host *P. verrucosa* and host *P. speciosa*, while host *G. fascicularis* showed overlap with both species (Fig. 4.1a). Principal component Dim1 explained 22.5% of the variability in the total fatty acid composition, with the fatty acids 20:5n-3, 16:1n-7, 18:1n-9, 20:1n-7, and 22:1n-7 contributing to the variability. Principal component Dim2 explained 18.5% of the variability due to the fatty acids 18:3n-6, 20:4n-6, 22:4n-6, and 18:2n-6. In the PCA of symbiont total fatty acid composition, *P. verrucosa* symbionts clearly separated from *G. fascicularis* and *P. speciosa* symbionts of which the latter two also occupied distinct space in the ordination plot (Fig. 4.1b). In the symbiont total fatty acid PCA, 28.2% of the variability was explained by the principal component Dim1 due to the fatty acids 22:6n-3, 16:0, and 18:0. Principal component Dim2 explained 26.6% of the variability in the symbiont fatty acid composition, with contributions from the fatty acids 20:5n-3, 20:0, and 15:0.

To investigate the similarity between host and symbiont fatty acid composition, the proportion of fatty acids were compared between coral host and symbiont tissue from individual coral colonies. The variation in host fatty acid proportions was reduced by taking into account symbiont proportions of the fatty acid, of which 14 individual fatty acids (comprising 47% of total fatty acids) had

significant models (Fig. S4.2). The proportion of the MUFA 20:1n-9, a common marker for copepod feeding, showed a strong relationship (adj. R^2= 0.84) between *P. verrucosa* host and symbionts. The model of the ∑ LC-MUFA index was also significant (Fig. S4.4).

The saturated fatty acid 16:0 was the most prevalent fatty acid in both the hosts and symbionts, with an average of 31.5 to 37.2% and 34.2 to 43.6%, respectively (Fig. S4.1, Table S4.1). With a greater proportion in host tissues (average 22.2 to 29.0%) compared to symbiont tissues (7.0 to 12.9%), the fatty acid 18:0 appears to be important for energy storage in the coral host tissue. The fatty acid 22:4n-6 was the third most dominant fatty acid in all host species (average 4.2 to 7.9%) but had much lower proportions in the symbionts (1.3 to 2.8%). The average composition of the MUFA 18:1n-9 was greatest in *P. verrucosa* hosts (4.2%) and symbionts (4.8%). The PUFA 20:4n-6 was also prevalent in coral host tissue, with the highest proportions in *G. fascicularis* (6.4%) and *P. speciosa* (6.2%). The highest proportion of 20:5n-3 was in the *G. fascicularis* host (6.5%) and symbionts (5.9%). The proportion of the fatty acid 22:5n-3 was greater in host *P. verrucosa* than host *P. speciosa* (ANOVA, $F_{2,27}$ = 5.861, p = 0.008; Tukey p = 0.006). In regard to n-6 PUFA, the proportions of the fatty acid 20:4n-6 was significantly higher in coral host tissue than symbiont tissue (ANOVA, $F_{2,54}$ = 4.135, p = 0.047). There was a significant interaction between coral species and tissue type for the proportion of the fatty acid 22:4n-6 (ANOVA, $F_{2,54}$ = 5.620, p = 0.006), which was greater in the host rather than symbiont tissue for both *G. fascicularis* and *P. speciosa* (p<0.001).

In addition to 16:0, the other prevalent fatty acids in the symbionts included 18:3n-6, 22:6n-3, 18:0, 18:4n-3, 20:5n-3, and 14:0, in order of higher to lower proportions (Table S4.1). The factors coral species and tissue type has a significant effect on the proportion of the fatty acid 18:3n-6 (ANOVA, $F_{2,54}$ = 3.459, p = 0.039), with differences between host and symbionts of *G. fascicularis* (p<0.001). Overall, the symbionts of the more autotrophic corals *G. fascicularis* and *P. speciosa* had similar proportions of the fatty acid 18:3n-6 (p = 0.190). The average proportions of 18:3n-6 (4.7 to 8.7%) and 18:4n-3 (5.2 to 6.9%) were higher in symbionts than in the coral host tissues, in which the sum of both fatty acids was <3.5%. The proportion of 22:6n-3 was also higher in symbionts, particularly in *P. verrucosa* (9.5%) and *G. fascicularis* (7.1%) symbionts, than in coral hosts (<3%). The average proportion of 18:2n-6 was highest in the symbionts of *G. fascicularis* and *P. speciosa*. Very low proportions of 18:3n-3 were found in the symbionts (average <0.1%) and this fatty acid was not found in any host samples. The most prevalent MUFA was 16:1n-7, which was highest in *G. fascicularis* symbionts (4.8%). Mass spectra showed that eight out of ten *P. speciosa* symbiont samples had the rather unusual fatty acid 24:6n-3. In addition to analyzing the proportion of fatty acids, the mass of

total fatty acids per tissue type of each coral species was quantified. Symbionts had considerably higher mass (8-16 fold) of total fatty acids compared to their coral hosts (Table S4.1).

4.4.4 Composition of polyunsaturated fatty acids (PUFA)

A PCA was used to examine the PUFA composition of the coral hosts and symbionts (all 12 PUFA, Table S4.1), with most important variables listed in order of higher to lower contribution. The 80% confidence interval ellipses showed separation of host *P. verrucosa* from host *P. speciosa* and host *G. fascicularis* (Fig. S4.3a). Principal component Dim1 explained 38.4% of the host PUFA variability, with a majority of the contribution from n-6 PUFA (18:3n-6, 20:4n-6, 22:4n-6, 18:2n-6, and 22:6n-3). Three n-3 PUFAs (22:5n-3, 22:6n-3, 20:4n-3) contributed the most to principal component Dim2, which explained 18.6% of the variability in the host PUFA composition. The fatty acid 20:5n-3 contributed to the similarity among the species along the Dim1 axis. In the PCA of symbiont PUFA, *P. verrucosa* symbionts were distinctly separated from *P. speciosa* symbionts and *G. fascicularis* symbionts, of which the latter two showed some overlap in their ellipses (Fig. S4.3b). Both n-3 and n-6 PUFA (22:4n-6, 18:4n-3, 22:6n-3, 20:4n-6, 22:5n-3, 18:3n-3) contributed to the principal component Dim1, which explained 39.9% of the variability in symbiont PUFA composition. Symbiont PUFA composition was also explained by the principal component Dim2 (28.7%), with contributions from the fatty acids 20:4n-3, 18:2n-6, 18:3n-6, 20:5n-3, and 20:3n-6.

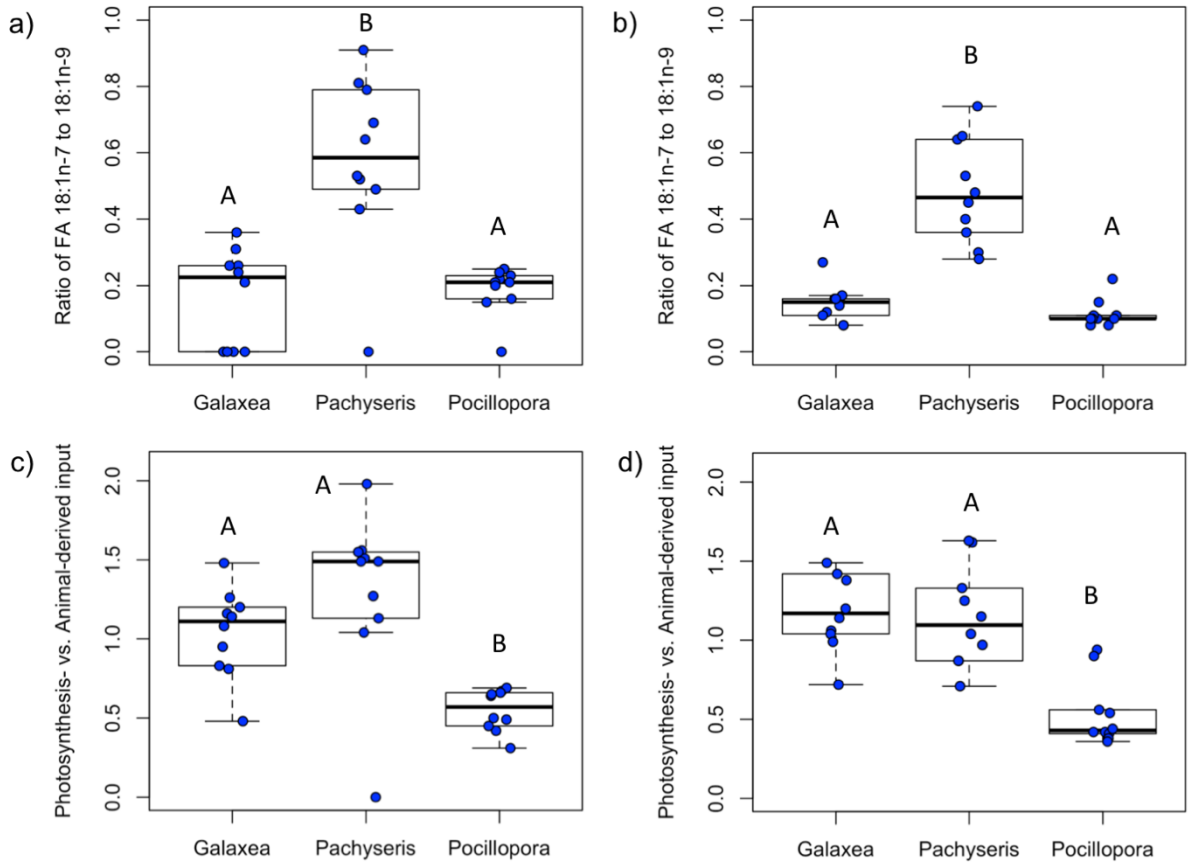

Figure 4.2. Established fatty acid indices are applied in a novel context as potential indicators of coral trophic strategies (autotrophy versus heterotrophy). The ratio of fatty acids 18:1n-7 to 18:1n-9 shows the relative proportion of photosynthesis-derived versus zooplankton-derived nutrition for *Galaxea fascicularis*, *Pachyseris speciosa*, and *Pocillopora verrucosa* a) coral hosts and b) their associated symbionts. An additional index of photosynthesis- versus animal-derived nutrition considers the input of typically photosynthesis-derived fatty acids (16:1n-7 and 18:1n-7) relative to typically animal-derived fatty acids (18:1n-9, 20:1n-9, and 22:1n-11) for c) coral hosts and d) their associated symbionts. Statistical differences are designated within each boxplot with letters (i.e., A and B).

4.4.5 Evaluating coral trophic strategies using fatty acid biomarker indices

An indicator of the degree of photosynthesis- versus zooplankton-derived nutrient input (i.e., ratio of 18:1n-7 to 18:1n-9) revealed that the ratio of 18:1n-7 to 18:1n-9 was highest in the host and symbionts of *P. speciosa* compared to the host and symbionts of *P. verrucosa* and *G. fascicularis* (Fig. 4.2). For the ratio of fatty acids 18:1n-7 to 18:1n-9, there were significant differences among the coral host species (ANOVA, $F_{2,27} = 17.74$, $p < 0.001$). Pairwise comparisons showed that host *P. speciosa* had significantly higher 18:1n-7 to 18:1n-9 ratios than host *G. fascicularis* ($p < 0.001$) and host *P.*

verrucosa ($p < 0.001$; Fig. 4.2a). Similarly, there were significant differences in the ratio of 18:1n-7 to 18:1n-9 among the symbionts (ANOVA, $F_{2,27} = 43.8$, $p < 0.001$) with a higher ratio in *P. speciosa* symbionts compared to *G. fascicularis* symbionts ($p < 0.001$) and *P. verrucosa* symbionts ($p < 0.001$; Fig. 4.2b).

The index of photosynthesis- (16:1n-7 and 18:1n-7) vs. animal-derived dietary input (18:1n-9, 20:1n-9, and 22:1n-11) differed among coral hosts (ANOVA, $F_{2,27} = 11.76$, $p < 0.001$), with a lower ratio in host *P. verrucosa* compared to host *P. speciosa* ($p < 0.001$) and host *G. fascicularis* ($p = 0.012$; Fig. 4.2c). The photosynthesis- vs. animal-derived dietary input index was also different among symbionts (ANOVA, $F_{2,27} = 11.76$, $p < 0.001$), with a higher ratio in *G. fascicularis* symbionts ($p < 0.001$) and *P. speciosa* symbionts ($p = 0.003$) compared to *P. verrucosa* symbionts (Fig. 4.2d).

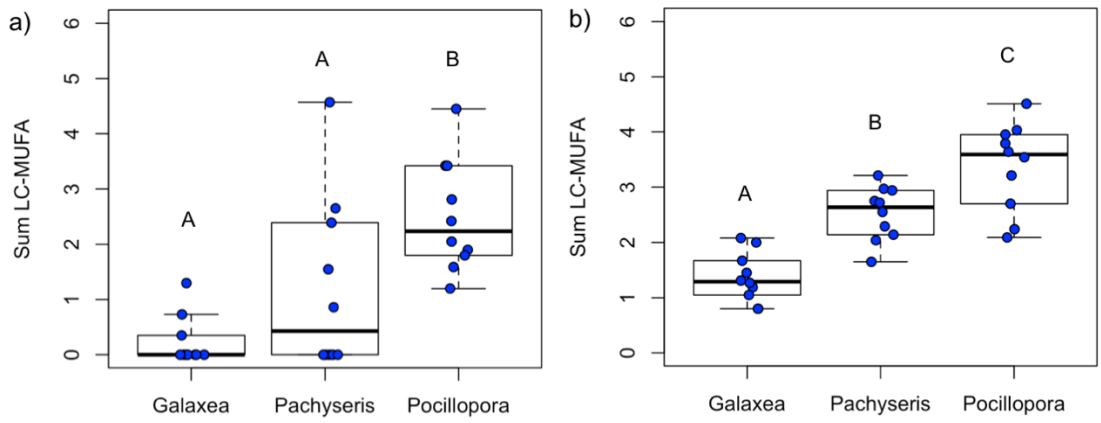

Figure 4.3. The fatty acid index of the sum of long-chain MUFA (LC-MUFA; ∑20:1 and ∑22:1) was used to evaluate the relative proportion of nutrition derived from copepods for *Galaxea fascicularis*, *Pachyseris speciosa*, and *Pocillopora verrucosa* a) coral hosts and b) their associated symbionts. Statistical differences are designated within each boxplot with letters (i.e., A and B).

The effect of coral species and tissue type were tested by evaluating the sum of LC-MUFA as an index of potential heterotrophic feeding on copepods. Coral species affected the sum of the long-chain MUFA (∑ LC-MUFA) among the coral hosts (ANOVA, $F_{2,27} = 10.52$, $p < 0.001$) with host *P. verrucosa* having a higher proportion of the ∑ LC-MUFA than host *G. fascicularis* ($p < 0.001$) and host *P. speciosa* ($p = 0.036$) (Fig. 4.3a). The proportion of ∑ LC-MUFA in host *P. speciosa* was variable, ranging from 0 to 4.6%. In symbionts, coral species also affected the proportion of ∑ LC-MUFA (ANOVA, $F_{2,27} = 28.35$, $p < 0.001$). The proportion of ∑ LC-MUFA in *P. verrucosa* symbionts was greater than *P. speciosa* symbionts ($p = 0.011$) and *G. fascicularis* symbionts ($p <$

0.001) (Fig. 4.3b). Further, the proportion of ∑ LC-MUFA was greater in *P. speciosa* symbionts than *G. fascicularis* symbionts ($p < 0.001$).

Table 4.1. Proportional contributions of the 95% confidence intervals and means of polyunsaturated fatty acids (PUFA) derived from copepods, diatoms, and symbionts estimated from the linear discriminant analysis. The particulate-derived source includes both copepods and diatoms as external food sources.

	Galaxea fascicularis	*Pachyseris speciosa*	*Pocillopora verrucosa*
95% CI			
Symbionts	0 ± 30	0 ± 70	0 ± 40
Particulates	70 ± 100	10 ± 80	60 ± 100
Mean			
Copepod	14	13	25
Diatom	81	65	66
Symbiont	5	22	9

4.4.6. Estimating coral autotrophy and heterotrophy from source PUFA

A linear discriminant analysis was used to estimate the proportion of coral PUFA derived from various potential sources including symbionts and various particulate prey items such as copepods and diatoms (Fig. 4.4). Overall, 95% confidence intervals indicated that species-specific symbiont PUFA has a lower contribution (0-40%) to coral host PUFA for both *G. fascicularis* and *P. verrucosa* while the contribution of symbiont-derived PUFA was variable but may be more important (0-88%) for coral host *P. speciosa* (Table 4.1). Particulate resources are likely an important source of PUFA for all coral hosts especially *G. fascicularis* and *P. verrucosa* (60-100%) as indicated by 95% confidence intervals. Between the particulate prey sources examined in the final model, copepod-derived PUFA was more important (mean 25%) for host *P. verrucosa* compared to the other species (mean 13-14%) while diatom-derived PUFA represented an important contribution to all host species (mean 65-81%).

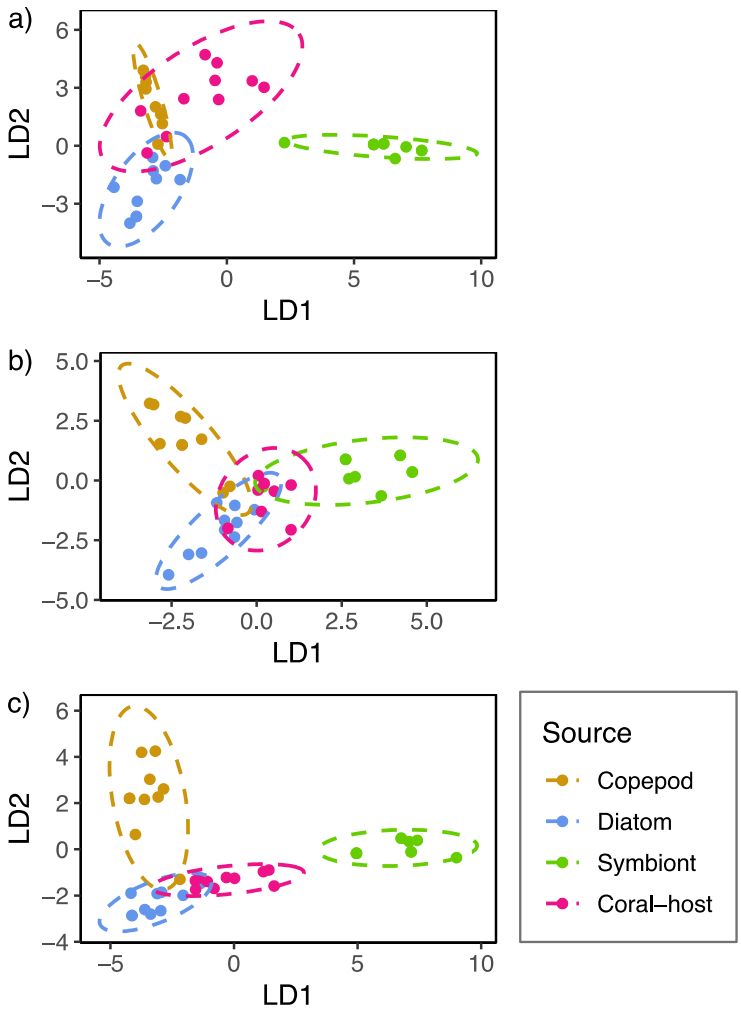

Figure 4.4. Linear discriminant analysis (LDA) based on PUFA composition (18:2n-6, 18:3n-3, 18:3n-6, 18:4n-3, 20:4n-6, 20:5n-3, 22:6n-3) was used to estimate the proportional contribution of different sources of PUFA to the coral host PUFA composition of the species a) *Galaxea fascicularis*, b) *Pachyseris speciosa*, and c) *Pocillopora verrucosa* with 95% confidence ellipses.

4.5 Discussion

The mixotrophic nature of reef-building corals enables them to live across a variety of environmental conditions. However, the complexity of coral symbiosis challenges our understanding of coral trophic strategies. Indeed, symbiont type can influence host trophic plasticity (Leal et al. 2015; Matthews et al. 2017). Biochemical tracers such as fatty acids are key to studying trophic ecology because multiple tracers provide insight into the origin of dietary resources (Kelly and Scheibling 2012). Despite the difference in the total mass of fatty acids between coral hosts and symbionts, there were significant relationships in the proportions of 14 individual fatty acids (comprising 47% of total fatty acids) between coral hosts and symbionts. Although early studies showed that fatty acids were synthesized

by symbionts and subsequently transferred to the coral host (Schlichter et al. 1984), the bidirectional interchange of fatty acids between coral host and symbionts is possible given that both partners can synthesize fatty acids *de novo* (Kabeya et al. 2018) and/or obtain nutrients from the diet (Houlbrèque and Ferrier-Pagès 2009; Jeong et al. 2012), with hosts capable of transferring fatty acids to symbionts (Imbs et al. 2014). Our study used several approaches to assess the contribution of host heterotrophy and symbiont autotrophy in coral fatty acid composition. A principal component analysis of total fatty acid composition of the three species of coral hosts revealed a difference between the more heterotrophic coral species *P. verrucosa* relative to the more autotrophic coral species *P. speciosa* (Fig. 4.1). The coral *G. fascicularis*, which can shift trophic strategies between shallow and deep reefs (Chapter 2), overlapped with the other two species but showed greater similarity with the fatty acid composition of *P. speciosa*. The similarity in the fatty acid composition of host *G. fascicularis* and host *P. speciosa* tissue supports carbon isotope data that showed that these species depend more on symbiont autotrophy than host heterotrophy (Chapter 2).

4.5.1 Coral trophic strategies as defined by fatty acids

Although PUFA composition is often used for coral chemotaxonomy (Imbs et al. 2007; Figueiredo et al. 2017), the analysis of PUFA composition in relation to coral nutrition is underutilized (Meyers 1979). A PCA of coral host PUFA showed separation of the more heterotrophic coral *P. verrucosa* and the more autotrophic coral *P. speciosa* while *G. fascicularis* showed overlap with both species (Fig. S4.3). Interestingly, three n-3 PUFAs (20:4n-3, 22:5n-3, 22:6n-3) contributed to the separation of *P. verrucosa* while five n-6 PUFAs (18:2n-6, 18:3n-6, 20:2n-6, 20:4n-6, 22:4n-6) drove the separation of *P. speciosa*. Symbionts are considered to be the primary source of 18:3n-6, which is found in higher proportions in symbionts than the host tissue (Imbs et al. 2014). In this study, the fatty acid 18:3n-6 was significantly higher in symbionts particularly in the more autotrophic corals *G. fascicularis* and *P. speciosa* (Fig. S4.2f). In contrast, the proportions of the longer chain n-6 PUFA, 20:4n-6 and 22:4n-6, were significantly higher in the host tissue. The fatty acid 22:4n-6 is particularly abundant (up to ~8% of total fatty acids) in the coral host tissue (Table S4.1, Imbs et al. 2007; Papina et al. 2007; Treignier et al. 2008), and has been suggested as a marker of the coral host (Imbs et al. 2014). Further evidence for host synthesis or assimilation of external sources of fatty acid 22:4n-6 was found in an experiment with symbiontic anemones incubated with ^{13}C-enriched DIC; the fatty acid 22:4n-6 was not labeled with ^{13}C despite ^{13}C incorporation in other n-6 PUFA earlier in the synthesis pathway (Dunn et al. 2012). Grouping of coral hosts according to PUFA composition further support the different species-specific trophic strategies of these three species. However,

whether the synthesis of n-3 and n-6 PUFA relate specifically to host and/or symbiont production requires further investigation (Imbs et al. 2010b; Imbs 2013).

The ratio of 18:1n-7 to 18:1n-9 fatty acids, which reflects photosynthesis- versus animal-derived input, showed patterns that reflect differences in coral trophic strategies (Fig. 4.3). The lower ratio of 18:1n-7 to 18:1n-9 fatty acids in *P. verrucosa* and *G. fascicularis* corals are consistent with a greater contribution from heterotrophic feeding, which is supported by carbon isotope ratios and experimental feeding (Chapter 2; Séré et al. 2010; Hoogenboom et al. 2015). The more heterotrophic coral *P. verrucosa* had a lower index of photosynthesis- vs. animal-derived dietary input compared to the more autotrophic corals *P. speciosa* and *G. fascicularis*. Studies comparing symbiotic and asymbiotic (without zooxanthellae) corals have shown that asymbiotic corals, which exclusively rely on heterotrophic feeding, have higher values of 22:5n-3 (Imbs et al. 2010a; Figueiredo et al. 2017). Among the three symbiotic corals in our study, host *P. verrucosa* had significantly higher proportions of 22:5n-3 than host *P. speciosa*. The coral *P. speciosa* had the highest ratio of 18:1n-7 to 18:1n-9, indicating a greater contribution from photosynthesis-derived products that may be due to higher symbiont autotrophy and/or nutrients from feeding on phytoplankton. Carbon isotope ratios and efficient photosynthesis across different light regimes indicates autotrophy is the primary trophic strategy of *P. speciosa* (Chapter 2; Cooper et al. 2011; Browne et al. 2014).

Several lines of evidence provide support for greater heterotrophic feeding by *P. verrucosa*, which can capture prey with its polyps using nematocysts as well as through extruding a mucus web (Séré et al. 2010). The fatty acid index of the ∑ LC-MUFA, an index characteristic of feeding on copepods, indicated that host *P. verrucosa* had the highest proportion of LC-MUFA potentially derived from copepods and was similar to previous results for this species from Vietnam (Latyshev et al. 1991). In particular, there was a strong relationship in the proportion of the common marker for copepod feeding (20:1n-9) between *P. verrucosa* host and symbionts (Fig. S4.2h). Further, the LDA model estimated the greatest PUFA contribution from copepods for the coral host *P. verrucosa* (25% average) compared to the other coral species (13-14%). The convergence of MUFA and PUFA results provide strong support for *P. verrucosa* heterotrophic feeding on copepods. Indeed, Pocilloporid corals consume a variety of taxa including copepods, microalgae, planktonic larvae, and rotifers (Séré et al. 2010; Leray et al. 2019) and water column primary productivity is an important driver of heterotrophy for Pocillopora species (Fox et al. 2018). Among the meiofauna of reef sediments, harpacticoid copepods are more abundant in outer reefs compared to lagoons of the Maldives (Semprucci et al. 2013). Despite the importance of zooplankton as a food source for marine fauna in

the Maldives, including corals, manta rays, blue whales, and whale sharks (Anderson and Ahmed 1993; Anderson et al. 2011, 2012), limited information is available about the zooplankton community in reef waters of the central Indian Ocean (Stebbing 1904; Vinogradov and Voronina 1962). Around the time of the coral sampling in the Maldives, calanoids dominated the copepod community in the lagoon of Kavaratti atoll (north of the Maldives) with a shift in copepod community composition and abundance following the thermal stress event of the 2016 El Niño (Vineetha et al. 2018). There is a clear need for research on zooplankton community structure and abundance across the reef water column throughout the Maldives archipelago.

4.5.2 Fatty acid composition distinguishes symbionts from different host species

Despite the difference in the total mass of fatty acids between coral hosts and symbionts, there were significant relationships in the proportions of 14 individual fatty acids (comprising 47% of total fatty acids) between coral hosts and symbionts. The potential for bidirectional interchange of fatty acids between coral host and symbionts is supported by the ability of both partners to synthesize fatty acids *de novo* (Kabeya et al. 2018) and/or to exchange nutrients obtained from the diet (Houlbrèque and Ferrier-Pagès 2009; Jeong et al. 2012). Indeed, symbiont-related factors can influence coral trophic plasticity (Leal et al. 2015). The PCA of symbiont composition for all 30 fatty acids also showed separation among the symbionts from the three different species of coral (Fig. 4.2b). Host *P. speciosa* and host *G. fascicularis*, both of which appear to rely more on autotrophy than heterotrophy (Chapter 2), had symbionts that grouped more closely together, but their ellipses showed minimal overlap. In contrast, symbionts from the more heterotrophic coral *P. verrucosa* were distinctly separated from the other symbionts. There is clear differentiation in the fatty acid composition among symbionts of different clades (ITS2 sequences types) and/or symbionts isolated from different coral hosts (LaJeunesse 2002; Zhukova and Titlyanov 2003; Wang et al. 2015). The coral host *P. speciosa* is known to have a stable association with *Symbiodinium* clade C (Bongaerts et al. 2011b; Cooper et al. 2011; Ziegler et al. 2015b) while *P. verrucosa* has a stable association with *Symbiodinium* clade A (Ziegler et al. 2014, 2015a). The ability of *G. fascicularis* to associate with two clades of *Symbiodinium* (C and D; Dong et al. 2009; Huang et al. 2011) supports the closer grouping of *G. fascicularis* symbionts with *P. speciosa* symbionts (Figs. 4.1b and S4.3b). The proportion of the fatty acid 18:2n-6 is lower in symbionts from lower light conditions (Papina et al. 2007), suggesting that relatively higher proportions of 18:2n-6 may indicate greater dependence on symbiont autotrophy. In our study, lower proportions of 18:2n-6 were found in the more heterotrophic *P. verrucosa* compared to symbionts of the more autotrophic coral species *P. speciosa* and *G. fascicularis*. Dinoflagellates are generally characterized by high proportions of n-3 PUFA (Dalsgaard et al. 2003), and it has been

previously hypothesized that n-3 PUFA are primarily synthesized by the coral symbiont (Imbs 2013). Generally, symbionts of the three species of coral had greater proportions of n-3 PUFA (Treignier et al. 2008; Imbs et al. 2010b; Teece et al. 2011) but only the proportion of fatty acid 22:6n-3 was significantly higher in symbionts than in host tissue (Fig. S4.2n). The fatty acid 22:6n-3 is considered a marker for dinoflagellates and microalgae (Dalsgaard et al. 2003; Seemann et al. 2013).

Differences in fatty acid metabolism of symbionts may be due to a combination of factors, including different clades of symbionts, host influence on symbiont metabolism, and/or environmental conditions (Bishop and Kenrick 1980; Treignier et al. 2008; Weng et al. 2014). For example, host feeding on PUFA-enriched plankton has been shown to positively affect autotrophy of *G. fascicularis* symbionts (Lim et al. 2017). Interestingly, the fatty acid 24:6n-3 was observed only in the symbiont tissue of *P. speciosa* and not in any host tissue. Certain C_{24} PUFA, including the fatty acid 24:6n-3, have been considered chemotaxonomic markers for octocorals with 24:6n-3 apparently yet to be identified in hexacorals (Imbs et al. 2010a; Figueiredo et al. 2017). However, the fatty acid 24:6n-3 is an intermediate product during the synthesis of 22:6n-3 (Gurr et al. 2002). Indeed, the symbionts of *P. speciosa* had less than half of the proportion of 22:6n-3 compared to the other two species' symbionts. The detection of 24:6n-3 may indicate that this fatty acid is a precursor to 22:6n-3 in the PUFA synthesis pathway and/or 24:6n-3 is important for the physiology of *P. speciosa* symbionts, warranting further investigation of symbiont biosynthesis pathways.

4.5.3 PUFA composition of coral hosts and potential resources

To evaluate the extent of autotrophy and heterotrophy in corals, it is necessary to consider potential fatty acid sources of these different trophic strategies. To estimate the relative importance of different sources of nutrition for the coral host, a linear discriminant analysis model was used to estimate the contribution of different potential sources of PUFA including species-specific symbionts and various plankton groups, which are well characterized by their PUFA composition (Bode et al. 2015; Galloway and Winder 2015). Overall, each species of coral host showed a distinct composition of PUFA compared to likely sources of potential prey in ordination space (Fig. 4.4).

Among the three species of coral hosts, a majority of PUFA (mean 70%) appeared to be derived from diatoms. The larger estimated contribution from diatom-derived fatty acids rather than copepod-derived fatty acids aligns with some of the passive feeding strategies exhibited by the corals (e.g., mucus webs, extracoelenteric feeding, mesenterial feeding) (Stafford-Smith and Ormond 1992; Wijgerde et al. 2011; Leray et al. 2019). Considering the high potential contribution of diatom-

derived PUFA to coral host nutrition, future work should investigate the prevalence of diatoms as an important source of food for corals. Phytoplankton can be an important source of nutrients for reef ecosystems (Ayukai 1995; Yahel et al. 1998; Genin et al. 2009). Notably, diatom depletion can be greater than zooplankton depletion in some reef systems (Glynn 1973) and diatom-derived organic matter can be a source of nutrients for coral reef sponges (de Goeij et al. 2008). Although zooplankton have been typically considered the primary particulate food source for reef-building corals (Goreau et al. 1971; Porter 1974; Muscatine and Porter 1977), the extent to which phytoplankton may contribute to coral nutrition remains poorly understood (Seemann et al. 2012; Seemann 2013; Leal et al. 2014). Despite the limited information on phytoplankton in tropical Indian Ocean waters, diatoms are among the dominant taxa recorded (Garrison et al. 1998; Stanca et al. 2013; Karati et al. 2017). Unfortunately, information regarding phytoplankton community structure and abundance is not available for fore reef slopes of the Maldives. However, in coral reef lagoons of the Maldives, dinoflagellates (class Dinophyceae) represented the majority of phytoplankton followed by diatoms (class Coscinodiscophyceae) (Stanca et al. 2013). Interestingly, a shift in the phytoplankton community from dinoflagellates (>50%) to diatoms (>50%) was observed in Kavaratti lagoon (north of the Maldives) following the 2016 El Niño (Karati et al. 2017). Karati et al. (2017) observed a phytoplankton community dominated by diatoms (55%) and cyanobacteria (33%) in May 2016. Although our sampling occurred in March-April 2017 in the Maldives, this provides insight into the potential changes in the phytoplankton community following the thermal stress coral bleaching event of 2016 (Ibrahim et al. 2017). Although this study cannot compare pre- and post-thermal stress coral fatty acids, symbionts showed higher proportions of the fatty acids 14:0 and 18:3n-6 that have been shown to increase under thermal stress conditions (Hillyer et al. 2017). For corals in the Maldives, the potential reliance on heterotrophy is supported by the estimates of the LDA model and the relatively greater heterotrophy compared to corals from other reef systems (Fox et al. 2018). Although coral fatty acid composition may change under thermal stress conditions that cause coral bleaching (Bachok et al. 2006), heterotrophic feeding during thermal stress conditions can mitigate the potential effect on coral fatty acids (Tolosa et al. 2011). Future work should investigate the potential effect of a trophic enrichment factor in the assimilation of fatty acids (heterotrophic feeding) and/or the transfer/synthesis of fatty acids in the nutrient exchange between coral hosts and their symbionts under normal conditions as well as thermal stress.

Despite their distribution across the shallow to deep reef slopes (10-30 m) of the central Maldives, the three species of coral in this study (*G. fascicularis*, *P. speciosa*, and *P. verrucosa*) had distinct differences in their fatty acid composition. The more heterotrophic coral *P. verrucosa* and the more

autotrophic coral *P. speciosa* appeared to have the greatest differences between their host and symbiont fatty acid composition (Figs. 4.1 and S4.3). Given the frequency of thermal stress events that cause recurring coral bleaching, it is especially important to characterize coral trophic strategies and investigate the mechanisms by which corals survive and recover (Grottoli et al. 2014; Schoepf et al. 2015; Hughes et al. 2018). The ability of corals to obtain nutrients from different resources is critical when the symbiosis and the presumably major autotrophic energy source is compromised (Grottoli et al. 2006; Tremblay et al. 2016). Mixotrophic organisms may become more heterotrophic under conditions of rising temperatures, but it is unclear if such changes in trophic behavior indicate underlying physiological stress or a sign of resilience (Hughes and Grottoli 2013; Wilken et al. 2013). Although thermal stress conditions can affect coral fatty acid composition and the expression of symbiont fatty acid desaturases (Bachok et al. 2006; Gierz et al. 2017; Hillyer et al. 2017), heterotrophic feeding can mitigate the potential effect of thermal stress conditions on coral fatty acids (Tolosa et al. 2011). In particular, feeding on PUFA-enriched particulate food sources can mitigate coral bleaching under thermal stress conditions (Tagliafico et al. 2017). Eight months following a thermal stress event in the Maldives, we show that host heterotrophy is the primary trophic strategy for all three species of coral. High primary productivity supported by deep-water upwelling sustains relatively high coral heterotrophy in the Maldives relative to corals from less productive reef systems (Fox et al. 2018). Whether the high levels of coral heterotrophy reflect the status quo supported by the productive waters of the Maldives or a prolonged stress response – heterotrophic compensation – by the corals (Hughes and Grottoli 2013) requires the regular monitoring of coral and symbiont fatty acid composition over time. This study demonstrates that the fatty acid composition of corals can be used to determine coral trophic strategies, with the fatty acid results aligning closely with previous carbon isotope results for the same three species of coral (Chapter 2). Of the three species, *P. verrucosa* depends more on heterotrophic feeding than *P. speciosa* while *G. fascicularis* shows a more generalist strategy, appearing to depend on both autotrophy and heterotrophy. If anthropogenic emissions continue according to the business-as-usual scenarios and frequent thermal stress events continue to devastate coral reefs worldwide (Hughes et al. 2018a), it is likely that species-specific trophic strategies will underlie the shifts in surviving coral communities.

4.6 Acknowledgements

We thank Aaron Galloway, Wilhelm Hagen, Gerhard Kattner, Alex Lowe, and Sami Taipale for their helpful advice and sharing zooplankton fatty acid data. We thank Kristen Brown, Dominic Bryant, Mary Bryant, Pete Dalton, Susie Green, Chris Hoegh-Guldberg, the Seaview Survey team, the Maldives Marine Research Centre, especially Shiham Adam and Nizam Ibrahim, the Ministry of

Fisheries and Agriculture, the Environmental Protection Agency, and the crew of the MV Emperor Atoll for their research support in the Maldives. This study was made possible by funding from the XL Catlin Seaview Survey (OHG and VZR), Australian Research Council (ARC) Centre of Excellence for Coral Reef Studies (SD and OHG), an ARC Laureate Fellowship (OHG), the University of Queensland Research Training Tuition Fee Scholarship (VZR), and the University of Washington Dale A. Carlson Endowed Faculty Support Fund (MB and VZR).

4.7 Supplementary Information

Table S4.1. Fatty acid composition (mean ± SD of % total fatty acids) of three species of coral hosts and their symbionts from the Maldives (n=10 samples for each species of host or symbiont).

	Galaxea fascicularis		*Pachyseris speciosa*		*Pocillopora verrucosa*	
Fatty acid	Host	Symbiont	Host	Symbiont	Host	Symbiont
14:0	1.5 ± 0.5	3.9 ± 2.0	1.6 ± 0.7	3.2 ± 0.8	3.2 ± 1.0	5.0 ± 0.6
14:1	0.0 ± 0.1	1.0 ± 2.3	0.0 ± 0.0	0.2 ± 0.2	0.0 ± 0.0	0.4 ± 0.6
15:0	0.1 ± 0.1	0.2 ± 0.1	0.1 ± 0.1	0.3 ± 0.1	0.4 ± 0.4	1.0 ± 0.4
16:0	37.2 ± 6.2	35.2 ± 8.5	31.5 ± 8.3	43.6 ± 10.5	36.9 ± 4.9	34.2 ± 6.7
16:1n-7	2.4 ± 0.7	4.8 ± 1.6	2.0 ± 1.1	2.6 ± 0.4	2.5 ± 0.3	3.1 ± 0.8
17:0	0.8 ± 1.6	0.5 ± 1.0	0.1 ± 0.2	0.0 ± 0.0	2.1 ± 3.3	0.3 ± 0.8
18:0	22.2 ± 3.7	7.0 ± 1.9	29.0 ± 6.4	12.9 ± 3.1	24.6 ± 3.9	8.5 ± 1.5
18:1n-7	0.5 ± 0.4	0.5 ± 0.1	1.4 ± 0.6	1.2 ± 0.2	0.7 ± 0.3	0.5 ± 0.1
18:1n-9	2.8 ± 0.5	3.5 ± 1.3	2.5 ± 1.1	2.7 ± 0.9	4.2 ± 0.9	4.8 ± 1.3
18:2n-6	1.0 ± 0.7	2.3 ± 0.6	1.0 ± 0.7	1.7 ± 0.6	0.6 ± 0.4	1.0 ± 0.3
18:3n-3	0.0 ± 0.0	0.1 ± 0.1	0.0 ± 0.0	0.0 ± 0.0	0.0 ± 0.0	0.1 ± 0.1
18:3n-6	2.3 ± 1.2	8.7 ± 2.7	2.0 ± 1.4	7.2 ± 3.0	1.5 ± 0.8	4.7 ± 1.1
18:4n-3	0.5 ± 0.5	6.4 ± 3.0	1.5 ± 1.9	5.2 ± 3.7	1.3 ± 0.8	6.9 ± 3.6
20:0	2.6 ± 0.7	0.8 ± 0.3	1.3 ± 0.5	1.0 ± 0.3	2.8 ± 0.4	1.6 ± 0.4
20:1n-11	0.0 ± 0.0	0.0 ± 0.0	0.0 ± 0.1	1.0 ± 0.7	0.0 ± 0.0	0.1 ± 0.1
20:1n-7	0.0 ± 0.0	0.0 ± 0.0	0.3 ± 0.8	0.0 ± 0.0	0.0 ± 0.0	0.1 ± 0.0
20:1n-9	0.0 ± 0.1	0.1 ± 0.1	0.1 ± 0.2	0.1 ± 0.2	2.1 ± 0.6	1.9 ± 0.7
20:2n-6	0.2 ± 0.4	0.3 ± 0.2	0.4 ± 0.5	0.4 ± 0.1	0.2 ± 0.3	0.3 ± 0.1
20:3n-6	2.4 ± 1.3	2.6 ± 1.2	0.6 ± 0.8	1.1 ± 0.7	2.5 ± 1.5	4.3 ± 1.1
20:4n-3	0.0 ± 0.0	0.2 ± 0.1	0.0 ± 0.0	0.1 ± 0.1	0.1 ± 0.2	0.6 ± 0.2
20:4n-6	6.4 ± 3.8	4.2 ± 2.1	6.2 ± 3.6	3.9 ± 2.8	3.2 ± 1.6	3.4 ± 1.9
20:5n-3	6.5 ± 6.1	5.9 ± 2.8	9.6 ± 17.6	4.7 ± 2.5	2.6 ± 2.5	3.0 ± 1.8
22:0	0.3 ± 0.3	0.3 ± 0.2	0.8 ± 0.6	0.6 ± 0.2	0.5 ± 0.3	0.3 ± 0.1
22:1n-11	0.0 ± 0.0	0.8 ± 0.5	0.0 ± 0.0	0.6 ± 0.2	0.0 ± 0.0	0.5 ± 0.3
22:1n-7	0.0 ± 0.0	0.0 ± 0.0	0.6 ± 1.0	0.0 ± 0.0	0.1 ± 0.2	0.0 ± 0.0
22:1n-9	0.2 ± 0.4	0.4 ± 0.5	0.1 ± 0.3	0.8 ± 0.4	0.3 ± 0.4	0.7 ± 0.4
22:4n-6	7.9 ± 2.5	2.8 ± 1.4	6.4 ± 2.3	1.3 ± 1.1	4.2 ± 2.0	2.4 ± 0.9
22:5n-3	0.2 ± 0.3	0.4 ± 0.2	0.0 ± 0.0	0.0 ± 0.1	0.5 ± 0.5	0.8 ± 0.6

22:6n-3	2.0 ± 1.6	7.1 ± 2.6	0.6 ± 0.8	3.4 ± 1.8	2.9 ± 1.4	9.5 ± 2.0
24:0	0.1 ± 0.2	0.0 ± 0.0	0.0 ± 0.0	0.1 ± 0.1	0.0 ± 0.0	0.1 ± 0.0
Total FA mass (10^{-3} mg per mg dry weight)	5.9	48.5	6.8	66.2	6.8	108

Table S4.2. Classification of different potential sources of polyunsaturated fatty acids (18:2n-6, 18:3n-6, 18:3n-3, 18:4n-3, 18:5n-3, 20:4n-6, 20:5n-3, 22:6n-3) evaluated in the original model of the linear discriminant analysis.

Coral species	Copepod	Cryptophyte	Cyanobacteria	Diatom	Dinoflagellate	Symbiont
Galaxea fascicularis	0.79	0.80	0.67	0.97	0.56	0.90
Pachyseris speciosa	0.77	0.84	0.67	0.97	0.50	0.90
Pocillopora verrucosa	0.79	0.80	0.67	0.97	0.50	1.00

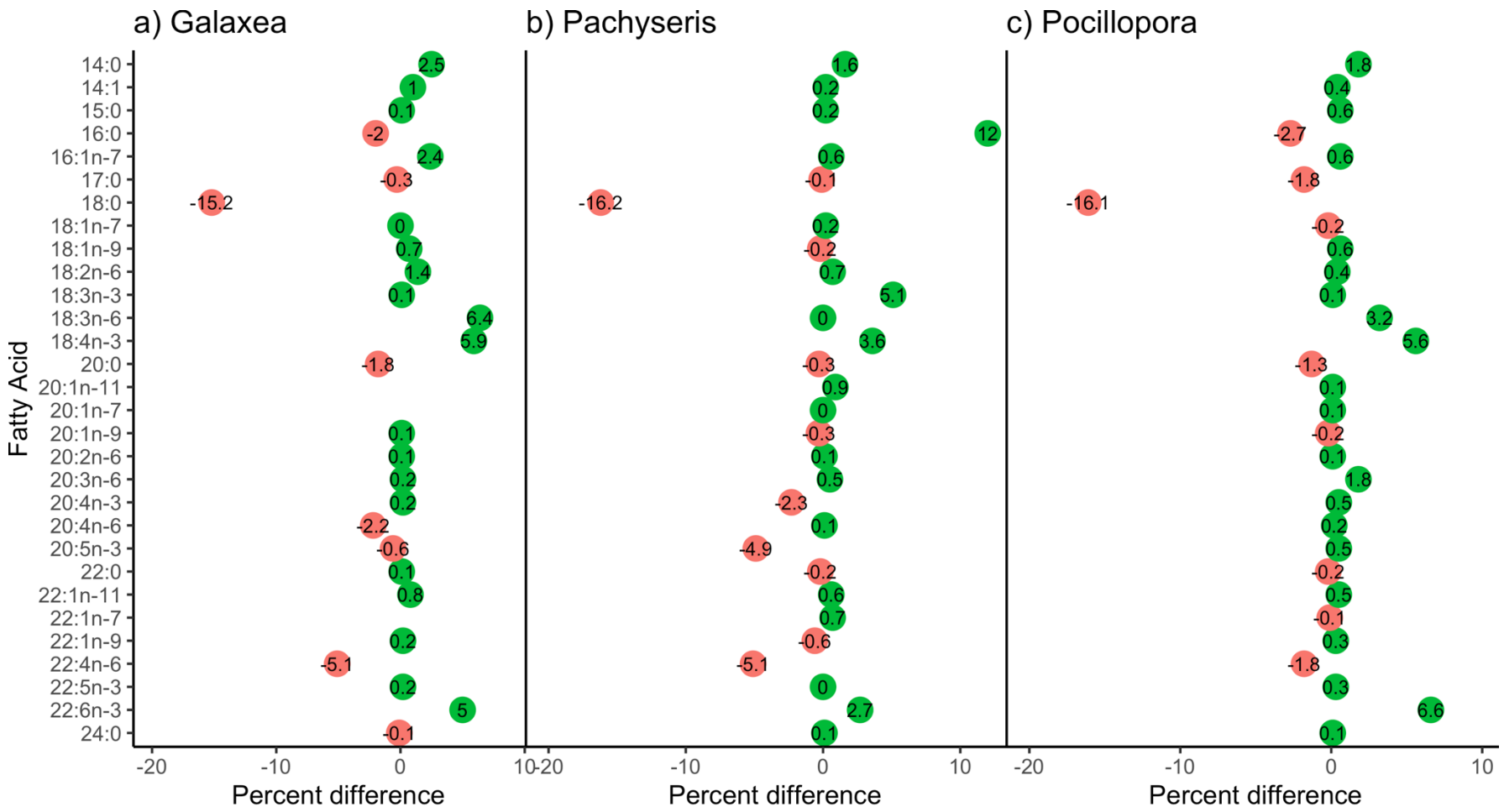

Figure S4.1. Comparison of the proportional difference of thirty fatty acids between coral hosts (red) and symbionts (green) for three species of corals a) *Galaxea fascicularis*, b) *Pachyseris speciosa*, and c) *Pocillopora verrucosa*. Number inside colored circle is the difference between coral host and symbiont fatty acid percentage, with color and x-axis position relative to zero signifying which partner has a greater proportion of a given fatty acid. A blank space is shown if there was zero percent of a given fatty acid. A negative number of host fatty acid percent difference is due to the position (left) in relation to zero on the x-axis.

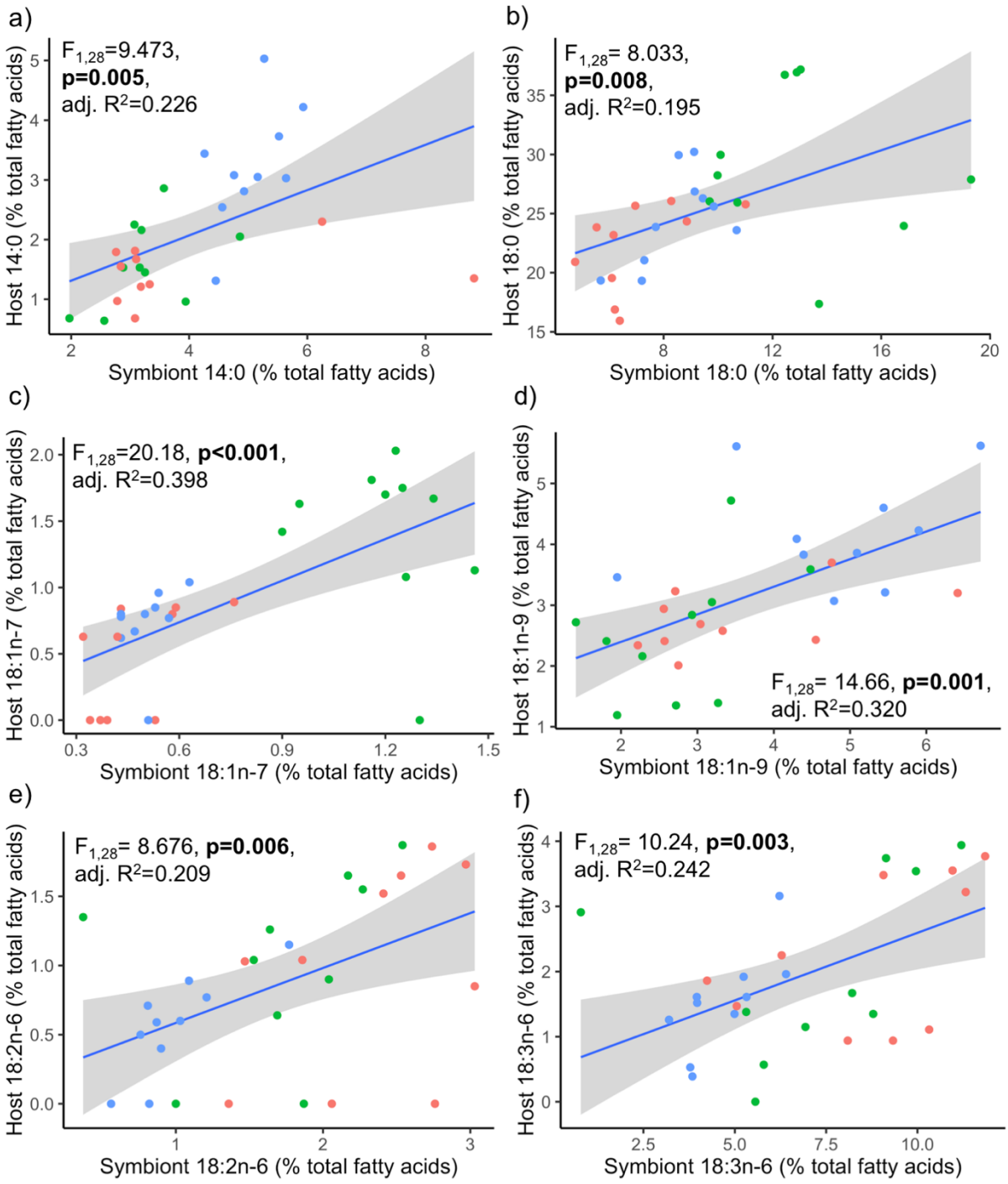
a)
$F_{1,28}$=9.473,
p=0.005,
adj. R^2=0.226
Host 14:0 (% total fatty acids)
Symbiont 14:0 (% total fatty acids)
b)
$F_{1,28}$= 8.033,
p=0.008,
adj. R^2=0.195
Host 18:0 (% total fatty acids)
Symbiont 18:0 (% total fatty acids)
c)
$F_{1,28}$=20.18, **p<0.001**,
adj. R^2=0.398
Host 18:1n-7 (% total fatty acids)
Symbiont 18:1n-7 (% total fatty acids)
d)
$F_{1,28}$= 14.66, **p=0.001**,
adj. R^2=0.320
Host 18:1n-9 (% total fatty acids)
Symbiont 18:1n-9 (% total fatty acids)
e)
$F_{1,28}$= 8.676, **p=0.006**,
adj. R^2=0.209
Host 18:2n-6 (% total fatty acids)
Symbiont 18:2n-6 (% total fatty acids)
f)
$F_{1,28}$= 10.24, **p=0.003**,
adj. R^2=0.242
Host 18:3n-6 (% total fatty acids)
Symbiont 18:3n-6 (% total fatty acids)

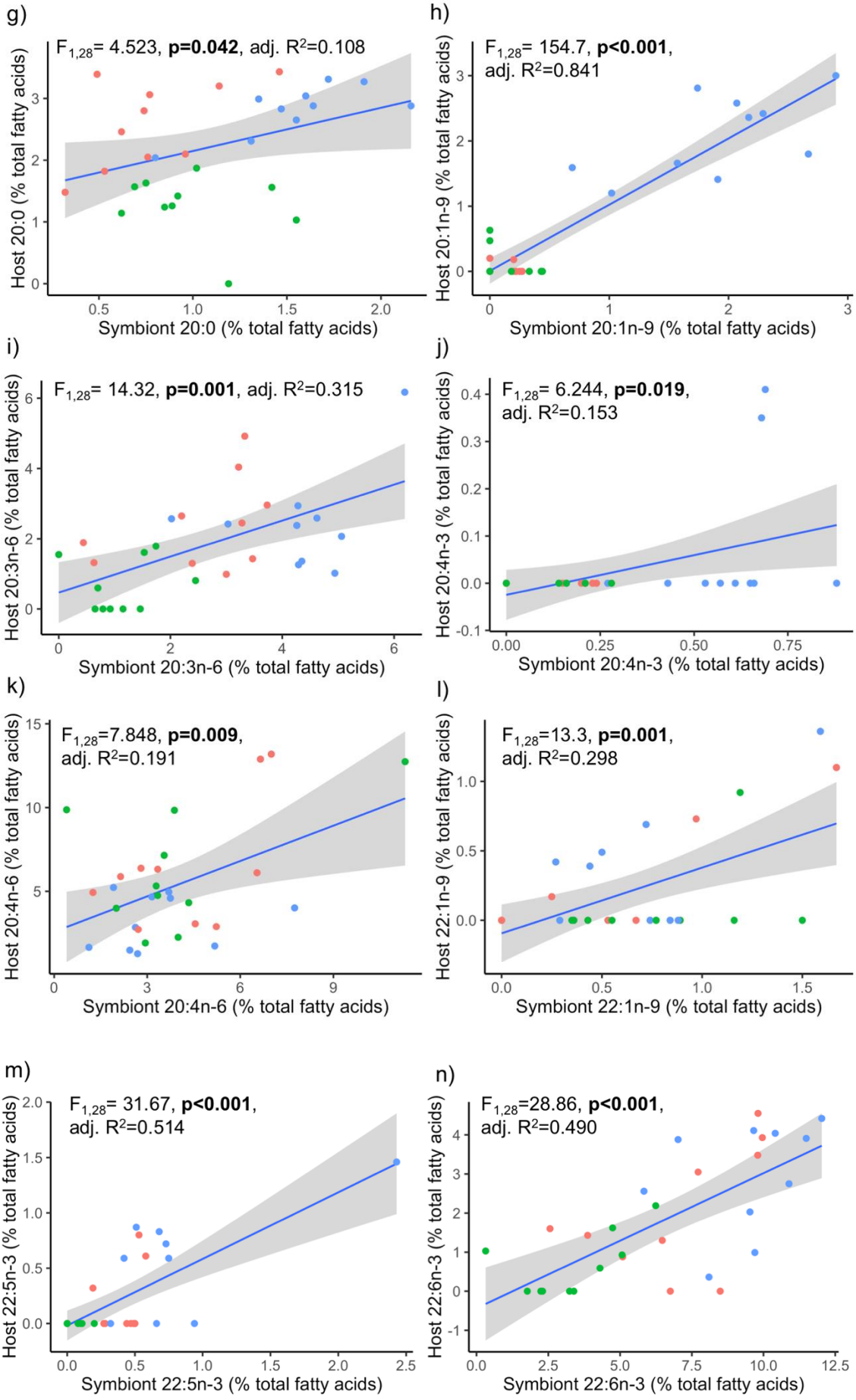
g)
$F_{1,28}$= 4.523, **p=0.042**, adj. R^2=0.108
Host 20:0 (% total fatty acids)
Symbiont 20:0 (% total fatty acids)
h)
$F_{1,28}$= 154.7, **p<0.001**,
adj. R^2=0.841
Host 20:1n-9 (% total fatty acids)
Symbiont 20:1n-9 (% total fatty acids)
i)
$F_{1,28}$= 14.32, **p=0.001**, adj. R^2=0.315
Host 20:3n-6 (% total fatty acids)
Symbiont 20:3n-6 (% total fatty acids)
j)
$F_{1,28}$= 6.244, **p=0.019**,
adj. R^2=0.153
Host 20:4n-3 (% total fatty acids)
Symbiont 20:4n-3 (% total fatty acids)
k)
$F_{1,28}$=7.848, **p=0.009**,
adj. R^2=0.191
Host 20:4n-6 (% total fatty acids)
Symbiont 20:4n-6 (% total fatty acids)
l)
$F_{1,28}$=13.3, **p=0.001**,
adj. R^2=0.298
Host 22:1n-9 (% total fatty acids)
Symbiont 22:1n-9 (% total fatty acids)
m)
$F_{1,28}$= 31.67, **p<0.001**,
adj. R^2=0.514
Host 22:5n-3 (% total fatty acids)
Symbiont 22:5n-3 (% total fatty acids)
n)
$F_{1,28}$=28.86, **p<0.001**,
adj. R^2=0.490
Host 22:6n-3 (% total fatty acids)
Symbiont 22:6n-3 (% total fatty acids)

Figure S4.2. The relationship between symbiont and host fatty acid proportions of fatty acids (a-n), isolated from individual coral colonies of *Galaxea fascicularis* (red), *Pachyseris speciosa* (green), and *Pocillopora verrucosa* (blue).

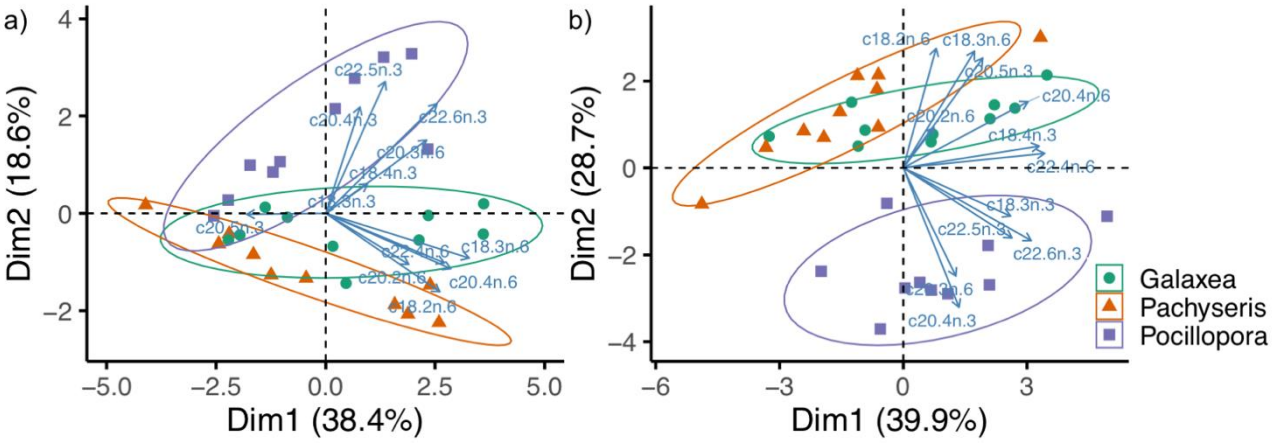

Figure S4.3. Principal component analysis based on composition of 12 polyunsaturated fatty acids (all PUFA, see Table S4.1) in *Galaxea fascicularis*, *Pachyseris speciosa*, and *Pocillopora verrucosa* a) coral hosts and b) their associated symbionts, with 80% concentration ellipses shown.

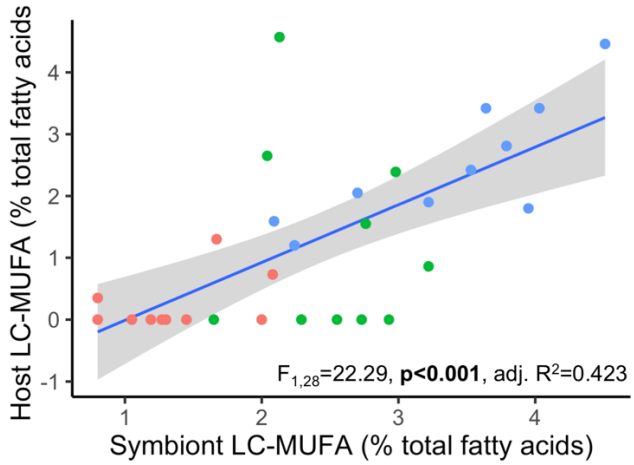

Figure S4.4. Proportion of the sum of long-chain MUFA (LC-MUFA) between symbionts and coral host of individual colonies *Galaxea fascicularis* (red), *Pachyseris speciosa* (green), and *Pocillopora verrucosa* (blue).

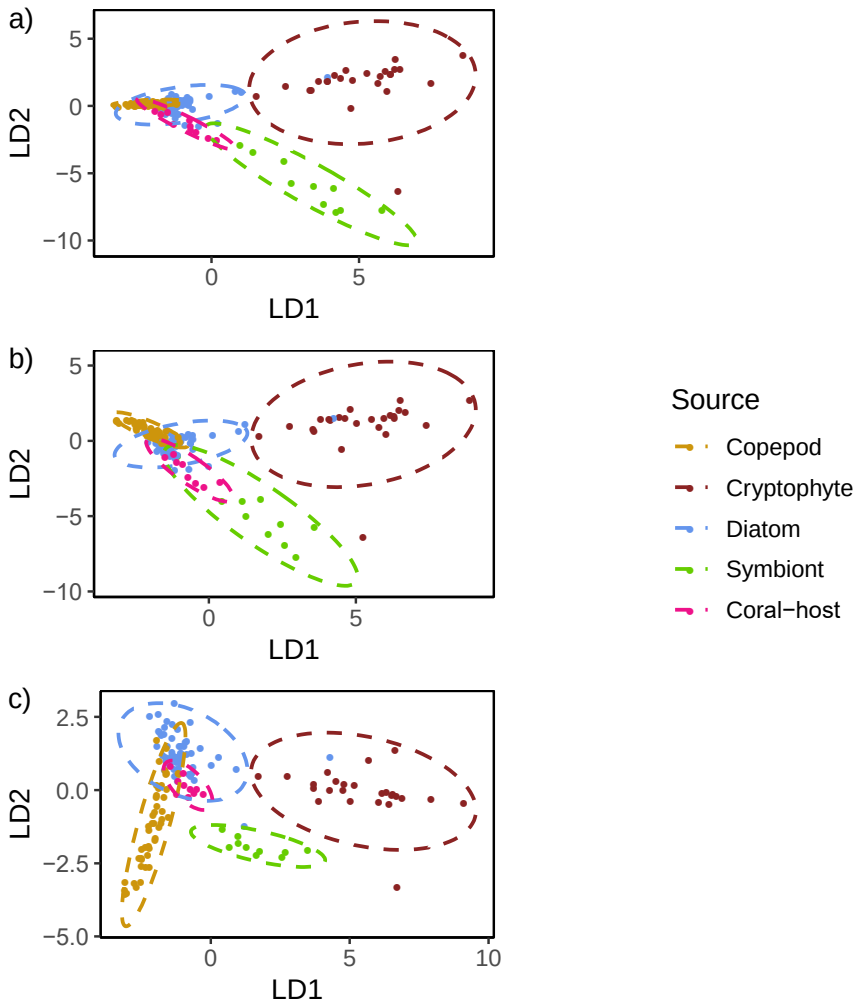

Figure S4.5. Linear discriminant analysis (LDA) based on the PUFA composition (18:2n-6, 18:3n-3, 18:3n-6, 18:4n-3, 18:5n-3, 20:4n-6, 20:5n-3, 22:6n-3) of coral hosts and potential food sources (original model). Potential sources include copepods, cryptophytes, diatoms, and symbionts specific to each coral host species a) *Galaxea fascicularis*, b) *Pachyseris speciosa*, and c) *Pocillopora verrucosa* (95% confidence level ellipse).

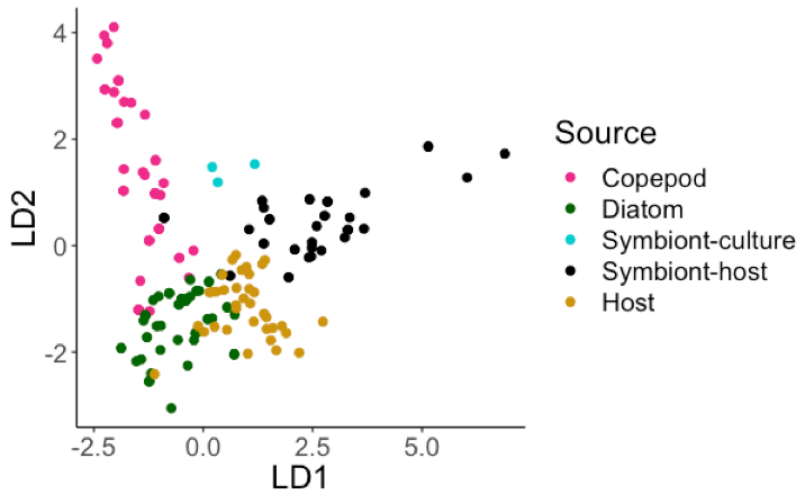

Figure S4.6. Linear discriminant analysis (LDA) based on the polyunsaturated fatty acid composition (18:2n-6, 18:3n-3, 18:3n-6, 18:4n-3, 20:4n-6, 20:5n-3, 22:6n-3) of coral hosts, most likely potential food sources (as per final LDA model), host-associated symbionts, and cultured symbionts. Despite the low sample size of cultured symbiont fatty acid data available in the literature, the cultured symbiont samples group closely together and do not clearly cluster with host-associated symbionts.

Chapter 5:

General Discussion

5.1 Autotrophy and heterotrophy of reef-building corals in the Maldives

The capacity of symbiotic reef-building corals to acclimatize to a wide range of environmental conditions is partly dependent on the plasticity of the host coral and its symbionts (LaJeunesse et al. 2004; Hoogenboom et al. 2008; Kenkel and Matz 2016). Consequently, an organism's ecological niche is constrained by habitat and resource related environmental factors (Hutchinson 1957), with trophic strategies and interactions contributing to an organism's trophic niche (Cohen 1977). The dimensions of the trophic niche can be analyzed using natural abundance stable isotope ratios (Newsome et al. 2007), with multivariate ellipses delineating niche size and position (Jackson et al. 2011). In this regard, isotopic niches are useful proxies for trophic niches given that they both depend on resource availability and feeding strategies (Layman et al. 2012). Biochemical tracers such as natural abundance stable isotope ratios and fatty acid trophic markers provide important new insights into marine food webs when combined with other ecological data (Pethybridge et al. 2018).

The present thesis focused on the trophic ecology of three species of reef-building coral (*G. fascicularis*, *P. speciosa*, and *P. verrucosa*) that are common to the Indo-Pacific region. Extensive sampling of coral hosts (n=399), their associated symbionts (n=393), and particulate resources (POM/plankton, n=192) revealed species-specific patterns of $\delta^{13}C$ values that indicate diverse trophic strategies that varied in space and time (Chapters 2 and 3). Species-specific trophic strategies were evident in both sampling years (Chapter 3) despite the occurrence of the thermal stress event in 2016. Furthermore, a different set of biochemical tracers based on 30 fatty acid trophic markers supported these species-specific trophic strategies (Chapter 4). In this regard, the same groupings of species were evident in both host and symbiont tissue with the results of the thesis research providing robust biochemical support for different trophic strategies by coral species on reef slopes from 10 m to 30 m depth. The extensive isotopic data set presented in this thesis was used to create three two-source carbon isotope mixing models (Model A, Model B, and Model C) to estimate the contribution of autotrophy and heterotrophy with standard error (Phillips and Gregg 2001).

To account for variation in coral $\delta^{13}C$ values in the Maldives, Model A set the autotrophy end member to +1.0‰ of the most autotrophic coral host (average $\delta^{13}C$ of deep host *P. speciosa* from 2015, prior to thermal stress event) while the heterotrophy end member was set as the average $\delta^{13}C$ value of plankton. The carbon isotope mixing Model A estimated that *P. speciosa* and shallow *G. fascicularis* from prior to the thermal stress event were predominantly autotrophic (~80%) whereas this model estimated a significant contribution (~50%) of heterotrophic carbon for *P. verrucosa* and deep *G. fascicularis* (Table 5.1).

Table 5.1. Model A- Carbon isotope mixing model estimates of the relative importance of autotrophy and heterotrophy for three species of reef-building coral. The end member for autotrophy was derived by adding 1.0‰ to the most autotrophic coral (average $\delta^{13}C$ of deep host *P. speciosa* from 2015, prior to the 2016 thermal stress event), and the heterotrophy end member is the average $\delta^{13}C$ value of plankton. The $\delta^{13}C$ values and proportions of contributions from autotrophy and heterotrophy are shown as average ± standard error, calculated using IsoError. Shallow (2015) and deep (2015 and 2017) populations of *G. fascicularis* were considered separately because of different average $\delta^{13}C$ values between depths.

			Coral Host Average	Autotrophy		Heterotrophy	
Species	Depth	Year	$\delta^{13}C$ (‰)	$\delta^{13}C$	%	$\delta^{13}C$	%
Pachyseris speciosa	Both	Both	-15.4 ± 0.1	-14.1 ± 0.2	82 ± 3	-21.5 ± 0.1	18 ± 3
Pocillopora verrucosa	Both	Both	-17.9 ± 0.1		49 ± 2		51 ± 2
Galaxea fascicularis	Shallow	2015	-15.5 ± 0.2		81 ± 4		19 ± 4
Galaxea fascicularis	Deep	Both	-17.6 ± 0.1		53 ± 2		47 ± 2

Table 5.2. Model B- Carbon isotope mixing model estimates of the relative importance of autotrophy and heterotrophy for three species of reef-building coral. The end member for autotrophy is the average of 20% of the most positive $\delta^{13}C$ values of symbionts, and the heterotrophy end member is the average $\delta^{13}C$ value of plankton. The $\delta^{13}C$ values and proportions of contributions from autotrophy and heterotrophy are shown as average ± standard error, calculated using IsoError. Shallow (2015) and deep (2015 and 2017) populations of *G. fascicularis* were considered separately because of different average $\delta^{13}C$ values between depths.

			Coral Host Average	Autotrophy		Heterotrophy	
Species	Depth	Year	$\delta^{13}C$ (‰)	$\delta^{13}C$	%	$\delta^{13}C$	%
Pachyseris speciosa	Both	Both	-15.4 ± 0.1	-12.7 ± 0.1	69 ± 2	-21.5 ± 0.1	31 ± 2
Pocillopora verrucosa	Both	Both	-17.9 ± 0.1		41 ± 1		59 ± 1
Galaxea fascicularis	Shallow	2015	-15.5 ± 0.2		68 ± 3		32 ± 3
Galaxea fascicularis	Deep	Both	-17.6 ± 0.1		44 ± 1		56 ± 1

An alternate carbon isotope mixing model (Model B) used a symbiont-derived autotrophy end member. Considering the variability in symbiont $\delta^{13}C$ values, a conservative approach was used to derive the autotrophy end member. The autotrophy end member was derived from the symbiont $\delta^{13}C$ values (the average of 20% of the most positive $\delta^{13}C$ values) and the plankton average $\delta^{13}C$ value represented the heterotrophy end member. Carbon isotope mixing Model B estimated a major proportion of carbon (55-60%) derived from heterotrophy for *P. verrucosa* and deep *G. fascicularis* while *P. speciosa* and shallow *G. fascicularis* populations were more autotrophic (65-70%) (Table 5.2).

Table 5.3. Model C- Carbon isotope mixing model estimates of the relative importance of autotrophy and heterotrophy for three species of reef-building coral. The end member for autotrophy is the average of species-specific symbiont $\delta^{13}C$ values, and the heterotrophy end member is the average $\delta^{13}C$ value of plankton. The $\delta^{13}C$ values and proportions of contributions from autotrophy and heterotrophy are shown as average ± standard error, calculated using IsoError. Shallow (2015) and deep (2015 and 2017) populations of *G. fascicularis* were considered separately because of different average $\delta^{13}C$ values between depths.

Species	Depth	Year	Coral Host Average $\delta^{13}C$ (‰)	Autotrophy		Heterotrophy	
				$\delta^{13}C$	%	$\delta^{13}C$	%
Pachyseris speciosa	Both	Both	-15.4 ± 0.1	-14.1 ± 0.2	82 ± 2		18 ± 2
Pocillopora verrucosa	Both	Both	-17.9 ± 0.1	-17.0 ± 0.1	80 ± 3		20 ± 3
Galaxea fascicularis	Shallow	2015	-15.5 ± 0.2	-15.0 ± 0.3	92 ± 5	-21.5 ± 0.1	8 ± 5
Galaxea fascicularis	Deep	Both	-17.6 ± 0.1	-16.8 ± 0.2	83 ± 4		17 ± 4

Finally, a third carbon isotope mixing model was considered (Model C). To account for potential variation in symbiont mixotrophy, the autotrophy end member was derived separately from the symbionts of each host species (average symbiont $\delta^{13}C$ values of each species) while the heterotrophy end member was the average $\delta^{13}C$ value of the plankton. Model C estimated that autotrophy was the dominant trophic strategy among all coral species but still showed a greater contribution from heterotrophy (mean 18-20% for *P. verrucosa* and *G. fascicularis*) than the commonly cited dogma of 90% of carbon derived from symbiont autotrophy (Table 5.3).

Table 5.4. Summary of estimates of Autotrophy and Heterotrophy contribution (average ± SE) calculated by averaging the results from carbon isotope mixing models A, B, and C (see Tables 5.1, 5.2, and 5.3).

Coral species	Depth	Year	Autotrophy %	Heterotrophy %
Pachyseris speciosa	Both	Both	78 ± 4	22 ± 4
Pocillopora verrucosa	Both	Both	57 ± 12	43 ± 12
Galaxea fascicularis	Shallow	2015	80 ± 7	20 ± 7
Galaxea fascicularis	Deep	Both	60 ± 12	40 ± 12

The estimates of the contribution of autotrophy and heterotrophy from all three carbon isotope mixing models (A, B, and C) were averaged to outline a conservative estimate of the trophic strategy of each coral species (Table 5.4). For *P. speciosa*, autotrophy (78 ± 4%) was estimated to provide a larger proportion of carbon than heterotrophy (22 ± 4%) while the proportions of estimated autotrophy (57 ± 12%) and heterotrophy (43 ± 12%) were similar for *P. verrucosa*. For shallow populations of *G. fascicularis* prior to the thermal stress event, autotrophy (80 ± 7%) was estimated to contribute more carbon than heterotrophy (20 ± 7%). For deep populations of *G. fascicularis* (both years), autotrophy and heterotrophy was estimated to contribute 60 ± 12% and 40 ± 12% of carbon, respectively.

Overall, all three of the carbon isotope mixing models estimated that there was an important input of heterotrophic carbon to coral host nutrition. Mixing models A and B estimated that coral hosts *P. verrucosa* and deep populations of *G. fascicularis* derived approximately 50% of carbon from heterotrophy. These mixing model estimates are further supported by other proxies for heterotrophy

(i.e., $\Delta^{13}C$), which also provide evidence for increased heterotrophy in the productive atoll system of the Maldives compared to other reef systems (Fox et al. 2018). Moreover, a different non-isotopic method also estimated high rates of heterotrophy for coral hosts *P. verrucosa* and *G. fascicularis*. Using PUFA data, a linear discriminant analysis estimated ~60-100% heterotrophy (95% confidence intervals) for coral hosts *P. verrucosa* and *G. fascicularis* (Chapter 4). The lower range of the linear discriminant analysis estimate of heterotrophy (60%) for *P. verrucosa* is consistent with the carbon isotope mixing Model B estimate of heterotrophic-derived carbon (59±1%). Therefore, the results show strong support for *P. verrucosa* heterotrophy and the similarity in model estimates provides evidence of the utility of both natural abundance stable isotopes and fatty acids in characterizing coral trophic strategies.

In contrast, mixing models A and B estimated that autotrophy was the major trophic strategy (~70-80%) for coral host *P. speciosa*. Similarly, the linear discriminant analysis estimated the highest potential contribution of autotrophy ranging from 0-87.5% (95% confidence interval) for coral host *P. speciosa* (Chapter 4). Generally, it appears that many populations of *P. speciosa* prefer shaded and/or deeper lower-light environments (Dinesen 1983; Ziegler et al. 2015b; DeVantier and Turak 2017), with *P. speciosa* recorded at mesophotic depths of 102 m (Bongaerts et al. 2011a). In the Maldives, *P. speciosa* was more abundant in deep reefs at the edge of the mesophotic (Chapter 3). Indeed, it has been shown that *P. speciosa* are efficient autotrophs in low light environments including deep reefs (e.g., up to 60 m; Cooper et al. 2011) and turbid reefs (Browne et al. 2014).

The fatty acid composition of the three species of coral hosts and their symbionts indicated similar patterns of trophic strategies as those outlined by the carbon isotope results (Chapter 4). As supported by $\delta^{13}C$ results (Chapters 2 and 3), total fatty acid composition also distinguished between the more heterotrophic coral *P. verrucosa* and the more autotrophic coral *P. speciosa*. The coral *G. fascicularis*, with different $\delta^{13}C$ values between shallow and deep populations, showed similarity to both *P. verrucosa* and *P. speciosa* fatty acid composition. Overall, ecological knowledge of these three species strongly support the conclusions of the carbon isotope mixing models and linear discriminant analysis (fatty acid data, Chapter 4).

A nitrogen isotope mixing model was also considered. Plankton from the Maldives reefs (Chapter 3) was used as the heterotrophy end member ($\delta^{15}N$ +6.4‰) and the isotopic signature for deep-water nitrate ($\delta^{15}N$ +5.0‰) as the autotrophy end member (symbiont nitrogen assimilation). However, the narrow range of $\delta^{15}N$ values of corals from the Maldives and the proximity of $\delta^{15}N$ values of the

potential end members resulted in a model with inadequate resolution. Overall, coral host tissues tend to have less variation in $\delta^{15}N$ values (2.5‰ range prior to thermal stress event; 3.7‰ range post thermal stress event) than $\delta^{13}C$ values (7.5‰, similar range before and after thermal stress). Across large depth gradients in other reef systems (1-2 to 50-60 m), similar ranges in coral host $\delta^{15}N$ values (~4.0‰ and ~1.5‰, respectively) have been observed among coral species (Muscatine and Kaplan 1994; Alamaru et al. 2009). Variation in coral host $\delta^{15}N$ values can reflect both the variability in nitrogen sources in the reef system and species-specific coral physiology. Minimal variation in the $\delta^{15}N$ values of different species of coral hosts may indicate the uptake of a similar nitrogen source in the reef system while marginal variation in the $\delta^{15}N$ values between coral hosts and symbionts of a given species indicate nitrogen recycling within the coral holobiont (Reynaud et al. 2009). Considering the lines of evidence presented in the three data chapters, the estimates of autotrophy versus heterotrophy from the three carbon isotope mixing models (A, B, and C), and the estimates of symbiont- versus particulate-derived PUFA (Chapter 4), heterotrophy plays an important role in coral nutrition throughout reefs of the Maldives archipelago.

5.2 Coral reefs, inorganic nutrients, and oceanography of the Maldives

The monsoon climate of the Maldives limits research on oceanic fore reefs to the relatively brief inter-monsoon periods (i.e. boreal inter-monsoon spring and fall periods). A low-nitrogen oligotrophic system was observed during the spring inter-monsoon. This oligotrophic regime was characterized by high residual $\delta^{15}N\text{-}NO_3^-$ values due to phytoplankton uptake, high residual $\delta^{18}O\text{-}NO_3^-$ values that were able to persist due to low nitrogen concentrations, and high Redfield ratios (Chapter 3). High $\delta^{18}O\text{-}NO_3^-$ values accompanied by high Redfield ratios suggest phosphate limitation, which supports the idea that atmospheric nitrate can accumulate in the surface waters. During the spring inter-monsoon period (March-April 2017), the $\delta^{18}O$ values of nitrate appear to reflect two groups of nitrate, including a nitrate source with a distinct high $\delta^{18}O$ signature. Due to the apparent limitation of nutrient(s) other than nitrate, which is likely to be phosphate, the preservation of these relatively high $\delta^{18}O$ values of nitrate recorded during the spring inter-monsoon provide evidence of a proportionally high input of atmospheric nitrate (Kendall et al. 2008; Granat et al. 2010; Das et al. 2011). In the Maldives, aerosol pollution originating from the south/southeast Asian region is highest during the northeast monsoon season with high levels of air pollution observed during the months of January-February (Ramana and Ramanathan 2006; Adhikary et al. 2007). Considering a fractionation factor of ~5‰, the $\delta^{15}N\text{-}NO_3^-$ values (10.8 ± 4.2‰) of surface waters likely reflect phytoplankton assimilation of a nitrate source of approximately 5‰ (Altabet 2001). The dual $\delta^{15}N$- and $\delta^{18}O\text{-}NO_3^-$ signature of marine-derived nitrate is further supported by the $\delta^{15}N$ values of POM

from 2015 (Regime 2 Upwelling: 5.3 ± 1.1‰) and POM (Regime 3 Oligotrophic: 6.5 ± 1.2‰) and reef plankton (6.4 ± 0.8‰) from 2017. In combination with the $\delta^{15}N$ values of coral hosts from 2015 (5.5 ± 0.5‰) and 2017 (6.0 ± 0.5‰), the biogeochemical evidence indicates that deep-water nitrate ($\delta^{15}N$ ~5-6‰) is an important nitrogen source for coral reefs across the Maldives.

Overall, the "unique geological, physical, biogeochemical, and ecological features of the Indian Ocean" has been declared one of six scientific themes of the 2nd International Indian Ocean Expedition (Hood et al. 2016; Singh et al. 2016). Greater focus, such as that offered by the ongoing 2nd International Indian Ocean Expedition (2015-2020), represents a collaborative opportunity to explore and fill these important gaps in our understanding of the central Indian Ocean and its response to global climate change. Indeed, there has been limited research on how the unique oceanography of the Maldives region affects coral reef ecology. To further investigate the complex nutrient dynamics of this region, it will be necessary to repeatedly survey oceanic reefs of the Maldives at greater depths and at multiple times during each monsoon season (as opposed to only the inter-monsoon periods). In this regard, access to a well-equipped oceanographic research vessel would be needed to accomplish further sampling.

5.3 Coral reefs from the central Indian Ocean under rapid climate change

The focal species of this thesis have been characterized by different genus-level susceptibilities to thermal stress related coral bleaching prior to the 2015-2016 event. The coral genus *Galaxea* has been characterized as resistant while corals from the genus *Pachyseris* have been described as tolerant or showing mixed status, and the genus *Pocillopora* has been characterised as susceptible to coral bleaching (McClanahan et al. 2007; Tkachenko 2015). Different bleaching responses of these three genera were observed during the mass coral bleaching event in the Maldives in 2016. Specifically, *Galaxea* was the most severely bleached, followed by *Pachyseris* and then *Pocillopora* (Ibrahim et al. 2017). In response to the thermal stress event, shallow populations of *G. fascicularis* appeared to shift from autotrophy to heterotrophy, while more heterotrophic populations from deep reefs occupied the same isotopic niche before and after the thermal stress (Chapter 3). Considering the ability of *G. fascicularis* to increase heterotrophy as a response to thermal stress (Ferrier-Pagès et al. 2010), our results support the life history strategy of *G. fascicularis* as a relatively "stress-tolerant" coral although it appears to be more of a generalist coral that has flexibility in its trophic strategy (Table S2.1). Although it is suggested that *P. speciosa* has a "generalist" life history strategy, this research found that *P. speciosa* was nearly absent in shallow depths of oceanic reefs; this could likely be due to the greater hydrodynamic forces of oceanic reefs compared to the reefs of the Inner Sea (Kench et

al. 2006). The results of this thesis support a “specialist” life history strategy of *P. speciosa*, which was abundant in deep reefs but more cryptic in shallow Inner Sea reefs (Table S2.1). The “competitive” life history strategy of *P. verrucosa* likely supports its dominance across reefs of the Indo-Pacific (Table S2.1; Brown and Dunne 1988; Reyes-Bonilla and López-Pérez 1998). Overall, the colony abundance of the three species remained similar before and after the thermal stress, indicating that at least a proportion of each of the populations had survived the mass coral bleaching event of 2016.

Based on optimistic climate scenarios (RCP 2.6) sea surface temperatures in the Maldives are projected to increase by 0.44ºC (range 0.40ºC - 0.47ºC) by the end of this century (Beyer et al. 2018). Specifically, the Maldives is projected to experience maximum monthly mean temperatures of 3.1ºC (range 2.1ºC - 4.6ºC) above historical means (Beyer et al. 2018). Recurrent mass coral bleaching and reef degradation will continue to impact the coral reefs of the central Indian Ocean as expected under the more frequent and intense extremes associated with climate change (Sheppard 2003; Riegl et al. 2015). In this regard, upwelling regions, such as the one focused on in this thesis, may have a role of providing potential refugia during environmental stress (Glynn 1996; Riegl and Piller 2003). Interestingly, the Maldives have been suggested as potential thermal refugia because of the low historical exposure to thermal stress, and the high warm-season variability of this region (Heron et al. 2016). However, our understanding of how shallow tropical coral reefs are affected by broader hydrodynamic processes, especially under global climate change, remains limited (Hoegh-Guldberg et al. 2014). Cooler seawater transported by upwelling to surface waters may support potential refugia areas for coral reefs in the face of climate change (Chollett and Mumby 2013; van Hooidonk et al. 2013). Global climate implications for oceanic circulation, however, may present serious challenges for marine ecosystems (Collins et al. 2010; Karnauskas and Cohen 2012). In order to understand the responses of coral reefs to shifting climate patterns, it is necessary to examine how upwelling affects coral reefs and how these will change in the future. Although there is comprehensive research examining how increasing ocean warming and ocean acidification affects coral reefs (Hoegh-Guldberg et al. 2017), it is imperative to simultaneously consider how coral reefs will respond to potential changes in regional oceanographic processes.

References

Adhikary B, Carmichael GR, Tang Y, Leung LR, Qian Y, Schauer JJ, Stone EA, Ramanathan V, Ramana M V. (2007) Characterization of the seasonal cycle of south Asian aerosols: A regional-scale modeling analysis. J Geophys Res 112:D22S22

Al-Moghrabi S, Allemand D, Couret JM, Jaubert J (1995) Fatty acids of the scleractinian coral Galaxea fascicularis: effect of light and feeding. J Comp Physiol B 165:183–192

Alamaru A, Loya Y, Brokovich E, Yam R, Shemesh A (2009) Carbon and nitrogen utilization in two species of Red Sea corals along a depth gradient: Insights from stable isotope analysis of total organic material and lipids. Geochim Cosmochim Acta 73:5333–5342

Altabet MA (2001) Nitrogen isotopic evidence for micronutrient control of fractional NO3− utilization in the equatorial Pacific. Limnol Oceanogr 46:368–380

Anderson C, Branch T, Alagiyawadu A, Baldwin R, Marsac F (2012) Seasonal distribution, movements and taxonomic status of blue whales (Balaenoptera musculus) in the northern Indian Ocean. J Cetacean Resour Manag 12:203–218

Anderson R, Adam M, Goes J (2011) From monsoons to mantas: seasonal distribution of Manta alfredi in the Maldives. Fish Oceanogr 20:104–113

Anderson RC, Ahmed H (1993) The Shark Fisheries of the Maldives.

Anthony KRN (2000) Enhanced particle-feeding capacity of corals on turbid reefs (Great Barrier Reef, Australia). Coral Reefs 19:59–67

Anthony KRN, Connolly SR (2004) Environmental limits to growth: physiological niche boundaries of corals along turbidity–light gradients. Oecologia 141:373–384

Bachar A, Achituv Y, Pasternak Z, Dubinsky Z (2007) Autotrophy versus heterotrophy: The origin of carbon determines its fate in a symbiotic sea anemone. J Exp Mar Bio Ecol 349:295–298

Bachok Z, Mfilinge P, Tsuchiya M (2006) Characterization of fatty acid composition in healthy and bleached corals from Okinawa, Japan. Coral Reefs 25:545–554

Baird A, Madin J, Álvarez-Noriega M, Fontoura L, Kerry J, Kuo C, Precoda K, Torres-Pulliza D, Woods R, Zawada K, Hughes T (2018) A decline in bleaching suggests that depth can provide a refuge from global warming in most coral taxa. Mar Ecol Prog Ser 603:257–264

Baker AC, Glynn PW, Riegl B (2008) Climate change and coral reef bleaching: An ecological assessment of long-term impacts, recovery trends and future outlook. Estuar Coast Shelf Sci 80:435–471

Baumann J, Grottoli AG, Hughes AD, Matsui Y (2014) Photoautotrophic and heterotrophic carbon in bleached and non-bleached coral lipid acquisition and storage. J Exp Mar Bio Ecol 461:469–478

Bednarz VN, Grover R, Maguer J-F, Fine M, Ferrier-Pagès C (2017) The Assimilation of Diazotroph-Derived Nitrogen by Scleractinian Corals Depends on Their Metabolic Status. MBio 8:e02058-16

Bessell-Browne P, Stat M, Thomson D, Clode PL (2014) Coscinaraea marshae corals that have survived prolonged bleaching exhibit signs of increased heterotrophic feeding. Coral Reefs 33:795–804

Betzler C, Fürstenau J, Lüdmann T, Hübscher C, Lindhorst S, Paul A, Reijmer JJG, Droxler AW (2013) Sea-level and ocean-current control on carbonate-platform growth, Maldives, Indian Ocean. Basin Res 25:172–196

Betzler C, Hübscher C, Lindhorst S, Reijmer JJG, Römer M, Droxler AW, Fürstenau J, Ludmann T (2009) Monsoon-induced partial carbonate platform drowning (Maldives, Indian Ocean). Geology 37:867–870

Beyer HL, Kennedy E V., Beger M, Chen CA, Cinner JE, Darling ES, Eakin CM, Gates RD, Heron SF, Knowlton N, Obura DO, Palumbi SR, Possingham HP, Puotinen M, Runting RK, Skirving WJ, Spalding M, Wilson KA, Wood S, Veron JE, Hoegh-Guldberg O (2018) Risk-sensitive planning for conserving coral reefs under rapid climate change. Conserv Lett e12587

Bishop DG, Kenrick JR (1980) Fatty acid composition of symbiotic zooxanthellae in relation to their hosts. Lipids 15:799–804

Bode M, Hagen W, Schukat A, Teuber L, Fonseca-Batista D, Dehairs F, Auel H (2015) Feeding strategies of tropical and subtropical calanoid copepods throughout the eastern Atlantic Ocean – Latitudinal and bathymetric aspects. Prog Oceanogr 138:268–282

Bongaerts P, Bridge TCL, Kline DI, Muir PR, Wallace CC, Beaman RJ, Hoegh-Guldberg O (2011a) Mesophotic coral ecosystems on the walls of Coral Sea atolls. Coral Reefs 30:335–335

Bongaerts P, Carmichael M, Hay KB, Tonk L, Frade PR, Hoegh-Guldberg O (2015) Prevalent endosymbiont zonation shapes the depth distributions of scleractinian coral species. R Soc Open Sci 2:140297–140297

Bongaerts P, Frade P, Ogier J (2013) Sharing the slope: depth partitioning of agariciid corals and associated Symbiodinium across shallow and mesophotic habitats (2-60 m) on a Caribbean reef. BMC Evol Biol 13:1–14

Bongaerts P, Sampayo E, Bridge T, Ridgway T, Vermeulen F, Englebert N, Webster J, Hoegh-Guldberg O (2011b) Symbiodinium diversity in mesophotic coral communities on the Great Barrier Reef: a first assessment. Mar Ecol Prog Ser 439:117–126

Borell EM, Yuliantri AR, Bischof K, Richter C (2008) The effect of heterotrophy on photosynthesis

and tissue composition of two scleractinian corals under elevated temperature. J Exp Mar Bio Ecol 364:116–123

Brett MT, Müller-Navarra DC, Persson J (2009) Crustacean zooplankton fatty acid composition. Lipids in Aquatic Ecosystems. Springer New York, New York, NY, pp 115–146

Brown BE, Dunne RP (1988) The Environmental Impact of Coral Mining on Coral Reefs in the Maldives. Environ Conserv 15:159

Brown KT, Bender-Champ D, Bryant DEP, Dove S, Hoegh-Guldberg O (2017) Human activities influence benthic community structure and the composition of the coral-algal interactions in the central Maldives. J Exp Mar Bio Ecol 497:33–40

Browne N, Precht E, Last K, Todd P (2014) Photo-physiological costs associated with acute sediment stress events in three near-shore turbid water corals. Mar Ecol Prog Ser 502:129–143

Browne NK, Smithers SG, Perry CT (2012) Coral reefs of the turbid inner-shelf of the Great Barrier Reef, Australia: An environmental and geomorphic perspective on their occurrence, composition and growth. Earth-Science Rev 115:1–20

Budge SM, Iverson SJ, Koopman HN (2006) Studying trophic ecology in marine ecosystems using fatty acids: a primer on analysis and interpretation. Mar Mammal Sci 22:759–801

Carder KL, Chen RF, Hawes SK (2003) Instantaneous Photosynthetically Available Radiation and Absorbed Radiation by Phytoplankton: Algorithm Theoretical Basis Document.

Cardini U, Bednarz VN, Naumann MS, van Hoytema N, Rix L, Foster RA, Al-Rshaidat MMD, Wild C (2015) Functional significance of dinitrogen fixation in sustaining coral productivity under oligotrophic conditions. Proceedings Biol Sci 282:20152257

Carpenter EJ, Montoya JP, Burns J, Mulholland MR, Subramaniam A, Capone DG (1999) Extensive bloom of a N2-fixing diatom/cyanobacterial association in the tropical Atlantic Ocean. Mar Ecol Prog Ser 185:273–283

Carpenter KE, Abrar M, Aeby G, Aronson RB, Banks S, Bruckner A, Chiriboga A, Cortés J, Delbeek JC, Devantier L, Edgar GJ, Edwards AJ, Fenner D, Guzmán HM, Hoeksema BW, Hodgson G, Johan O, Licuanan WY, Livingstone SR, Lovell ER, Moore JA, Obura DO, Ochavillo D, Polidoro BA, Precht WF, Quibilan MC, Reboton C, Richards ZT, Rogers AD, Sanciangco J, Sheppard A, Sheppard C, Smith J, Stuart S, Turak E, Veron JEN, Wallace C, Weil E, Wood E (2008) One-third of reef-building corals face elevated extinction risk from climate change and local impacts. Science 321:560–3

Casciotti KL (2016) Nitrogen and Oxygen Isotopic Studies of the Marine Nitrogen Cycle. Ann Rev Mar Sci 8:379–407

Casciotti KL, Sigman DM, Galanter MH, Böhlke JK, Hilkert A (2002) Measurement of the Oxygen

Isotopic Composition of Nitrate in Seawater and Freshwater Using the Denitrifier Method.

Chen H-K, Song S-N, Wang L-H, Mayfield AB, Chen Y-J, Chen W-NU, Chen C-S (2015) A Compartmental Comparison of Major Lipid Species in a Coral-Symbiodinium Endosymbiosis: Evidence that the Coral Host Regulates Lipogenesis of Its Cytosolic Lipid Bodies. PLoS One 10:e0132519

Chollett I, Mumby PJ (2013) Reefs of last resort: Locating and assessing thermal refugia in the wider Caribbean. Biol Conserv 167:179–186

Ciarapica G, Passeri L (1993) An overview of the Maldivian coral reefs in Felidu and North Malé Atoll (Indian Ocean): Platform drowning by ecological crises. Facies 28:33–65

Cohen JE (1977) Food webs and the dimensionality of trophic niche space. Proc Natl Acad Sci U S A 74:4533–6

Collins M, An S-I, Cai W, Ganachaud A, Guilyardi E, Jin F-F, Jochum M, Lengaigne M, Power S, Timmermann A, Vecchi G, Wittenberg A (2010) The impact of global warming on the tropical Pacific Ocean and El Niño. Nat Geosci 3:391–397

Cooper TF, Ulstrup KE, Dandan SS, Heyward AJ, Kühl M, Muirhead A, O'Leary RA, Ziersen BEF, Van Oppen MJH (2011) Niche specialization of reef-building corals in the mesophotic zone: metabolic trade-offs between divergent Symbiodinium types. Proc Biol Sci 278:1840–50

Courtial L, Planas Bielsa V, Houlbrèque F, Ferrier-Pagès C (2018) Effects of ultraviolet radiation and nutrient level on the physiological response and organic matter release of the scleractinian coral Pocillopora damicornis following thermal stress. PLoS One 13:e0205261

Crabbe MJC, Smith DJ (2006) Modelling variations in corallite morphology of Galaxea fascicularis coral colonies with depth and light on coastal fringing reefs in the Wakatobi Marine National Park (S.E. Sulawesi, Indonesia). Comput Biol Chem 30:155–9

Cui G, Liew YJ, Li Y, Kharbatia N, Zahran NI, Emwas A-H, Eguíluz VM, Lastra MA (2018) Meta-analysis reveals host-dependent nitrogen recycling as a mechanism of symbiont control in Aiptasia. bioRxiv 269183

Dalsgaard J, St John M, Kattner G, Müller-Navarra D, Hagen W (2003) Fatty acid trophic markers in the pelagic marine environment. Adv Mar Biol 46:225–340

Darling ES, Alvarez-Filip L, Oliver TA, McClanahan TR, Côté IM (2012) Evaluating life-history strategies of reef corals from species traits. Ecol Lett 15:1378–1386

Darling ES, McClanahan TR, Côté IM (2013) Life histories predict coral community disassembly under multiple stressors. Glob Chang Biol 19:1930–1940

Darwin C (1842) The structure and distribution of coral reefs. Being the first part of the geology of the voyage of the Beagle, under the command of Capt. Fitzroy, R.N. during the years 1832 to

1836. Smith Elder and Co, London

Das R, Granat L, Leck C, Praveen PS, Rodhe H (2011) Chemical composition of rainwater at Maldives Climate Observatory at Hanimaadhoo (MCOH). Atmos Chem Phys 11:3743–3755

DeVantier L, Turak E (2017) Species Richness and Relative Abundance of Reef-Building Corals in the Indo-West Pacific. Diversity 9:25

Dimond J, Carrington E (2008) Symbiosis regulation in a facultatively symbiotic temperate coral: zooxanthellae division and expulsion. Coral Reefs 27:601–604

Dinesen ZD (1983) Shade-dwelling corals of the Great Barrier Reef. Mar Ecol Prog Ser 10:173–185

Dong Z-J, Huang H, Huang L-M, Li Y-C (2009) Diversity of symbiotic algae of the genus Symbiodinium in scleractinian corals of the Xisha Islands in the South China Sea. J Syst Evol 47:321–326

Dorado S, Rooker J, Wissel B, Quigg A (2012) Isotope baseline shifts in pelagic food webs of the Gulf of Mexico. Mar Ecol Prog Ser 464:37–49

Doty MS, Oguri M (1956) The Island Mass Effect. ICES J Mar Sci 22:33–37

Dubinsky Z, Falkowski PG, Porter JW, Muscatine L (1984) Absorption and Utilization of Radiant Energy by Light- and Shade-Adapted Colonies of the Hermatypic Coral Stylophora pistillata. Proc R Soc B Biol Sci 222:203–214

Dunn SR, Thomas MC, Nette GW, Dove SG (2012) A Lipidomic Approach to Understanding Free Fatty Acid Lipogenesis Derived from Dissolved Inorganic Carbon within Cnidarian-Dinoflagellate Symbiosis. PLoS One 7:e46801

Einbinder S, Mass T, Brokovich E, Dubinsky Z, Erez J, Tchernov D (2009) Changes in morphology and diet of the coral Stylophora pistillata along a depth gradient. Mar Ecol Prog Ser

Enríquez S, Méndez ER, Iglesias-Prieto R (2005) Multiple scattering on coral skeletons enhances light absorption by symbiotic algae. Limnol Oceanogr 50:1025–1032

Ezzat L, Fine M, Maguer J-F, Grover R, Ferrier-Pagès C (2017) Carbon and nitrogen acquisition of shallow and deep holobionts of the scleractinian coral S. pistillata. Front Mar Sci 4:102

Ezzat L, Towle E, Irisson J-O, Langdon C, Ferrier-Pagès C (2016) The relationship between heterotrophic feeding and inorganic nutrient availability in the scleractinian coral T. reniformis under a short-term temperature increase. Limnol Oceanogr 61:89–102

Falk-Petersen S, Hagen W, Kattner G, Clarke A, Sargent J (2000) Lipids, trophic relationships, and biodiversity in Arctic and Antarctic krill. Can J Fish Aquat Sci 57:178–191

Falk-Petersen S, Hopkins CCE, Sargent JR (1990) Trophic relationships in the pelagic, Arctic food web. 315–333

Falkowski PG, Dubinsky Z (1981) Light-shade adaptation of Stylophora pistillata, a hermatypic coral from the Gulf of Eilat. Nature 289:172–174

Falkowski PG, Dubinsky Z, Muscatine L, McCloskey L (1993) Population Control in Symbiotic Corals. Bioscience 43:606–611

Falkowski PG, Dubinsky Z, Muscatine L, Porter JW (1984) Light and the Bioenergetics of a Symbiotic Coral. Bioscience 34:705–709

Farquhar G, Ehleringer J, Hubick K (1989) Carbon isotope discrimination and photosynthesis. Annu Rev Plant Physiol Plant Mol Biol 40:503–537

Fay F, Obando Claudia Z, Isabelle L, Laurent D, Mayalen Z, Alina T-L, Jean T, Isabelle G, Réjean T, Karine R (2017) Fatty Acid Profiling of Tropical Microalgae and Cyanobacteria Strains Isolated From Southwest Indian Ocean Islands. J Mar Biol Aquac 3:1–14

Ferrier-Pagès C, Rottier C, Beraud E, Levy O (2010) Experimental assessment of the feeding effort of three scleractinian coral species during a thermal stress: Effect on the rates of photosynthesis. J Exp Mar Bio Ecol 390:118–124

Figueiredo C, Baptista M, Rosa IC, Lopes AR, Dionísio G, Rocha RJM, Cruz ICS, Kikuchi RKP, Simões N, Leal MC, Tojeira I, Bandarra N, Calado R, Rosa R (2017) 3D chemoecology and chemotaxonomy of corals using fatty acid biomarkers: Latitude, longitude and depth. Biochem Syst Ecol 70:35–42

Folch J, Lees M, Sloane Stanley GH (1957) A simple method for the isolation and purification of total lipides from animal tissues. J Biol Chem 226:497–509

Fox MD, Smith EA, Smith JE, Newsome SD High trophic plasticity and intercolony variation in a common reef-building coral: Insights from δ13C analysis of amino acids. Proc R Soc B *Under review.*

Fox MD, Williams GJ, Johnson MD, Radice VZ, Zgliczynski BJ, Kelly ELA, Rohwer FL, Sandin SA, Smith JE (2018) Gradients in Primary Production Predict Trophic Strategies of Mixotrophic Corals across Spatial Scales. Curr Biol 28:3355–3363.e4

Frade PR, Bongaerts P, Winkelhagen AJS, Tonk L, Bak RPM (2008a) In situ photobiology of corals over large depth ranges: A multivariate analysis on the roles of environment, host, and algal symbiont. Limnol Oceanogr 53:2711–2723

Frade PR, Englebert N, Faria J, Visser PM, Bak RPM (2008b) Distribution and photobiology of Symbiodinium types in different light environments for three colour morphs of the coral Madracis pharensis: is there more to it than total irradiance? Coral Reefs 27:913–925

Frankowiak K, Wang XT, Sigman DM, Gothmann AM, Kitahara M V., Mazur M, Meibom A, Stolarski J (2016) Photosymbiosis and the expansion of shallow-water corals. Sci Adv

2:e1601122–e1601122

Fricke H, Meischner D (1985) Depth limits of Bermudan scleractinian corals: a submersible survey. Mar Biol 88:175–187

Fricke H, Vareschi E, Schlichter D (1987) Photoecology of the coral Leptoseris fragilis in the Red Sea twilight zone (an experimental study by submersible). Oecologia 73:371–381

Fry B (2006) Stable Isotope Ecology. Springer-Verlag New York, New York, NY

Fry B, Anderson RK, Entzeroth L, Bird JL, Parker PL (1984) 13C enrichment and oceanic food web structure in the northwestern Gulf of Mexico.

Fry B, Wainright SC (1991) Diatom sources of 13C-rich carbon in marine food webs. 76:149–157

Furla P, Galgani I, Durand I, Allemand D (2000) Sources and mechanisms of inorganic carbon transport for coral calcification and photosynthesis. J Exp Biol 203:3445–57

Galloway AWE, Winder M (2015) Partitioning the Relative Importance of Phylogeny and Environmental Conditions on Phytoplankton Fatty Acids. PLoS One 10:e0130053

Garrison DL, Gowing MM, Hughes MP (1998) Nano- and microplankton in the northern Arabian Sea during the Southwest Monsoon, August–September 1995 A US–JGOFS study. Deep Sea Res Part II Top Stud Oceanogr 45:2269–2299

Gibbin EM, Krueger T, Putnam HM, Barott KL, Bodin J, Gates RD, Meibom A (2018) Short-Term Thermal Acclimation Modifies the Metabolic Condition of the Coral Holobiont. Front Mar Sci 5:10

Glynn PW (1996) Coral reef bleaching: facts, hypotheses and implications. Glob Chang Biol 2:495–509

Godinot C, Houlbrèque F, Grover R, Ferrier-Pagès C, Larsen A (2011) Coral Uptake of Inorganic Phosphorus and Nitrogen Negatively Affected by Simultaneous Changes in Temperature and pH. PLoS One 6:e25024

Goreau TF, Goreau NI, Yonge CM (1971) Reef corals: autotrophs or heterotrophs? Biol Bull 141:247–260

Gove JM, McManus MA, Neuheimer AB, Polovina JJ, Drazen JC, Smith CR, Merrifield MA, Friedlander AM, Ehses JS, Young CW, Dillon AK, Williams GJ (2016) Near-island biological hotspots in barren ocean basins. Nat Commun 7:10581

Gove JM, Williams GJ, McManus MA, Heron SF, Sandin SA, Vetter OJ, Foley DG (2013) Quantifying Climatological Ranges and Anomalies for Pacific Coral Reef Ecosystems. PLoS One 8:e61974

Gower J, King S (2011) A Global Survey of Intense Surface Plankton Blooms and Floating Vegetation Using MERIS MCI. In: Tang D. (eds) Remote Sensing of the Changing Oceans.

Springer, Berlin, Heidelberg, pp 99–121

Graeve M, Kattner G, Piepenburg D (1997) Lipids in Arctic benthos: does the fatty acid and alcohol composition reflect feeding and trophic interactions? Polar Biol 18:53–61

Granat L, Engström JE, Praveen S, Rodhe H (2010) Light absorbing material (soot) in rainwater and in aerosol particles in the Maldives. J Geophys Res 115:D16307

Grottoli AG, Rodrigues LJ (2011) Bleached Porites compressa and Montipora capitata corals catabolize δ13C-enriched lipids. Coral Reefs 30:687–692

Grottoli AG, Rodrigues LJ, Juarez C (2004) Lipids and stable carbon isotopes in two species of Hawaiian corals, Porites compressa and Montipora verrucosa, following a bleaching event. Mar Biol 145:621–631

Grottoli AG, Rodrigues LJ, Palardy JE (2006) Heterotrophic plasticity and resilience in bleached corals. Nature 440:1186–9

Grottoli AG, Warner ME, Levas SJ, Aschaffenburg MD, Schoepf V, McGinley M, Baumann J, Matsui Y (2014) The cumulative impact of annual coral bleaching can turn some coral species winners into losers. Glob Chang Biol 20:3823–3833

Grover R, Maguer J-F, Allemand D, Ferrier-Pagès C (2003) Nitrate uptake in the scleractinian coral Stylophora pistillata. Limnol Oceanogr 48:2266–2274

Grover R, Maguer J-F, Allemand D, Ferrier-Pagès C (2008) Uptake of dissolved free amino acids by the scleractinian coral Stylophora pistillata. J Exp Biol 211:860–865

Gurr MI, Harwood JL, Frayn KN (2002) Lipid biochemistry. Blackwell Science,

Halpern BS, Walbridge S, Selkoe KA, Kappel C V, Micheli F, D'Agrosa C, Bruno JF, Casey KS, Ebert C, Fox HE, Fujita R, Heinemann D, Lenihan HS, Madin EMP, Perry MT, Selig ER, Spalding M, Steneck R, Watson R (2008) A global map of human impact on marine ecosystems. Science 319:948–52

Harland AD, Navarro JC, Spencer Davies P, Fixter LM (1993) Lipids of some Caribbean and Red Sea corals: total lipid, wax esters, triglycerides and fatty acids. Mar Biol 117:113–117

Harrington R, Woiwod I, Sparks T (1999) Climate change and trophic interactions. Trends Ecol Evol 14:146–150

Heron SF, Maynard JA, van Hooidonk R, Eakin CM (2016) Warming Trends and Bleaching Stress of the World's Coral Reefs 1985–2012. Sci Rep 6:38402

Hii Y-S, Soo C-L, Liew H-C (2009) Feeding of scleractinian coral, Galaxea fascicularis, on Artemia salina nauplii in captivity. Aquac Int 17:363–376

Hillyer KE, Dias DA, Lutz A, Wilkinson SP, Roessner U, Davy SK (2017) Metabolite profiling of symbiont and host during thermal stress and bleaching in the coral Acropora aspera. Coral

Reefs 36:105–118

Hoegh-Guldberg O (1999) Climate change, coral bleaching and the future of the world's coral reefs. Mar Freshw Res 50:839

Hoegh-Guldberg O, Bruno JF (2010) The impact of climate change on the world's marine ecosystems. Science 328:1523–8

Hoegh-Guldberg O, Cai R, Poloczanska ES, Brewer PG, Sundby S, Hilmi K, Fabry VJ, Jung S (2014) The Ocean. In: Barros V.R., Field C.B., Dokken D.J., Mastrandrea M.D., Mach K.J., Bilir T.E., Chatterjee M., Ebi K.L., Estrada Y.O., Genova R.C., Girma B., Kissel E.S., Levy A.N., MacCracken S., Mastrandrea P.R., White L.L. (eds) Climate Change 2014: Impacts, Adaptation, and Vulnerability. Part B: Regional Aspects. Contribution of Working Group II to the Fifth Assessment Report of the Intergovernmental Panel on Climate Change. Cambridge University Press, Cambridge, United Kingdom and New York, NY, U.S.A., pp 1655–1731

Hoegh-Guldberg O, Fine M, Skirving W, Johnstone R, Dove S, Strong A (2005) Coral bleaching following wintry weather. Limnol Oceanogr 50:265–271

Hoegh-Guldberg O, Mumby PJ, Hooten AJ, Steneck RS, Greenfield P, Gomez E, Harvell CD, Sale PF, Edwards AJ, Caldeira K, Knowlton N, Eakin CM, Iglesias-Prieto R, Muthiga N, Bradbury RH, Dubi A, Hatziolos ME (2007) Coral reefs under rapid climate change and ocean acidification. Science 318:1737–42

Hoegh-Guldberg O, Poloczanska ES, Skirving W, Dove S (2017) Coral Reef Ecosystems under Climate Change and Ocean Acidification. Front Mar Sci 4:158

Hoegh-Guldberg O, Smith GJ (1989) The effect of sudden changes in temperature, light and salinity on the population density and export of zooxanthellae from the reef corals Stylophora pistillata Esper and Seriatopora hystrix Dana. J Exp Mar Bio Ecol 129:279–303

Hoegh-Guldberg O, Williamson J (1999) Availability of two forms of dissolved nitrogen to the coral Pocillopora damicornis and its symbiotic zooxanthellae. Mar Biol

Hoins M, Eberlein T, Van de Waal DB, Sluijs A, Reichart G-J, Rost B (2016) CO2-dependent carbon isotope fractionation in dinoflagellates relates to their inorganic carbon fluxes. J Exp Mar Bio Ecol 481:9–14

Hood RR, Urban ER, McPhaden MJ, Su D, Raes E (2016) The 2 nd International Indian Ocean Expedition (IIOE-2): Motivating New Exploration in a Poorly Understood Basin. Limnol Oceanogr Bull 25:117–124

Hoogenboom M, Rottier C, Sikorski S, Ferrier-Pagès C (2015) Among-species variation in the energy budgets of reef-building corals: scaling from coral polyps to communities. J Exp Biol 218:3866–77

Hoogenboom MO, Campbell DA, Beraud E, DeZeeuw K, Ferrier-Pagès C (2012) Effects of Light, Food Availability and Temperature Stress on the Function of Photosystem II and Photosystem I of Coral Symbionts. PLoS One 7:e30167

Hoogenboom MO, Connolly SR, Anthony KRN (2008) Interactions between morphological and physiological plasticity optimize energy acquisition in corals. Ecology 89:1144–1154

van Hooidonk R, Maynard JA, Planes S (2013) Temporary refugia for coral reefs in a warming world. Nat Clim Chang 3:508–511

Houlbrèque F, Ferrier-Pagès C (2009) Heterotrophy in tropical scleractinian corals. Biol Rev Camb Philos Soc 84:1–17

Houlbrèque F, Tambutté E, Richard C, Ferrier-Pagès C (2004) Importance of a micro-diet for scleractinian corals. Mar Ecol Prog Ser 282:151–160

Howell KL, Pond DW, Billett DSM, Tyler PA (2003) Feeding ecology of deep-sea seastars (Echinodermata: Asteroidea): a fatty-acid biomarker approach. Mar Ecol Prog Ser 255:193–206

Hu C, Lee Z, Franz B (2012) Chlorophyll-a algorithms for oligotrophic oceans: A novel approach based on three-band reflectance difference. J Geophys Res Ocean 117:2156–2202

Huang H, Dong Z, Huang L, Yang J, Di B, Li Y, Zhou G, Zhang C (2011) Latitudinal variation in algal symbionts within the scleractinian coral Galaxea fascicularis in the South China Sea. Mar Biol Res 7:208–211

Hughes A, Grottoli A, Pease T, Matsui Y (2010) Acquisition and assimilation of carbon in non-bleached and bleached corals. Mar Ecol Prog Ser 420:91–101

Hughes AD, Grottoli AG (2013) Heterotrophic compensation: a possible mechanism for resilience of coral reefs to global warming or a sign of prolonged stress? PLoS One 8:e81172

Hughes TP, Anderson KD, Connolly SR, Heron SF, Kerry JT, Lough JM, Baird AH, Baum JK, Berumen ML, Bridge TC, Claar DC, Eakin CM, Gilmour JP, Graham NAJ, Harrison H, Hobbs J-PA, Hoey AS, Hoogenboom M, Lowe RJ, McCulloch MT, Pandolfi JM, Pratchett M, Schoepf V, Torda G, Wilson SK (2018a) Spatial and temporal patterns of mass bleaching of corals in the Anthropocene. Science (80-) 359:80–83

Hughes TP, Barnes ML, Bellwood DR, Cinner JE, Cumming GS, Jackson JBC, Kleypas J, van de Leemput IA, Lough JM, Morrison TH, Palumbi SR, van Nes EH, Scheffer M (2017) Coral reefs in the Anthropocene. Nature 546:82–90

Hughes TP, Kerry JT, Baird AH, Connolly SR, Dietzel A, Eakin CM, Heron SF, Hoey AS, Hoogenboom MO, Liu G, McWilliam MJ, Pears RJ, Pratchett MS, Skirving WJ, Stella JS, Torda G (2018b) Global warming transforms coral reef assemblages. Nature 556:492–496

Hutchinson GE (1957) Concluding Remarks. Cold Spring Harb Symp Quant Biol 22:415–427

Ibrahim N, Mohamed M, Basheer A, Ismail H, Nistharan F, Schmidt A, Naeem R, Abdulla A, Grimsditch G (2017) Status of Coral Bleaching in the Maldives in 2016.

Iglesias-Prieto R, Trench RK (1994) Acclimation and adaptation to irradiance in symbiotic dinoflagellates. I. Responses of the photosynthetic unit to changes in photon flux density. Mar Ecol Prog Ser 113:163–175

Imbs A, Latyshev N, Dautova T, Latypov Y (2010a) Distribution of lipids and fatty acids in corals by their taxonomic position and presence of zooxanthellae. Mar Ecol Prog Ser 409:65–75

Imbs AB (2013) Fatty acids and other lipids of corals: Composition, distribution, and biosynthesis. Russ J Mar Biol 39:153–168

Imbs AB, Demidkova DA, Latypov YY, Pham LQ (2007) Application of Fatty Acids for Chemotaxonomy of Reef-Building Corals. Lipids 42:1035–1046

Imbs AB, Yakovleva IM, Dautova TN, Bui LH, Jones P (2014) Diversity of fatty acid composition of symbiotic dinoflagellates in corals: Evidence for the transfer of host PUFAs to the symbionts. Phytochemistry 101:76–82

Imbs AB, Yakovleva IM, Latyshev NA, Pham LQ (2010b) Biosynthesis of polyunsaturated fatty acids in zooxanthellae and polyps of corals. Russ J Mar Biol 36:452–457

Iverson SJ (2009) Tracing aquatic food webs using fatty acids: from qualitative indicators to quantitative determination. Lipids in Aquatic Ecosystems. Springer New York, New York, NY, pp 281–308

Jackson AL, Inger R, Parnell AC, Bearhop S (2011) Comparing isotopic niche widths among and within communities: SIBER - Stable Isotope Bayesian Ellipses in R. J Anim Ecol 80:595–602

Jackson JB (1991) Adaptation and Diversity of Reef Corals. Bioscience 41:475–482

Jaleel A (2013) The status of the coral reefs and the management approaches: The case of the Maldives. Ocean Coast Manag 82:104–118

Jeong H, Yoo Y, Kang N, Lim A, Seong K, Lee S, Lee M, Lee K, Kim H, Shin W, Nam S, Yih W, Lee K (2012) Heterotrophic feeding as a newly identified survival strategy of the dinoflagellate Symbiodinium. Proc Natl Acad Sci 109:12604–12609

Jones RJ, Hoegh-Guldberg O, Larkum AWD, Schreiber U (1998) Temperature-induced bleaching of corals begins with impairment of the CO2 fixation mechanism in zooxanthellae. Plant, Cell Environ 21:1219–1230

Kabeya N, Fonseca MM, Ferrier DEK, Navarro JC, Bay LK, Francis DS, Tocher DR, Castro LFC, Monroig Ó (2018) Genes for de novo biosynthesis of omega-3 polyunsaturated fatty acids are widespread in animals. Sci Adv 4:EAAR6849

Kabeya N, Sanz-Jorquera A, Carboni S, Davie A, Oboh A, Monroig O (2017) Biosynthesis of Polyunsaturated Fatty Acids in Sea Urchins: Molecular and Functional Characterisation of Three Fatty Acyl Desaturases from Paracentrotus lividus (Lamark 1816). PLoS One 12:e0169374

Kahng S, Hochberg E, Apprill A, Wagner D, Luck D, Perez D, Bidigare R (2012) Efficient light harvesting in deep-water zooxanthellate corals. Mar Ecol Prog Ser 455:65–77

Kaniewska P, Magnusson SH, Anthony KRN, Reef R, Kühl M, Hoegh-Guldberg O (2011) Importance of macro- versus microstructure in modulating light levels inside coral colonies. J Phycol 47:846–860

Karati KK, Vineetha G, Madhu N V., Anil P, Dayana M, Shihab BK, Muhsin AI, Riyas C, Raveendran T V. (2017) Variability in the phytoplankton community of Kavaratti reef ecosystem (northern Indian Ocean) during peak and waning periods of El Niño 2016. Environ Monit Assess 189:653

Karnauskas KB, Cohen AL (2012) Equatorial refuge amid tropical warming. Nat Clim Chang 2:530–534

Karnauskas KB, Cohen AL, Gove JM (2016) Mitigation of Coral Reef Warming Across the Central Pacific by the Equatorial Undercurrent: A Past and Future Divide. Sci Rep 6:21213

Kassambara A, Mundt F (2017) factoextra: Extract and Visualize the Results of Multivariate Data Analyses.

Kattner G, Hagen W (2009) Lipids in marine copepods: latitudinal characteristics and perspective to global warming. Lipids in Aquatic Ecosystems. Springer New York, New York, NY, pp 257–280

Kelly J, Scheibling R (2012) Fatty acids as dietary tracers in benthic food webs. Mar Ecol Prog Ser 446:1–22

Kench PS, Brander RW, Parnell KE, McLean RF (2006) Wave energy gradients across a Maldivian atoll: Implications for island geomorphology. Geomorphology 81:1–17

Kendall C, Elliott EM, Wankel SD (2008) Tracing Anthropogenic Inputs of Nitrogen to Ecosystems. Stable Isotopes in Ecology and Environmental Science. Blackwell Publishing Ltd, Oxford, UK, pp 375–449

Kenkel CD, Matz M V. (2016) Gene expression plasticity as a mechanism of coral adaptation to a variable environment. Nat Ecol Evol 1:0014

Kleypas JA, McManus JW, Menez LAB (1999) Environmental limits to coral reef development: Where do we draw the line? Am Zool 39:146–159

Knowlton N, Jackson JBC (1994) New taxonomy and niche partitioning on coral reefs: jack of all

trades or master of some? Trends Ecol Evol 9:7–9

Kumar GS, Prakash S, Ravichandran M, Narayana AC (2016) Trends and relationship between chlorophyll-a and sea surface temperature in the central equatorial Indian Ocean. Remote Sens Lett 7:1093–1101

Kürten B, Al-Aidaroos AM, Struck U, Khomayis HS, Gharbawi WY, Sommer U (2014) Influence of environmental gradients on C and N stable isotope ratios in coral reef biota of the Red Sea, Saudi Arabia. J Sea Res 85:379–394

LaJeunesse T, Bhagooli R, Hidaka M, deVantier L, Done T, Schmidt G, Fitt W, Hoegh-Guldberg O (2004) Closely related Symbiodinium spp. differ in relative dominance in coral reef host communities across environmental, latitudinal and biogeographic gradients. Mar Ecol Prog Ser 284:147–161

LaJeunesse TC (2002) Diversity and community structure of symbiotic dinoflagellates from Caribbean coral reefs. Mar Biol 141:387–400

Lasagna R, Albertelli G, Colantoni P, Morri C, Bianchi CN (2010) Ecological stages of Maldivian reefs after the coral mass mortality of 1998. Facies 56:1–11

Latyshev NA, Naumenko N V., Svetashev VI, Latypov YY (1991) Fatty acids of reef-building corals. Mar Ecol Prog Ser 76:295–301

Layman CA, Araujo MS, Boucek R, Hammerschlag-Peyer CM, Harrison E, Jud ZR, Matich P, Rosenblatt AE, Vaudo JJ, Yeager LA, Post DM, Bearhop S (2012) Applying stable isotopes to examine food-web structure: an overview of analytical tools. Biol Rev 87:545–562

Le S, Josse J, Husson F (2008) FactoMineR: An R Package for Multivariate Analysis. J Stat Softw 25:1–18

Leal MC, Ferrier-Pagès C, Calado R, Thompson ME, Frischer ME, Nejstgaard JC (2014) Coral feeding on microalgae assessed with molecular trophic markers. Mol Ecol 23:3870–3876

Leal MC, Hoadley K, Pettay DT, Grajales A, Calado R, Warner ME (2015) Symbiont type influences trophic plasticity of a model cnidarian-dinoflagellate symbiosis. J Exp Biol 218:858–63

Leichter J, Genovese S (2006) Intermittent upwelling and subsidized growth of the scleractinian coral Madracis mirabilis on the deep fore-reef slope of Discovery Bay, Jamaica. Mar Ecol Prog Ser 316:95–103

Leichter J, Shellenbarger G, Genovese S, Wing S (1998) Breaking internal waves on a Florida (USA) coral reef: a plankton pump at work? Mar Ecol Prog Ser 166:83–97

Leichter JJ, Paytan A, Wankel S, Hanson K, Miller S, Altabet MA (2007) Nitrogen and oxygen isotopic signatures of subsurface nitrate seaward of the Florida Keys reef tract. Limnol

Oceanogr 52:1258–1267

Lesser M, Falcon L, Rodriguez-Roman A, Enriquez S, Hoegh-Guldberg O, Iglesias-Prieto R (2007) Nitrogen fixation by symbiotic cyanobacteria provides a source of nitrogen for the scleractinian coral Montastraea cavernosa. Mar Ecol Prog Ser 346:143–152

Lesser MP, Slattery M, Leichter JJ (2009) Ecology of mesophotic coral reefs. J Exp Mar Bio Ecol 375:1–8

Lesser MP, Slattery M, Stat M, Ojimi M, Gates RD, Grottoli A (2010) Photoacclimatization by the coral Montastraea cavernosa in the mesophotic zone: light, food, and genetics. Ecology 91:990–1003

Letourneur Y, Briand MJ, Graham NAJ (2017) Coral reef degradation alters the isotopic niche of reef fishes. Mar Biol 164:224

Levas S, Grottoli AG, Schoepf V, Aschaffenburg M, Baumann J, Bauer JE, Warner ME (2016) Can heterotrophic uptake of dissolved organic carbon and zooplankton mitigate carbon budget deficits in annually bleached corals? Coral Reefs 35:495–506

Levas SJ, Grottoli AG, Hughes A, Osburn CL, Matsui Y (2013) Physiological and Biogeochemical Traits of Bleaching and Recovery in the Mounding Species of Coral Porites lobata: Implications for Resilience in Mounding Corals. PLoS One 8:e63267

Li J, Chen Q, Zhang S, Huang H, Yang J, Tian X-P, Long L-J (2013) Highly heterogeneous bacterial communities associated with the South China Sea reef corals Porites lutea, Galaxea fascicularis and Acropora millepora. PLoS One 8:e71301

Lim C-S, Bachok Z, Hii Y-S (2017) Effects of supplementary polyunsaturated fatty acids on the health of the scleractinian coral Galaxea fascicularis (Linnaeus, 1767). J Exp Mar Bio Ecol 491:1–8

Liu G, Heron S, Eakin C, Muller-Karger F, Vega-Rodriguez M, Guild L, De La Cour J, Geiger E, Skirving W, Burgess T, Strong A, Harris A, Maturi E, Ignatov A, Sapper J, Li J, Lynds S (2014) Reef-Scale Thermal Stress Monitoring of Coral Ecosystems: New 5-km Global Products from NOAA Coral Reef Watch. Remote Sens 6:11579–11606

Lønborg C, Álvarez-Salgado XA, Duggan S, Carreira C (2018) Organic matter bioavailability in tropical coastal waters: The Great Barrier Reef. Limnol Oceanogr 63:1015–1035

Lowe A (2018) Local ecological modulation of global environmental change and its influence on benthic foundation species. University of Washington

Lowe RJ, Falter JL (2015) Oceanic Forcing of Coral Reefs. Ann Rev Mar Sci 7:43–66

Madin JS, Anderson KD, Andreasen MH, Bridge TCL, Cairns SD, Connolly SR, Darling ES, Diaz M, Falster DS, Franklin EC, Gates RD, Hoogenboom MO, Huang D, Keith SA, Kosnik MA,

Kuo C-Y, Lough JM, Lovelock CE, Luiz O, Martinelli J, Mizerek T, Pandolfi JM, Pochon X, Pratchett MS, Putnam HM, Roberts TE, Stat M, Wallace CC, Widman E, Baird AH, Baird AH (2016a) The Coral Trait Database, a curated database of trait information for coral species from the global oceans. Sci Data 3:160017

Madin JS, Hoogenboom MO, Connolly SR, Darling ES, Falster DS, Huang D, Keith SA, Mizerek T, Pandolfi JM, Putnam HM, Baird AH (2016b) A Trait-Based Approach to Advance Coral Reef Science. Trends Ecol Evol 31:419–428

Maier C, Weinbauer M, Pätzold J (2010) Stable isotopes reveal limitations in C and N assimilation in the Caribbean reef corals Madracis auretenra, M. carmabi and M. formosa. Mar Ecol Prog Ser 412:103–112

Maritorena S, Payri C, Babin M, Claustre H, Bonnafous L, Morel A, Rodière M (2002) Photoacclimatization in the zooxanthellae of Pocillopora verrucosa and comparison with a pelagic algal community. Oceanol Acta 25:125–134

Marshall PA, Baird AH (2000) Bleaching of corals on the Great Barrier Reef: differential susceptibilities among taxa. Coral Reefs 19:155–163

McClanahan T, Ateweberhan M, Graham N, Wilson S, Sebastián C, Guillaume M, Bruggemann J (2007) Western Indian Ocean coral communities: bleaching responses and susceptibility to extinction. Mar Ecol Prog Ser 337:1–13

McClanahan TR (2000) Bleaching damage and recovery potential of Maldivian coral reefs. Mar Pollut Bull 40:587–597

Meyers PA (1979) Polyunsaturated fatty acids in corals: indicators of nutritional sources. Mar Biol Lett 1:69–75

Meyers PA, Porter JW, Chad RL (1978) Depth analysis of fatty acids in two caribbean reef corals. Mar Biol 49:197–202

Minagawa M, Wada E (1986) Nitrogen isotope ratios of red tide organisms in the East China Sea: A characterization of biological nitrogen fixation. Mar Chem 19:245–259

Mocking RJT, Assies J, Lok A, Ruhé HG, Koeter MWJ, Visser I, Bockting CLH, Schene AH (2012) Statistical Methodological Issues in Handling of Fatty Acid Data: Percentage or Concentration, Imputation and Indices. Lipids 47:541–547

Monroig Ó, Tocher D, Navarro J (2013) Biosynthesis of Polyunsaturated Fatty Acids in Marine Invertebrates: Recent Advances in Molecular Mechanisms. Mar Drugs 11:3998–4018

Montoya J (2008) Nitrogen stable isotopes in marine environments. Nitrogen in the Marine Environment. Academic Press, pp 1277–1297

Montoya JP (2007) Natural Abundance of 15N in Marine Planktonic Ecosystems. In: Michener R.,

Lajtha K. (eds) Stable Isotopes in Ecology and Environmental Science. Blackwell Publishing Ltd, Oxford, UK, pp 176–201

Montoya JP, Carpenter EJ, Capone DG (2002) Nitrogen fixation and nitrogen isotope abundances in zooplankton of the oligotrophic North Atlantic. Limnol Oceanogr 47:1617–1628

Morillo-Velarde PS, Briones-Fourzán P, Álvarez-Filip L, Aguíñiga-García S, Sánchez-González A, Lozano-Álvarez E (2018) Habitat degradation alters trophic pathways but not food chain length on shallow Caribbean coral reefs. Sci Rep 8:4109

Mortillaro JM, Pitt KA, Lee SY, Meziane T (2009) Light intensity influences the production and translocation of fatty acids by zooxanthellae in the jellyfish Cassiopea sp. J Exp Mar Bio Ecol 378:22–30

Muir PR, Marshall PA, Abdulla A, Aguirre JD (2017) Species identity and depth predict bleaching severity in reef-building corals: shall the deep inherit the reef? Proc R Soc B Biol Sci 284:20171551

Muscatine L, Falkowski P, Dubinsky Z, Cook P, McCloskey L (1989a) The Effect of External Nutrient Resources on the Population Dynamics of Zooxanthellae in a Reef Coral. Proc R Soc B Biol Sci 236:311–324

Muscatine L, Falkowski PG, Porter JW, Dubinsky Z (1984) Fate of Photosynthetic Fixed Carbon in Light- and Shade-Adapted Colonies of the Symbiotic Coral Stylophora pistillata. Proc R Soc B Biol Sci 222:181–202

Muscatine L, Goiran C, Land L, Jaubert J, Cuif J-P, Allemand D (2005) Stable isotopes (delta13C and delta15N) of organic matrix from coral skeleton. Proc Natl Acad Sci U S A 102:1525–30

Muscatine L, Kaplan I (1994) Resource partitioning by reef corals as determined from stable isotope composition II. 15N of zooxanthellae and animal tissue versus depth. Pacific Sci 48:304–312

Muscatine L, Porter JW (1977) Reef Corals: Mutualistic Symbioses Adapted to Nutrient-Poor Environments. Bioscience 27:454–460

Muscatine L, Porter JW, Kaplan IR (1989b) Resource partitioning by reef corals as determined from stable isotope composition: I. d13C of zooxanthellae and animal tissue vs depth. Mar Biol 100:185–193

Nagle DG, Paul VJ (1998) Chemical defense of a marine cyanobacterial bloom. J Exp Mar Bio Ecol 225:29–38

Newsome SD, Martinez del Rio C, Bearhop S, Phillips DL (2007) A niche for isotopic ecology. Front Ecol Environ 5:429–436

van Os N, Massé LM, Séré MG, Sara JR, Schoeman DS, Smit AJ (2012) Influence of heterotrophic

feeding on the survival and tissue growth rates of Galaxea fascicularis (Octocorralia: Occulinidae) in aquaria. Aquaculture 330–333:156–161

Owen A, Kruijsen J, Turner N, Wright K (2011) Marine Energy in the Maldives: Pre-feasibility report on Scottish Support for Maldives Marine Energy Implementation, Part II, Annex III: Currents.

Palardy JE, Grottoli AG, Matthews KA (2005) Effects of upwelling, depth, morphology and polyp size on feeding in three species of Panamanian corals. Mar Ecol Prog Ser 300:78–89

Palardy JE, Rodrigues LJ, Grottoli AG (2008) The importance of zooplankton to the daily metabolic carbon requirements of healthy and bleached corals at two depths. J Exp Mar Bio Ecol 367:180–188

Papina M, Meziane T, van Woesik R (2003) Symbiotic zooxanthellae provide the host-coral Montipora digitata with polyunsaturated fatty acids. Comp Biochem Physiol Part B Biochem Mol Biol 135:533–7

Papina M, Meziane T, van Woesik R (2007) Acclimation effect on fatty acids of the coral Montipora digitata and its symbiotic algae. Comp Biochem Physiol Part B Biochem Mol Biol 147:583–589

Patton JS, Abraham S, Benson AA (1977) Lipogenesis in the intact coral Pocillopora capitata and its isolated zooxanthellae: Evidence for a light-driven carbon cycle between symbiont and host. Mar Biol 44:235–247

Pernice M, Meibom A, Van Den Heuvel A, Kopp C, Domart-Coulon I, Hoegh-Guldberg O, Dove S (2012) A single-cell view of ammonium assimilation in coral-dinoflagellate symbiosis. ISME J 6:1314–24

Perry CT, Morgan KM (2017) Bleaching drives collapse in reef carbonate budgets and reef growth potential on southern Maldives reefs. Sci Rep 7:40581

Peterson B, Fry B (1987) Stable isotopes in ecosystem studies. Annu Rev Ecol Syst 18:293–320

Pethybridge HR, Choy CA, Polovina JJ, Fulton EA (2018) Improving Marine Ecosystem Models with Biochemical Tracers. Ann Rev Mar Sci 10:199–228

Peyou-Ndi MM, Watts JL, Browse J (2000) Identification and Characterization of an Animal Δ12 Fatty Acid Desaturase Gene by Heterologous Expression in Saccharomyces cerevisiae. Arch Biochem Biophys 376:399–408

Phillips DL, Gregg JW (2001) Uncertainty in source partitioning using stable isotopes. Oecologia 127:171–179

Pichon M, Benzoni F (2007) Taxonomic re-appraisal of zooxanthellate Scleractinian Corals in the Maldive Archipelago. Zootaxa 21–33

Pinheiro J, Bates D, DebRoy S, Sarkar D, Team RC (2018) nlme: Linear and Nonlinear Mixed Effects Models (R package version 3.1-137).

Pisapia C, Burn D, Yoosuf R, Najeeb A, Anderson KD, Pratchett MS (2016) Coral recovery in the central Maldives archipelago since the last major mass-bleaching, in 1998. Sci Rep 6:34720

Plass-Johnson JG, Bednarz VN, Hill JM, Jompa J, Ferse SCA, Teichberg M (2018) Contrasting Responses in the Niches of Two Coral Reef Herbivores Along a Gradient of Habitat Disturbance in the Spermonde Archipelago, Indonesia. Front Mar Sci 5:32

Pogoreutz C, Rädecker N, Cárdenas A, Gärdes A, Voolstra CR, Wild C (2017) Sugar enrichment provides evidence for a role of nitrogen fixation in coral bleaching. Glob Chang Biol

Porter JW (1976) Autotrophy, Heterotrophy, and Resource Partitioning in Caribbean Reef-Building Corals. Am Nat 110:731–742

Preu C, Engelbrecht C (1991) Patterns and processes shaping the present morphodynamic of coral reef islands: Case study from the North-Male Atoll, Maldives (Indian Ocean). In: Brückner H., Radtke U. (eds) Von der Nordsee bis zum Indischen Ozean. Franz Steiner Verlag, Stuttgart, pp 209–220

Qasim SZ (1970) Some characteristics of a Trichodesmium bloom in the Laccadives. Deep Sea Res Oceanogr Abstr 17:

R-Core-Team (2018) R: A Language and Environment for Statistical Computing.

Rädecker N, Pogoreutz C, Voolstra CR, Wiedenmann J, Wild C (2015) Nitrogen cycling in corals: the key to understanding holobiont functioning? Trends Microbiol 23:490–497

Rahav O, Dubinsky Z, Achituv Y, Falkowski PG (1989) Ammonium Metabolism in the Zooxanthellate Coral, Stylophora pistillata. Proc R Soc B Biol Sci 236:325–337

Ramana M V., Ramanathan V (2006) Abrupt transition from natural to anthropogenic aerosol radiative forcing: Observations at the ABC-Maldives Climate Observatory. J Geophys Res 111:D20207

Redfield AC (1958) The biological control of chemical factors in the environment. Am Sci 46:205–221

Redfield AC (1963) The influence of organisms on the composition of sea-water. In: Hill M.N. (eds) The Sea: Ideas and Observations on Progress in the Study of the Seas, Vol. 2: The Composition of Seawater: Comparative and Descriptive Oceanography. Interscience, New York, pp 26–77

Reyes-Bonilla H, López-Pérez A (1998) Biogeography of the stony corals (Scleractinia) of the Mexican Pacific. Ciencias Mar 24:211–224

Reynaud S, Ferrier-Pagès C, Sambrotto R, Juillet-Leclerc A, Jaubert J, Gattuso J (2002) Effect of

feeding on the carbon and oxygen isotopic composition in the tissues and skeleton of the zooxanthellate coral Stylophora pistillata. Mar Ecol Prog Ser 238:81–89

Reynaud S, Martinez P, Houlbrèque F, Billy I, Allemand D, Ferrier-Pagès C (2009) Effect of light and feeding on the nitrogen isotopic composition of a zooxanthellate coral: role of nitrogen recycling. Mar Ecol Prog Ser 392:103–110

Riegl B, Glynn PW, Wieters E, Purkis S, d'Angelo C, Wiedenmann J (2015) Water column productivity and temperature predict coral reef regeneration across the Indo-Pacific. Sci Rep 5:8273

Riegl B, Piller WE (2003) Possible refugia for reefs in times of environmental stress. Int J Earth Sci 92:520–531

Risk MJ, Dunn JL, Allison WR, Horrill C (1993) Reef monitoring in Maldives and Zanzibar: low-tech and high-tech science. 66–72

Roder C, Fillinger L, Jantzen C, Schmidt G, Khokiattiwong S, Richter C (2010) Trophic response of corals to large amplitude internal waves. Mar Ecol Prog Ser 412:113–128

Roder C, Jantzen C, Schmidt GM, Kattner G, Phongsuwan N, Richter C (2011) Metabolic plasticity of the corals Porites lutea and Diploastrea heliopora exposed to large amplitude internal waves. Coral Reefs 30:57–69

Rodrigues LJ, Grottoli AG (2006) Calcification rate and the stable carbon, oxygen, and nitrogen isotopes in the skeleton, host tissue, and zooxanthellae of bleached and recovering Hawaiian corals. Geochim Cosmochim Acta 70:2781–2789

Rodrigues LJ, Grottoli AG (2007) Energy reserves and metabolism as indicators of coral recovery from bleaching. Limnol Oceanogr 52:1874–1882

Rodrigues LJ, Grottoli AG, Pease TK (2008) Lipid class composition of bleached and recovering Porites compressa Dana, 1846 and Montipora capitata Dana, 1846 corals from Hawaii. J Exp Mar Bio Ecol 358:136–143

Rodríguez-Troncoso AP, Carpizo-Ituarte E, Cupul-Magaña AL (2016) Physiological response to high temperature in the Tropical Eastern Pacific coral *Pocillopora verrucosa*. Mar Ecol 37:1168–1175

Roemmich D, McGowan J (1995) Climatic warming and the decline of zooplankton in the California Current. Science (80-) 267:1324–6

Rowan R, Knowlton N (1995) Intraspecific diversity and ecological zonation in coral-algal symbiosis. Proc Natl Acad Sci 92:2850–2853

Sampayo EM, Ridgway T, Bongaerts P, Hoegh-Guldberg O (2008) Bleaching susceptibility and mortality of corals are determined by fine-scale differences in symbiont type. Proc Natl Acad

Sci U S A 105:10444–9

Sargent JR, Falk-Petersen S (1981) Ecological investigations on the zooplankton community in balsfjorden, northern Norway: Lipids and fatty acids in Meganyctiphanes norvegica, Thysanoessa raschi and T. inermis during mid-winter. Mar Biol 62:131–137

Sasamal SK (2006) Island mass effect around the Maldives during the winter months of 2003 and 2004. Int J Remote Sens 27:5087–5093

Sasamal SK (2007) Island wake circulation off Maldives during boreal winter, as visualised with MODIS derived chlorophyll-a data and other satellite measurements. Int J Remote Sens 28:891–903

Sawall Y, Khokiattiwong S, Jompa J, Richter C (2014) Calcification, photosynthesis and nutritional status of the hermatypic coral Porites lutea: contrasting case studies from Indonesia and Thailand. Galaxea, J Coral Reef Stud 16:1–10

Schlichter D, Kremer BP, Svoboda A (1984) Zooxanthellae providing assimilatory power for the incorporation of exogenous acetate in Heteroxenia fuscescens (Cnidaria: Alcyonaria). Mar Biol 83:277–286

Schmidt G, Phongsuwan N, Jantzen C, Roder C, Khokiattiwong S, Richter C (2012) Coral community composition and reef development at the Similan Islands, Andaman Sea, in response to strong environmental variations. Mar Ecol Prog Ser 456:113–126

Schnack-Schiel SB, Niehoff B, Hagen W, Bottger-Schnack R, Cornils A, Dowidar MM, Pasternak A, Stambler N, Stubing D, Richter C (2008) Population dynamics and life strategies of Rhincalanus nasutus (Copepoda) at the onset of the spring bloom in the Gulf of Aqaba (Red Sea). J Plankton Res 30:655–672

Schoepf V, Grottoli AG, Levas SJ, Aschaffenburg MD, Baumann JH, Matsui Y, Warner ME (2015) Annual coral bleaching and the long-term recovery capacity of coral. Proc R Soc London B Biol Sci 282:20151887

Schukat A, Auel H, Teuber L, Lahajnar N, Hagen W (2014) Complex trophic interactions of calanoid copepods in the Benguela upwelling system. J Sea Res 85:186–196

Schulte S, Rostek F, Bard E, Rullkötter J, Marchal O (1999) Variations of oxygen-minimum and primary productivity recorded in sediments of the Arabian Sea. Earth Planet Sci Lett 173:205–221

Schutter M, van Velthoven B, Janse M, Osinga R, Janssen M, Wijffels R, Verreth J (2008) The effect of irradiance on long-term skeletal growth and net photosynthesis in Galaxea fascicularis under four light conditions. J Exp Mar Bio Ecol 367:75–80

Sebens KP, Vandersall KS, Savina LA, Graham KR (1996) Zooplankton capture by two

scleractinian corals,Madracis mirabilis andMontastrea cavernosa, in a field enclosure. Mar Biol 127:303–317

Seemann J (2013) The use of 13C and 15N isotope labeling techniques to assess heterotrophy of corals. J Exp Mar Bio Ecol 442:88–95

Seemann J, Sawall Y, Auel H, Richter C (2013) The Use of Lipids and Fatty Acids to Measure the Trophic Plasticity of the Coral Stylophora subseriata. Lipids 48:275–286

Semprucci F, Colantoni P, Baldelli G, Sbrocca C, Rocchi M, Balsamo M (2013) Meiofauna associated with coral sediments in the Maldivian subtidal habitats (Indian Ocean). Mar Biodivers 43:189–198

Séré MG, Massé LM, Perissinotto R, Schleyer MH (2010) Influence of heterotrophic feeding on the sexual reproduction of Pocillopora verrucosa in aquaria. J Exp Mar Bio Ecol 395:63–71

Sheppard CRC (2003) Predicted recurrences of mass coral mortality in the Indian Ocean. Nature 425:294–297

Sigman DM, Altabet MA, McCorkle DC, Francois R, Fischer G (2000) The δ15N of nitrate in the Southern Ocean: Nitrogen cycling and circulation in the ocean interior. J Geophys Res Ocean 105:19599–19614

Sigman DM, Casciotti KL, Andreani M, Barford C, Galanter M, Böhlk JK (2001) A Bacterial Method for the Nitrogen Isotopic Analysis of Nitrate in Seawater and Freshwater.

Sigman DM, DiFiore PJ, Hain MP, Deutsch C, Wang Y, Karl DM, Knapp AN, Lehmann MF, Pantoja S (2009a) The dual isotopes of deep nitrate as a constraint on the cycle and budget of oceanic fixed nitrogen. Deep Sea Res Part I Oceanogr Res Pap 56:1419–1439

Sigman DM, Karsh K, Casciotti KL (2009b) Ocean process tracers: Nitrogen isotopes in the ocean. Encycl Ocean Sci 4138–4153

Singh A, Kürten B, Cedras R, Fernandes M, Kumar N, et al. (2016) Perspectives on future Indian Ocean research from early career scientists. Curr Sci 111:1741–1742

Soares MA, Bhaskar P V., Naik RK, Dessai D, George J, Tiwari M, Anilkumar N (2015) Latitudinal δ13C and δ15N variations in particulate organic matter (POM) in surface waters from the Indian ocean sector of Southern Ocean and the Tropical Indian Ocean in 2012. Deep Sea Res Part II Top Stud Oceanogr 118:186–196

Sorokin YI (1973) On the feeding of some scleractinian corals with bacteria and dissolved organic matter. Limnol Oceanogr 18:380–386

Spychalla JP, Kinney AJ, Browse J (1997) Identification of an animal omega-3 fatty acid desaturase by heterologous expression in Arabidopsis. Proc Natl Acad Sci U S A 94:1142–7

Stafford-Smith M, Ormond R (1992) Sediment-rejection mechanisms of 42 species of Australian

scleractinian corals. Mar Freshw Res 43:683

Stanca E, Roselli L, Durante G, Seveso D, Galli P, Basset A (2013) A checklist of phytoplankton species in the Faafu atoll (Republic of Maldives). Transitional Waters Bull 7:133–144

Starzak DE, Quinnell RG, Nitschke MR, Davy SK (2014) The influence of symbiont type on photosynthetic carbon flux in a model cnidarian–dinoflagellate symbiosis. Mar Biol 161:711–724

Stebbing TRR (1904) Marine Crustaceans. XII Isopoda, with Description of a New Genus (with Plates XLIX-LIII). In: Gardiner S.J. (eds) The Fauna and Geography of the Maldive and Laccadive Archipelagoes: Being the Account of the Work carried on and of the Collections made by an Expedition during the years 1899 and 1900. Volume II, Part III. Cambridge University Press, Cambridge, pp 699–721

Steen R (1986) Evidence for heterotrophy by zooxanthellae in symbiosis with Aiptasia pulchella. Biol Bull 170:267–278

Stimson JS (1987) Location, Quantity and Rate of Change in Quantity of Lipids in Tissue of Hawaiian Hermatypic Corals. Bull Mar Sci 41:889–904

Strutton PG, Coles VJ, Hood RR, Matear RJ, McPhaden MJ, Phillips HE (2015) Biogeochemical variability in the central equatorial Indian Ocean during the monsoon transition. Biogeosciences 12:2367–2382

Stuhldreier I, Sánchez-Noguera C, Roth F, Cortés J, Rixen T, Wild C (2015) Upwelling Increases Net Primary Production of Corals and Reef-Wide Gross Primary Production Along the Pacific Coast of Costa Rica. Front Mar Sci 2:113

Swart PK, Saied A, Lamb K (2005) Temporal and spatial variation in the δ15N and δ13C of coral tissue and zooxanthellae in Montastraea faveolata collected from the Florida reef tract. Limnol Oceanogr 50:1049–1058

Sydeman WJ, García-Reyes M, Schoeman DS, Rykaczewski RR, Thompson SA, Black BA, Bograd SJ (2014) Climate change and wind intensification in coastal upwelling ecosystems. Science 345:77–80

Tagliafico A, Rudd D, Rangel M, Kelaher B, Christidis L, Cowden K, Scheffers S, Benkendorff K (2017) Lipid-enriched diets reduce the impacts of thermal stress in corals. Mar Ecol Prog Ser 573:129–141

Taipale S, Strandberg U, Peltomaa E, Galloway A, Ojala A, Brett M (2013) Fatty acid composition as biomarkers of freshwater microalgae: analysis of 37 strains of microalgae in 22 genera and in seven classes. Aquat Microb Ecol 71:165–178

Taipale SJ, Kainz MJ, Brett MT (2011) Diet-switching experiments show rapid accumulation and

preferential retention of highly unsaturated fatty acids in Daphnia. Oikos 120:1674–1682

Tanaka Y, Grottoli AG, Matsui Y, Suzuki A, Sakai K (2015) Partitioning of nitrogen sources to algal endosymbionts of corals with long-term 15N-labelling and a mixing model. Ecol Modell 309:163–169

Tanaka Y, Miyajima T, Koike I, Hayashibara T, Ogawa H (2006) Translocation and conservation of organic nitrogen within the coral-zooxanthella symbiotic system of Acropora pulchra, as demonstrated by dual isotope-labeling techniques. J Exp Mar Bio Ecol 336:110–119

Tanaka Y, Ogawa H, Miyajima T (2011) Production and bacterial decomposition of dissolved organic matter in a fringing coral reef. J Oceanogr 67:427–437

Tanaka Y, Suzuki A, Sakai K (2018) The stoichiometry of coral-dinoflagellate symbiosis: carbon and nitrogen cycles are balanced in the recycling and double translocation system. ISME J 12:860–868

Tchernov D, Lipschultz F (2008) Carbon isotopic composition of Trichodesmium spp. colonies off Bermuda: effects of colony mass and season. J Plankton Res 30:21–31

Teece MA, Estes B, Gelsleichter E, Lirman D (2011) Heterotrophic and autotrophic assimilation of fatty acids by two scleractinian corals, Montastraea faveolata and Porites astreoides. Limnol Oceanogr 56:1285–1296

Teuber L, Schukat A, Hagen W, Auel H (2014) Trophic interactions and life strategies of epi- to bathypelagic calanoid copepods in the tropical Atlantic Ocean. J Plankton Res 36:1109–1123

Tkachenko KS (2015) Impact of repetitive thermal anomalies on survival and development of mass reef-building corals in the Maldives. Mar Ecol 36:292–304

Tolosa I, Treignier C, Grover R, Ferrier-Pagès C (2011) Impact of feeding and short-term temperature stress on the content and isotopic signature of fatty acids, sterols, and alcohols in the scleractinian coral Turbinaria reniformis. Coral Reefs 30:763–774

Treignier C, Grover R, Ferrier-Pagès C, Tolosa I (2008) Effect of light and feeding on the fatty acid and sterol composition of zooxanthellae and host tissue isolated from the scleractinian coral Turbinaria reniformis. Limnol Oceanogr 53:2702–2710

Tremblay P, Gori A, Maguer JF, Hoogenboom M, Ferrier-Pagès C (2016) Heterotrophy promotes the re-establishment of photosynthate translocation in a symbiotic coral after heat stress. Sci Rep 6:38112

Tremblay P, Maguer JF, Grover R, Ferrier-Pagès C (2015) Trophic dynamics of scleractinian corals: stable isotope evidence. J Exp Biol 218:1223–34

Tyrrell T (1999) The relative influences of nitrogen and phosphorus on oceanic primary production. Nature 400:525–531

UNEP-WCMC, WorldFish, WRI, TNC (2010) Global distribution of warm-water coral reefs, compiled from multiple sources including the Millennium Coral Reef Mapping Project, Version 1.3. http://data.unep-wcmc.org/datasets/1

Venables WN, Ripley BD (2002) Modern Applied Statistics with S. Springer, New York

Vermeij MJA, Bak RPM (2003) Species-Specific Population Structure of Closely Related Coral Morphospecies Along a Depth Gradient (5–60 m) Over a Caribbean Reef Slope. Bull Mar Sci 73:725–744

Veron JEN (2000) Corals of the world. Australian Institute of Marine Science, Townsville

Veron JEN, Hoegh-Guldberg O, Lenton TM, Lough JM, Obura DO, Pearce-Kelly P, Sheppard CRC, Spalding M, Stafford-Smith MG, Rogers AD (2009) The coral reef crisis: The critical importance of less than 350 ppm CO2. Mar Pollut Bull 58:1428–1436

Vineetha G, Karati KK, Raveendran T V., Idrees Babu KK, Riyas C, Muhsin MI, Shihab BK, Simson C, Anil P (2018) Responses of the zooplankton community to peak and waning periods of El Niño 2015–2016 in Kavaratti reef ecosystem, northern Indian Ocean. Environ Monit Assess 190:465

Vinogradov ME, Voronina N (1962) The distribution of different groups of plankton in accordance with their trophic level in the Indian Equatorial Current Area (No. 33). Raport et Proces-Verbaux des Reunions (Vol. 153). pp 200–205

de Vos A, Pattiaratchi CB, Wijeratne EMS (2014) Surface circulation and upwelling patterns around Sri Lanka. Biogeosciences 11:5909–5930

Walther G-R, Post E, Convey P, Menzel A, Parmesan C, Beebee TJC, Fromentin J-M, Hoegh-Guldberg O, Bairlein F (2002) Ecological responses to recent climate change. Nature 416:389–395

Wang, Douglas (1998) Nitrogen recycling or nitrogen conservation in an alga-invertebrate symbiosis? J Exp Biol 201:2445–2453

Wang L-H, Chen H-K, Jhu C-S, Cheng J-O, Fang L-S, Chen C-S (2015) Different strategies of energy storage in cultured and freshly isolated *Symbiodinium* sp. J Phycol 51:1127–1136

Wang XT, Sigman DM, Cohen AL, Sinclair DJ, Sherrell RM, Cobb KM, Erler D V., Stolarski J, Kitahara M V., Ren H (2016) Influence of open ocean nitrogen supply on the skeletal δ15N of modern shallow-water scleractinian corals. Earth Planet Sci Lett 441:125–132

Ward S (1995) Two patterns of energy allocation for growth, reproduction and lipid storage in the scleractinian coral Pocillopora damicornis. Coral Reefs 14:87–90

Weis VM (2008) Cellular mechanisms of Cnidarian bleaching: stress causes the collapse of symbiosis. J Exp Biol 211:3059–3066

Weng L-C, Pasaribu B, -Ping Lin I, Tsai C-H, Chen C-S, Jiang P-L (2014) Nitrogen Deprivation Induces Lipid Droplet Accumulation and Alters Fatty Acid Metabolism in Symbiotic Dinoflagellates Isolated from Aiptasia pulchella. Sci Rep 4:680–685

West JM, Salm R V. (2003) Resistance and Resilience to Coral Bleaching: Implications for Coral Reef Conservation and Management. Conserv Biol 17:956–967

Wickham H (2009) ggplot2: Elegant Graphics for Data Analysis. Springer-Verlag New York,

Wijgerde T, Diantari R, Lewaru MW, Verreth JAJ, Osinga R (2011) Extracoelenteric zooplankton feeding is a key mechanism of nutrient acquisition for the scleractinian coral Galaxea fascicularis. J Exp Biol 214:3351–7

Wilke CO (2017) cowplot: Streamlined Plot Theme and Plot Annotations for "ggplot2."

Wilkerson FP, Muller G, Muscatine PL (1983) Temporal patterns of cell division in natural populations of endosymbiotic algae. Limnol Oceanogr 28:1009–1014

Wilkinson C, Linden O, Cesar H, Hodgson G, Rubens J, Strong A (1999) Ecological and socioeconomic impacts of 1998 coral mortality in the Indian Ocean: an ENSO impact and a warning of future change. Ambio 28:188–196

Williams EH, Bunkley-Williams L (1990) The world-wide coral reef bleaching cycle and related sources of coral mortality. Atoll Res Bull 335:1–71

Williams GJ, Sandin SA, Zgliczynski BJ, Fox MD, Gove JM, Rogers JS, Furby KA, Hartmann AC, Caldwell ZR, Price NN, Smith JE (2018) Biophysical drivers of coral trophic depth zonation. Mar Biol 165:60

Williams PM, Gordon LI (1970) Carbon-13: carbon-12 ratios in dissolved and particulate organic matter in the sea. Deep Sea Res Oceanogr Abstr 17:19–27

Winder M, Schindler DE (2004) Climate change uncouples trophic interactions in an aquatic ecosystem. Ecology 85:2100–2106

Wyatt ASJ, Falter JL, Lowe RJ, Humphries S, Waite AM (2012) Oceanographic forcing of nutrient uptake and release over a fringing coral reef. Limnol Oceanogr 57:401–419

Yamashiro H, Oku H, Higa H, Chinen I, Sakai K (1999) Composition of lipids, fatty acids and sterols in Okinawan corals. Comp Biochem Physiol Part B Biochem Mol Biol 122:397–407

Yamashiro H, Oku H, Onaga K (2005) Effect of bleaching on lipid content and composition of Okinawan corals. Fish Sci 71:448–453

Yamazaki A, Watanabe T, Ogawa NO, Ohkouchi N, Shirai K, Toratani M, Uematsu M (2011) Seasonal variations in the nitrogen isotope composition of Okinotori coral in the tropical western Pacific: A new proxy for marine nitrate dynamics. J Geophys Res 116:G04005

Zhou X-R, Green AG, Singh SP (2011) *Caenorhabditis elegans* Δ12-Desaturase FAT-2 Is a

Bifunctional Desaturase Able to Desaturate a Diverse Range of Fatty Acid Substrates at the Δ12 and Δ15 Positions. J Biol Chem 286:43644–43650

Zhukova N V, Titlyanov EA (2003) Fatty acid variations in symbiotic dinoflagellates from Okinawan corals. Phytochemistry 62:191–195

Ziegler M, Roder C, Büchel C, Voolstra C (2015a) Niche acclimatization in Red Sea corals is dependent on flexibility of host-symbiont association. Mar Ecol Prog Ser 533:149–161

Ziegler M, Roder CM, Büchel C, Voolstra CR (2014) Limits to physiological plasticity of the coral Pocillopora verrucosa from the central Red Sea. Coral Reefs 33:1115–1129

Ziegler M, Roder CM, Büchel C, Voolstra CR (2015b) Mesophotic coral depth acclimatization is a function of host-specific symbiont physiology. Front Mar Sci 2:4

(2013) NOAA Coral Reef Watch Daily Global 5-km Satellite Virtual Station Time Series Data for Maldives. http://coralreefwatch.noaa.gov/vs/index.php

(2018) Daily wind data for Hulhule (Kaafu Atoll).